ABSTRACT

Radical Fragmentation Towards the Synthesis of **FS-2**

Renata Xavier Kover

May, 1999.

Radical fragmentation studies of cyclic thionocarbonates attached to five-membered rings aimed at the synthesis of sesquiterpene micotoxin FS-2 are presented. The synthetic strategy targeted the formation of a rigid tricycle [5.4.0.$0^{2,6}$]-undecane skeleton with well-defined geometry to take advantage of face-selective reactions to install the necessary functionality in a stereoselective manner. The final product could be unraveled at the last step of the synthesis *via* a radical fragmentation cascade. The rigid skeleton was assembled by an intramolecular [2+2] photoaddition to set the relative stereochemistry of the two adjacent quaternary centers characteristic of the trichothecene natural products. The fragmentation of a model system demonstrated the feasibility of this approach. The stereochemistry at the ring junction enabled the control of the selectivity of the fragmentation. The *cis* fused system leads to the formation of the secondary radical while the *trans* fused system gives a primary radical at a ratio greater than 20:1. Fragmentation of the cyclobutylcarbinyl radical derived from the thionocarbonate fragmentation selectively cleaved the exocyclic C-C bond to give the more stable radical resembling the trichothecene skeleton.

This methodology offers an entry for the preparation of the trichothecene family of compounds *via* control of the stereochemistry at the thionocarbonate ring junction. The radical fragmentation of the *cis*-fused system leads to the formation of trichothecenes

with the FS-2 type skeleton, while fragmentation of the *trans*-fused system leads to the formation of the tricyclic type trichothecene skeleton upon biomimetic cyclization.

Geometry *ab initio* calculations were conducted to better understand the origin of the observed selectivity in the fragmentation reactions. A series of differently substituted cyclic thionocarbonates were analyzed with respect to energy, charge distribution, geometry and an "offset-from-ideal-angle" quantity to gage angle-strain. Additionally, the intermediates and transition states involved in the radical fragmentation reactions were investigated in the context of the *cis* and *trans* ring junction. These calculations indicate that secondary radical is favored over primary unless the system is highly strained as represented by the offset-from-ideal-angle. For these highly strained molecules, release of strain may determine the preferred pathway of the reaction overcoming the natural thermodynamical tendencies of the system.

Radical Fragmentation Towards the Synthesis of **FS-2**

A Dissertation

Presented to the Faculty of the Graduate School

of

Yale University

in Candidacy for the Degree of

Doctor of Philosophy

by

Renata Xavier Kover

Dissertation Director: Dr. Frederick E. Ziegler

May, 1999

For my parents.

And my family,

Jon and Clawed.

Acknowledgements

As I get to the end of this journey it is time to acknowledge the people that made it all possible. The presentation of a Ph. D. thesis marks the end of endless years of research; it reflects a process of maturing and learning that had an impact in all aspects of my life. It required me to get acquainted with the techniques in organic synthesis, with the literature in the different subjects I studied and with the thought processes necessary to address the questions encountered in the way; but it also required perseverance, enthusiasm, the need to challenge the generally accepted truth (sometimes) and TO GO ON, when everything else fails. Many people helped me succeed in such an undertaking, and these people helped shaping the final me. At this point it is important that I thank them.

I'd like to start at the beginning, with my parents without whom I would not have made it beyond the first steps. I'd like to thank my mother for being there the whole time and for teaching me how to live and love life. I'd like to thank my dad who set the standards high from the start, who was always willing to teach and push me a little forward, but never willing to just give the answer. The years we were together at UFRJ brought us very close. And I'd like to thank my sister, Paula who has been supportive throughout the years and is always full of challenges.

I thank my advisor, Frederick E. Ziegler for the opportunity to work in this project. I also thank my committee members, John L. Wood and J. Michael McBride, for reading my thesis and for offering comments and suggestions that helped improve the final product. I thank my former committee members Alanna Schepartz and Jerome

Berson for constructive criticism and discussions during committee meetings during the years.

I'd like to thank Prof. Kenneth Wiberg for helping with *ab initio* calculations conducted in this thesis, as well as Prof. Paul Rablen, Dr. Henry Castejon and Jack Hammer for holding my hand when I had no idea how to even submit one of these gaussian calculations to the computer.

I thank Prof. Donald Crothers for being great. He was always supportive and just genuinely interested in people and their well being, and I thank him for sharing some of that with me.

I'd like to thank all the members of the Ziegler lab, past and present and the other people I was lucky to interact with in the various labs in the department, you have made my stay here a memorable one. There are too many of you to mention everyone, but thank you. I would especially like to thank the students and post-docs in the Danishefski lab for being my extended lab for many years.

I have been fortunate to have made MANY friends and colleagues during my years at Yale. To adequately express my gratitude to them would require writing another volume to this thesis. I cannot mention everyone, but I must mention the following people. John Bembow, Mike Biewer, Julie Carruthers, Margareth Chu-Moyer, Lissa Fowley, John Gehman, Meg Gross, Pat Harran, Cherryl and Matt Hayward, Chet Metcalf, Dave Nakaji, John Peterson, Mary Kay and Derek Pflum, Rich Roberts, Dan Rush, Julian Tirados, Leslie Sloan, Fred Vehrnes, Mike Wendt. I should also thank my friends in Brasil that gave me the courage to come to Yale: Beto, Marcos, Elaine, Heloisa, Feto, Aylene.

Jon Lapham may be the only person who has (or will ever) read every single word of this thesis. You have been my partner in research and in life. Having the privilege of sharing all this time with someone as intelligent and passionate about life as you are gave me the courage to face whatever uncertainties were encountered in completing this thesis. Thank you.

TABLE OF CONTENTS:

LIST OF COMPOUNDS: 4

CHAPTER I: INTRODUCTION 7

- **TRICHOTHECENES: 7**

1. ORIGIN 7
2. STRUCTURE 10
3. BIOLOGICAL ACTIVITY 13

- **FS-2 16**
- **PREVIOUS SYNTHETIC APPROACHES: 18**

1. GENERAL: 18
2. ALDOL APPROACH 19
3. BIOMIMETIC APPROACH: 21
4. OTHER APPROACHES: 23
5. OPTICALLY ACTIVE SYNTHESIS 27
6. QUATERNARY CENTERS: 28
7. INTERCONVERSION OF TRICHOTHECENES: 30

- **RETROSYNTHETIC ANALYSIS: 31**
- **REVISED STRUCTURE: 34**

CHAPTER II: SYNTHESIS OF THE TRICYCLO-UNDECANE COMMOM INTERMEDIATE **38**

- **SYNTHESIS OF THE FIVE AND SIX-MEMBERED RING PRECURSORS 39**
- **INTERMOLECULAR PHOTOADDITION 45**
- **INTRAMOLECULAR PHOTOADDITION 46**

1. ETHER TETHER STRATEGY: WILLIAMSON ETHER SYNTHESIS 47
2. ETHER TETHER STRATEGY: FAILED ALTERNATIVES 51
3. THE ESTER TETHER STRATEGY 57
4. SILICON TETHER STRATEGY 63
5. PHOTOADDITION 66

- **OLEFIN FORMATION 69**
- **CONCLUSION 73**

CHAPTER III: RADICAL FRAGMENTATION - MODEL SYSTEMS **75**

- **INTRODUCTION 75**
- **RADICAL FRAGMENTATION BACKGROUND 76**

1. FRAGMENTATION OF THIONOCARBONATES 78
2. BETA-OXYGEN EFFECT 91
3. FRAGMENTATION OF CYCLOBUTYLCARBINYL SYSTEMS 94

4. FRAGMENTATION OF OXIRANYLCARBINYL RADICALS 98
• **PREPARATION OF THE MODEL SYSTEMS** **104**
1. MODEL SYSTEM 1 104
2. MODEL SYSTEM 2 107
3. MODEL SYSTEM 3 111
4. MODEL SYSTEM 4 113
• **FRAGMENTATION OF THE MODEL SYSTEMS** **115**
1. MODEL SYSTEM 1 116
2. MODEL SYSTEM 2 121
• **CONCLUSION** **122**

CHAPTER IV: ELABORATION OF THE FRAGMENTATION INTERMEDIATE. **125**

• **INTRODUCTION** **125**
• **FUNCTIONALIZATION ALPHA TO THE CARBONYL:** **126**
1. STRATEGY I: α-BROMINATION 126
2. STRATEGY II: α-OXIDATION 131
3. STRATEGY III: THE MORIARTY ROUTE 137
• **KETONE REDUCTION:** **139**
• **FUTURE DEVELOPMENTS:** **142**

CHAPTER V: EXPERIMENTAL PROCEDURES **144**

• **GENERAL** **144**
• **SPECIFIC COMPOUNDS** **147**

ADDENDUM I: SELECTED ^{1}H NMR SPECTRA **192**

• **RESULTS OF NOE EXPERIMENTS CHAPTER 3** **231**
1. COMPOUND 91 231
2. COMPOUND 94 232
3. COMPOUND 96 233
4. COMPOUND 99 234
5. COMPOUND 100 235
• **RESULTS OF NOE EXPERIMENTS CHAPTER 4** **236**
1. COMPOUND 112 236
2. COMPOUND 121 237
3. COMPOUND 122 238
4. COMPOUND 124 239
5. COMPOUND 126 240

ADDENDUM II: SELECTED ^{13}C NMR SPECTRA **241**

ADDENDUM III: CONFORMATION ANALYSIS OF FS-2 - MONTE CARLO SIMULATION **277**

ADDENDUM IV: AB INITIO CALCULATIONS ON THE CYCLIC THIOCARBONATE SYSTEM **309**

- **INTRODUCTION: 309**
- **THE AB INITIO PROCEDURE: 311**
- **SAMPLE CALCULATION: 314**

1. CIS DIMETHYL CARBONATE GEOMETRY CALCULATION INPUT FILE: 315
2. GEOMETRY CALCULATION – RESULTS: 316
3. FREQUENCY CALCULATION – RESULTS: 316
4. GEOMETRY – PDB FILE: 317
5. CALCULATED OFFSET-FROM-THE-IDEAL-ANGLE: 317
6. GRAPHICAL REPRESENTATION: 318

- **RESULTS: SUBSTITUENT EFFECTS ON THE CARBONATE RING: 319**
- **RESULTS: FRAGMENTATION REACTION - CIS: 323**
- **RESULTS: FRAGMENTATION REACTION - TRANS: 329**

ADDENDUM V: PERL SCRIPTS **335**

- **ANGLE_STRAIN.PL 335**
- **GET_CHARGE.PL 337**
- **GET_SPIN.PL 339**
- **GAUSSIAN2PDB.PL 340**
- **ZMATRIXEXTRACT 341**
- **PDBCLEAN.PL 341**
- **SUM_ANGLE_STRAIN.PL 342**

LIST OF COMPOUNDS:

Compound 7: 4, 5, 6, 7-Tetrahydrocyclopenta-[a]-[1, 3]-dioxin-5-one 147

Compound 5: 2-(Hydroxymethyl)-3-methyl-2-cyclopenten-1-one 148

Compound 18: 2-(Chloromethyl)-3-methyl-2-cyclopenten-1-one 149

Compound 8: 3-Trimethylsilyloxy-1-methyl-1, 3-cyclohexadiene 150

Compound 9: 6-(Benzyloxymethyl)-3-methyl-2-cyclohexen-1-one 151

Compounds 6a and 6b: (1R*, 6S*)-6-(Benzyloxymethyl)-3-methyl-2-cyclohex-2-ene-1-ol and (1R*, 6R*)-6-(Benzyloxymethyl)-3-methyl-2-cyclohex-2-ene-1-ol 153

Compound 10: 6-Hydroxymethyl-3-methyl-(1R*, 6S*)-2-cyclohexen-1-ol 154

Compound 11: 7-Methyl-(4aR*, 8aR*)-5H, 6H-benzo[a][1, 3]dioxin-2-one 155

Compound 12: 6-Hydroxymethyl-3-methyl-(1R*, 6R*)-2-cyclohexen-1-ol 156

Compound 13: 7-Methyl-(4aR*, 8aS*)-5H, 6H-benzo[a][1, 3]dioxin-2-one 157

Compound 4: 2-(6-Benzyloxymethyl-3-methyl-(1R*, 6S*)-2-cyclohexenyloxymethyl)-3-methyl-2-cyclopenten-1-one 158

Compound 17: 3-[(Benzyloxy)-methyl]-5a, 5b-dimethyl-(2aR*, 3S*, 5aR*, 5bS*, 8aR*, 8bS*)-perhydro-2-xacyclopenta[4, 1]cyclobuta[c, d]-inden-8-one 160

Compound 39: 3-Hydroxymethyl-5a, 5b-dimethyl-(2aR*, 3S*, 5aR*, 5bS*, 8aR*, 8bS*)-perhydro-2-oxacyclopenta[4, 1]cyclobuta[c, d]-inden-8-one 161

Compound 3: 5a, 5b-Dimethyl-3-methylene-(2aR*, 5aR*, 5bS*, 8aR*, 8bS*) perhydro-2-oxacyclopenta[4, 1]cyclobuta[c, d]inden-8-one 162

Compound 91: 5a, 5b-Dimethyl-3-methylene-(2aR*, 5aR*, 5bS*, 8S*, 8aR*, 8bS*) perhydro-2-oxacyclopenta [4, 1] cyclobuta [c, d] inden-8-ol 163

Compound 92: 7b-(Hydroxymethyl)-3a, 3b, 6-trimethyl-(1R*, 3aR*, 3bS*, 7aR*, 7bS*)-2, 3, 3a, 3b, 4, 5, 7a, 7b-octahydro-1*H*-cyclopenta[3, 4]cyclobuta[a]benzen-1-ol 164

Compound 94: 6a, 6b, 9-Trimethyl-(4aR*, 6aR*, 6bS*, 10aR*, 10bS*)-4a, 5, 6, 6a, 6b, 7, 8, 10a-octahydrobenzo[3', 4']cyclobuta[2, 3]cyclopenta[d][1, 3]dioxin-3-thione 165

Compound 95: 6a, 6b, 9-Trimethyl-(4aR*, 6aR*, 6bS*, 10aR*, 10bS*)-4a, 5, 6, 6a, 6b, 7, 8, 10a-octahydrobenzo[3', 4']-cyclobuta[2, 3]cyclopenta[d][1, 3]-dioxin-3-one 166

Compound 96: 1a, 3a, 3b-Trimethyl-(1aR*, 3aS*, 3bR*, 5aR*, 9aS*, 9bS*, 9cR*)-perhydrooxireno[2''', 3''':3'', 4'']benzo[3', 4']cyclobuta[2, 3]cyclopenta[d][1, 3] dioxin-7-one 167

Compounds 97 and 98: 6a-Hydroxymethyl-1a, 3a, 3b-trimethyl-(1aR*, 3aR*, 3bS*, 6S*, 6aR*, 6bS*, 6cS*)perhydrocyclopenta[3 , 4]cyclobuta[3, 4]benzo[b]oxiren-6-ol and 3, 5a, 5b-

Trimethyl-(2aR*, 3R*, 5aR*, 5bS*, 8S*, 8aR*, 8bS*)-perhydro-2-oxacyclopenta[4, 1]cyclobuta[c, d]indene-3, 8-diol 168

Compound 99: 1a, 3a, 3b-Trimethyl-(1aR*, 3aS*, 3bR*, 5aR*, 9aS*, 9bS*, 9cR*)-perhydrooxireno [2''', 3''':3'', 4''] benzo [3', 4'] cyclobuta [2, 3] cyclopenta[d][1, 3] dioxin-7-thione 170

Compound 100: 5a, 5b-Dimethyl-3-methylene-(2aR*, 5aR*, 5bS*, 8R*, 8aR*, 8bS*) perhydro-2-oxacyclopenta[4, 1]cyclobuta[c, d]inden-8-ol 171

Compound 101: 7b-(Hydroxymethyl)-3a, 3b, 6-trimethyl-(1R*, 3aS*, 3bR*, 7aS*, 7bR*)-2, 3, 3a, 3b, 4, 5, 7a, 7b-octahydro-1*H*-cyclopenta [3, 4] cyclobuta [a] benzen-1-ol 173

Compound 102: 6a, 6b, 9-Trimethyl-(4aR*, 6aS*, 6bR*, 10aS*, 10bR*)-4a, 5, 6, 6a, 6b, 7, 8, 10a-octahydrobenzo[3', 4']-cyclobuta[2, 3]cyclopenta[d][1, 3]-dioxin-3-thione 174

Compound 103: 5a, 5b-dimethyl-3-methylene-(2aR*, 5aR*, 5bS*, 8aR*, 8bS*)-[(2a, 3, 4, 5, 5a, 5b, 6, 8b-octahydro-2-oxacyclopenta[4, 1]cyclobuta[c, d]inden-8-yl)oxy](triisopropyl)silane 175

Compound 105: 7b-(Hydroxymethyl)-3a, 3b, 6-trimethyl-(3aR*, 3bS*, 7aR*, 7bS*)-2, 3, 3a, 3b, 4, 5, 7a, 7b-octahydro-1*H*-cyclopenta[3, 4]cyclobuta[a]benzen-1-one 176

Compound 106: 1a, 3a, 3b-trimethyl-6a-{[(1, 1, 1-trimethylsilyl)oxy]methyl}-(1aR*, 3aR*, 3bS*, 6aR*, 6bS*, 6cS*)-perhydrocyclopenta[3 , 4]cyclobuta[3, 4] benzo[b]oxiren-6-one 177

Compounds 107 and 108: 3a, 3b, 6-Trimethyl-(1R*, 3aS*, 3bS*, 7aR*, 8aS*)-1, 2, 3, 3a, 3b, 4, 5, 7a, 8, 8a-decahydrocyclopenta[a]inden-1-ol and 3(1, 4-Dimethyl-(1R*)-2-cyclohexenyl)-3-methyl-2-methylene-(1R*, 3R*)-cyclopentan-1-ol 179

Fragmentation of compound 99 180

Compound 112: 7-Bromo-5a, 5b-dimethyl-3-methylene-(2aR*, 5aR*, 5bS*, 7R*, 8aR*, 8bS*)perhydro-2-oxacyclopenta[4, 1]cyclobuta[c, d]inden-8-one 181

Compound 116: 7-Bromo-5a, 5b-dimethyl-3-methylene-(2aR*, 5aR*, 5bS*, 7S*, 8S*, 8aR*, 8bS*)perhydro-2-oxacyclopenta[4, 1]cyclobuta[c, d]inden-8-ol 182

Compound 118: 7b-(Hydroxymethyl)-3a, 3b, 6-trimethyl-(1R*, 2R*, 3aR*, 3bS*, 7aR*, 7bS*)-2, 3, 3a, 3b, 4, 5, 7a, 7b-octahydro-1*H*-2-bromo-cyclopenta[3, 4] cyclobuta[a]benzen-1-ol 183

Compound 114: 7-Hydroxy-5a, 5b-dimethyl-3-methylene-(2aR*, 5aR*, 5bS*, 8aR*, 8bS*)-2a, 3, 4, 5, 5a, 5b, 8, 8b-octahydro-2-oxacyclopenta[4, 1]cyclobuta[c, d]inden-8-one 184

Compound 124: 5a, 5b-dimethyl-3-methylene-(2aR*, 5aR*, 5bS*, 7S*, 8aR*, 8bS*)-perhydro-2-oxacyclopenta[4, 1]cyclobuta[c, d]inden-7-ol-8-one 185

Compound 121: 5a, 5b-Dimethyl-3-methylene-(2aR*, 5aR*, 5bS*, 7S*, 8S*, 8aR*, 8bS*)-perhydro-2-oxacyclopenta[4, 1]cyclobuta[c, d]inden-7, 8-diol 187

Compound 122: 5a, 5b-dimethyl-methylene-(2aR*, 5aR*, 5bS*, 6aS*, 9aR*, 9bR*, 9cS*)-perhydro[1]benzoxolo[3'', 4'':2', 3', 4']cyclobuta[4, 5] cyclopenta[d][1,3]dioxole-8-thione 188

Compound 123: 7b-(Hydroxymethyl)-3a, 3b, 6-trimethyl-(1R*, 2S*, 3aR*, 3bS*, 7aR*, 7bS*)- 2, 3, 3a, 3b, 4, 5, 7a, 7b-octahydro-1*H*-cyclopenta[3, 4] cyclobuta[a]benzen-1, 2-diol 189

Compound 126: 5a, 5b-Dimethyl-3-methylene-(2aR*, 5aR*, 5bS*, 7S*, 8R*, 8aR*, 8bS*)-perhydro-2-oxacyclopenta[4, 1]cyclobuta[c, d]inden-7, 8-diol **190**

CHAPTER I: INTRODUCTION

- *Trichothecenes:*

1. Origin

"Trichothecene contamination of human food and animal feed is a continuing worldwide problem".[1] Multiyear surveys in the US and Canada indicate that maize and wheat are often contaminated with trichothecenes but at levels that are generally below the recommended tolerance level of 2 ppm.

Trichothecenes are widely occurring fungal metabolites and they have been linked to outbreaks of alimentary toxic aleukia that occurred in the former Soviet Union in the 1940's (1942-1947) and outbreaks of a similar disease called akakabi-byo or red mold disease in Japan.[2] Trichothecenes are responsible for moldy corn toxicosis in the USA, and stachybotryotoxicosis in central Europe. Dendrochiotoxicosis of horses in Europe is also presumed to be induced by these secondary metabolites, since the responsible fungus, *Dendrodochium toxicum,* is synonymous with *Myrothecium rodium,* which is able to produce a macrocyclic trichothecene.[3] The most controversial aspect of human exposure to trichothecene toxins has been the charge that they were used as chemical warfare agents in South Asia in the early 1980's, as part as the agent known as yellow rain.[1] Reports

---

[1] Desjardins, A. E.; Hohn, T. M.; McCormick, S. P. *Microb. Rev.* **1993**, *57*, 595.
[2] Joffe, A. Z. *Fusarium Species - Their Biology and Toxicology*; John Wiley & sons: New York, **1986**.

denouncing the use of "yellow rain" in Laos were obtained in 1975-76. Similar reports and evidence were received from Kampuchia (1978) and Afghanistan (1979). Scientists believed that the principal active compound of yellow rain was T2-toxin.[2] This hypothesis was later disputed[4] because it takes six to eight weeks of ingestion of food intoxicated with T2-toxin to kill, therefore this trichothecene alone may not be the agent responsible for the sudden death toxic syndrome associated with yellow rain.

The trichothecenes are a group of closely related sesquiterpenoid mycotoxins[5] produced by various species of fungus imperfecti.[6] The first compounds of this class were discovered at Imperial Chemical Industries in 1946 during an extensive search for new antibiotics. Historically, glutinosin was the first trichothecene isolated, but it was later shown to be a mixture of verrucarins A and B. The name trichothecene is derived from the first isolated and purified member of the class, trichothecin, from the fungus *Trichotecium roseum,* in 1948. Since that date, over 80 trichothecenes have been identified from nine genera of fungi: *Fusarium, Myrothecium, Trichothecium, Trichoderma, Cephalosporium, Cyclindrocarpen, Stachybotrys, Verticimonosporium* and *Calonectria.*[7]

---

[3] Ueno, Y. *Pure Appl. Chem.* **1977**, *49*, 1737.

[4] From a letter to *Science* by Rosen, J. D. *Science* **1983**, 222 (4622), p 698:"I firmly believe that is not possible to isolate *Fusarium* species of the sporotrichiella section from tropical regions (Laos and Cambodia) or Subtropical areas with warm climate (India or Israel) but only from cold temperature climate regions. Therefore I cannot agree with the notion that the trichothecenes isolated from yellow rain samples are associated with natural occurrences in Southeast Asia"

[5] Mycotoxins means: fungal toxins that affect animals.

[6] McDougal, P. G.; Schmuff, N. R. In *Progress in the Chemistry of Organic Natural Products*; Herz, W., Grisebach, H., Kirby, G. W., Eds.; Springer - Verlag: New York, **1985**; Vol. 47, p 153.

[7] Corley, D. G.; Rottinghaus, G. E.; Tracy, J. K.; Tempesta, M. S. *Tetrahedron Lett.* **1986**, *27*, 4133.

The *Fusarium* genus, which are isolated only from temperate regions, produces the most toxic trichothecene metabolites. The most toxic trichothecenes isolated to date are T2-toxin, HT2-toxin, neosolaniol, diacetoxy scirpenol, nivalenol, fusarion-x and deoxynivalenol.[2]

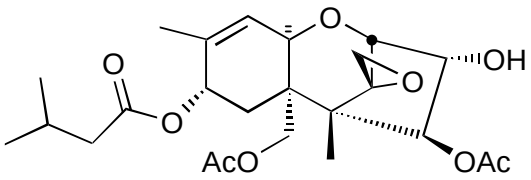

T2-toxin

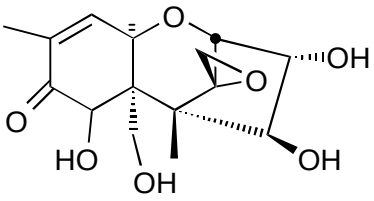

Nivalenol

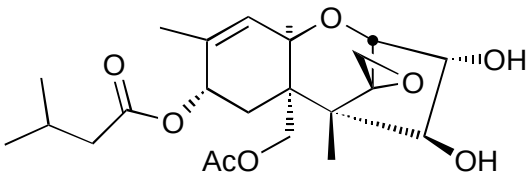

HT2-toxin

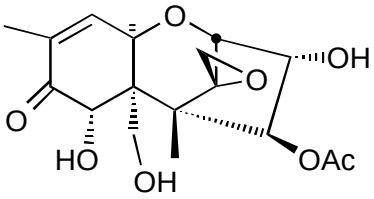

Fusarion-x

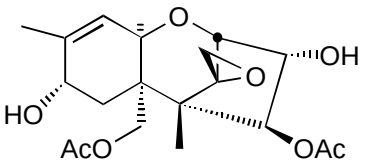

Neosolaniol

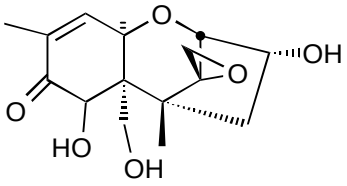

Deoxynivalenol

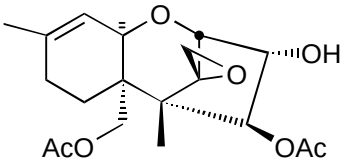

Diacetoxy scirpenol

The only known occurrence of these metabolites in higher plants is from an extract of the Brazilian shrub *Baccharis megapotamica,*[8] which exhibited *in vivo* antileukemic activity and led to the isolation of new macrocyclic trichothecenes, the "baccharins". These shrubs are resistant to trichothecenes and actually accumulate them on their seed

coats. It was originally suggested[9] that the baccharins are fungal metabolites absorbed from the soil and subsequently biotransformed by the plants. This hypothesis was refuted after further investigation as the baccharins were confirmed to originate from the plant.

2. Structure

The original structure proposed for the skeleton of the trichothecene molecules was derived from chemical reactivity studies in the laboratories of Freeman,[10] Tamm[11] and Fishman.[12] This structure was later revised[13] based on the x-ray analysis of a single crystal of the p-bromobenzoate derivative of trichodermol. The originally proposed structure was more closely related to the apotrichothecane skeleton obtained from the rearrangement of the trichothecenes.

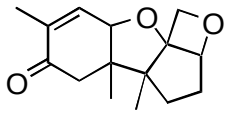

Proposed Structure

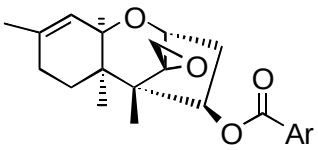

p-Bromobenzoate derivative of trichodermol (X-ray structure)

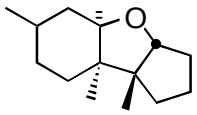

Apotrichothecane skeleton

[8] Jarvis, B. B.; Stahly, G. P.; Pavanasasivam, G.; Midiwo, J. O.; DeSilva, T.; Holmlund, C. E.; Mazolla, E. P.; Geoghegan Jr, R. F. *J. Org. Chem.* **1982**, *47*, 1117.

[9] Jarvis, B. B.; Stahly, G. P.; Pavanasasivam, G.; Mazzola, E. P. *J. Med. Chem.* **1980**, *23*, 1054.

[10] Freeman, G. G.; Gill, J. E.; Waring, W. S. *J. Chem. Soc.* **1959**, 1105.

[11] Harri, E.; Loeffler, W.; Sigg, H. P.; Stahelin, H.; Stoll, C.; Tamm, C. H.; Wiesinger, D. *Helv. Chim. Acta* **1962**, *45*, 839.

[12] Fishman, J.; Jones, E. R. H.; Lowe, G.; Whiting, M. C. *J. Chem. Soc.* **1960**, 3948.

[13] Jarvis, B. B.; Vrudhula, V. M.; Midiwo, J. O.; Mazzola, E. P. *J. Org. Chem.* **1983**, *48*, 2576.

To date, over 80 naturally occurring trichothecenes have been identified and can be classified into three distinct structural groups:[14] simple trichothecenes, macrocycle trichothecenes and the recently discovered trichoverroids. Their chemical structures vary in both the position and the number of hydroxylations as well as in the position and complexity of esterification.

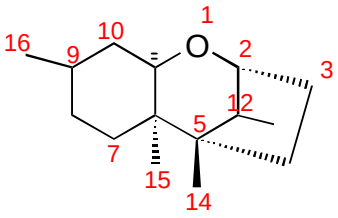

Trichothecane revised skeleton

The simple trichothecenes contain the basic mono- or polyhydroxylated sesquiterpene skeleton, with zero, one or more of the hydroxyl groups esterified. Examples include trichodermin, anguidine, T2- toxin, trichothecin and verrucarol.

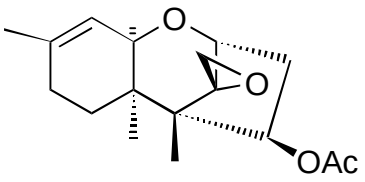

Trichodermin

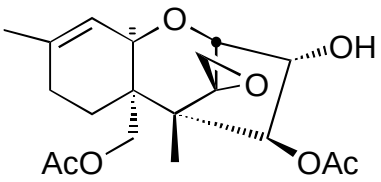

Anguidine

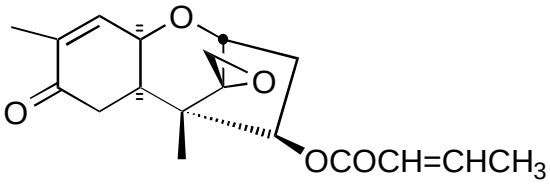

Trichothecin

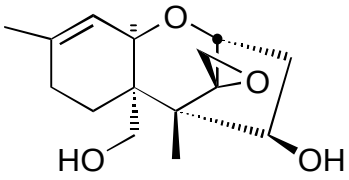

Verrucarol

[14]Corley, D. G.; Rottinghaus, G. E.; Tempesta, M. S. *Tetrahedron Lett.* **1986**, *27*, 427.

In the second structural group, the macrocyclic trichothecenes, a di- or tri-lactide ribbon bridges the hydroxy groups at C-4 and C-15. Verrucarol is most often the sesquiterpene onto which the macrocycle is attached. Examples in this class are: verrucarin-A, roridin-A, verrucarin K[15] and the baccharins (which were discussed earlier). Verrucarin K was the first trichothecene isolated that lacks the 12,13-epoxide unit.

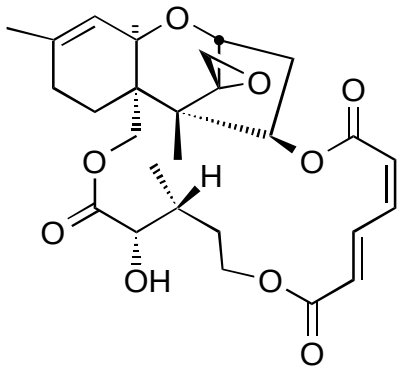

Verrucarin A

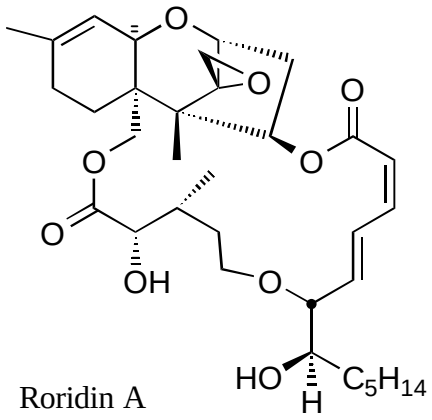

Roridin A

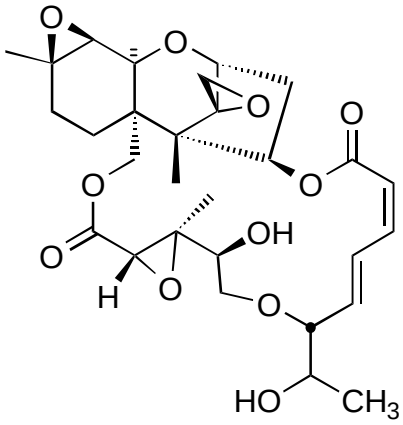

Baccharin B5(13'-R)

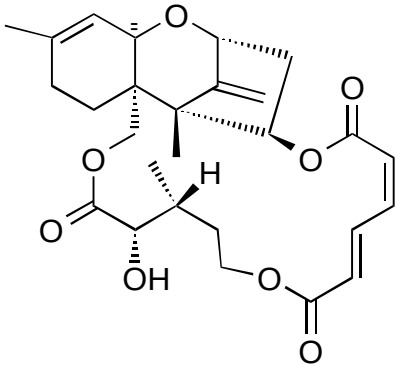

Verrucarin K

The last group of trichothecenes is the trichoverroids. These *seco* macrocyclic metabolites have either partial or complete carbon chains at C-4 and C-15 characteristic of

[15] Breitenstein, W.; Tamm, C. *Helv. Chim. Acta* **1977**, *60*, 1522.

the macrocyclic compounds but lack the requisite ring forming bonds. Other trichothecenes that cannot be classified into any of the above categories include Sambucoin and Sambucinol.[16]

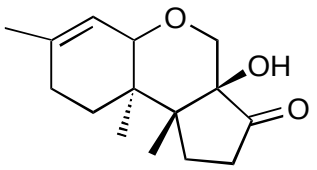

Sambucoin

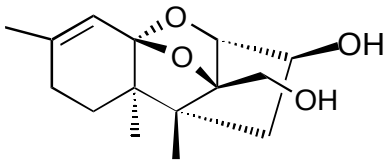

Sambucinol

3. Biological Activity

All animal species that have been tested appear to be sensitive to trichothecene toxins. A wide variety of biological activities have been ascribed to the Trichothecene mycotoxins.[17,18,19] These include alimentary toxic aleukia,[20] vomiting, weight loss, skin inflammation, anorexia, inflammation of the gastrointestinal tract, hypo-tension, anemia, diarrhea, ataxia, hematuria, leukopenia, lymphoid necrosis, immunosuppression, hemorrhage, emesis, degeneration of nerve cells in the central nervous system, degeneration and hemorrhaging of cardiac muscle, lymph nodes, testis and thymus, feed

---

[16] Mohr, P.; Tamm, C.; Zucher, W.; Zehnder, M. *Helv. Chim. Acta* **1984**, *67*, 406.

[17] Corley, D. G.; Rottinghaus, G. E.; Tempesta, M. S. *J. Org. Chem.* **1987**, *52*, 4405.

[18] Oltz, E. M.; Nakanishi, K.; Yagen, B.; Corley, D. G.; Rottinghaus, G. E.; Tempesta, M. S. *Tetrahedron* **1986**, *42*, 2615.

[19] Cole, R. J.; Cox, R. H. In *Handbook of Toxic Fungal Metabolites*; Academic Press: New York, **1981**; Vol. 5, p 152.

[20] Since the number of white blood cells of the patients decreased markedly, the diagnostic name ATA (alimentary toxic aleukia) was given to the disease.

refusal and death in humans and farm animals from ingestion of infected grains. There is evidence that they are teratogenic but not carcinogenic.[13]

An extensively studied and potentially important property of the trichothecenes is their cytostatic activity. In 1962, Harri[11] and coworkers found that verrucarin-A caused 50% inhibition of mouse tumor cell *P-815* growth at a concentration of 0.6 ng/mL, making it one of the most active cytostatic agents known. This activity is not limited to the macrocyclic trichothecenes, as anguidine has exhibited cytopathogenic effects against baby hamster kidney cells at a concentration of 1.5 ng/mL. In fact, the majority of the trichothecenes have been shown to possess *in vitro* cytotoxic activity. Anguidine has completed Phase II in clinical trials against colon and breast cancer conducted by the National Cancer Institute.

The trichothecene mycotoxins induce cellular damage characterized by karyorrhexis[21] and destruction of the actively dividing cells in the thymus, testis, intestines, spleen and others. These observations led scientists to believe that this type of mycotoxin interferes with the synthesis of biomolecules. Comparative toxicology with various kinds of trichothecenes has revealed that all the tested compounds inhibit protein[22] and DNA synthesis, in whole cell and in cell-free systems.[3, 23] No inhibitory effect was observed on bacterial replication. Inhibition[24] is believed to be caused by the binding of trichothecene

---

[21] Karyorrhexis means the destruction of the nucleus.

[22] Inhibition of protein synthesis in humans was verified in experiments using HeLa cells as well as cell-free systems. The cell-free system is more sensitive than the whole cell, therefore it is suggested that trichothecenes have some effect on cell membrane permeability.

[23] Ueno, Y.; Hosoya, M.; Ishikawa, Y. *J. Biochem. (Tokyo)* **1969**, *66*, 419.

[24] Welch, S. C.; Rao, A. S. C. P.; Gibbs, C. G.; Wong, R. Y. *J. Org. Chem.* **1980**, *45*, 4077.

to polysomes and ribosomes (80 S) from eukaryotic cells,[25] followed by inactivation of protein translation. The trichothecenes affect protein synthesis by interfering with the active site of peptidyl transferase on ribosomes[19] and consequently inhibit the initiation, elongation or termination steps of protein synthesis.

Trichothecenes have been shown to inhibit DNA synthesis in Ehrlich ascited tumor cells[3], but the mechanism of this inhibition is not known. No inhibitory effect on RNA transcription was observed.

The molecular basis of the biological activity for these compounds is still unclear. Ueno has presented evidence that the trichothecenes react with thiol residues at the peptidyl transferase active site in the ribosome. Grove[26] suggested that the 12,13-epoxide in the trichothecane framework might serve as the electrophylic site responsible for this reactivity.[27] Other structure-activity relationship studies demonstrated that the

---

[25] No detectable binding of the trichothecenes with the individual 30S or 50S sub-units of the ribosome was observed.

[26] Grove, J. F. *J. Chem. Soc. Perkin Trans. I* **1985**, 1731.

[27] This assumption is not completely supported since it is difficult to reconcile it with the established low reactivity of the 12,13-epoxide unit under non-acidic SN_2 conditions. Normally, the epoxide is protected from rear side nucleophilic attack by ring A and by rigid oxabicyclo[3.2.1]octane system rings B/C so the reactivity of these trichothecenes depends on the ease of generation of ionic centers which can participate *via* an intramolecular attack on the epoxide, this process is frequently accompanied by skeletal rearrangement.

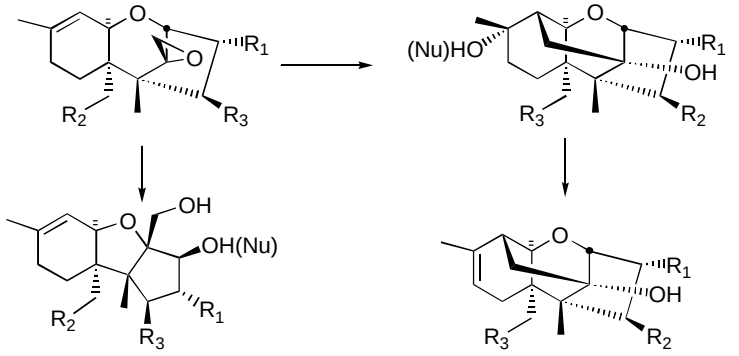

saponification of the esters as well as the hydrogenation of the 9-10 olefin leads to a decrease in toxicological activity.[3]

- *FS-2*

In 1987, Tempesta[17] isolated two new secondary metabolites from fermentation of *Fusarium sporotrichioides* (MC - 72083): FS-2 and trichotriol. FS-2 was isolated in 30 ppb (2 mg) from culture on corn medium at 10 ^{o}C, after incubation in the dark for 21 days. Its structure was elucidated with the aid of high-resolution mass spectroscopy, UV, ^{1}H-NMR (COSY and difference NOE experiments) and ^{13}C-NMR. Its absolute stereochemistry was assigned based on analogy with other trichothecenes.

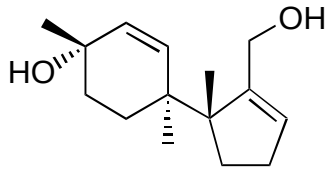

FS-2

FS-2 was tested for toxicity using the chicken-egg-yolk-sac inoculation bioassay and the results indicated an LD_{50} of 55 ng/egg, similar to T2-toxin embryotoxicity. This suggests that the tetrahydropyran ring (absent in this case) may play only a minor role for toxicity in most trichothecenes.

FS-2, and other closely related compounds recently isolated,[17, 28] represent important clues for the elucidation of the biosynthetic pathway of the trichothecenes and thus presents itself as an interesting target for synthetic organic chemists.

The structure of FS-2 is unusual among the trichothecenes because it lacks the oxygen bridge between C-2 and C-11 (trichothecene numbering, structure section of this chapter) that forms ring B. The absence of ring B increases the flexibility of the molecule and makes the task of controlling the stereochemistry of its substituents during synthesis more difficult, especially for the two adjacent quaternary centers at positions C-5 and C-6 (trichothecene numbering).

[28] Other natural products bearing similar structures include trichodiol, trichotriol and FS-4.

- *Previous synthetic approaches:*

1. General:

Extensive research has been conducted towards the synthesis of the trichothecene family of sesquiterpenes culminating in the total synthesis of trichodermin[29], 12,13-epoxytrichothec-9-ene,[30] verrucarol,[31] trichodermol,[32] calonectrin,[33] trichodiene,[34] anguidine[35] and sporol.[36]

The synthesis of trichothecenes was originally divided into four main synthetic approaches based on the final development of the tricyclic skeleton, according to

---

[29] Colvin, E. W.; Malchenko, S.; Raphael, R. A.; Roberts, J. S. *J. Chem. Soc. Perkin Trans. I* **1973**, 1989.

[30] (a) Fujimoto, Y.; Yokura, S.; Nakamura, T.; Morikawa, T.; Tatsuno, T. *Tetrahedron Lett.* **1974**, 2523; (b) Masuoka, N.; Kamikawa, T. *Tetrahedron Lett.* **1976**, 1691; (c) Masuoka, N.; Kanikawa, T.; Kubota, T. *Chem. Lett.* **1974**, 751; (d) Hua, D. H.; Venkataraman, S.; Chan-Yu-King, R.; Paukestelis, J. V . *J. Am. Chem. Soc.* **1988**, *110*, 4741; (e) Hua, D. H.; Venkataraman, S.; Coulter, M. J.; Sinai-Zingde, G. *J. Org. Chem.* **1987**, *52*, 719; (f) Pearson, A. J.; O'Brien, M. K. *J. Org. Chem.* **1989**, *54*, 4663.

[31] (a) Trost, B. M.; Rigby, J. H. *J. Org. Chem.* **1978**, *43*, 2938; (b) White, J. D.; Matsui, T.; Thomas, J. A. *J. Org. Chem.* **1981**, *46*, 3376; (c) Roush, W. R.; D'Ambra, T. E. *J. Am. Chem. Soc.* **1983**, *105*, 1058; (d) Trost, B. M.; McDougal, P. G.; Haller, K. J. *J. Am. Chem. Soc.* **1984**, *106*, 383; (e) Koreeda, M.; Ricca, D. J.; Luengo, J. I. *J. Org. Chem.* **1988**, *53*, 5586; (f) White, J. D.; Kim, N.-S.; Hill, D. E.; Thomas, J. A. *Synthesis - Stuttgard* **1998**, 619; (g) Ishihara, J.; Nonaka, R.; Terasawa, Y.; Shiraki, R.; Yabu, K.; Kataoka, H.; Ochiai, Y.; Tadano, K.-I. *Tetrahedron Lett.* **1998**, *38*, 8311; (h) Ishihara, J.; Nonaka, R.; Terasawa, Y.; Shiraki, R.; Yabu, K.; Kataoka, H.; Ochiai, Y.; Tadano, K. *J. Org. Chem.* **1998**, *63*, 2679.

[32] Still, W. C.; Tsai, M.-Y. *J. Am. Chem. Soc.* **1980**, *102*, 3654.

[33] Kraus, G. A.; Roth, B.; Frazier, K.; Shimagaki, M. *J. Am. Chem. Soc.* **1982**, *104*, 1116.

[34] (a) Suda, M. *Tetrahedron Lett.* **1982**, *23*, 427; (b) Schlessinger, R. H.; Schultz, J. A. *J. Org. Chem.* **1983**, *48*, 407; (c) Snowden, R. J.; Sonnay, P. *J. Org. Chem.* **1984**, *49*, 1464; (d) Harding, K. E.; Clement, K. S. *J. Org. Chem.* **1984**, *49*, 3870; (e) Gilbert, J. C.; Wiechman, B. E. *J. Org. Chem.* **1986**, *51*, 258; (f) Gilbert, J. C.; Kelly, T. A. *J. Org. Chem.* **1986**, *51*, 4485; (g) Van Middlesworth, F. L. *J. Org. Chem.* **1986**, *51*, 5019; (h) Kraus, G. A.; Thomas, P. J. *J. Org. Chem.* **1986**, *51*, 503; (i) Harding, K. E.; Clement, K. S.; Tseng, C.-Y. *J. Org. Chem.* **1990**, *55*, 4403; (j) Tanaka, M.; Sakai, K. *Tetrahedron Lett.* **1991**, *32*, 5581; (k) Gilbert, J. C.; Selliah, R. D. *J. Org. Chem.* **1993**, *58*, 6255; (l) Lemieux, R. M.; Meyers, A. I. *J. Am. Chem. Soc.* **1998**, *120*, 5453.

[35] (a) Brooks, D. W.; Grothaus, P. G.; Mazdiyasni, H. *J. Am. Chem. Soc.* **1983**, *105*, 4472; (b) Brooks, D. W.; Grothaus, P. G.; Palmer, J. T. *Tetrahedron Lett.* **1982**, *23*, 4187.

McDougal and Schmuff,[6] as shown in Figure 1.1. Two approaches involved formation of the C ring via an intramolecular aldol reaction (paths a and b). The other two involved the formation of the B ring in a similar manner to the model proposed for the biosynthesis of the trichothecene family (paths c and d) and are referred to as the biomimetic approach.

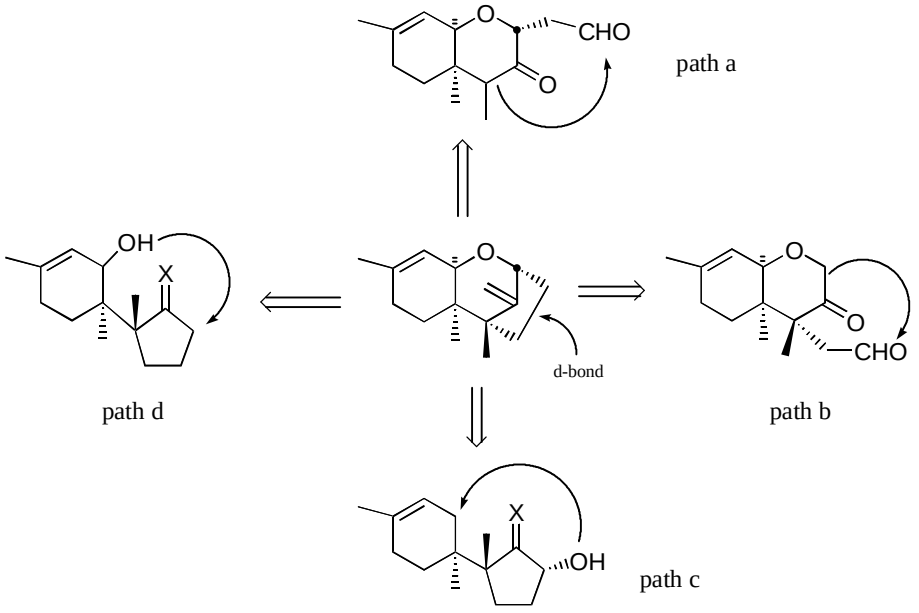

Figure 1.1

2. Aldol approach

The first trichothecene total synthesis was effected by Raphael[29,37] in 1973. He successfully prepared racemic trichodermin following the path-a aldol disconnection (see Figure 1.2).

---

[36] Ziegler, F. E.; Metcalf III, C. A.; Schulte, G. *Tetrahedron Lett.* **1992**, *33*, 3117.

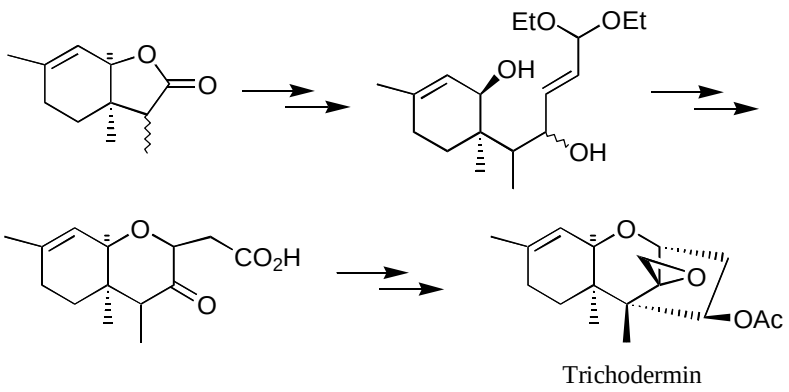

Trichodermin

Figure 1.2

The path-b aldol disconnection was employed successfully in the synthesis of calonectrin by Kraus,[33] T-2 tetraol by Colvin[38] and the preparation of 12,13-epoxytrichothec-9-ene by Fujimoto.[30a] Figure 1.3 illustrates the path-b aldol disconnection for Fujimoto's synthesis of 12,13-epoxytrichothec-9-ene.

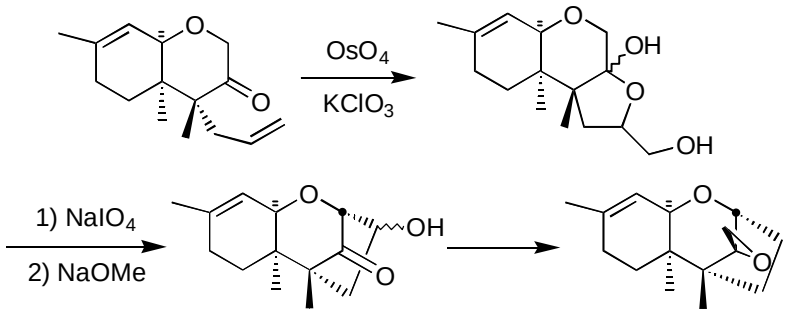

12,13-epoxy-
trichothec-9-ene

Figure 1.3

[37] Colvin, E. W.; Malchenko, S.; Raphael, A.; Roberts, J. S. *J. Chem. Soc. Perkin Trans. I* **1978**, 658.
[38] Colvin, E. W.; Egan, M. J.; Kerr, F. W. *J. Chem. Soc. Chem. Comm.* **1990**, 1200.

3. Biomimetic approach:

Many synthetic endeavors have followed the path-c biomimetic strategy, including Masuoka[30b-c] with the synthesis of 12,13-trichothec-9-ene, the application of chiral sulfoxides developed by Hua,[30d-e] the synthesis of enantiomerically pure anguidine by Brooks[35] and the preparation of an advanced intermediate towards the synthesis of anguidine by Ziegler.[39] Still[32] utilized the path-c biomimetic approach in his synthesis of trichodermol as shown in Figure 1.4. The synthesis starts with a Diels-Alder reaction followed by the Favorskii rearrangement and anionic fragmentation to prepare rings A and C and set the relative stereochemistry of the two quaternary centers.

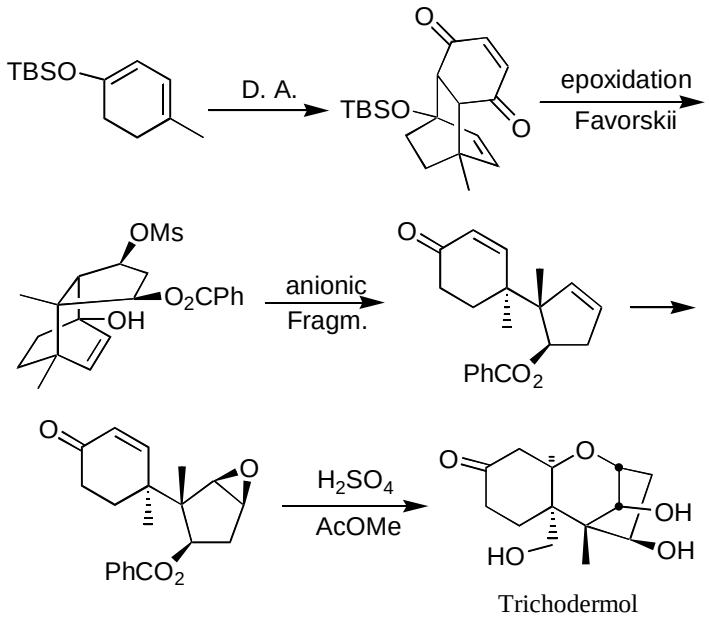

Figure 1.4

[39] Ziegler, F. E.; Sobolov, S. B. *J. Am. Chem. Soc.* **1990**, *112*, 2749.

The path-d biomimetic approach involves the attack of ring C by a nucleophilic oxygen substituent in ring A. This approach proved to be effective for Pearson's[30f,40] synthesis of trichodermol and Roush's[31c,41] synthesis of verrucarol. Anderson[42] was studying the entry to the trichothecene ring system while looking at compounds with an aromatic ring A and Nemoto[43] developed the aromatic ring A strategy further by elaborating the tricyclic skeletons into nivalenol-type compounds. Nemoto's approach (see Figure 1.5) was based on the elaboration of a ketone into a cyclobutanone and then an allylic cyclobutene that could undergo Palladium mediated regiocontrolled ring expansion to form ring C. A path-d biomimetic cyclization finalized the assembly of the skeleton.

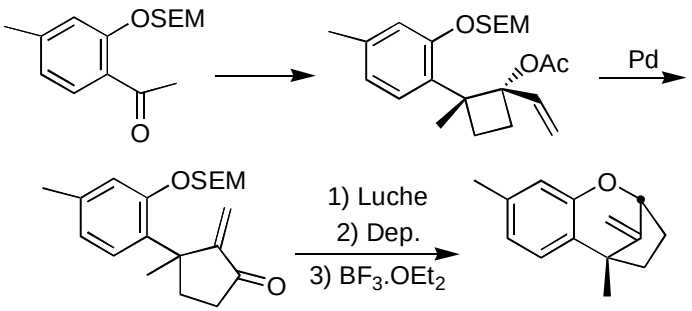

Figure 1.5

---

[40] (a) Pearson, A. J.; O'Brien, M. K. *J. Chem. Soc. Chem. Comm.* **1987**, 1445; (b) O'Brien, M. K.; Pearson, A. J.; Pinkerton, A. A.; Schimidt, W.; Willman, K. *J. Am. Chem. Soc.* **1989**, *111*, 1499.

[41] (a) Roush, W. R.; D'Ambra, T. E. *J. Org. Chem.* **1981**, *46*, 5045; (b) Roush, W. R.; D'Ambra, T. E. *J. Org. Chem.* **1980**, *45*, 3927.

[42] Anderson, W. K.; La Voie, E. J.; Lee, G. E. *J. Org. Chem.* **1977**, *42*, 1045.

[43] (a) Nemoto, H.; Miyata, J.; Fukumoto, K. *Heterocycles* **1997**, *44*, 125; (b) Nemoto, H.; Miyata, J.; Fukumoto, K. *Tetrahedron* **1996**, *52*, 10363; (c) Nemoto, H.; Miyata, J.; Fukumoto, K. *Heterocycles* **1996**, *42*, 165.

4. Other approaches:

Some synthetic approaches developed for the assembly of trichothecenes don't fall into any of the above disconnection categories. Fraser-Reid[44] developed a chiral synthetic entry into the tricyclic skeleton starting from D-glucose for preparation of the A/B ring system followed by formation of the C ring via the "d-bond" closure (see Figure 1.1). In the synthesis of neosporol[45] (see Figure 1.6), a Claisen rearrangement set the stereochemistry of the two quaternary centers. The placement of the double bonds in the A and C rings solved previous problems involving mixtures of E and Z olefin geometries that resulted in low selectivity. The methodology developed for the assembly of the trichothecene skeleton involved the epoxidation of the allylic alcohol followed by intramolecular ketal formation and inversion of the alcohol to prompt transketalization. This methodology was applied successfully again for the synthesis of Sporol.[36]

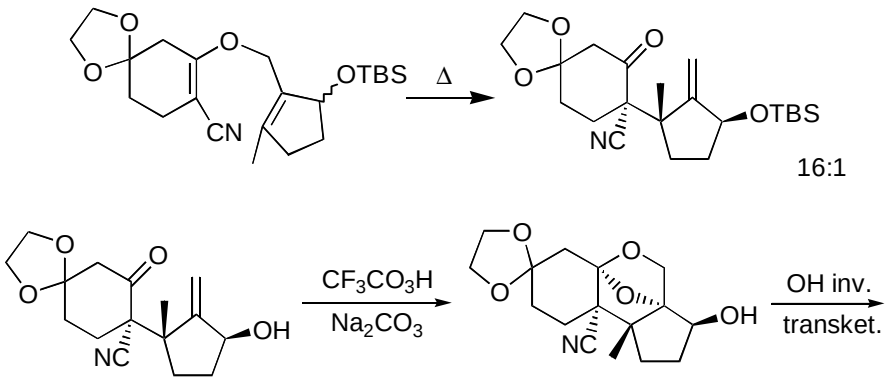

[44] Tsang, R.; Fraser-Reid, B. *J. Org. Chem.* **1985**, *50*, 4659.
[45] Ziegler, F. E.; Nangia, A.; Schulte, G. Tetrahedron *Lett.* **1988**, *29*, 1669.

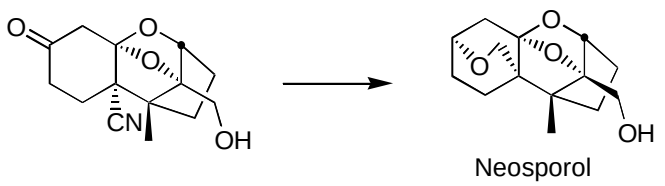

Figure 1.6

Trost[31d,46] accomplished the synthesis of verrucarol shown in Figure 1.7 by use of a tandem Diels-Alder-ene reaction to set the adjacent quaternary centers followed by a retro-ene and a ring expansion/fragmentation reaction to assemble the final skeleton.

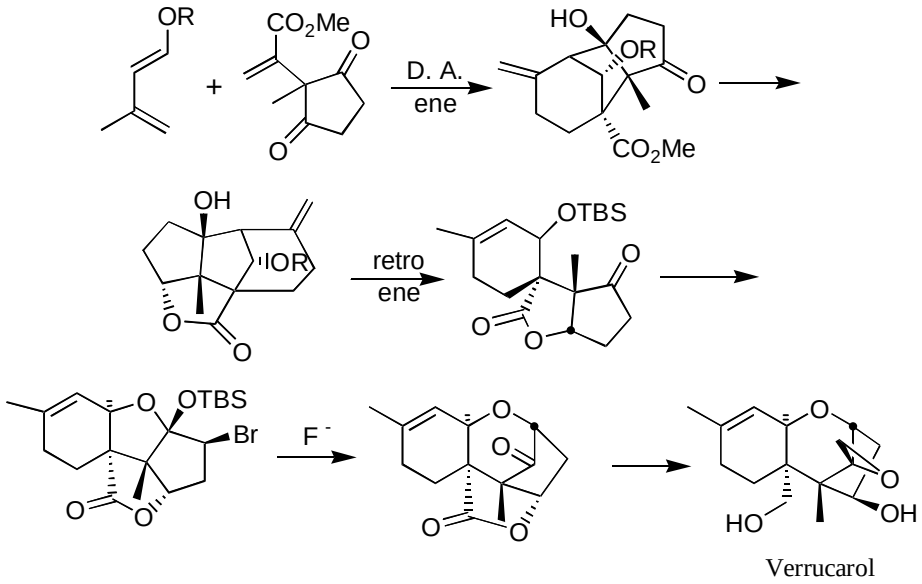

Figure 1.7

Assembly of Ring A via an intramolecular Diels-Alder reaction during flash chromatography in neutral alumina was the final bond connection employed by Koreeda[31e]

---

[46] Trost, B. M.; McDougal, P. G. *J. Am. Chem. Soc.* **1982**, *104*, 6110.

on his formal synthesis of verrucarol (see Figure 1.8). This synthesis merges with Trost's lactone advanced intermediate shown in Figure 1.7.

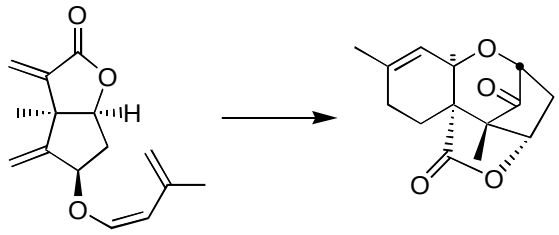

Figure 1.8

White's approach[31b,f,47] for the formal synthesis of Verrucarol took advantage of the Cargill rearrangement (see Figure 1.9). The strategy involved formation of the A/B ring system via a Diels-Alder reaction and introduction of the C ring in the form of a cyclobutene via photochemical reaction with acetylene. Acid catalyzed ring expansion proceeded via cyclobutene fragmentation to give a 6-5-5 tricyclic skeleton. Palladium catalyzed skeleton rearrangement assembled the trichothecene skeleton. The final product is the same lactone previously prepared by Trost[31d] in his synthesis of Verrucarol (Figure 1.7).

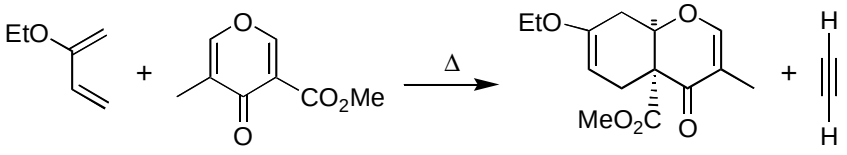

[47] Fetizon, M.; Khac, D. D.; Tho, N. D. *Tetrahedron Lett.* **1986**, *26*, 1777.

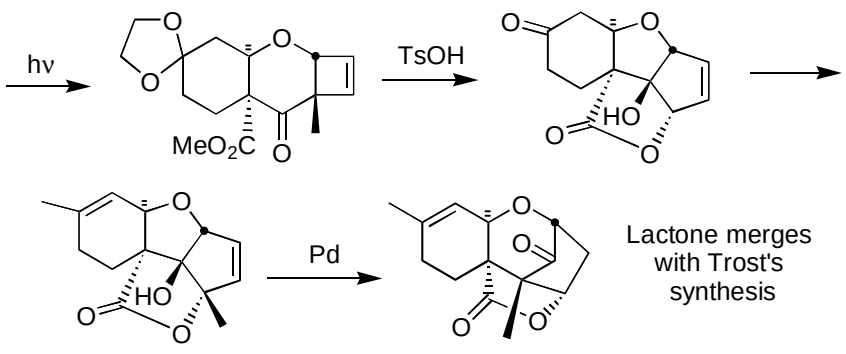

Figure 1.9

Ishihara[31g-h,48] was responsible for the first preparation of Verrucarol in optically active form (Figure 1.10). Starting from D-glucose, elaboration of ring A took advantage of Trost's recognition that the *cis* stereochemistry between rings A and B could be better controlled *via* the formation of a 6-5 ring system. Stereoselective quaternization α to the carbonyl of the lactone took advantage of the stereochemistry bias of the bicyclic molecule. Elaboration of ring C followed via a Dieckmann cyclization, Barton-Crich decarboxylative oxygenation and ring expansion (also developed by Trost, see Figure 1.7).

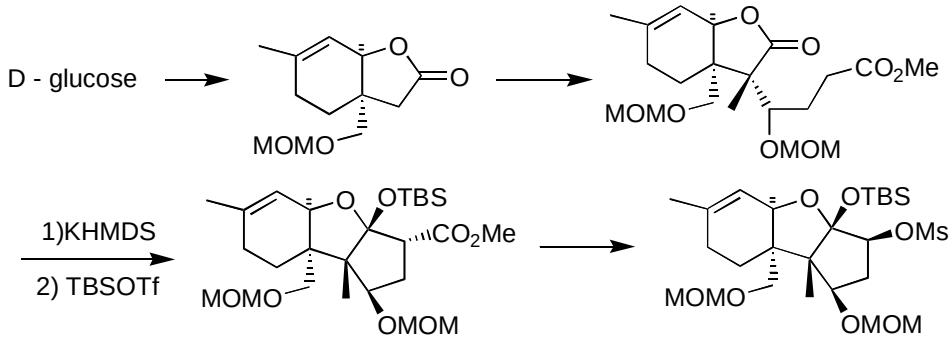

[48] Ishihara, J.; Nonaka, R.; Terasawa, Y.; Tadano, K.-i.; Ogawa, S. *Tetrahedron Assym.* **1994**, *5*, 2217.

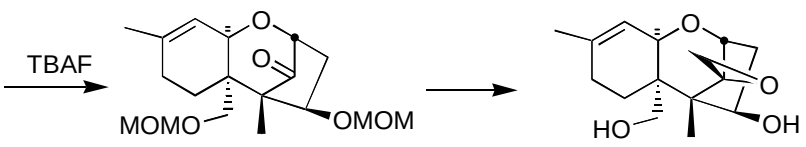

Verrucarol

Figure 1.10

5. Optically active synthesis

Other optically active synthesis of trichothecenes were the synthesis of 12,13-epoxytrichothec-9-ene employing chiral sulfoxides by Hua,[30d-e] an approach towards the synthesis of Anguidine by Enholm[49] starting from the readily available L-(+)-arabinose. Two independent chiral syntheses of trichodiene were accomplished. One by Gilbert,[50] taking advantage of Bakers' yeast reduction of a ketone in 45% ee, and one by Meyers[34l] (see Figure 1.11). Meyers used a chiral auxiliary derived from an amino acid to set the two quaternary centers in trichodiene via a thio-Claisen rearrangement.

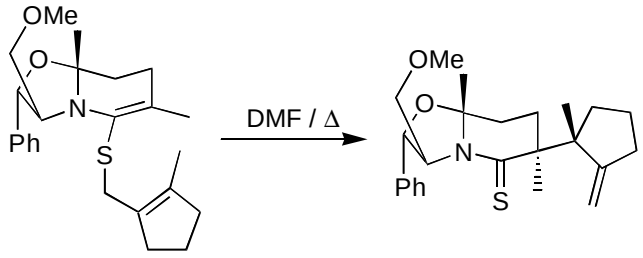

Figure 1.11

[49] Enholm, E. J.; Satici, H.; Trivellas, A. *J. Org. Chem.* **1989**, *54*, 5841.
[50] Gilbert, J. C.; Kelly, T. A. *Tetrahedron Lett.* **1989**, *30*, 4193.

6. Quaternary centers:

A series of syntheses of trichodiene addressed the issue of construction of the two adjacent quaternary centers. These include the use of the Nazarov[34d,i] reaction to introduce the stereochemistry in an electrocyclic fashion. A series of Claisen[51] approaches including the ester enolate Ireland-Claisen[52] adaptation was investigated in detail. The low selectivity of this rearrangement was attributed to the lack of selectivity of E/Z geometry at the double bonds. This problem was solved by incorporating the olefins into rings for the Claisen reaction to achieve selectivity as high as 16:1.[45] Another solution was found by use of chelate controlled Ireland ester enolate Claisen to get as high as 92:8 selectivity, such as Gilbert's synthesis of optically active (-) trichodiene in 1993 (see Figure 1.12).

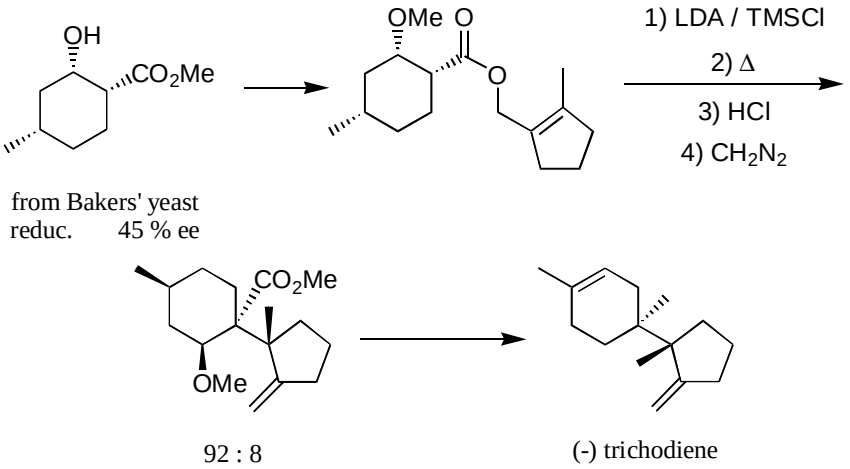

Figure 1.12

---

[51] Ziegler, F. E.; Nangia, A.; Schulte, G. *J. Am. Chem. Soc.* **1987**, *109*, 3987; also see references 34a, 34e, 36 and 48.

[52] (a) Gilbert, J. C.; Selliah, R. D. *Tetrahedron Lett.* **1992**, *33*, 6259; (b) Gilbert, J. C.; Selliah, R. D. *Tetrahedron* **1994**, *50*, 1651; also see references 34f,g,h,k, and ref. 55.

An organometallic reaction involving tin enolates coupling to cyclohexadienyl iron complexes[40] posed as a potential convergent entry to the system as was shown by Pearson in his syntheses of trichodiene[40b] (see Figure 1.13) and trichodermol.[40c]

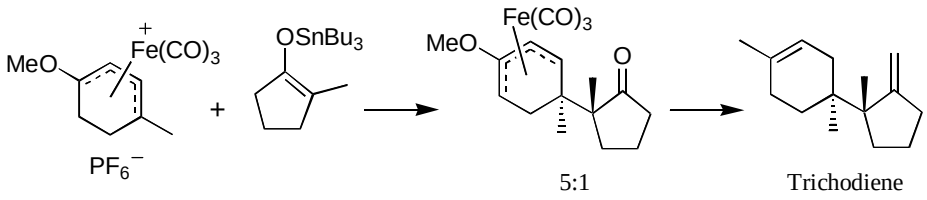

Figure 1.13

The application of a Prins reaction[39] to establish the relative stereochemistry between the two adjacent quaternary centers was showcased in an attempt to prepare anguidine (see Figure 1.14).

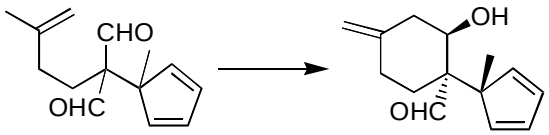

Figure 1.14

A [2+2] intermolecular photoaddition[53] was attempted without much success resulting in a mixture of regioisomers at about 1:1 ratio. A thio-Claisen rearrangement,[34l] aided by a chiral auxiliary, prepared the optically active bond connection. A novel ring transformation involving aldol acetylation and Grob fragmentation was developed by

Tanaka[34js] in a synthesis of trichodiene starting from a prostaglandin type intermediate and is illustrated in Figure 1.15.

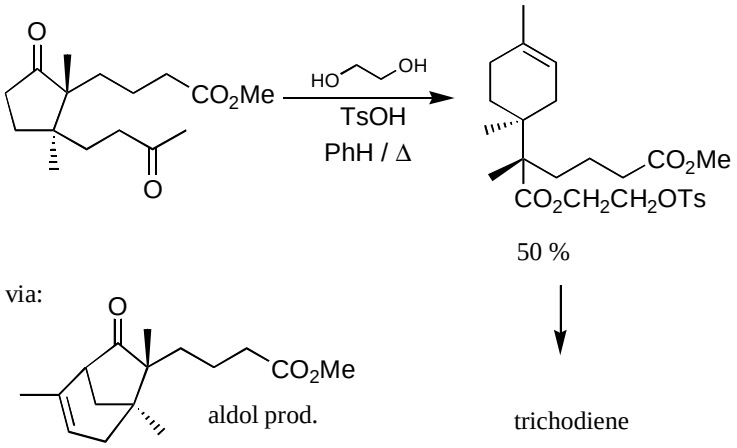

Figure 1.15

For other isolated solutions, an extensive review in the subject has been written by Martin[54] and should be consulted.

7. Interconversion of trichothecenes:

Some attention has been focused on developing the more complicated trichothecenes from readily available intermediates deriving from natural products, such as anguidine and verrucarol. Anguidine can be obtained in 250 to 300 mg/mL from aerated

---

[53] (a) Yamakawa, K.; Sakaguchi, R.; Nakamura, T.; Watanabe, K. *Chem. Lett.* **1976**, 991; (b) Yamakawa, K.; Kurita, J.; Sakaguchi, R. *Tetrahedron Lett.* **1973**, 3877.

[54] Martin, S. F. *Tetrahedron* **1980**, *36*, 419.

culture of *fusarium* fungi in pure crystalline form.[55] It has been used as the starting material for the interconversion of trichothecenes because C-15 and C-4 hydroxyl groups are protected as acetate groups while the C-3 is a free hydroxyl. This approach has been the focus of the research of Tamm,[56] Colvin[57] and Wani[58] and has resulted in the synthesis of Verrucarin A, Calonectrin, HT-2 toxin, Neosolaniol, T-2 toxin, Sporotrichiol, Deoxynivalenol (Vomitoxin), Verrucinol and Verrucene. One asymmetrical synthesis of the dilactide ribbon involved in the macrocyclic trichothecenes was reported by Tamm[59] and it involved a Sharpless epoxidation as the source of asymmetry.

- *Retrosynthetic analysis:*

The synthesis of FS-2 was envisioned to start by construction of a rigid structure with well-defined concave and convex faces followed by introduction of the necessary functionality *via* face selective reactions. The desired trichothecene skeleton would be unraveled at the end, with the application of a radical fragmentation methodology under investigation in our laboratory. This methodology offered the possibility of control of the regiochemistry of the fragmentation of a six-membered cyclic thionocarbonate ring fused to a five-membered ring by manipulation of the relative stereochemistry at the ring

---

[55] Brian, P. W.; Dawkwns, A. W.; Grove, J. F.; Hemming, A. G.; Lowe, D. *J. Exp. Bot.* **1961**, *12*, 1.

[56] (a) Mohr, P.; Tori, M.; Grossen, P.; Herold, P.; Tamm, C. *Helv. Chim. Acta* **1982**, *65*, 1412; (b) Jeker, N.; Mohr, P.; Tamm, C. *Tetrahedron Lett.* **1984**, *25*, 5637; (c) Jeker, N.; Tamm, C. *Helv. Chim. Acta* **1988**, *71*, 1904; (d) Jerker, N.; Tamm, C. *Helv. Chim. Acta* **1988**, *71*, 1895.

[57] (a) Colvin, E. W.; Cameron, S. *J. Chem. Soc. Chem. Comm.* **1986**, 1642; (b) Colvin, E. W.; Cameron, S. *Tetrahedron Lett.* **1988**, *29*, 493; (c) Cameron, S.; Colvin, E. W. *J. Chem. Soc. Perkin Trans. I* **1989**, 887.

[58] Wani, M. C.; Rector, H.; Cook, C. E. *J. Org. Chem.* **1987**, *52*, 3468.

junction. The radical methodology tolerates a wide array of functionality in the molecule at the time of the fragmentation and offers an entry to the synthesis of trichothecenes of the FS-2 type skeleton and to the normal trichothecene skeleton, making this a general approach to the family.

The radical fragmentation *per se* will be discussed in more detail in chapter three, along with the discussion of results obtained during the study of the fragmentation of some model systems. The transformation proposed is depicted in the scheme below.

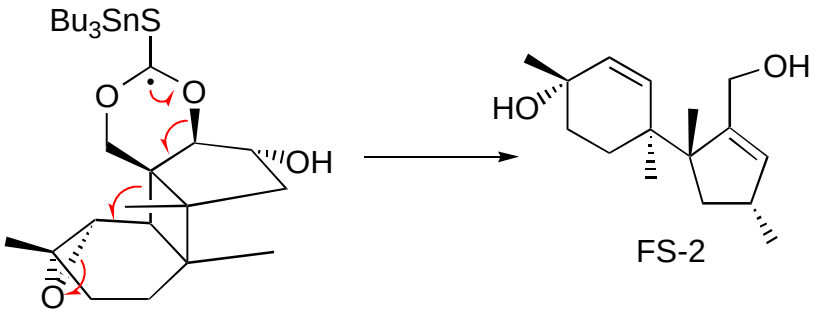

The radical fragmentation methodology required the preparation of cyclic thionocarbonate **1** (see Figure 1.16). Preparation of this intermediate could be derived from the epoxidation of the parent olefin and selective cyclization of the 1,3 diol. This strategy assumes that reaction with the primary alcohol would be faster than reaction with the secondary alcohol and that formation of the six-membered ring would be favored over the seven-membered ring alternative. Intermediate **2** was the logical precursor and could be prepared from ketone **3** by stereoselective introduction of a hydroxyl at C-3 (trichothecene numbering) followed by reduction of the ketone and the allylic ether.

---

[59] Herold, P.; Mohr, P.; Tamm, C. *Helv. Chim. Acta* **1983**, *66*, 744.

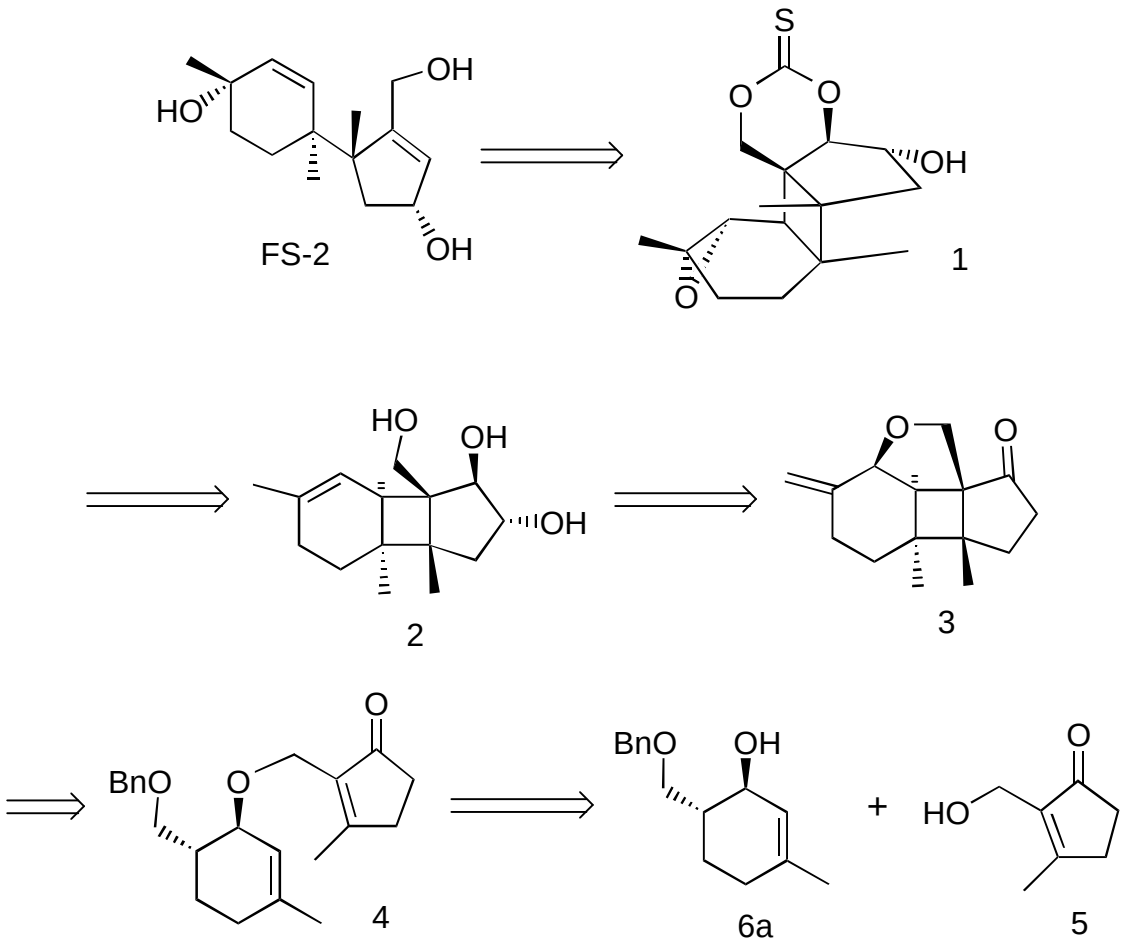

Figure 1.16 : Retrosynthetic Analysis

Preparation of the cyclobutane and control of the stereochemistry of the two emerging quaternary centers in ketone **3** could be accomplished through the photoaddition of substrate **4** or an analog. Synthesis of the requisite five- and six-membered ring precursors could be achieved from commercially available material.

- *Revised Structure:*

In 1993, Gilbert[60] published a proposed revision for the structure of FS-2 in which the hydroxyl at C-9 was reassigned as 9-β hydroxy (R) contrary to the original configuration assignment of 9-α (S).[17] This change was a result of research conducted on two molecules, trichodiol and trichotriol, which are structurally related to FS-2.

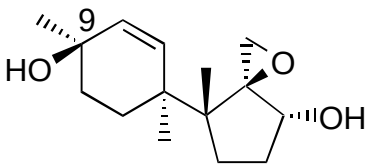

Trichodiol

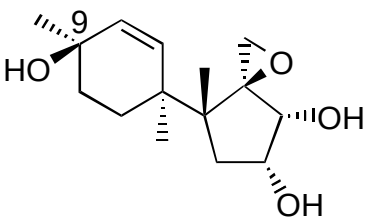

Trichotriol

Gilbert's assignments for the stereochemistry of trichodiol and its triol partner were confirmed by through-bond NMR, ^{1}H-^{1}H COSY and ^{1}H-^{13}C COSY. The reassignment of the stereochemistry of FS-2 and other naturally occurring products is based solely on the comparative analysis of Gilbert's ^{13}C NMR of trichodiol and trichotriol, which were recorded in $CDCl_3$, and the previously published values[17] of the chemical shifts for FS-2, which were recorded in acetone-d_6. In Gilbert's examples, C-9 bearing an α-OH is consistently at 69 ppm, and the β-OH counterpart appears between 65 and 66 ppm. It should be noted that the reassignment of FS-2 is based on this comparison of the 3-4 ppm difference in the ^{13}C NMR chemical shift data for C-9, collected in two different solvents, in different laboratories.

Computational conformation studies, using Monte Carlo simulations,[61] of both the originally reported configuration (Tempesta) and the reassigned structure (Gilbert) were carried out in order to clarify the structure of FS-2 by comparing the low energy structures for both molecules against the available NMR data. The details of the experiment and the explicit results are presented in Addendum III. The Tempesta configuration can adopt six distinct conformations within 4 Kcal/mol and the Gilbert configuration offers the possibility for a total of nine different conformations within 4 Kcal/mol. The large number of possible conformations within a narrow range of energy for each configuration makes it difficult to choose one conformation based on thermodynamics alone.

The fifteen conformations generated by the Monte Carlo simulations were analyzed against the difference NOE and COSY results reported by Tempesta.[17] The magnitude of the NOEs were not reported in the original paper, which suggested that only strong NOEs (within 3Å) were considered. Because the different conformations are very close in energy, one possibility was that the NOE and coupling constants observed actually represent a fast exchange time averaged structure in solution. That possibility is not likely since the coupling constants reported reflect specific angles encountered in some of the conformations and not an intermediate value.

Analysis of the differential NOE results reported against the calculated structures for the Tempesta and the Gilbert series suggests that conformation #3 of the Tempesta

---

[60] Hesketh, A. R.; Gledhill, L.; Bycroft, B. W.; Dewick, P. M.; Gilbert, J. *Phytochemistry* **1993**, *32*, 93 - 104.

[61] See Addendum III for details on the Monte Carlo simulations.

series is the one that best fits the data, presenting no NOE violations and satisfying the available coupling constant data. Shown below is a 3-dimensional view of Tempesta's conformation #3 with the NOEs reported in Tempesta's paper marked in red. Following that, conformation #1 of the Gilbert configuration is also shown with the same NOEs drawn for comparison.

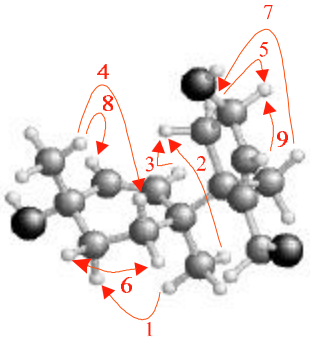

FS-2
Tempesta

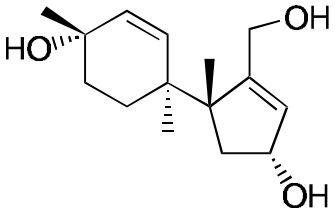

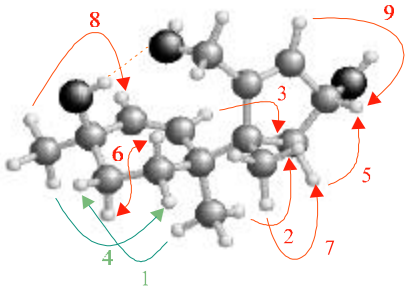

FS-2
Gilbert

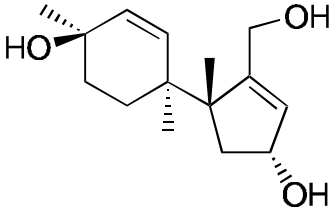

NOE #	Tempesta (Å)	Gilbert (Å)
1	2.142	3.755
2	2.220	2.239
3	2.246	2.174
4	2.375	4.842
5	2.475	2.461
6	2.481	3.072
7	2.577	2.556
8	2.691	2.562
9	2.744	2.733

The NMR data, along with the Monte Carlo simulations results support the structure assignment published by Tempesta, but this is still not conclusive data to assign the relative stereochemistry of FS-2. The decision to proceed with the original plan of synthesizing the α-hydroxy FS-2 (9-S configuration, Tempesta's original proposal) now had the added intention of establishing the stereochemistry of the hydroxyl at position C-9 for the natural product.

CHAPTER II: *SYNTHESIS OF THE TRICYCLO-UNDECANE COMMOM INTERMEDIATE*

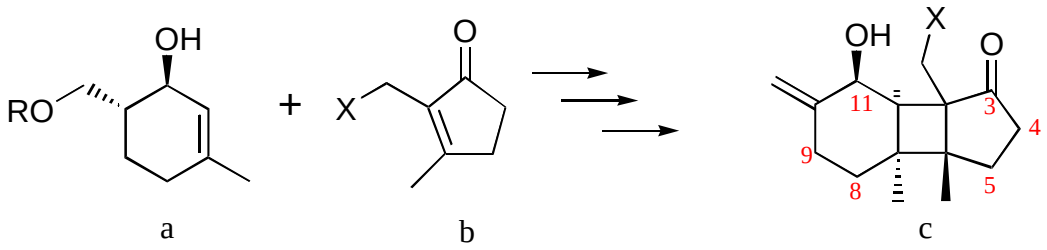

Figure 2.1

The synthesis of FS-2 required some way to control the many stereocenters present in the molecule, particularly the two adjacent quaternary centers at C-6 and C-7 (C-5 and C-6 in the trichothecene numbering system). The synthesis of a rigid intermediate with a well-defined geometry to enable face selectivity was envisioned to circumvent the need to introduce functionality in a stereoselective manner on a flexible molecule. This rigid intermediate could then be unraveled into FS-2 in the final step of the synthesis *via* a radical fragmentation. A tricycle [5.4.0.$0^{2,6}$] undecane skeleton (**c**) was designed as a precursor for simple model systems that could test the fragmentation theory and as an entry for the more advanced fragmentation intermediate needed for the synthesis of FS-2. This tricycle undecane skeleton required functionalization on its 2- and 3-positions for introduction of the cyclic thionocarbonate and a handle for introduction of a double bond at C-10 for later functional group elaboration. This common intermediate (**c**) was envisioned to arise in a convergent fashion from a [2+2] photo-addition reaction

between a five- and a six-membered ring intermediates (**a** and **b**) which would set the relative stereochemistry of the two adjacent quaternary centers upon formation of the four-membered ring.

- *Synthesis of the five and six-membered ring precursors*

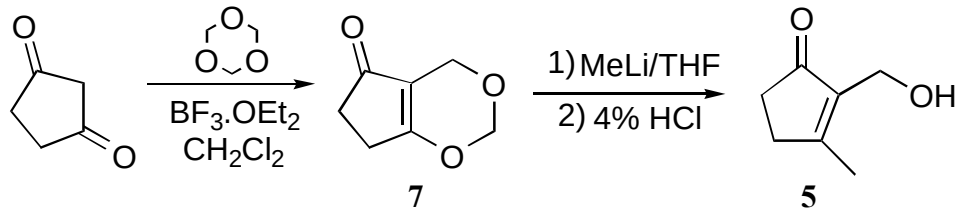

7 **5**

The five- and the six-membered ring intermediates (**a** and **b**) were synthesized independently. The five-membered ring component, an α-hydroxymethyl cyclopentenone, was prepared following Smith's procedure[62] with only minor modifications.[63] Applying an acid catalyzed aldol reaction,[64] commercially available 1,3 cyclopentadione was treated with 1,3,5-trioxane in the presence of $BF_3.OEt_2$ (3 eq.) to give the 1,3-dioxin-vinylogous-ester **7** in 96% yield. It should be noted that an excess of $BF_3.OEt_2$ (3 eq.) was used in the reaction, rather then a catalytic amount (0.33 eq.), to minimize the formation of propellane side products.[62]

---

[62] Methodology developed by Bolte, M. L.; Crow, W. D.; Yoshida, S. *Aust. J. Chem.* **1982**, *35*, 1411. Amos Smith prepared compound **1** by the same procedure in Smith, A.; Dorsey, B. D.; Ohba, M.; Lupo-Jr., A. T.; Malamas, M. S. *J. Org. Chem.* **1988**, *53*, 4315.

[63] Smith used trioxane according to his table of results, but in the experimental there are reports only on the use of paraformaldehyde.

[64] A similar reaction on an enol system was previously investigated by Williams, P. H.; Ecke, G. G.; Ballard, S. A. *J. Am. Chem. Soc.* **1950**, *72*, 5738.

Addition of methyllithium or, in some experiments, a methyl Grignard reagent[65] to enone **7** (THF, -78° C, 90 min), followed by carbonyl transposition via acid hydrolysis of the intermediate (4% HCl, 0° C, 3.5 hrs) gave the desired allylic alcohol **5** in 79% yield. Derivatives of alcohol **5** could be easily prepared to activate the molecule towards nucleophilic substitution, as will be shown later for the ether coupling.

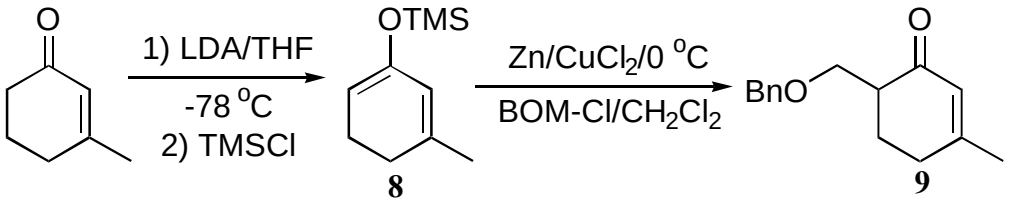

8 **9**

The six-membered ring moiety was prepared by alkylation of commercially available 3-methyl-2-cyclohexen-1-one. Initially the alkylation was attempted directly on the enolate in a basic medium, but the desired product **9** was not stable under alkaline conditions, giving mostly elimination side products.[65] To resolve the problem of product stability, an alternative approach to the alkylation was pursued using acidic conditions. A two step procedure in the presence of a Lewis acid was studied. The enone was first converted into its TMS enol ether **8** by kinetically controlled deprotonation of the ketone with LDA and trapping of the resulting lithium enolate with chlorotrimethylsilane (-78° C, THF, 40 min) in 98% yield according to the procedure of Rubottom[66] and Ainsworth.[67]

---

[65] Brown E. and Nylund C. S. Progress Reports, **1979**, in this laboratory.
[66] Rubottom, G. M.; Gruber, J. M. *J. Org. Chem.* **1978**, *43*, 1599.
[67] Ainsworth, C.; Chen, F.; Kuo, Y. N. *J. Organomet. Chem.* **1972**, *46*, 59.

Alkylation of the known[68] enol-silyl ether **8** with BOM-Cl[69] was tried in the presence of several different Lewis acid systems ($TiCl_4$,[70] $BF_3.OEt_2$, TMSI,[71] TMSOTf,[72] $ZnBr_2$[73] and activated Zn[74]) in an attempt to optimize the yield of **9** and minimize the formation of undesired products. Titanium tetrachloride and $BF_3.OEt_2$ degraded the starting material (**8)** and no product (**9)** was obtained. When TMSI was used, product **9** could be isolated in 50-72% yield, but the reaction was not consistently reproducible. According to Noyori's procedure,[73] a solution of formaldehyde dibenzylacetal, enol-silyl ether **8** and 2,6-di-*tert*-butylpyridine was treated with 15-mol % of TMSOTf at 10^o C. Very little conversion was observed as evidenced by recovery of 81% of the starting material, 3-methyl-2-cyclohexen-1-one. The ketone was recovered due to hydrolysis of unreacted TMS-enolether **8** during purification of the products. The alkylation of the TMS-enol ether did not go to completion even after the reaction was conducted for 4 days, and more formaldehyde dibenzylacetal was added; instead, side products started to form.

The best results for alkylation were obtained using zinc bromide[73] (BOM-Cl, CH_2Cl_2, 0^o C, 3 hrs) in small-scale reactions (< 500 mg) which afforded **9** in 49% yield. When the procedure was tried on a larger scale poor yields (12-15 %) were obtained. It is

---

[68] Iwata, C.; Takemoto, Y.; Nakamura, A.; Imanishi, T. *Tetrahedron Lett.* **1985**, *26*, 3227 reported the first preparation of this compound, in a table of results, but no characterization data was reported.

[69] An alternative where BOM-I was used instead of the chloride was reported with great success by Kucera, D. J.; O'Connor, S. J.; Overman, L. E. *J. Org. Chem.* **1993**, *58*, 5304 and also by Ditrich, K.; Reinhard, W.; Hoffman, R. W. *Liebigs Ann. Chem.* **1990**, 15.

[70] Mukaiyama, T.; Banno, K.; Narasaka, K. *J. Am. Chem. Soc.* **1974**, *96*, 7503.

[71] Sakurai; Hosomi *Chem Lett.* **1983**, 405.

[72] Murata, S.; Suzuki, M.; Noyori, R. *Tetrahedron Lett.* **1980**, 2527.

[73] Paterson, I.; Fleming, I. *Tetrahedron Lett.* **1979**, *20*, 2179.

important to note that one must sublime the catalyst (flame, under vacuum) just prior to use because any HBr present in the system is enough to compromise the reaction. Another solution was sought for situations when large-scale versions of the reaction were needed. Activated zinc,[74] in the form of Simmon-Smith's catalyst (Zn, CuCl, CH_2I_2, BOM-Cl, CH_2Cl_2, 0^o C, 10 hrs) was used with success, giving 58% yield on large scale reactions up to 24 g.

Contrary to previous reports,[65] compound **9** was stable after purification. Compound **9** degrades rapidly under the reaction conditions; therefore, it requires immediate purification via flash chromatography using 1 % diethyl ether in methylene chloride as the eluent. Product **9** was found to be particularly prone to degradation when zinc bromide was used as the catalyst.

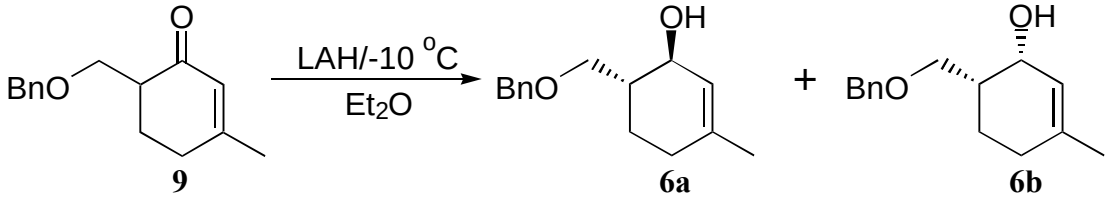

9 **6a** **6b**

Reduction of compound **9** was accomplished with good selectivity using lithium aluminum hydride as the reducing agent (Et_2O, -10^o C, 3 hrs). A mixture of *cis* and *trans* alcohols was obtained in 85% yield. The ^{1}H NMR integration ratios of the crude reaction mixture indicated a 7:1 distribution in favor of the desired *trans* product **6a** (threo). The

[74] Shono, T.; Nishigushi, I.; Komaniura, T.; Sasaki, M. *J. Am. Chem. Soc.* **1979**, *101*, 984.

two isomers **6a** and **6b** could be separated by flash chromatography using 5 % diethyl ether, 1 % benzene in methylene chloride as the eluent.

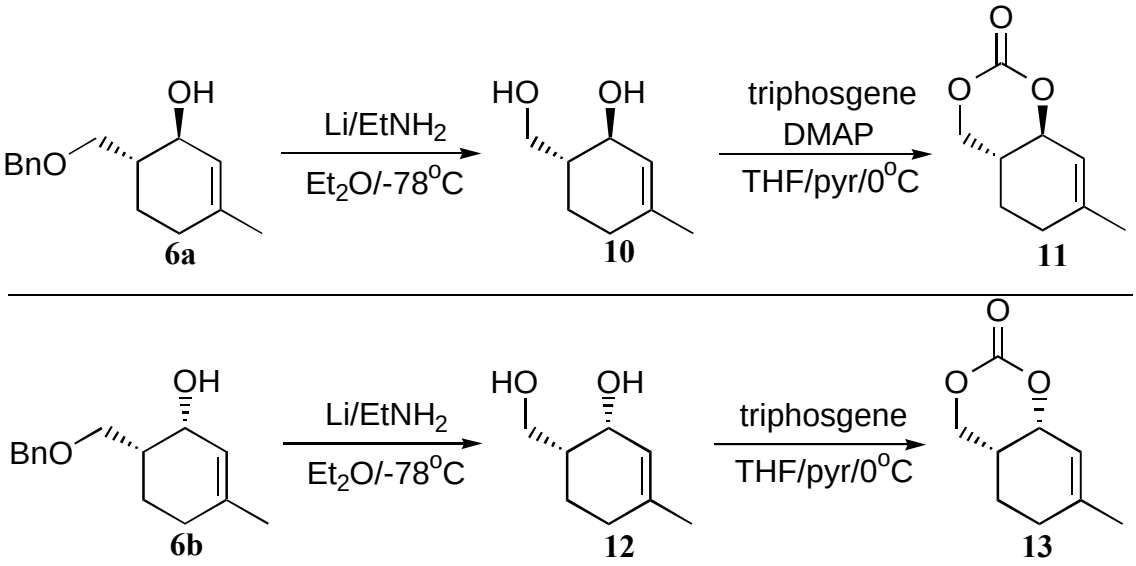

The relative stereochemistry of the two alcohols was tentatively assigned based on their ^{3}J coupling constants (*trans* 8.4 Hz and *cis* 4.0 Hz) of protons attached to C-1 and C-6 in the ^{1}H NMR. These stereochemical assignments of **6a** and **6b** were further supported by converting each product to its corresponding cyclic carbonate, where the coupling constants could be used for assignment in a more confident fashion once the two systems were locked in a rigid geometry. The conversion of the two alcohols **6a** and **6b** to the cyclic carbonates **11** and **13** was done independently by first deprotection of the benzyl protecting group with Li/$EtNH_2$ (Et_2O/ -78^{o} C) to give the respective diols, *trans* (**10)** in 97% yield and *cis* (**12)** in 90% yield. These diols were in turn converted to the corresponding cyclic carbonates by treatment with triphosgene. The best conditions for this transformation were 4-dimethylaminopyridine, pyridine, THF, 0^{o} C, 7 hrs for the *trans* system **11** (93% yield) and pyridine, THF, 0^{o} C, 7 hrs for the *cis* system **13** (89% yield).

The reaction gave very poor yields for the *cis* product (**13**) when 4-DMAP was used. When ^{3}J coupling constants of the protons attached to C-1 and C-6 were examined they were found to be 9.5 Hz for compound **11** and 4.3 Hz for compound **13**.

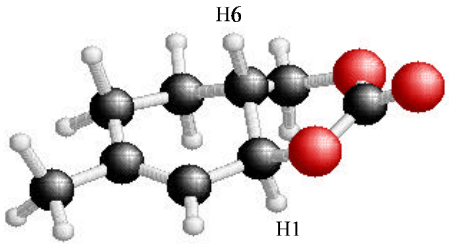

Compound 9
trans-carbonate

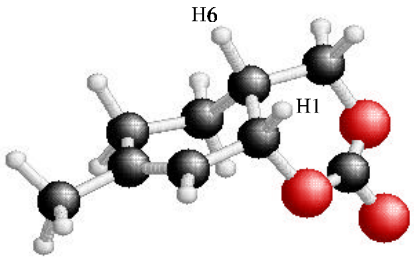

Compound 10
cis-carbonate

According to the Karplus[75] equation and based on the predicted dihedral angles of the energy minimized structures[76] for these two compounds (*trans* 124.9° and 48.4° for the *cis*), their coupling constants were predicted to be 10.5 Hz for the *trans* compound and 3.2 Hz for the *cis*). Based on these observations compound **11** was assigned as the *trans* carbonate and compound **13** as the *cis* carbonate.

---

[75] Karplus, M. *J. Chem. Phys*. **1959**, *30*, 11.

[76] Energy minimizations were performed using MacroModel version 4.5 developed by Prof. Clark Still at Columbia University. Conformational searches were conducted using the Monte Carlo simulation package and the MM2 minimization force field. One conformation was found for the *trans* compound and 3 conformations were found for the *cis* system within 50 Kcal/mol. The lowest energy in each case was used to evaluate the angles. The *trans* compound was found to be more stable by ΔE=0.12 Kcal/mol.

- *Intermolecular photoaddition*

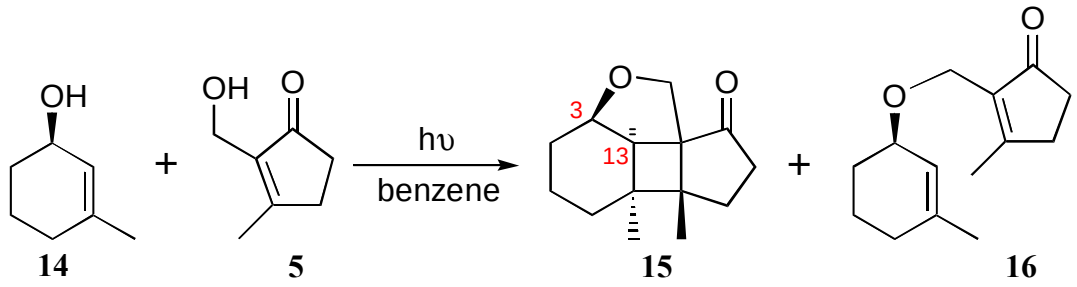

With the two precursors in hand, initial studies[65] to couple the five- and six-membered rings involved an intermolecular photo-addition. The reaction was carried out under the following conditions: alcohol **14** (10 eq.), alcohol **5** (1 eq.), benzene (0.02 M on alcohol **5**) and UV photo-irradiation of the deoxygenated solution for 20 hrs at room temperature. This gave a 7% yield of the head-to-head product **15** as was evidenced by the absence of vinylic protons on the ^{1}H NMR and shift of the enone IR band from 1696 cm^{-1} to that of a ketone at 1729 cm^{-1}. Evidence for the formation of the four-membered ring consisted of the presence of a resonance at δ 2.27 ppm, a doublet (J = 6.3 Hz) corresponding to H-13, coupled to a multiplet at δ 3.99-3.93 ppm associated with H-3, in the ^{1}H NMR spectrum. There was no evidence for the formation of head-to-tail products.

The absence of the head-to-tail product can be justified by arguing that the exciplex is pre-organized due to hydrogen bonding between the two reagents as shown in the scheme on the right. Other isolated compounds included the unreacted starting materials: alcohol **14 (**47%) and alcohol **5** (80%), along with the byproduct ether **16** (8%). The observation that ether **16** is formed during the course of

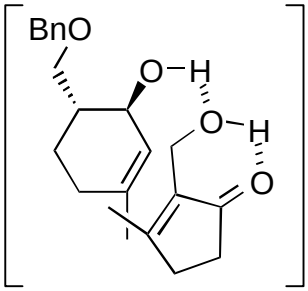

this reaction is further support for the idea that hydrogen bonding is in effect between the five- and six-membered ring reagents. The low yield of the desired photoaddition product **15** obtained under these conditions prompted us to investigate intramolecular analogs of the same reaction.

- *Intramolecular photoaddition*

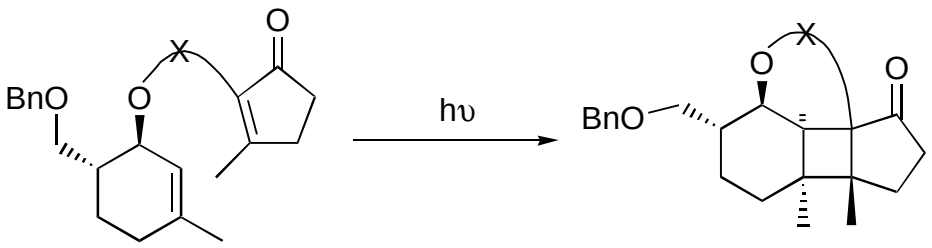

Intramolecular reactions are preferred over crossed-cyclo-additions because they minimize undesired homo-dimerizations and allow for regio-control of the photoaddition. The intermolecular version of the reaction would also offer better control over the relative stereochemistry of the four newly formed stereocenters by transferring chirality from the six-membered ring alcohol **6a** to the product. Wender supports this prediction in a report where he states "When the ground state alkene is facially differentiated, addition of the excited state enone will occur preferentially to the less encumbered face of the alkene".[77] This statement is based on assumptions that the stereochemistry integrity of ground state

[77] Wender, P. In *Photochemistry in Organic Synthesis*; Coyle, J. D., Ed.; Royal Soc. of Chem.: London, **1986**; Vol. 57, p 163.

cyclic alkenes is preserved, and also that the exo product is favored unless there are geometric constraints in the molecule that would favor the endo product.

In an attempt to tether the five- and six-membered ring precursors **5** and **6a** for an intramolecular version of the photoaddition, three main strategies were pursued: ether link, ester link and silicon tether. All three strategies will be discussed, but ultimately, the ether link strategy gave the most promising results and the Williamson ether synthesis was incorporated in the final photoaddition scheme.

1. Ether tether strategy: Williamson ether synthesis

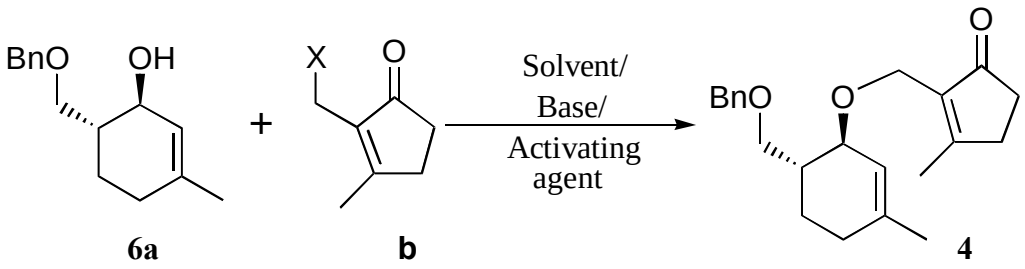

6a **b** **4**

The Williamson ether synthesis methodology was the first ether link strategy pursued. The best coupling results were obtained using the six-membered ring alcohol **6a** as the nucleophile and activating the five-membered ring component towards substitution. The benefits of using the five-membered ring as the electrophile are two fold: one does not have to worry about SN_2' reactions competing with the desired direct displacement on the six-membered ring and the displacement is expected to occur on the primary site of the electrophile thus minimizing steric effects.

Following successful ether formation, the intramolecular photoaddition reaction of compound **4** could follow two pathways in which both faces of the double bonds could react to give two isomeric *syn* products. In order to induce the face selectivity, only the *trans* alcohol **6a** was used. Thus the oxygen stereochemistry at C-1 of the substrate **4** would induce formation of the 1R*, 8R*, 9S*, 13S* relative stereochemistry in photoadduct **17**. The alkyl group at C-6 would further ensure this face selectivity by increasing the steric hindrance on the opposite side of the molecule.

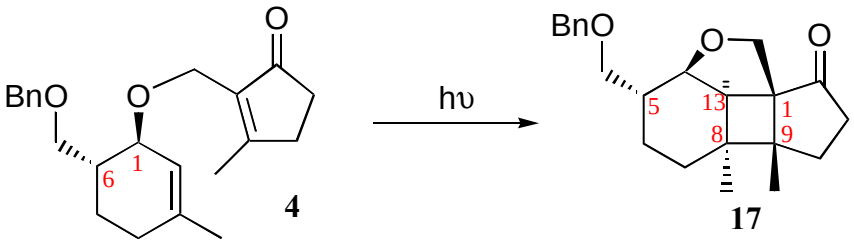

4 **17**

During the course of optimizing the ether synthesis, several issues had to be examined: best leaving group, activation of the electrophile, solvent effects and choice of base. On trying to select the best leaving group, two issues were considered: the ease of preparation of the derivative and the effect of the leaving group in the coupling reaction. Attempts included the derivatization of alcohol **5** as its mesylate (X = OMs), chloride (X = Cl), bromide (X = Br) and iodide (X = I). The mesylate (MsCl, Et_3N, CH_2Cl_2, 0^o C) was prepared in 40 % yield. The chloride ($SOCl_2$, $CHCl_3$, room temperature) was obtained in 96 % yield. The bromide was prepared in a two step process starting from formation of the mesylate and displacement with bromide (LiBr, acetone, 0^o C) to obtain the desired derivative in 46% yield (18% overall from alcohol **5**). The iodide was also prepared in a

two step process (NaI, acetone, room temperature) giving the desired product in 61% yield (25% overall from alcohol **5**).

With the derivatives in hand, coupling of the mesylate (10 eq. of alcohol **6a**, 1 eq. mesylate, ^{t}BuOK) gave ether **4** in 24 % yield. For the reactions involving the halide electrophiles, silver triflate was used as an activating agent (in CH_2Cl_2, and base). Under these reaction conditions the iodide derivative reacts only slightly better (38 % yield of **4**) than the bromide (34 % yield of **4**) and the chloride (35 % yield of **4**). Since there was not much difference on the efficiency of the different leaving groups, the chloride derivative was chosen because it could be prepared in higher yield.

Various silver salts were investigated to determine which one would work best in activating the electrophile in the Williamson ether synthesis. Silver nitrate, silver carbonate and silver tetrafluoroborate were tried unsuccessfully. The best results were obtained using a silver triflate catalyst to activate chloride **18** towards coupling. Under these conditions AgCl starts precipitating immediately upon addition so, provided there is free silver salt in solution, activation of the chloride is not the rate-determining factor. Note that excess silver triflate (3 eq.) was necessary, possibly because some of the silver salt complexes to the oxygens in the product during the course of the reaction.

The solvent of choice was methylene chloride, a non-coordinating solvent. Experiments that utilized coordinating solvents such as THF or acetonitrile led to no reaction, even when ten equivalents of silver triflate were used. Attempts were also made with benzene as an option for solvent, but ether formation proceeded in low yield (<10%).

Base was required to scavenge any acid formed during the course of the reaction; experiments conducted in the absence of base gave poor results. Four bases were tried,

triethylamine, pyridine, 2,6-lutidine and 2,6-di-*tert*-butylpyridine. When only one equivalent of the silver salt is used with one equivalent of either TEA, pyridine or 2,6-lutidine, no product formed, which suggests that the base complexes with the salt. To prevent this complexation, the more hindered base, 2,6-di-*tert*-butylpyridine was used successfully. It is worth mentioning that chloride **18** is unstable to nucleophilic bases probably due to degradation leading to diene type elimination products. This is evidenced by the increased signal in the vinylic region of the ^{1}H NMR.

The possibility that the reaction catalyzed by silver triflate involved substitution of the halide in compound **b** and formation of a triflate intermediate (X = OTf) prior to coupling with alcohol **6a** was investigated. Attempts to pre-form the triflate of alcohol **5** *in situ* (triflic anhydride, CH_2Cl_2, 0^o C, 30 min), followed by addition of alcohol **6a** and di-tert-butylpyridine was unsuccessful, yielding only 24% of the desired ether **4**. Optimization was focussed again on the chloride displacement reaction.

Studies involving changes in the order of addition of the reagents, testing the stability of the reagents in the reaction mixture and stoichiometric dependence of the reaction led to the conclusion that, provided the base was hindered enough, the only variable that affected reaction yield was the slow addition of chloride **18**. The slow addition requirement probably reflects the fast activation of the chloride generating an unstable electrophile. It is important to keep the chloride concentration low throughout the course of the reaction to maximize ether formation.

Attempts to scale up the reaction were not as successful. This could be due to surface area restraints that seem to play an important role in this reaction. Consequently, the yield was higher if several small reactions (300 mg) were conducted side by side rather

than one large-scale reaction. It is also important that no moisture be present in the reaction media to prevent the nucleophilic attack of water on the activated chloride. For that reason, the reaction was always conducted in the presence of 4Å molecular sieves.

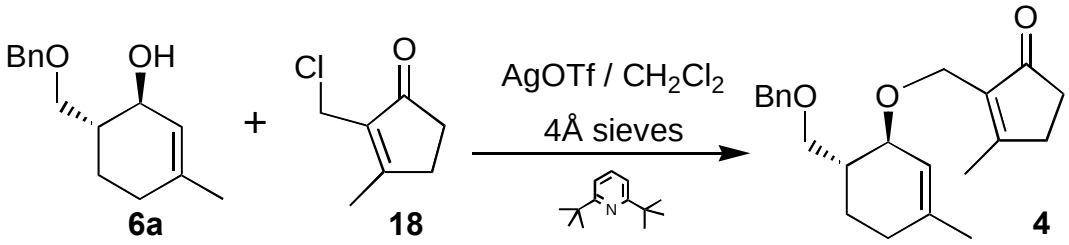

The optimized reaction conditions for the Williamson ether synthesis involves slow addition of the chloride **18** (1 eq.) to a solution protected from light containing alcohol **6a** (1 eq.), 2,6-di-*tert*-butyl-pyridine (3 eq.), silver triflate (3 eq.) and 4Å molecular sieves, in methylene chloride. Under these conditions, provided the scale was no more than 300 mg, compound **4** was consistently isolated in 57% yield.

2. Ether tether strategy: failed alternatives

Attempts to overcome the low yield obtained for the Williamson ether synthesis strategy involved experiments under different ether forming conditions or modification of the five-membered ring coupling-partner. These options are presented below.

The first approach involved formation of the tin-oxide derivative[78] of alcohol **6a** in an attempt to make the oxygen of the alcohol more nucleophilic.

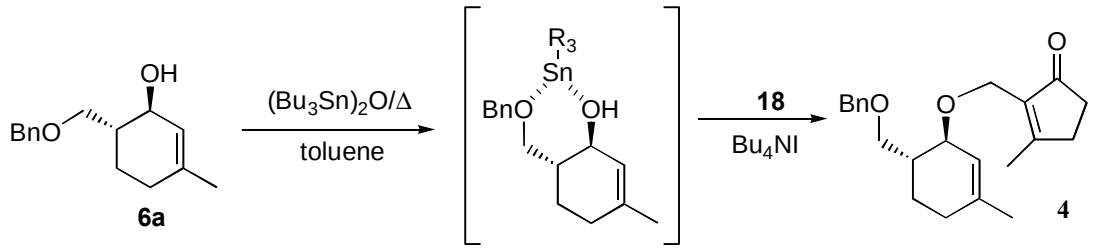

Alcohol **6a** was first treated with bis-(tributyltin)-oxide, (toluene, reflux, 4 hrs, 4Å molecular sieves) and then reacted with chloride **18**, in the presence of Bu_4NI, (80^o C). After 70 hrs only unreacted starting material was recovered.

Trost[79] and Hirama[80] successfully applied oxygen nucleophiles in intramolecular palladium-coupling reactions. Attempts to effect the intermolecular version of this reaction and form the ether through a π-allyl intermediate was conducted in two fronts.

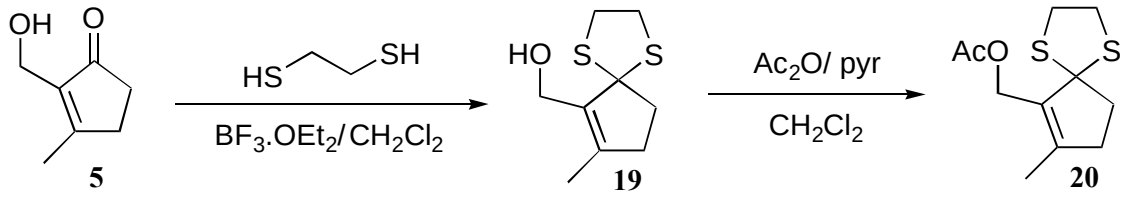

[78] Alais, J.; Veyrieres, A. *J. Chem. Soc. Perkin Trans. I* **1981**, 377. This reaction was first tried by Nylund, C. S., see ref 4.
[79] Trost, B. M.; Tenaglia, A. *Tetrahedron Lett.* **1988**, *29*, 2927.
[80] Suzuki, T.; Sato, O.; Hirama, M. *Tetrahedron Lett.* **1990**, *31*, 4747.

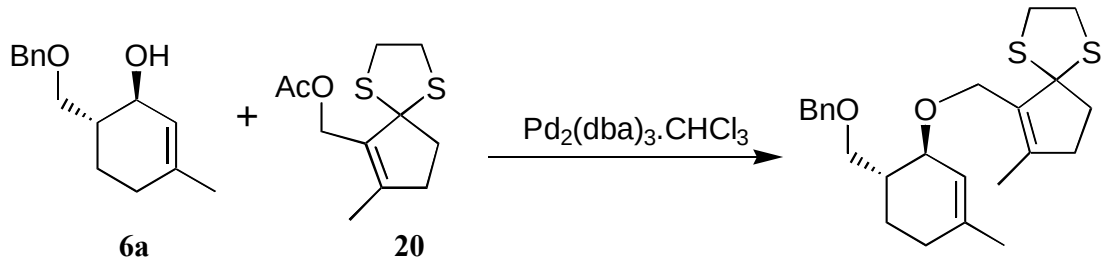

6a **20**

The first possibility was to form the π-allyl on the five-membered ring and use the six-membered ring as the nucleophile. This required masking of the ketone in the five-membered ring in order to form the π-allyl complex effectively, introducing an extra step to the reaction sequence. It also resulted in an increase of the ring strain on the π-allyl complex and of the steric hindrance around the reaction center. The carbonyl in compound **5** was first protected as a thioketal to give compound **19** by treatment with 1,2-ethane dithiol (methylene chloride, room temperature, $BF_3.OEt_2$, 8 hrs. 80% yield). The allylic alcohol portion of the molecule was activated as an acetate by treatment with acetic anhydride to give compound **20** (pyridine, CH_2Cl_2, room temperature, 16 hrs, 77% yield) which was then reacted with $Pd_2(dba)_3.CHCl_3$ (THF, PPh_3, room temperature, 15 min) to form the π-allyl complex. This intermediate was transferred *via cannula* into a solution containing alcohol **6a** and sodium hydride in THF. No coupling product was isolated even after the reaction proceeded for 20 hrs at room temperature.

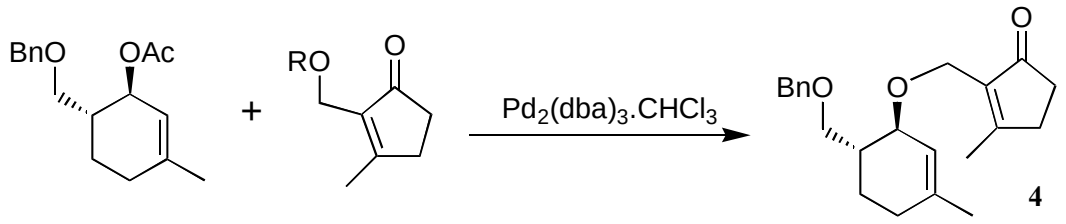

R = H comp. **5**

R = Bu_3Sn comp. **21**

The second possibility for the palladium coupling was the reverse of the previous strategy. The π-allyl-palladium complex was formed on the six-membered ring and the five-membered ring acted as the nucleophile. This approach should be favored since the nucleophile attacking the complex would be located on a primary center. Attack of the π-allyl should be selective with the nucleophile approaching from the least hindered side, giving ether **4**. Two versions of the coupling were tried against the possibility that the dipolar moment of the carbonyl on **5** would interfere with the nucleophilic attack of the palladium complex: one with the carbonyl protected as the thioketal (compound **19**), and the other with the carbonyl unprotected (compound **5**). In addition, following suggestions that hard nucleophiles are generally poor reaction partners for π-allyl-palladium complexes, the tin ether[78] of alcohol **5** was pre-formed and used as the nucleophile (compound **21**). The stannyl derivative experiment, as was also observed in Trost's experiments,[81] gave the same result as the respective alcohol.

Alcohol **6a** was first acetylated (Ac_2O, pyridine, CH_2Cl_2, room temperature, 4 hrs, 66% yield) then submitted to π-allyl formation. Treatment of the acetyl derivative of **6a** with $Pd_2(dba)_3{\cdot}CHCl_3$ (THF, PPh_3, room temperature), then addition of alcohol **5** or

alcohol **19** (reflux for 2 hrs) resulted in recovery of the five-membered ring piece intact. Attempts to form the π-allyl complex by treatment with $Pd(Ph_3P)_4$ in THF, or with $Pd(PPh_3)_4$ and $Ph_2PCH_2CH_2PPh_2$ in CH_2Cl_2 resulted in no reaction and both starting materials were recovered with no evidence of formation of the complex. Due to the lack of success with the palladium coupling strategy, this approach was abandoned.

A different strategy for the ether synthesis involved modification of the five-membered ring coupling-partner based on the premise that the dipole moment of the ketone was favoring elimination side products and deactivating substitution pathways.

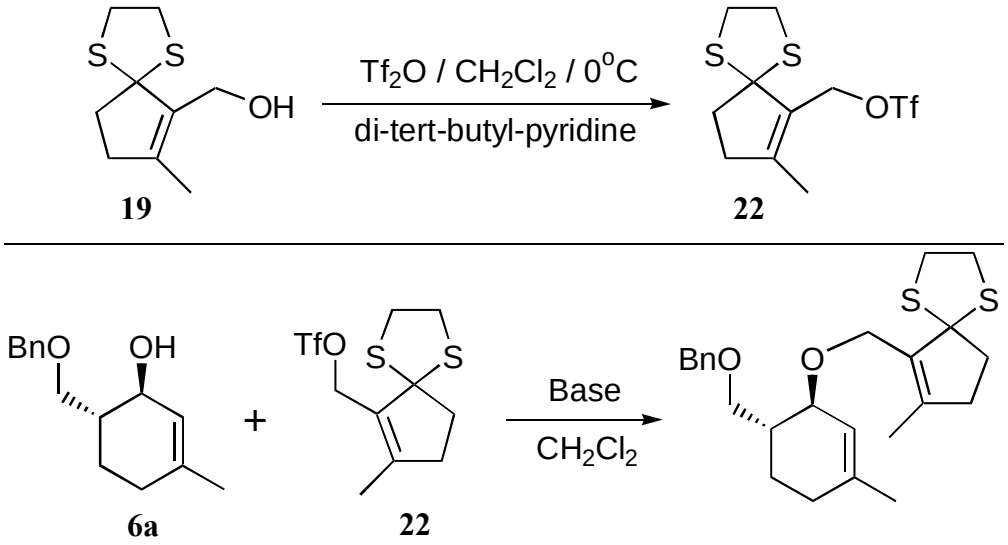

One attempt involved masking the ketone as a thioketal. The thioketal derivative was activated towards coupling by reaction with triflic anhydride (di-*tert*-butyl-pyridine, CH_2Cl_2, 0^o C, 30 min) followed by addition of alcohol **6a**, then the reaction mixture was

[81] Trost, B. M.; Tenaglia, A. *Tetrahedron Lett.* **1988**, *29*, 2931.

allowed to slowly warm to room temperature. Even after 4 hrs, only 8% yield of an ether could be isolated.

Another attempt to modify the five-membered ring component (**5**) involved reduction of the enone to an allylic alcohol and protection as a silyl ether.

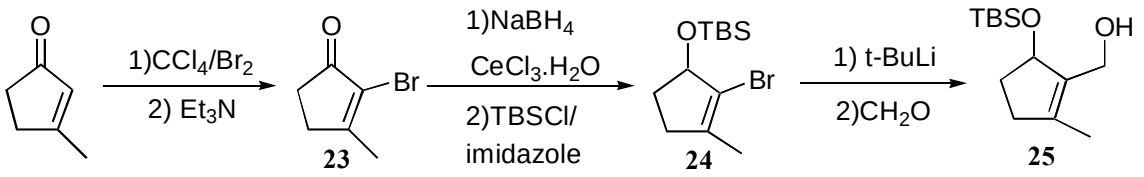

Compound **25** could be obtained from 3-methylcyclopentenone by first treating the starting material with bromine in carbon tetrachloride, followed by elimination in the presence of triethylamine to give the α-keto-bromide **23** in 66% yield.[82] Reduction of the carbonyl according to Luche's procedure[83] ($CeCl_3.7H_2O$, $NaBH_4$, EtOH, room temperature) and protection of the resulting allylic alcohol by reaction with TBSCl in the presence of imidazole[84] (DMAP, CH_2Cl_2, 0^o C) occurred smoothly giving the desired silyl ether precursor **24** in 76% yield. Transmetallation[85] with t-BuLi in pentane-ether at -78^o C, followed by trapping the anion with para-formaldehyde gave the requisite five-membered ring compound **25** in 68% yield.

Incorporation of **25** into the ether coupling schemes required activation of its alcohol functionality as either the chloride or the mesylate. However, preparation of these

---

[82] Smith, A.; Branca, S. J.; Pilla, N. N.; Guaciaro, M. A. *J. Org. Chem.* **1982**, *47*, 1855-1869.
[83] Gemal, A. L.; Luche, J.-L. *J. Am. Chem. Soc.* **1981**, *103*, 5454.
[84] Tanner, D.; Somfai, P. *Tetrahedron* **1988**, *44*, 619.

derivatives using the procedures discussed previously produced mostly degradation products along with byproducts deriving from silicon group migration.

3. The ester tether strategy

The second strategy pursued to tether the precursors for the intramolecular photoaddition scheme was to use an ester link, a two oxidation-level higher version of the ether coupling. An advantage of the ester link is that there are many reagents available for the coupling. A disadvantage is that the ester introduces rigidity into the tethering chain, which may hinder proper alignment of the double bonds in the subsequent photochemistry step. Two substrates were prepared, a one-carbon chain ester (compound **29**) that was analogous to the ether tether, and a two-carbon chain ester (compound **32**) designed to add flexibility to the tether. Ester formation was accomplished in acceptable yields for both the one and two carbon chain esters, but the photochemistry of these substrates was not successful.

Preparation of the one carbon chain ester (compound **29**) was accomplished by first synthesizing the carboxylic acid derivative of the five-membered ring piece (compound **28**), and then coupling it with alcohol **6a**.

[85] (a) Bailey, W. F.; Punzalan, E. R. *J. Org. Chem.* **1990**, *55*, 5404; (b) Negishi, E.-I.; Swanson, D. R.; Rousset, C. J. *J. Org. Chem.* **1990**, *55*, 5406.

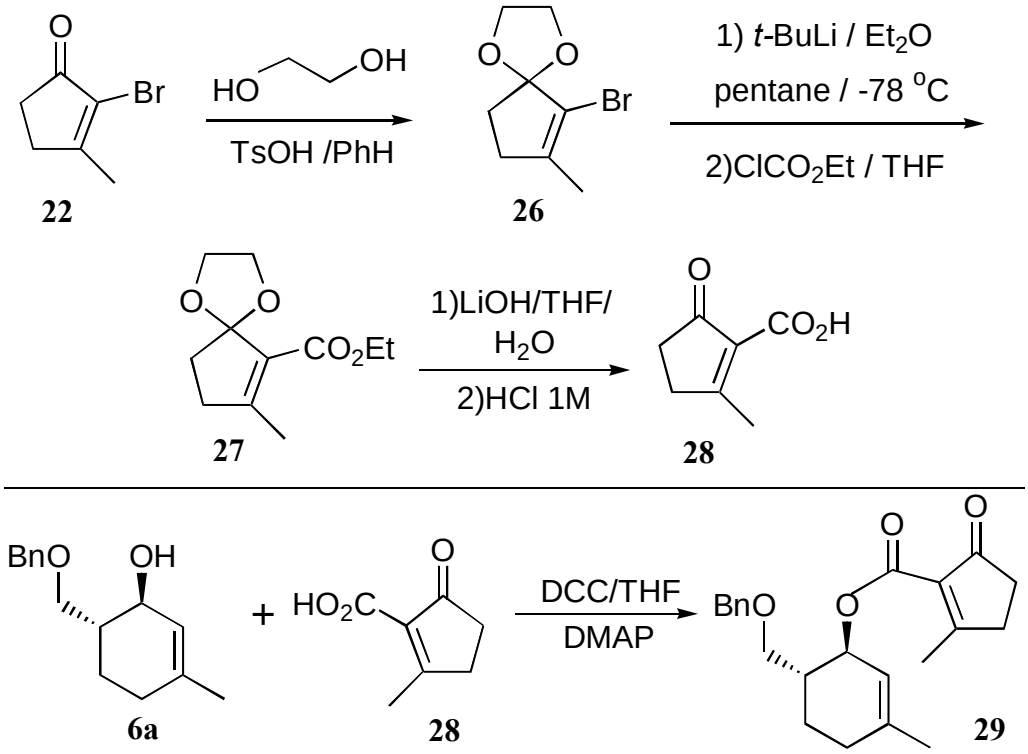

Protection of the carbonyl of 2-bromo-3-methylcyclopentenone **22** as the ketal[86] proceeded smoothly by treatment of the substrate with ethylene glycol in the presence of p-toluene sulfonic acid in benzene, under reflux (90% yield). Transmetallation[85] with t-butyllithium in pentane-ether at -78° C followed by trapping the anion with ethyl chloroformate gave ester **27** in 90% yield. Hydrolysis into the carboxylic acid **28** using LiOH[87] (THF, H_2O, 15° C), followed by acidic work-up (1M HCl) gave the five-membered ring substrate **31** in 78% yield. Note that the ketal protecting-group was also

[86] Daignault, R. A.; Eliel, E. L. *Org. Syn. coll.* **1973**, *vol 5*, 303.
[87] Ziegler, F. E.; Harran, P. G. *J. Org. Chem.* **1993**, *58*, 2768.

removed during the course of the hydrolysis. Esterification[88] of carboxylic acid **28** with alcohol **6a**, using DCC and DMAP in THF gave the desired ester **29** in 41% yield.

For the longer chain analog, furfural was used as the starting material for the synthesis of the five-membered ring precursor (compound **31**) which was then coupled to alcohol **6a**.

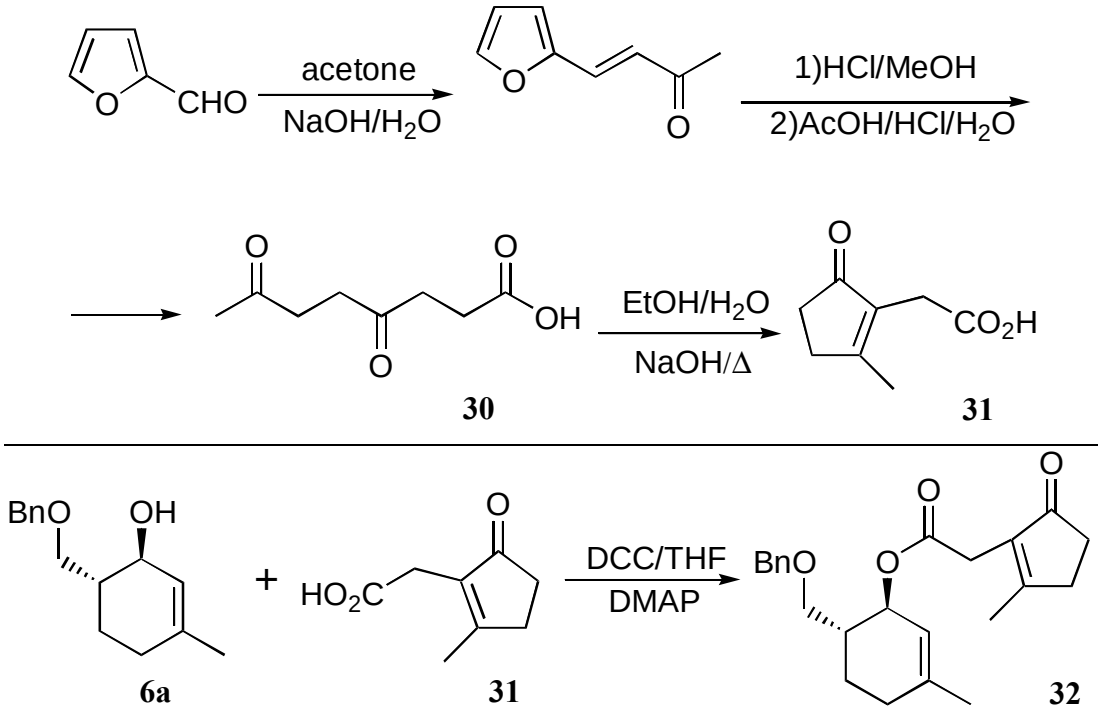

Furfural was condensed with acetone under basic conditions[89] (NaOH, H_2O, 80° C, 6 hrs, 53 % yield). The resulting furfurylidene-acetone was treated with HCl in methanol[90] to give the methyl ester of **30**, according to Marckwald's reaction.[91] This

[88] Ziegler, F. E.; Berger, G. D. *Syn. Comm.* **1979**, *9*, 539; also see Neises, B.; Steglich, W. *Ang. Chem. Int. Ed. Eng.* **1978**, *17*, 522 and Hassner, A.; Alexanian, V. *Tetrahedron Lett.* **1978**, 4475.
[89] Midorikawa, H. *Bull. Chem. Soc. Japan* **1954**, *27*, 210.
[90] Birch, A. J.; Keogh, K. S.; Mandaprer, V. R. *Aust. J. Chem.* **1973**, *26*, 2671.
[91] (a) Hunsdiecker, H. *Chem. Ber.* **1942**, *75B*, 447, (b) Abeysekura, A. M.; Amaralinge, S.; Grunshaw, J.; Jayeweera, N.; Sinanayake, G. *J. Chem. Soc. Perkin Trans. I* **1991**, 2021.

intermediate was then transesterified in the presence of acetic acid, HCl and water, to give the carboxylic acid **30** in 45 % yield. An intramolecular Knöevenagel cyclization[92] in NaOH (EtOH, H_2O, reflux, 20 hrs) gave the desired carboxylic acid **31** in quantitative yield. Esterification[88] of carboxylic acid **31** with alcohol **6a**, using DCC and DMAP in THF at room temperature gave the desired ester **32** in 49 % yield.

Photoaddition reactions were tried on both the one[93] (compound **29**) and the two[94] (compound **32**) carbon-tethered systems. Optimization of the reaction conditions included use of different solvents (benzene, cyclohexane, acetonitrile, methylene chloride, tetrahydrofuran, acetone, methanol, ethylene glycol and glyme), glass filters[95,96] (quartz, Vycor, Corex, Pyrex and uranium) and the use of sensitizers[97] (acetone, E_τ= 79 Kcal/mol, acetophenone, E_τ= 74 Kcal/mol, and benzophenone, E_τ= 69 Kcal/mol). None of these conditions gave the desired [2+2]-photoaddition product with most of the reactions resulting on recovery of unreacted starting material or decomposition into baseline products.

---

[92] (a) Johnson, W. S.; Gravestock, M. B.; McCarry, B. E. *J. Am. Chem. Soc.* **1971**, *93*, 4332; (b) McMurry, P. M. J.; Singh, R. K. *J. Org. Chem.* **1974**, *39*, 2316.

[93] UV absorption maximum at 220 nm in methanol.

[94] UV absorption maximum at 232 nm in methanol.

[95] UV cutoffs for glass width of 2mm: quartz (<200 nm), Vycor 7910 (<230 nm), Corex D (<270 nm), Pyrex 7740 (<290 nm), uranium (<320 nm).

[96] Coyle, J. D. *Photochemistry in Organic Synthesis*; Burlington House: London, **1986**.

[97] The energy for the first triplet state of cyclopentenones is reported to be at E_3=74 Kcal/mol in Turro, N. J. *Modern Molecular Photochemistry*; Benjamin/Cummings Pub. Co.: Menlo Park, Califronia, 1978.

E - conformation Z - conformation

Figure 2.2

Most esters tend to favor E-conformations over Z-conformations (see Figure 2.2), thus setting the two double bonds in esters **29** and **32** involved in the photoaddition reaction far apart. This preference for the E-conformation for the ground state of esters **29** and **32** make the success of the [2+2] cyclization dependent on the lifetime of the excited state of the chromophore. The excited state must live long enough for conformational change to occur prior to cycloaddition and avoid other relaxation pathways that would lead to side reactions such as Norrish cleavage, etc. Also, [2+2] intramolecular addition of the ester with the longer tether (compound **32**) must be accompanied by formation of a six-membered ring, which is generally disfavored, entropically, on intramolecular photoadditions.[98] Attempts to run the reaction at a higher temperature favored the formation of products derived from these undesired "side reactions" (mostly baseline material).

Monte Carlo simulations were carried out in order to evaluate the population distribution of the different conformations that compounds **4**, **29** and **32** are able to adopt. Analysis of the results was based on the assumption that the excited state resembles the geometry of the ground state and that for the reaction to occur the double bonds must be

close in space in order to be able to interact. Since this is an intramolecular reaction, the distance between the two methylene-carbons next to a methyl in each double bond can represent the distance of the two olefins in each one of the compounds. The results comparing the distance between the olefins to the energy of the conformer are graphed below; conformations with shorter distances and lower relative energy are more likely to undergo the desired reaction.

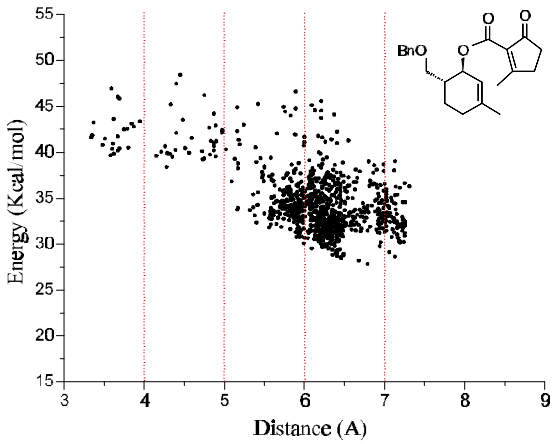

compound 29

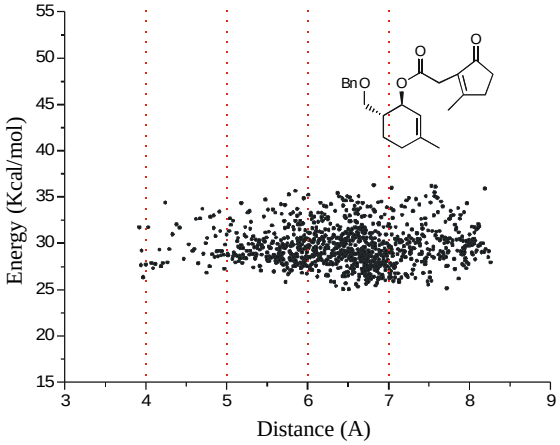

compound 32

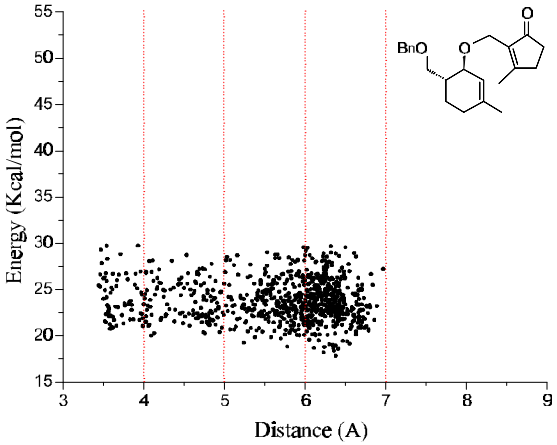

compound 4

Monte Carlo simulation parameters included minimization of 10,000 conformations for each of the three compounds using the MM2 force field available with MacroModel. Structures within 20 Kcal/mol of the lowest energy structure for each compound were saved.

[98] "Rule of five" - Crimmins, M. T. *Chem. Rev.* **1988**, 1453.

The Monte Carlo simulation results indicate that a significant percentage of the possible conformations of ether **4** allow for the [2+2] photoaddition to occur. In contrast, the preferred conformations for esters **29** and **32** tend to place the two double bonds further apart and at higher relative energy. Assuming that the relative ground state energies reflect the relative excited state energies, the lifetime of the excited state is probably too short for the esters to adopt conformations where the distance between the olefins is small enough to result in reaction. [2+2] Photoaddition was successful for ether **4** (see section 5 in this chapter for more details) while it failed for the two esters **29** and **32**.

4. Silicon tether strategy

The third strategy pursued to tether the precursors for the intramolecular photoaddition scheme was to use a temporary silicon connection. This methodology has been employed successfully by Stork[99] and Crimmins.[100] The silicon atom adds the versatility of being able to be removed in an oxidative[101] or reductive[102] fashion, as required. The silicon-oxygen bond is longer than the carbon-oxygen bond adding more range of motion to the tether; this may help align the double bonds in the cyclization step. The major disadvantage to the silicon tether strategy is that the silicon-oxygen bond is

[99] Stork, G.; La Clair, J. *J. Am. Chem. Soc.* **1996**, *118*, 247.
[100] Crimmins, M. T.; Guise, L. E. *Tetrahedron Lett.* **1994**, *35*, 1657.
[101] Tamao, K.; Ishida, N.; Kumada, M. *J. Org. Chem.* **1983**, *48*, 2120.

often unstable to chromatography in silica gel, making it difficult to purify the intermediates. Two silicon-tethered substrates were envisioned: a two and a three-atom chain. The two-atom tether satisfies the "rule of five"[98] for the subsequent photoaddition reaction, but it requires the insertion of an additional carbon at C-2 (tricyclic-undecane numbering, see Figure 2.1) for the proper functionalization of "common intermediate **c** . The three-atom tether carries the necessary number of carbons for the thionocarbonate formation, but it requires the formation of a six-membered ring in the photochemical step.

For the two atom tether, vinyl bromide **26** was transmetallated with t-BuLi[85] (ether, pentane, -78° C) and then treated with $Me_2Si(NEt_2)Cl$[103,104] at -78° C. The crude reaction mixture was concentrated and the residue was treated with alcohol **6a** in the presence of triethylamine in methylene chloride at 0° C to give the desired product **33** in 13% yield.

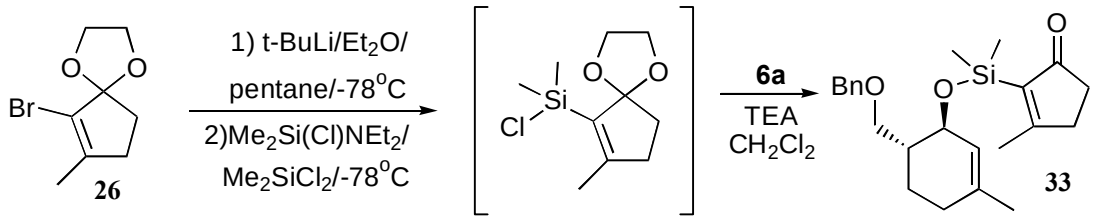

Due to the low yield of this coupling and considering the additional steps required to introduce the carbon at C-2 to form the cyclic thionocarbonate, this system was abandoned in favor of pursuing the three-atom chain analog.

---

[102] (a) Stork, G.; Sofia, M. *J. Am. Chem. Soc.* **1986**, *108*, 6826; (b) Hale, M. R.; Hoveyda, A. H. *J. Org. Chem.* **1992**, *57*, 1643.
[103] Stork, G.; Keitz, P. F. *Tetrahedron Lett.* **1989**, *30*, 6981.

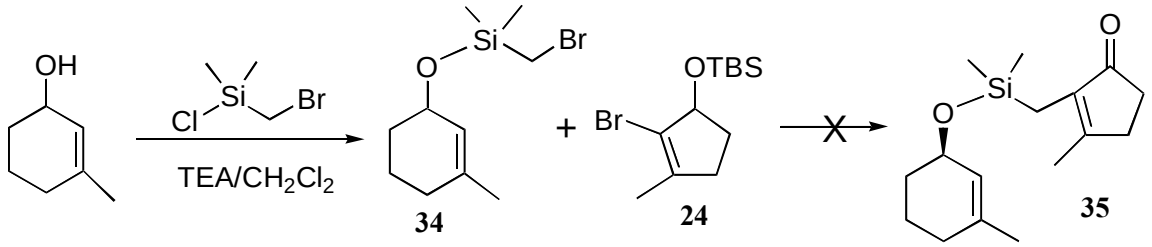

The bromide necessary to try the coupling for the three-atom chain compound was prepared from 3-methylcyclohexenone by reduction with $LiAlH_4$ (Et_2O, 0^o C, 30 min, 74 % yield), followed by treatment of the allylic alcohol with (bromomethyl)-chlorodimethylsilane[105] (triethylamine, CH_2Cl_2, 0^o C). Silylation gave the desired bromide **34** in 98 % yield. The higher-order vinylic-cuprate[106] of **24** was freshly prepared by addition of the alkyllithium derivative of **24**[85] to a solution containing 2-lithiothiophene and CuCN in THF at -78° C. The coupling with the six-membered ring halo-silicon intermediate **34** was performed by addition of the THF solution of the cuprate to **34** at -78° C; the reaction mixture was then allowed to warm to 0° C. The reaction was unsuccessful, giving none of the desired product. On a model system, the cuprate of geranyl bromide[107] could be coupled to **34** under the same conditions, which suggested that the difficulties observed for the desired coupling resided in the five-membered ring coupling-partner **24**. Further attempts to synthesize the silicon tether precursor were abandoned in favor of optimization of the Williamson ether synthesis, discussed earlier.

---

[104] Washburn, S. S.; W. R. Peterson, J. *J. Organomet. Chem.* **1970**, *21*, 59.
[105] Stork, G.; Kahn, M. *J. Am. Chem. Soc.* **1985**, *107*, 500.
[106] Lipshutz, B. H.; Moretti, R.; Crow, R. *Org. Syn.* , *Coll vol VIII*, 33 (or Lipshutz, B. H.; Moretti, R.; Crow, R. *Org. Syn.* **1990**, *69*, 80).

5. Photoaddition

The product of the Williamson ether synthesis, compound **4**, was submitted to photoaddition conditions to promote [2+2] cyclization in order to produce the desired tricycle[5.4.0.0^{2,6}]undecane **17**.

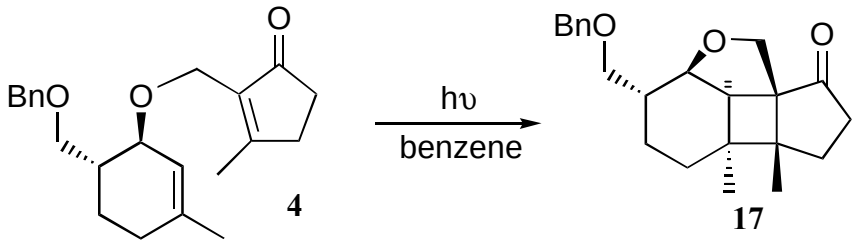

4 **17**

Irradiation of compound **4** was conducted using a medium pressure 450 W Hanovia UV lamp, at 8.75 mM concentration, in benzene. Other than [2+2] cyclization, enones can also undergo photoreduction, oxetane formation, Norrish type I cleavage and Norrish type II cleavage. The benzene[108] solvent probably acts as a filter, preventing the above side reactions (Norrish type I cleavage products were observed in other solvent systems such as cyclohexane). Three products were obtained, a [2+2] photoadduct, and two other products that could not be separated from each other by flash chromatography.

Only one isomer of the cyclized [2+2] photoadduct product was observed as evidenced by the presence of only two methyl singlets at δ 1.11 and 1.09 ppm in the ^{1}H NMR and the presence of 19 of 22 resolved peaks in the ^{13}C NMR. This isomer was

[107] Taylor, R. J. K. *Synthesis-Stuttgart* **1985**, *4*, 364.

tentatively assigned with the relative stereochemistry shown in compound **17** assuming that the stereochemistry of the ether would bias the face selectivity to cause the five-membered ring to approach the six-membered ring from the same side as the oxygen in the ether tether. This face selectivity should also be enforced by the presence of a bulky group (the benzyl ether) on the opposite side of the substrate. The assignment of compound **17** also presumes that most intramolecular photocycloadditions result in a *cis* ring fusion between five- and four-membered rings due to ring strain.[100] The assignment is supported by the measured ^{3}J between the protons at C-4 and C-13 of 6.0 Hz for the cyclized [2+2] photoadduct indicating a *cis* relationship between the two hydrogens.

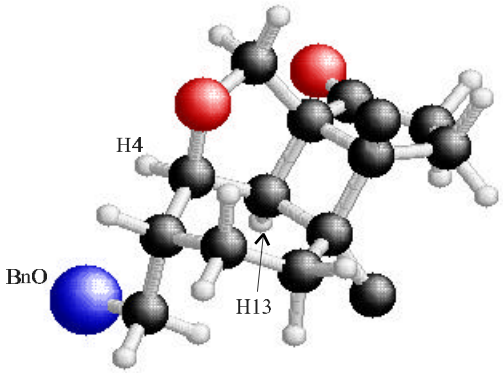

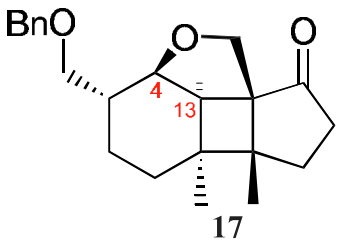

17

Energy Minimization

This assignment was in agreement with the ^{3}J value (6.9 Hz) for compound **17** predicted by MM2 energy minimization.[109] The identity of compound **17** was later

---

[108] UV absorption maximum at. 200 nm (ε 6300) and 255 nm (ε 200).

[109] Energy minimizations were performed using MacroModel version 4.5 developed by Prof. Clark Still at Columbia University. Conformational searches were conducted using the Monte Carlo simulation package and the MM2 minimization force field. Found 277 conformations within 50 Kcal/mol, mostly due to chain conformational changes. The lowest energy structure was used to evaluate the dihedral angle witch was 25.6 degrees.

confirmed by 1D-proton difference NOE experiments performed on products derived from this photoadduct, at subsequent steps in the synthesis. See chapter 3 for details.

The two other products, which were inseparable by flash chromatography, derived from disproportionation of the diradical intermediate **36** followed by 1,5 hydrogen shift.

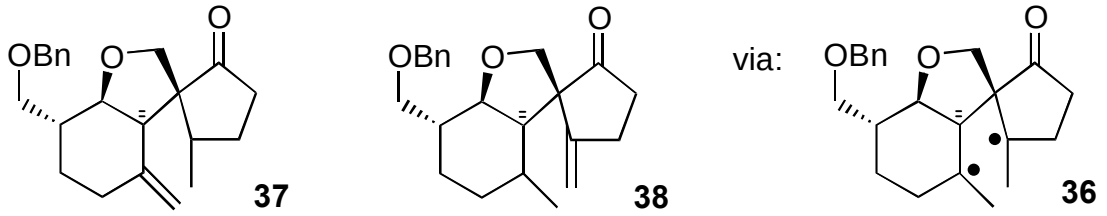

They were assigned as compounds **37** and **38**, which is supported in the ^{1}H NMR spectrum of the mixture of the two compounds (roughly 1:1), by a pair of doublets at δ 0.77 and 1.14 ppm (both J ~ 6.5 Hz), corresponding to the two methyl groups next to methine hydrogens. Additionally, four other peaks were observed at δ 4.64, 4.88, 5.22 and 5.28 ppm corresponding to the vinylic protons of the terminal olefins. Low-resolution GC-Ms traces indicated a mass of 340 for both compounds, as two separate peaks.

Product **17** was also photoreactive; therefore, the reaction could not be run to completion without degradation of the desired product. Best results were obtained when the reaction was run to 50 % conversion of the starting material, usually about 4 hours. After purification, the unreacted starting material could be resubmitted to the reaction conditions for further conversion. Product **17** was obtained in 78 % yield and the two byproducts together amounted to 9.5 % after three cycles of reaction.

- *Olefin formation*

Introduction of the double bond at C-5 could be accomplished by deprotection of the benzyl group followed by elimination of a water molecule. The double bond would be used later as a handle for the introduction of an epoxide as it is present in FS-2.

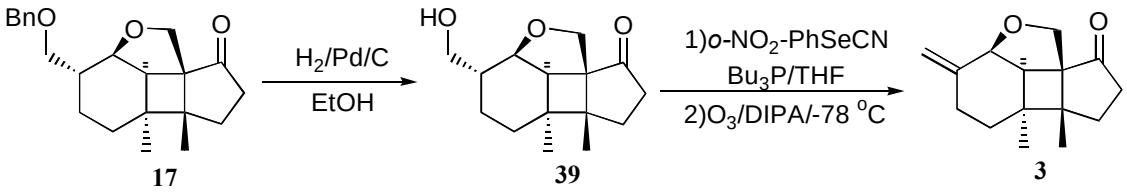

17 **39** **3**

The benzyl-protecting group was removed by catalytic hydrogenation (H_2, Pd/ charcoal, in EtOH, at 40 psi) and alcohol **39** was obtained in 98% yield. The double bond formation could be accomplished by transforming the alcohol into the o-nitroselenide and inducing elimination upon oxidation, following Grieco's methodology.[110]

Grieco reported that substituents on the β and/or γ carbons of primary alkyl-phenyl-selenoxides result in low yields of terminal olefins. A solution for this problem was developed by Sharpless.[111] He verified that electron-withdrawing groups on the aromatic ring of alkyl-selenides enhance the rate of elimination of the respective selenoxides. Hence the use of an *o*-nitrophenyl substituent promotes the elimination of primary selenoxides yielding terminal olefins in high yield.

Alcohol **39** was first converted into a selenide using *o*-NO_2-phenyl selenium cyanide in the presence of tributyl phosphine in THF. The crude product was then

[110] Grieco, P. A.; Gilman, S.; Nishizawa, M. *J. Org. Chem.* **1976**, *41*, 1485.

oxidized to promote elimination giving the desired olefin **3**. The conventional method to carry out this oxidation involves the use of *m*-CPBA or H_2O_2.[112] However, these reagents were not compatible with the five-membered ring ketone present in the molecule. Attempted oxidation of the selenide using the literature conditions led to a mixture of the desired olefin **3** along with the Baeyer-Villiger product **40**.

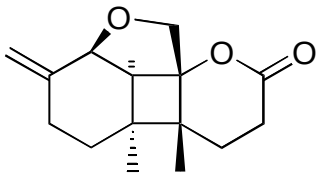

40

Other examples of Baeyer-Villiger reactions have been previously reported, along with epoxidation of olefins[113] under similar conditions. Both results were attributed to formation of benzeneperoxyseleninic acid **41** from organo selenides.[114]

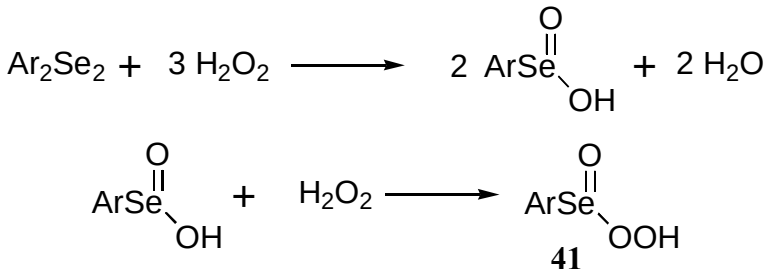

[111] Sharpless, K. B.; Young, M. W. *J. Org. Chem.* **1975**, *40*, 947.
[112] (a) Grieco, P. A.; Saki, Y.; Xler, D. *J. Am. Chem. Soc.* **1975**, *97*, 1597; (b) Grieco, P.; Noguez, J. A.; Masaki, Y. *Tetrahedron Lett.* **1975**, *48*, 4213.
[113] (a) Grieco, P. A.; Yokoyama, Y.; Gilman, S. *J. Chem. Soc. Chem. Comm.* **1977**, *23*, 870; (b) Grieco, P. A.; Yokoyama, Y.; Gilman, S.; Nishizawa, M. *J. Org. Chem.* **1977**, *42*, 2034.
[114] McCullogh, J. *J. Am. Chem. Soc.* **1949**, *71*, 674.

The oxidation step could be effected by ozonolysis of the selenide intermediate thus preventing formation of the Baeyer-Villiger side product **40**.

Another byproduct that was observed during the course of optimizing this reaction was formation of cyanohydrin **42**.

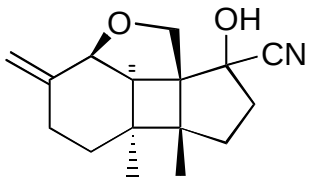

42

This result also has precedent in the work of Grieco[115] in which he observed that, at room temperature in the presence of tributyl phosphine, aryl selenocyanates react rapidly with aldehydes to give cyano-selenides. When ketones were present in the media he observed rapid formation of cyanohydrins. Cyanohydrin formation could be reversed by treatment of the crude reaction mixture with base to regenerate the desired ketone **3**.

The best conditions found[116] to carry out this transformation were to first prepare the selenide with o-nitroselenyl cyanide in the presence of tri-n-butylphosphine with THF as the solvent. The THF was evaporated and the crude product was oxidized by ozonolysis in methylene chloride (-78^{o} C), in the presence of di-isopropylamine. This process provided the desired olefin **3** in 75 % yield for the two steps.

---

[115] Grieco, P. A.; Yokoyama, Y. *J. Am. Chem. Soc.* **1977**, *99*, 5210.
[116] Optimized by Nathan Yee in this laboratory.

The assignment of the structures for compounds **3**, **40** and **42** was based primarily on their ^{13}C NMR spectra and was supported by their ^{1}H NMR, infrared and mass spectra. These assignments relied heavily on the ^{13}C NMR spectra because their ^{1}H NMR spectra were very similar. Furthermore it was difficult to obtain a molecular ion for the cyanohydrin from the mass spectra (EI and CI), and the fragmentation pattern for the cyanohydrin was similar to that of the ketone. Analysis of the ^{13}C NMR showed that compound **42,** assigned as the cyanohydrin, had 16 peaks, no carbonyls, and showed a signal at δ 120.0 ppm in agreement with having a cyano group. The infrared bands seen at 2249 cm^{-1} and 3585 cm^{-1}, characteristic of cyanides and alcohols respectively, further confirmed the presence of the cyano and hydroxyl groups. Chemical evidence for the assignment of compound **42** was that this cyanohydrin could be converted to compound **3** by treatment with base (15 % aqueous NaOH). Compound **3** showed a characteristic carbonyl resonance in both the ^{13}C NMR (δ 217.6 ppm) and the infrared (1722 cm^{-1}) spectra. Evidence for lactone **40** comes primarily from an infrared band at 1745 cm^{-1} and is supported by the presence of a carbon resonance in the ^{13}C NMR at δ 171.5 ppm. The molecular ion M^{+} (248, EI) could be observed for this lactone, offering further support to the assigned structure.

- *Conclusion*

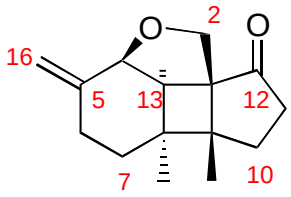

3

8,9–Dimethyl–5–methylidene-(1R*, 4R*, 8R*, 9S*, 13S*)–3-oxatetracyclo [6.4.1.$0^{1,9}$.$0^{4,13}$] tridecan-12-one (compound **3**) was synthesized. This compound fulfills the necessary requirements of the retrosynthetic-analysis for the synthesis of FS-2. It is a tricyclo [5.4.0.$0^{2,6}$] undecane carbon skeleton with two quaternary centers at C-8 and C-9, oxygen functionalization at C-2 and C-12 for introduction of the cyclic thionocarbonate and a handle for introduction of a double bond at C-5 to C-4.

Compound **3** was prepared in a convergent fashion, from a [2+2] intramolecular photo-addition reaction between a five-membered ring enone (compound **5**) and a six-membered ring olefin (compound **6a)**. The two precursors were tethered through an ether link *via* a Williamson ether synthesis using silver triflate to activate the electrophile. The *trans* stereochemistry of alcohol **6a** was used to control the relative stereochemistry of the four new stereocenters in the molecule, including the two adjacent quaternary centers.

After the photoaddition, the olefin functionality was unraveled by removal of the benzyl protecting group and elimination of a molecule of water following Grieco's methodology.

With compound **3** in hand, research was conducted on two fronts. The first was the preparation of model systems to test the scope of the radical fragmentation proposed

in the retrosynthetic plan. They will be discussed in chapter 3. The second was the further functionalization of the skeleton towards the synthesis of FS-2; this effort will be discussed in chapter 4.

CHAPTER III: *RADICAL FRAGMENTATION - MODEL SYSTEMS*

- *Introduction*

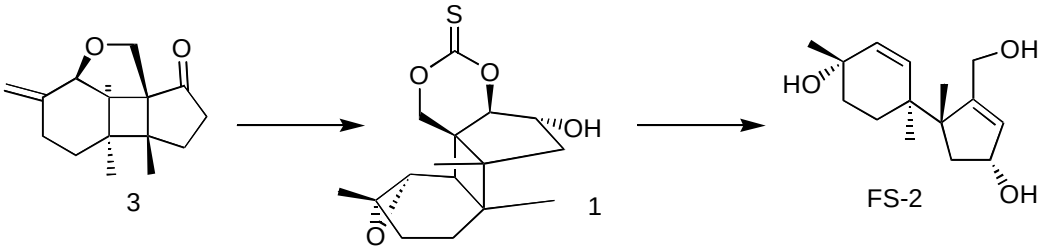

The synthesis of intermediate **3** enabled the investigation of the radical fragmentation theory originally proposed in chapter 1. A number of model systems were constructed from this intermediate, which could serve as a handle to determine what factors controls the selectivity of the fragmentation at the different steps of the reaction regarding thermodynamics and strain factors.

This chapter will first present background information on radical fragmentation reactions in general and discuss specific considerations that may affect the reactions proposed in this synthesis. This involves the selectivity of the cyclic thiocarbonate fragmentation to generate the primary or secondary radical, the fragmentation of the cyclobutyl carbinyl radical to give exocyclic or endocyclic bond cleavage, and the opening of the epoxide. The preparation of the model compounds will then be discussed along with the results of the fragmentation reactions.

- *Radical Fragmentation Background*

Reactions involving radical intermediates have been known since the beginning of the century,[117] but they were not often incorporated in synthetic plans because they were regarded as unpredictable and complex. Radicals react at a high absolute rate, which may suggest low selectivity, but it is the relative rates between the competing reaction paths that are important for selectivity.

Radicals can react with another radical or with a non-radical molecule. Radical-radical reactions occur by combination or disproportionation at rates approaching the diffusion controlled limit. These reactions are undesirable for most synthetic applications and can be avoided or limited by conducting the experiments under high dilution.[118] Radical-molecule reactions occur with a wide spectrum of rates and can be both chemo and regioselective.

Radical-molecule reactions allow for bond formation and bond cleavage to occur in a neutral environment. Under these conditions most functional groups may be left unprotected. The products of these reactions can be more predictable than the outcome of complex polar reactions. Steric crowding,[119] particularly on the radical center, is often tolerated. The reaction is not subjected to large solvent effects or ion pairing and aggregation issues. The choice of solvents is based on boiling point and hydrogen donating ability, and the volume of solvent used can dramatically influence the product

---

[117] Gomberg, M. *J. Am. Chem. Soc*. **1900**, 22, 757.
[118] Curran, D. Synthesis **1988**, 417.
[119] Barton, D. R.; Motherwell, R. S. H. *Pure and Appl. Chem*. **1981**, 53, 15.

ratio when one or more second order reactions are involved as a consequence of changes in reagent concentration.

Radical reactions can be advantageous over polar reactions in that they are less prone to rearrangement. In the example shown in Figure 3.1 Lange[120] observed the formation of ring expansion product **44** when he submitted compound **43** to radical fragmentation conditions. When the same substrate **43** was submitted to cationic solvolysis conditions (AgOAc, TFA), skeletal rearrangements were observed with products **45** and **46** deriving from both possible four-membered ring bond-migrations.

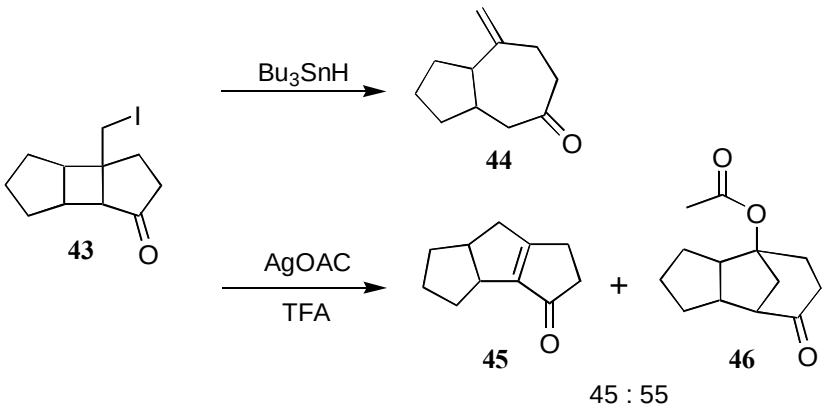

Figure 3.1

The product of a radical reaction is another radical; therefore tandem or sequential reactions are a natural development. It is possible to effect radical additions to unactivated alkenes and to introduce functionalization at remote positions. Barton[121] took

[120] Lange, G. L.; Gottardo, C. *J. Org. Chem.* **1995**, 60, 2183.
[121] Barton, D. H. R.; Beaton, J. M.; Geller, L. E.; Pechet, M. M. *J. Am. Chem. Soc* **1961**, *83*, 4076.

advantage of radical reactions in the synthesis of steroids where he used a 1,5-H migration to introduce functionalization at unactivated areas of the steroid skeleton (see Figure 3.2).

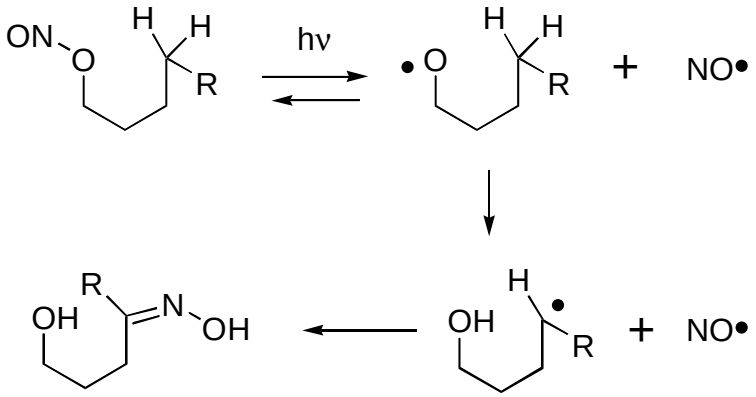

Figure 3.2

1. Fragmentation of Thionocarbonates

The fragmentation mechanism of the thionocarbonate system is well understood.[122] It involves rapid, reversible addition of the stannyl radical to the thiocarbonyl group followed by slower fragmentation of the adduct radical with cleavage of the carbon-oxygen bond.

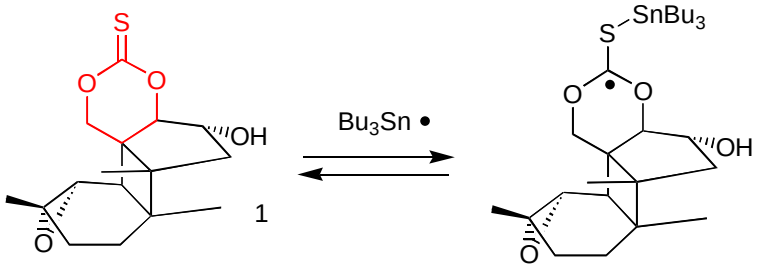

Carbon-oxygen bonds are usually very strong (BDE_{298K} ~83 Kcal/mol),[123] therefore they do not readily undergo β-fission. However under favorable conditions the C-O bond can be broken as in the transformation of a weak C=S bond into a strong C=O.

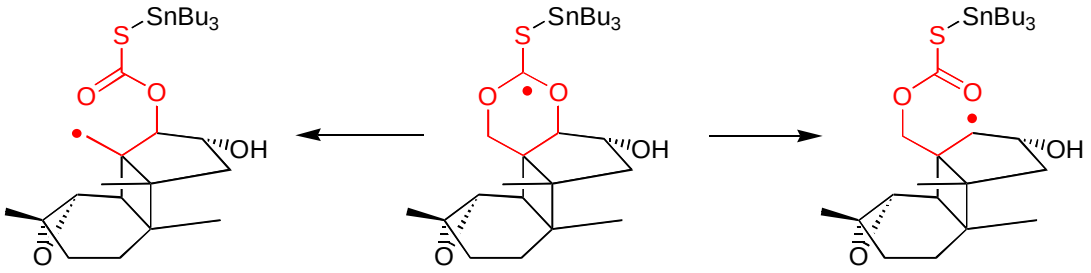

For the fragmentation precursor of FS-2 (shown above), the product of the addition of the stannyl radical to the thiocarbonyl group is locally symmetric. Fragmentation can occur in either direction to generate a primary alkyl radical or a secondary alkyl radical. A number of factors have been discussed in the literature as being important for determining the relative rates that establish the selectivity in this fragmentation; such as orbital overlap,[118] stability of the product radicals[124] or release of strain.[125]

For example, in sugars, primary versus secondary radical selectivity always favors formation of the secondary radical. Barton[124] argues that the failure to form primary derivatives is due to lesser stability of primary relative to secondary radicals. Figure 3.3

---

[122] Crich, D.; Beckwith, A. L. J.; Chen, C.; Yao, Q. W.; Davidson, I. G. E.; Longmore, R. W.; Deparrodi, C. A.; Quinterocortes, L. and Sandovalramirez, J. *J. Am. Chem. Soc*. **1995**, 117, 8757.
[123] Hartwig, W. *Tetrahedron* **1983**, 39, 2609.
[124] Barton, D. R. and Subramarian, R. *J. Chem. Soc. Perkin Trans. I* **1977**, 1718.
[125] Ruchardt, C. *Angew. Chem. Int. Ed. Eng.* **1970**, 9, 830.

illustrates the fragmentation of a five-membered ring cyclic thionocarbonate.[126] Formation of the secondary radical **48** was the preferred pathway for this reduction reaction supporting Barton's hypothesis. Along with the product deriving from the primary radical (**49**), other side products included reduction of the thiocarbonyl (compound **50**) and compound **51** which is a product of the Schönberg rearrangement.[127]

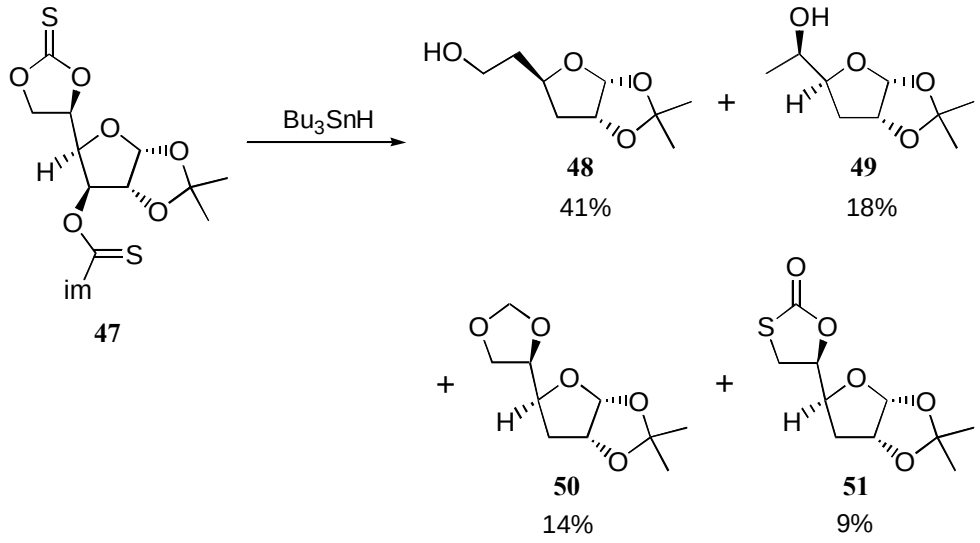

Figure 3.3

The stability of the radical, however, does not always determine the selectivity of the reaction. Studies of Barton-McCombie reactions on the taxol skeleton[128] serve to illustrate the role of strain in determining selectivity. In the example below (Figure 3.4), the presence of an acetate substituent in the eight-membered ring of compound **55** was important for determining the outcome of the reaction. When the acetate group was next

---

[126] De Bernardo, S.; Tenge, J. P.; Sasso, G. and Weigele, M. *Tetrahedron Lett*. **1988**, 29, 4077.

[127] (a) Schönberg, A.; Vargha, L. v. *Ber. Dtsch. Chem. Ges.* **1930**,. *63*, 178; (b) Schönberg, A.; Vargha, L. v.; Paul, W. *Liebigs Ann. Chem.* **1930**,. *483*, 107.

to the carbonyl the major product (**56**) was derived from the tertiary radical; when the acetate group was not present the major product (**53**) was derived from the secondary radical and the product derived from the tertiary radical (**54**) was obtained in only 8% yield. This change in selectivity can be explained by the increase in ring strain as a consequence of conformational changes induced in the ring by the presence of the acetate. This result is contrary to Barton reports[119,124] that: tri-butyltinhydride mediated deoxygenation of diol-thionocarbonates proceeded regioselectively to introduce hydride at the more substituted carbon due to a preference to form the more stable radical.

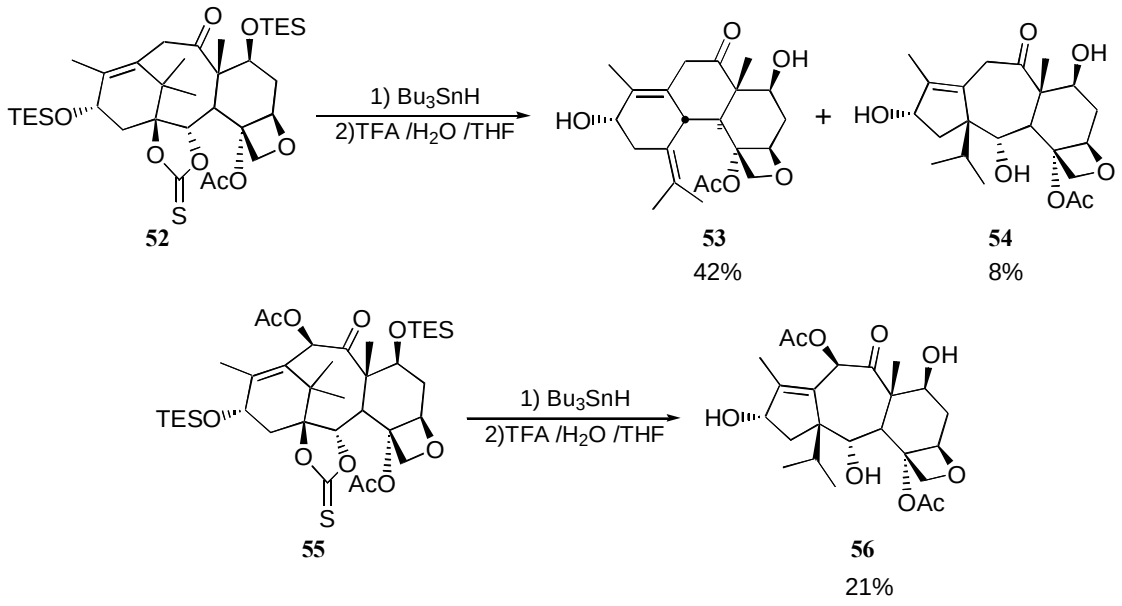

Figure 3.4

[128] Chen, S. H.; Huang, S.; Gao, Q.; Golik, J. and Farina, V. *J. Org. Chem*., **1994**, 59, 1475.

In the example below, Ziegler[129] observed that radical fragmentation of the six-membered ring thiocarbonate gave rise to a product that derived from a primary radical. The system then underwent cyclobutylcarbinyl fragmentation to yield the ring expansion product. The experiment was repeated after introduction of a deuterium label at a specific position. Scrambling of the label was observed indicating that preference for formation of the primary radical was not due to bond overlap in a concerted process. Also, examination of structural models suggests that both C-O bonds have good orbital overlap for fragmentation.

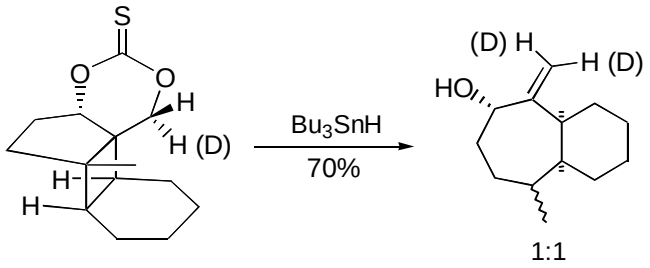

[129] Ziegler, F. E.; Zheng, Z. L. *J. Org. Chem*, **1990**, 55, 1416.

Further studies of this reaction, in a simplified system, showed that the four-membered ring was not required for the observed course of bond cleavage of the cyclic thionocarbonate.

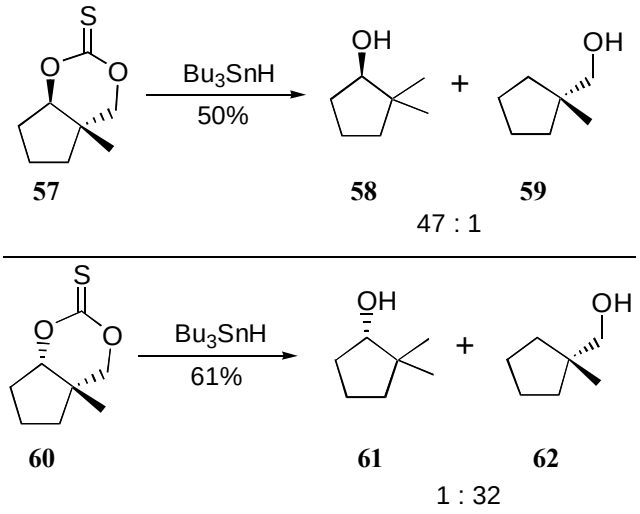

Figure 3.5

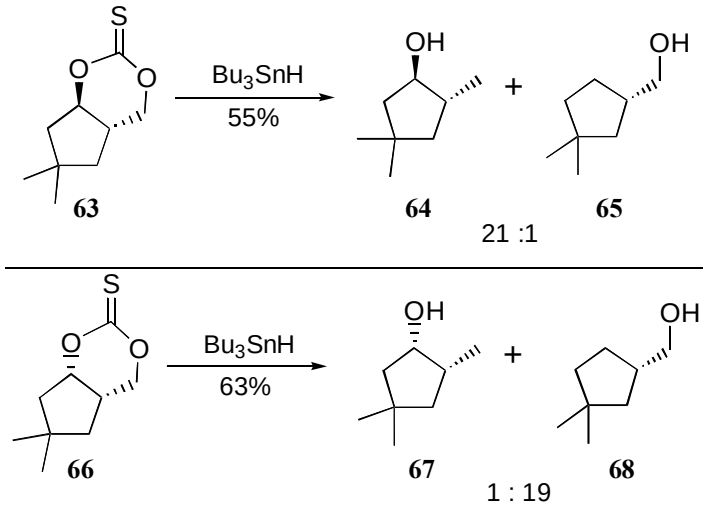

Figure 3.6

The stereochemistry at the ring junction between the five-membered ring and the cyclic thionocarbonate controls the selectivity of the fragmentation reaction (Figures 3.5 and 3.6). When the ring junction between the cyclic thionocarbonate and the five-membered ring is *trans* (compounds **57** and **63**), fragmentation of the cyclic thionocarbonate will favor the product deriving from the primary radical (compounds **58** and **64**) at a ratio of 47:1 and 21:1 respectively. When the ring junction is *cis* (compounds **60** and **66**), the major product is derived from the secondary radical (compounds **62** and **68**) at a ratio of 1:32 and 1:19 respectively. Experimental results suggest that local steric aspects do not play a role in the selectivity, as the reaction is successful with (Figure 3.5) and without (Figure 3.6) the methyl group substitution at the ring junction. The observed *cis*-*trans* selectivity suggests that relief of strain during the fragmentation reaction, due to difference in the conformation adopted by the molecules, is the causative agent.

Barton reports[124] suggest that the stability of the radicals is the dominant factor in determining selectivity, while the experiments conducted in the Ziegler lab support Ruchardt's theory[125] that strain plays a crucial role in determining the selectivity in the radical formation. Given these different views, a more in depth analysis of the selectivity issues for thionocarbonate fragmentation was explored.

Initially, an attempt to model the transition state for the radical cleavage reaction was done using the software package MacroModel.[130] The transition state was mimicked by stretching the bond that would eventually cleave to generate the radical. The simulations were carried out on the carbonate equivalent of the 6-5 thionocarbonate

[130] MacroModel v 4.5 developed by Prof. Clark Still at Columbia University.

simplified model system shown above. Primary and secondary radical formation was examined. These studies concluded that bond-angle-bending strain plays a major role in the regioselectivity of these reactions.

In an attempt to get a better understanding of what was determining the selectivity, *ab initio* calculations were used to evaluate the fragmentation reaction. The *ab initio* method offers the opportunity to examine the energy, charge distribution and geometry of each of the intermediate radicals and transition states involved in the fragmentation. Geometry calculations were conducted on a simplified version of the fragmentation system. Initially, a series of molecules were examined to determine if there was something inherently different about the 6-5 ring system (molecules **9**-**12**) versus a 6-6 ring system (molecules **5**-**8**) or a dimethyl substituted six-membered ring thionocarbonate (molecules **1**-**4**), in the context of *cis* versus *trans* substitution. Details about how the calculations were carried out and the specific results obtained can be found in Addendum 4. Here will be presented the conclusions derived from the calculations.

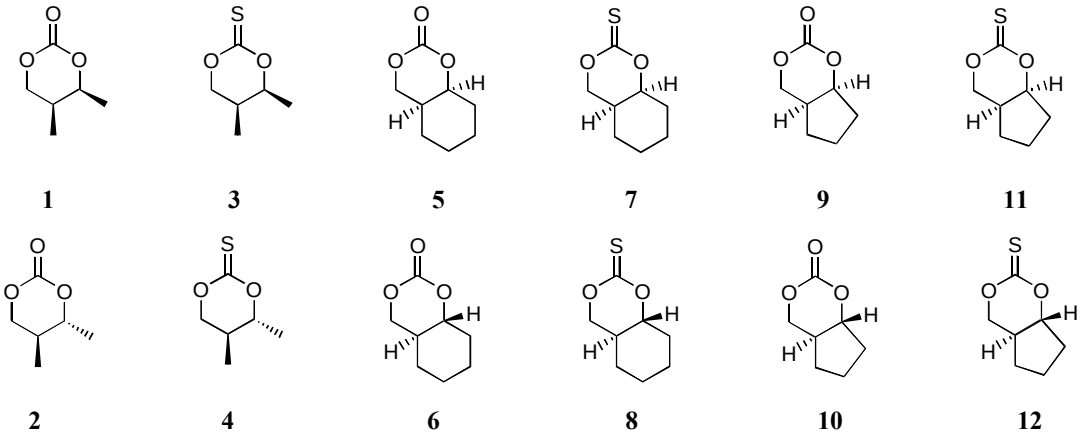

1 **3** **5** **7** **9** **11**

2 **4** **6** **8** **10** **12**

The results from the *ab initio* calculations conducted on compounds **1** through **12** demonstrated that *cis* and *trans* molecules have similar energies (Figure 3.7a). The charge distribution results indicated that charge was not a factor in determining the selectivity. Angle-offset[131] calculations showed that the carbonates display a smaller offset than the respective thionocarbonates except for the 6-5 series (compounds **9**, **10**, **11** and **12**) in which the offset associated with *cis* thionocarbonate **11** is smaller than its carbonate counterpart (Figure 3.7b).

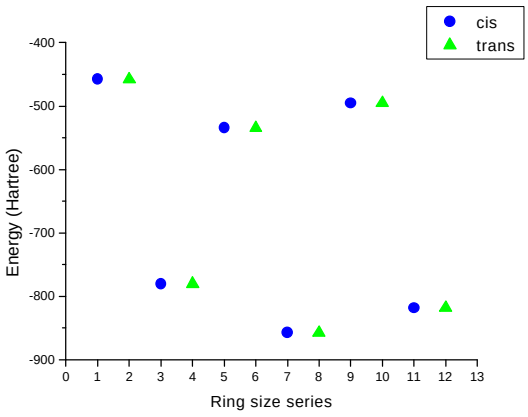

Compound Number	Total Offset	Energy (Hartree)
1	0.7587	-457.6375
2	0.7741	-457.6393
3	0.8198	-780.2564
4	0.8298	-780.2582
5	0.7533	-534.5498
6	0.6915	-534.5501
7	0.8147	-857.1689
8	0.7375	-857.1689
9	0.8878	-495.5063
10	1.2122	-495.4997
11	0.3847	-818.1251
12	1.2646	-818.1182

Figure 3.7 (a) Energy calculation

[131] Angle-offset calculations based on the minimized geometries obtained from the *ab initio* calculations mimc the effect of bond-angle-strain energy associated with these molecules. See Addendum IV for more details.

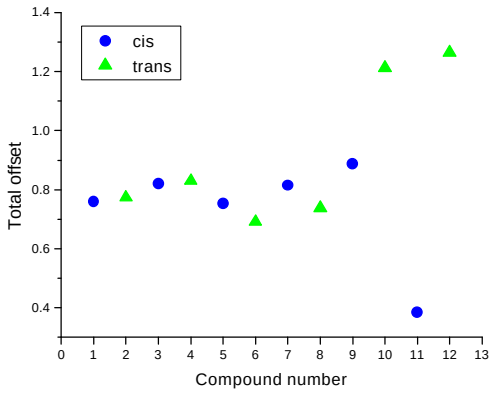

Figure 3.7 (b) Angle-offset estimation

Additionally, the fragmentation reaction itself was examined starting from molecule **11**, representing the *cis* configuration and **12**, representing the *trans* configuration.

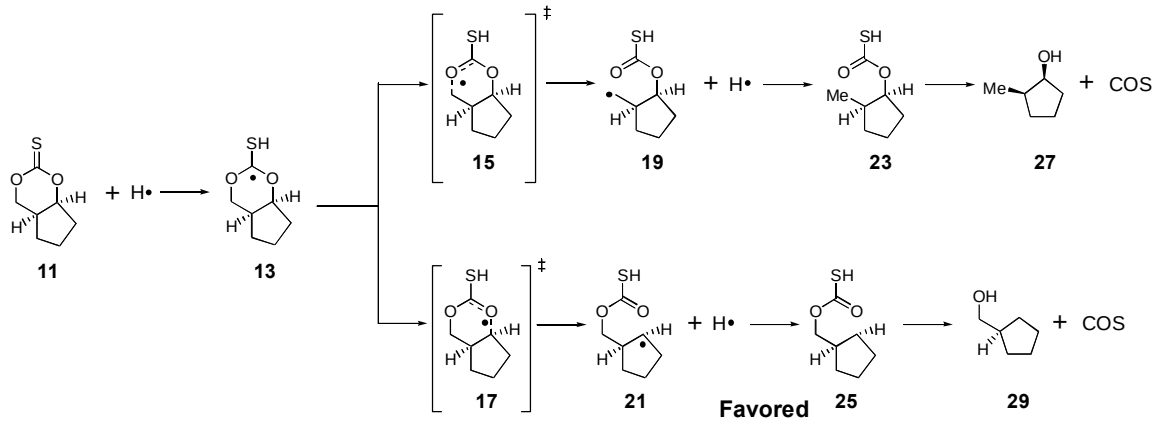

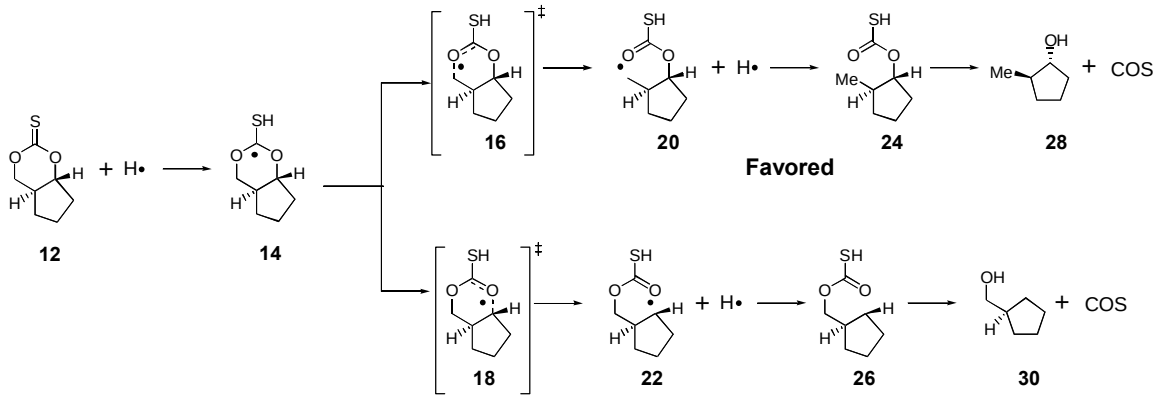

Simple thermodynamical analysis of the reactions (see the graph and chart in Figure 3.8) would indicate preference for the formation of the secondary radical (**21** and **22**) in both the *cis* and the *trans* series. Secondary radical **21** is more stable than primary radical **19** by 6.36 x 10^{-4} Hartrees (0.399 Kcal/mol) which should give an approximate 2:1 selectivity[132] at 25 ^{o}C for formation of the secondary radical. Meanwhile, the secondary radical **22** is more stable than the primary radical **20** by 2.04 x 10^{-3} Hartrees (1.28 Kcal/mol) which should give an approximate 6:1 selectivity at 25 ^{o}C for formation of the secondary radical. This agrees with what is expected based on stability of secondary *versus* primary radical analysis but is not in agreement with the experimental observation that the primary radical (**20**) is the preferred product for the *trans* system.

[132] Based on $\Delta G = - RT \ln K$ where R= 1.9872 cal/molK.

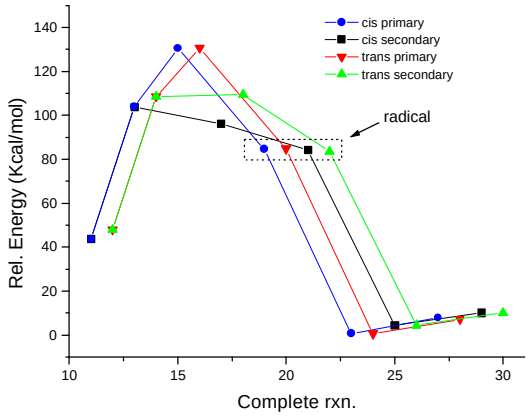

Compd. Number	Energy (Hartree) ab initio		Rxn. Energy (Hartree) ab initio	Rxn. Energy (Kcal/mol) relative
11	-818,1251	H-H	-819,2519	43,6499
12	-818,1182	H-H	-819,2450	47,9797
13	-818,6578	H•	-819,1560	103,8280
14	-818,6504	H•	-819,1486	108,4716
15	-818,6152	H•	-819,1134	130,5599
16	-818,6489	H•	-819,1134	130,5599
17	-818,6699	H•	-819,1681	96,2352
18	-818,6489	H•	-819,1471	109,4129
19	-818,6884	H•	-819,1867	84,5823
20	-818,6881	H•	-819,1863	84,8082
21	-818,6891	H•	-819,1873	84,1807
22	-818,6901	H•	-819,1884	83,5281
23	-819,3204		-819,3204	0,6843
24	-819,3205		-819,3206	0,5713
25	-819,3145		-819,3145	4,3489
26	-819,3145		-819,3145	4,3489
27	-309,0482	COS	-819,3088	7,9195
28	-309,0497	COS	-819,3103	7,0033
29	-309,0447	COS	-819,3053	10,1157
30	-309,0447	COS	-819,3053	10,1157
H•	-0,4982			
COS	-510,2606			
H-H	-1,1268			

Figure 3.8

For the *cis* reaction, analysis of the offset-from-the-ideal-angle associated with the ring portion of each intermediate of the fragmentation process showed an increase in the offset for the formation of both radicals. Formation of the primary radical (**13** to **19**) resulted in a change in ring-offset of 0.12, while the formation of the secondary radical (**13** to **21**) resulted in a change in ring-offset of 0.21, as shown in the graph in Figure 3.9.

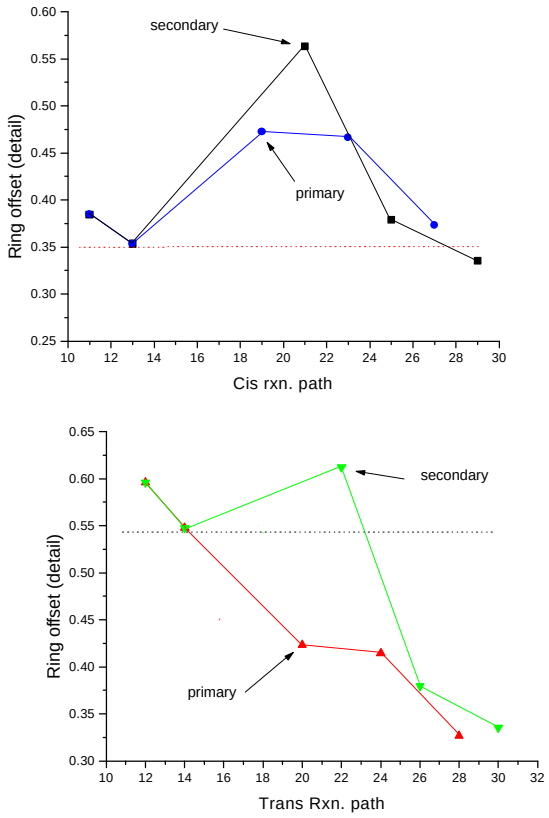

Compound Number	Total Strain	Ring Strain
11	0,3847	0,3847
12	1,2646	0,5961
13	1,1524	0,3535
14	1,3420	0,5476
15	1,7867	0,3979
16	1,5677	0,4528
17	6,5950	2,9316
18	1,2623	0,5476
19	0,9894	0,4723
20	0,9370	0,4230
21	1,1768	0,5634
22	1,2241	0,6124
23	0,9933	0,4667
24	0,9351	0,4144
25	0,9949	0,3792
26	0,9949	0,3792
27	0,9197	0,3733
28	0,8803	0,3266
29	0,8493	0,3352
30	0,8493	0,3352

Figure 3.9 (a) Ring Offset-cis rxn path; (b) Ring Offset-trans rxn path

For the *trans* reaction, the two possible radicals show opposite trends. Formation of the primary radical (**14** to **20**) is favored due to decrease in ring-offset of 0.13. Formation of the secondary radical (**14** to **22**) is unfavorable due to an increase of ring-offset of 0.07 (see Figure 3.9).

Based on these observations, it may be concluded that the *trans* series selectivity is controlled by the release of the offset-from-the-ideal-angle associated with the ring portion of the intermediates, while thermodynamics (*via* formation of the more stable secondary radical) controls the *cis* series selectivity. The *trans* series has greater overall offset-from-

the-ideal-angle than the *cis* series and therefore changes in the offset are proportionally more important and thus play a bigger role in defining selectivity towards formation of the primary radical and overcomes the thermodynamical tendencies of the system.

2. Beta-oxygen effect

The reaction rate of radical formation is accelerated by the presence of an oxygen substituent beta to the site of radical formation. Barton[133] first reported the β-oxygen effect where he stated that "various thiocarbonyl esters bearing alkoxy or acyloxy groups in the β-position underwent deoxygenation upon treatment with tri-butyltinhydride at lower temperatures than the corresponding unsubstituted species". He explained this result by stating that the "β-bonded oxygen has a marked effect in stabilizing carbon radicals thus permitting homolytic fission not seen otherwise".

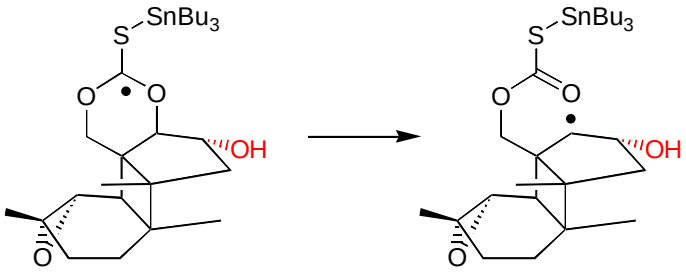

Figure 3.10

Beckwith[122] further investigated Barton's results and found that the β-oxygen effect was small, corresponding to a difference of only 1 Kcal/mol in activation energy at

110 °C. The observed reaction rates were faster for OH substituted substrates, but this was highly dependent on the conformation of the molecule. He observed that compounds that had a flexible frame did not exhibit the Barton β-oxygen effect and that in conformationally rigid species, stereochemistry played an important role in the magnitude of the effect. Further studies indicated that the results could be explained in terms of differing torsional and ring strain energies present in the various radicals. Beckwith suggested that relief of unfavorable dipolar interactions between synclinal carbon-oxygen bonds also played an important role and may be dominant in certain cases. This relief of dipolar interactions may be the underlying reason for the rate differences originally noted by Barton for highly functionalized acyclic systems, rather than stabilization effects. In the competition experiment shown in Figure 3.11, an axial xanthate was found to be more reactive than an equatorial xanthate when neither is subject to severe 1,3-diaxial steric interactions.

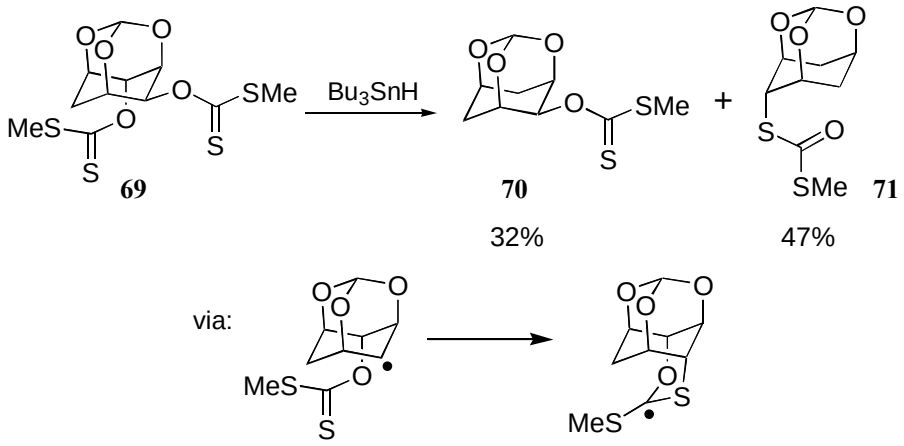

Figure 3.11

[133] Barton, D. H. R.; Hartwig, W.; Motherwell, W. B. *J. Chem. Soc. Chem. Comm.* **1982**, 447.

Compound **69** has one xanthate group which has two synclinal β-oxygens substituents and another xanthate which has two antiperiplanar β-oxygens. The xanthate, adjacent to two synclinal β-oxygens, cleaved faster to give compound **71** in 47% yield. Cleavage of the xanthate adjacent to two antiperiplanar oxygens was slower affording compound **70** in 32% yield. This ratio of roughly 1:1.5 in favor of cleavage of the equatorial xanthate suggests that the original β-oxygen effect is at least in part stereoelectronic in nature (relief of the dipolar interactions) and is maximized when the scissile C-O bond is synclinal to the β–oxygen bond.

Contrary to the results from other conformationally rigid compounds mentioned earlier, Beckwith did not observe β-oxygen effects for the cyclic thionocarbonate shown below.

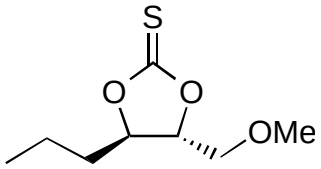

Given this observation, the fragmentation of the FS-2 precursor should experience no β-oxygen effect because it is also a rigid cyclic thiocarbonate. However, if there were a significant β-oxygen effect, one would expect that for the *cis* ring-junction fragmentation precursor, the selectivity towards the secondary site would be enhanced and for the *trans* ring-junction fragmentation precursor, the selectivity towards primary site would be diminished.

3. Fragmentation of Cyclobutylcarbinyl systems

Under normal circumstances, ring opening of a cyclobutylcarbinyl radical is not reversible,[134] especially in [3.2.0]bicyclohept-2-enyl radicals (**74**). The rate of ring closure of 5-pentenyl radical (**73**) was measured to be ~ 250 s^{-1} at 80° C and it was observed only when the cyclized form was stabilized by substituents.[134],[135] Substitution at the radical center has little effect on the magnitude of the fragmentation rate constant.

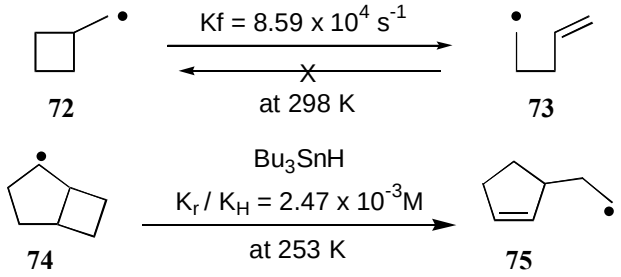

Figure 3.12

The cyclobutylcarbinyl radicals in this study were generated from the fragmentation of cyclic thionocarbonates (as shown in Figure 3.13, in red) and can fragment further to give either endocyclic or exocyclic bond cleavage.

[134] Beckwith, A. L. J.; Moad, G. *J. Chem. Soc. Perkin Trans. II*, **1980**, 1083.
[135] Castaing, M.; Pereyre, M.; Ratier, M.; Blum, P. M.; Davies, A. G. *J. C. Soc. Perkin II* **1979**, 287.

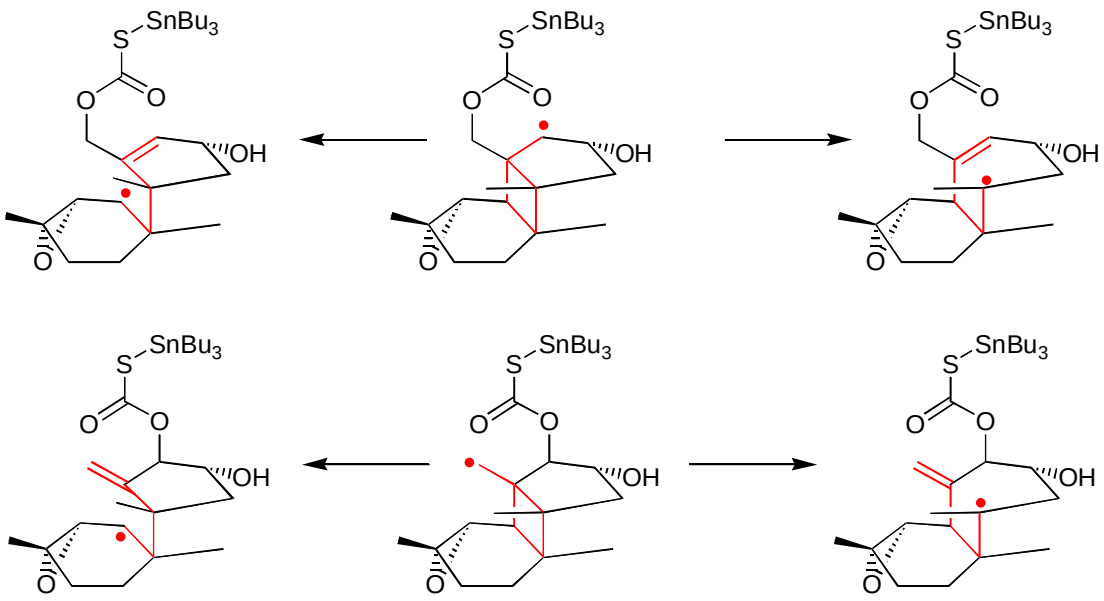

Figure 3.13

Based on thermodynamic calculations, Beckwith[134] demonstrated that the ring expansion product **77** arising from the fragmentation of [3.2.0]bicyclohept-2-enyl radicals **74** (endocyclic bond cleavage) is 2.0 Kcal/mol more stable than compound **76** (exocyclic bond cleavage). He proposed that the regiospecific ring opening of the bicyclic system to give the less stable product **76** is consistent with the view that β-fission requires efficient overlap between the semi-occupied orbital and the sigma orbital of the bond to be cleaved.[136] This is the opposite of what is seen in cationic examples where formation of the more stable cation directs the reaction towards endocyclic bond fragmentation[137].

---

[136] Batey, R. A.; Grice, P.; Harling, J. D.; Motherwell, W. B.; Rzepa, S. *J. Chem. Soc. Chem. Comm.* **1992**, 942.

[137] (a) Shubin, V. G. *Top. Curr. Chem.* **1984**, *116-117*, 267. (b) Olah, G. A.; Liang, G.; Mo, Y. K. *J. Am. Chem. Soc.* **1972**, *94*, 3544. (c) Prelog, V.; Trayham, J. G. In *Molecular Rerrangements*; de Mayo, P., Ed.; Wiley - Interscience: New York, **1963**, 593.

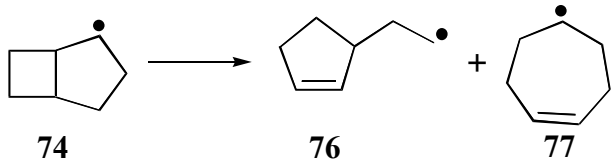

74 **76** **77**

Beckwith's prediction is supported by the results observed in a synthesis of (±)-silphinene (**80**),[138] where β-scission of the four-membered ring of compound **78** provided regiospecific introduction of the double bond in the natural product. No product deriving from the competing tertiary radical was observed.

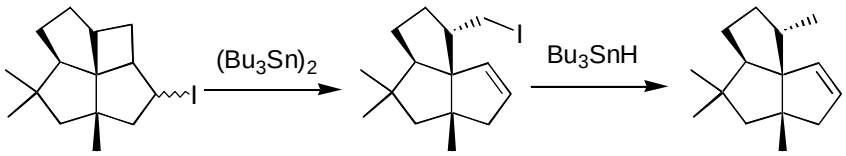

78 **79** **80**

Crimmins[139] explored the selectivity of the fragmentation of cyclobutyl carbinyl radicals by looking at substituent effects. When there were no substituents in the δ-position relative to the radical center (compound **81**), ring expansion was observed to give the more stable tertiary radical with cleavage of the endocyclic bond to give compound **82** in 80% yield. If instead, there was an electron-withdrawing substituent α to the carbonyl (δ to the radical center) as in the example shown for compound **83**, the product resulting from the exocyclic bond fragmentation (compound **84**) was obtained.

---

[138] Crimmins, M. T.; Mascarella, S. W. *Tetrahedron Lett.* **1987**, *28*, 5063.
[139] Crimmins, M. T.; Dudek, C. M.; Cheung, A. W. H. *Tetrahedron Lett.* **1992**, 33, 181.

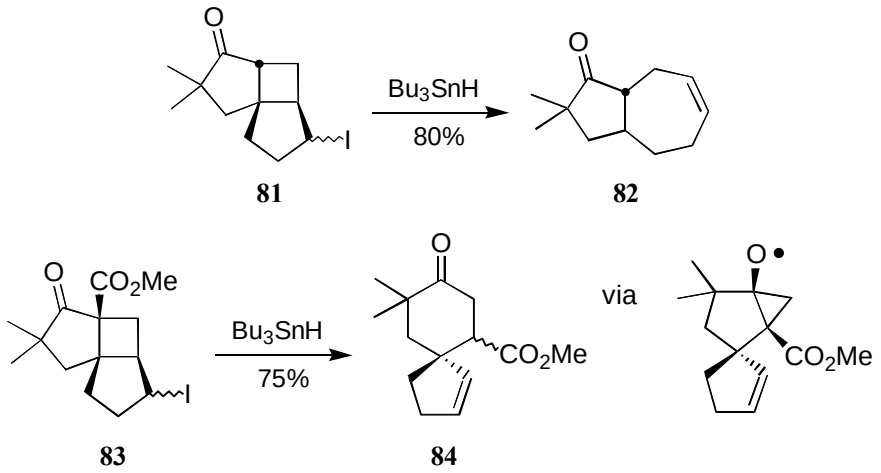

In the example shown in Figure 3.14 cyclobutylcarbinyl fragmentation of iodide **85** yielded only ring expansion products.[140] The more stable allylic radical was favored over formation of the secondary radical deriving from exocyclic bond cleavage. This selectivity was not based on orbital overlap, since good overlap is possible for breaking both bonds. Based on this experiment one could argue that the stability of the final radical determined the outcome of the reaction. Since there is no obvious difference in stability between the two possible allylic radicals, the final product was determined by the rate of hydrogen atom transfer. The slowest reducing system (SmI_2 / solvent) allowed for the formation of the more stable double bond and product **86** was the major product observed. For the faster reducing system (tri-butyltinhydride) the exocyclic double bond was favored and compound **87** was the major product observed.

[140] Lange, G. L.; Gottardo, C. *Tetrahedron Lett.* **1994**, 35, 6607.

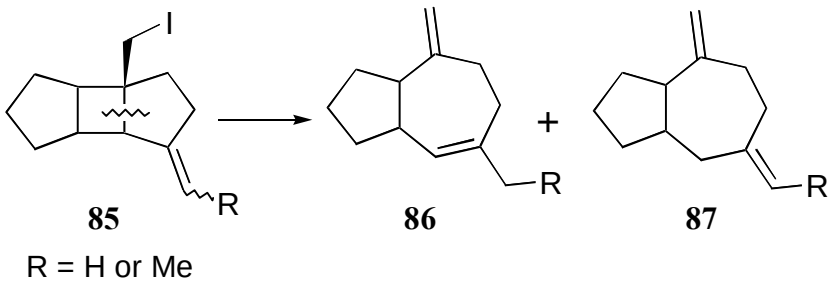

Figure 3.14

The results presented in this section are in agreement with the observation that cyclobutylcarbinyl radicals bearing substituents at the γ-position undergo ring opening to afford preferentially the more stable radical.[134] This can be explained on the basis that during bond fission the transition state is very product-like. The α-carbon has undergone little re-hybridization but the γ carbon is transformed from sp^3 to sp^2 hybridization and the resulting change in configuration relieves ring-strain. So for these radicals the rate and mode of fragmentation is dependent on strain release, orbital overlap and stability of the products formed.

4. Fragmentation of oxiranylcarbinyl radicals

In theory, oxiranylcarbinyl radicals can fragment in two possible ways: by breaking the C-O bond or the C-C bond. Based on simple bond dissociation energy, one would predict that epoxides would fragment the C-C bond preferentially by 5 Kcal/mol.[141]

[141] Lee, M. S.; Jackson, J. E. *Abstr Pap Am Chem Soc*. **1993**, *205*, 104.

However, if the dipolar nature of the transition state[142] is important in determining the course of the reaction, cleavage of the C-O bond would be the preferred pathway. Pasto[143] calculated that the activation barriers for fragmentation of the oxiranylcarbinyl radicals are 3.57 Kcal/mol for C-O bond cleavage and 14.7 Kcal/mol for breaking the C-C bond. This gives a difference of 11.13 Kcal/mol (or 6.7 Kcal/mol according to Jackson calculations)[144] in favor of C-O fragmentation (which would roughly correspond to 98% of C-O bond breaking to 2% of C-C bond breaking at 25 ^{o}C).

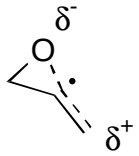

Experimentally it has been verified that the C-O bond is usually the preferred cleavage site, especially for alkyl substituted epoxides. However, C-C bond cleavage has been observed to occur when the cleaved radical product is stabilized by the presence of vinyl or aryl groups,[145] as shown below.

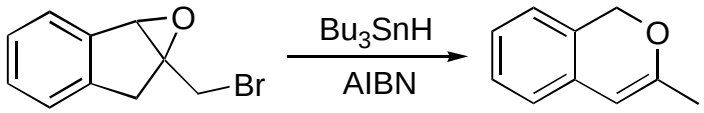

[142] Nonhebel, D. C.; Suarez, E. *Chem. Soc. Rev* **1993**, 347.
[143] Pasto, D. J. *J. Org. Chem.* **1996**, *61*, 252.
[144] Jackson (see ref. 141) calculated the activation barrier for C-O bond cleavage at 4.8 Kcal/mol and for C-C cleavage at 11.5 Kcal/mol.
[145] Murphy, J. A.; Patterson, C. W. *Tetrahedron Lett.* **1993**, 34, 867.

If the desired exocyclic bond cleavage is the favored pathway for the fragmentation of the cyclobutylcarbinyl radical under study, an oxiranylcarbinyl radical will be the product of the reaction. This product can fragment further to give C-O or C-C bond cleavage as shown on Figure 3.15. Cleavage of the C-O bond is expected to be the preferred pathway since there is no vinyl or aryl stabilization to favor C-C cleavage.

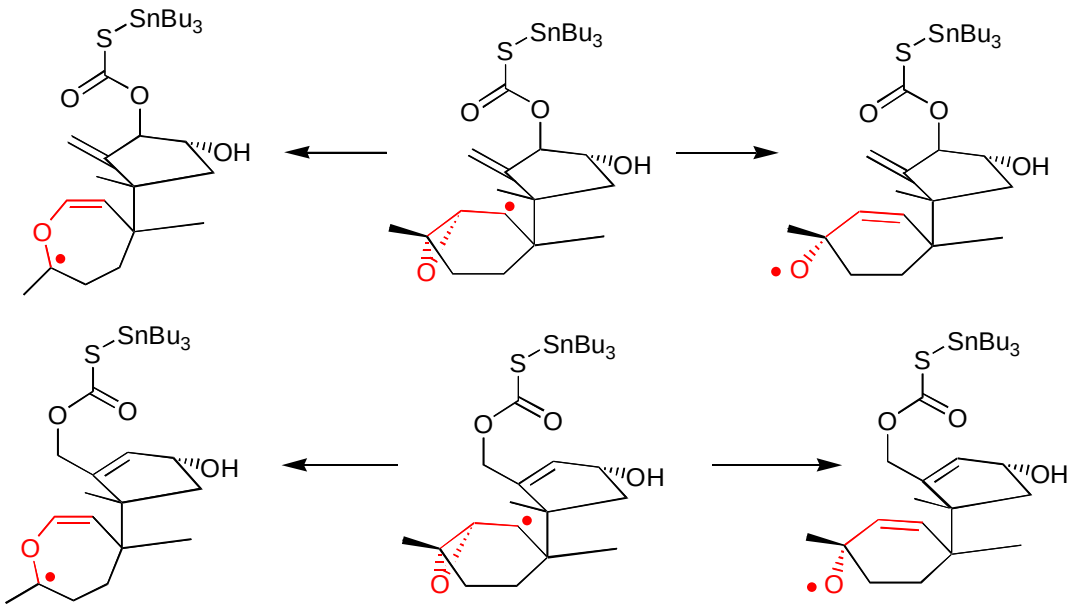

Figure 3.15

Rawal[146] measured the C-O bond cleavage rate at 3.2 x 10^{10} s^{-1} at 30° C as shown below. Ziegler's experiments[147] demonstrated that the opening of oxiranylcarbinyl radical is reversible, reporting the rate of the reverse reaction at 2 x 10^{9} s^{-1} at 80° C. Jackson and Pasto's calculations corroborates these results, predicting fast equilibrium between the

[146] Krishnamurthy, V.; Rawal, V. H. *J. Org. Chem.* **1997**, *62*, 1572.

closed form and the C-O cleaved form based on the low activation barrier and the "near thermo-neutrality" of the system (ΔH = -2.6 Kcal/mol). Additionally, Scaiano measured the quenching step for alkoxide radicals at 2.2 x 10^8 M^{-1} s^{-1}.[148]

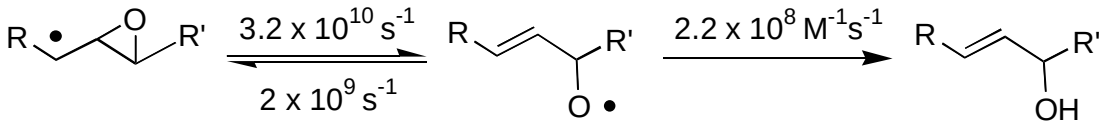

The reactivity of the alkoxide radical formed upon fragmentation must be examined. It is possible for this radical to undergo hydrogen shift or cyclize; further fragmentation of the six-membered ring was not considered a real possibility in the system under investigation.

Some literature examples were examined in order to illustrate the reactivity of alkoxide radicals. For instance, in the example below,[149] when compound **88** was submitted to fragmentation conditions the radical which derived from C-O cleavage of the oxiranylcarbinyl radical could be quenched as allylic alcohol **90** or could undergo 1,5-hydrogen shift, which was then followed by 1,5-cyclization to give the alcohol **89**.

---

[147] Ziegler, F. E.; Petersen, A. K. *J. Org. Chem.* **1994**, 59, 2707 and Ziegler, F. E.; Petersen, A. K. *J. Org. Chem.* **1995**, *60*, 2666.
[148] Scaiano, J. C. *J. Am. Chem. Soc.* **1980**, *102*, 5399.
[149] Rawal, V. H.; Newton, R. C.; Krishnamurthy, V. *J. Org. Chem.* **1990**, 55, 5181.

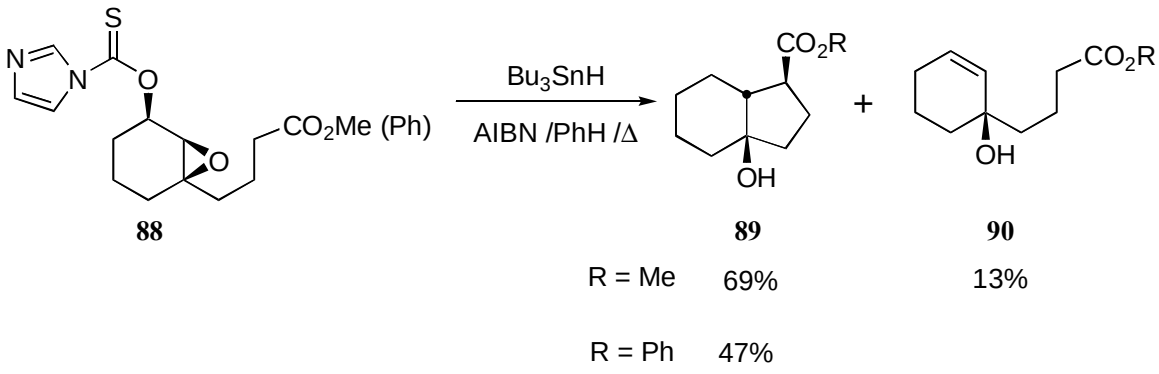

88 **89** **90**

R = Me 69% 13%

R = Ph 47%

The possibility of further fragmentation of the alkoxide radical is considered in the two examples below. In the first example, [150] in Figure 3.16, the ester group directs the fragmentation of the six-membered ring from the oxygen-centered radical towards ring expansion.

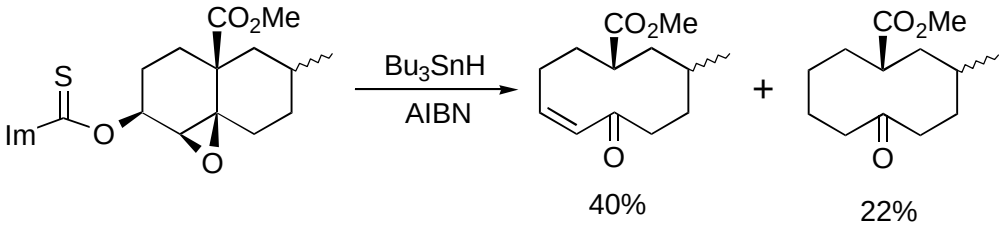

40% 22%

Figure 3.16

For the second example,[151] in Figure 3.17, epoxide fragmentation is followed by fragmentation of the external bond of the cyclohexane. The final product was derived from exocyclic bond cleavage, likely due to the greater stability of the tertiary radical. Exocyclic bond fragmentation also results in greater strain release for the system.

[150] Corser, D. A.; Marples, B. A.; Zaidi, N. A. *Tetrahedron Lett.* **1989**, 30, 3343.

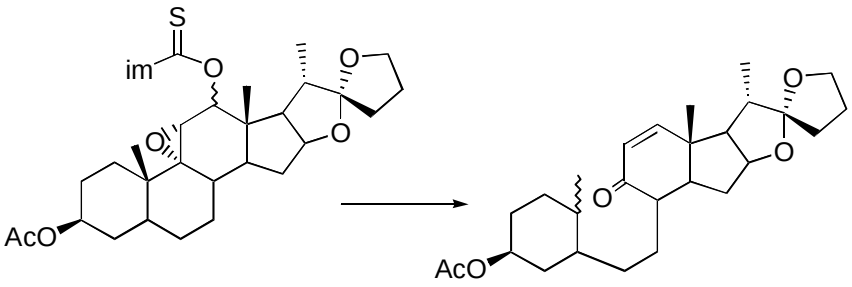

Figure 3.17

To address the issue of further cyclization of the alkoxide radical, an example was found in which the possibility of cyclization was in competition with fragmentation of cyclopropylcarbinyl radical as shown in the Figure 3.18. In this example, [152] β-scission of the C-C bond was shown to occur faster than the radical could cyclize. Based on this result and on direct competition experiments between fragmentation of cyclopropylcarbinyl and oxiranylcarbinyl radicals where only products deriving from epoxide fragmentation were observed,[153] C-O bond cleavage should also be faster than the competing cyclization reaction.

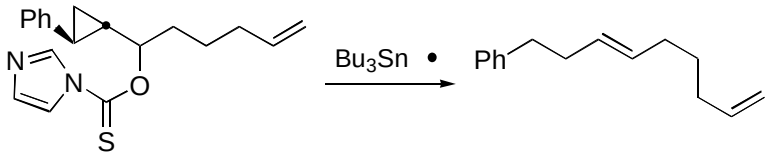

Figure 3.18

[151] Barton, D. H. R.; Motherwell, R. S. H.; Motherwell, W. B. *J. Chem. Soc. Perkin Trans. I* **1981**, 2363.
[152] Johns, A.; Murphy, J. A.; Patterson, C. W.; Wooster, N. F. *J. Chem. Soc. Chem. Comm.* **1987**, 1238.
[153] Newcomb, M.; Glenn, A. G. *J. Am. Chem. Soc.* **1989**, *111*, 275.

- *Preparation of the model systems*

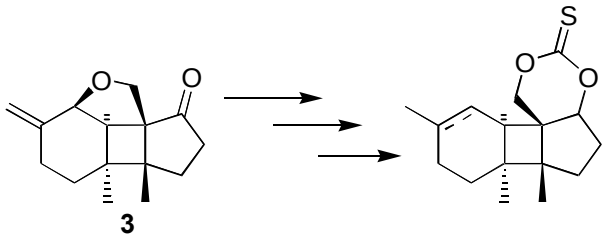

3

The preparation of model systems to test the fragmentation step required the elaboration of intermediate **3** into a series of compounds containing the six-membered ring cyclic thionocarbonate fused to [3.2.0]bicycloheptane ring-system. This transformation required the reduction of the carbonyl, reduction of the cyclic ether and preparation of the cyclic thionocarbonate.

1. Model system 1

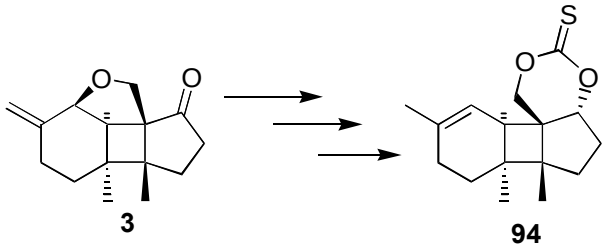

3 **94**

The first model system (cyclic thionocarbonate **94**) was constructed with the objective of determining the selectivity of the cyclic thionocarbonate fragmentation. The *trans* ring junction between the five-membered ring and the cyclic thionocarbonate should induce formation of the primary radical upon C-O bond cleavage. This model system

would also serve to verify if the cyclobutylcarbinyl radical would fragment *via* endocyclic or exocyclic bond cleavage.

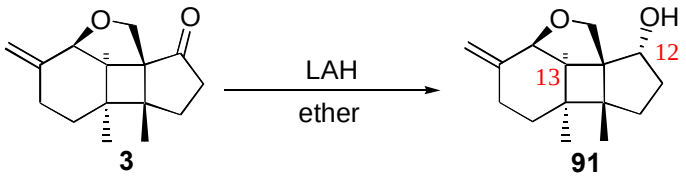

3 **91**

Reduction of the ketone in compound **3** was accomplished successfully using lithium aluminum hydride at 0° C (Et_2O, 89% yield) giving the desired alcohol **91**. Hydride was delivered from the less hindered face of the molecule to yield the hydroxyl group at C-12 in the α-configuration. No by-product due to reduction of the allylic ether was observed. The relative stereochemistry of the hydroxyl in the final product was confirmed by 1D-proton difference NOE experiments. The absence of an NOE between H-12 and H-13, which was seen for compound **100**, confirmed the R relative stereochemistry of the hydroxyl at C-12 (see Addendum I for details). A 2D-proton COSY experiment was used to aid in the peak assignments.

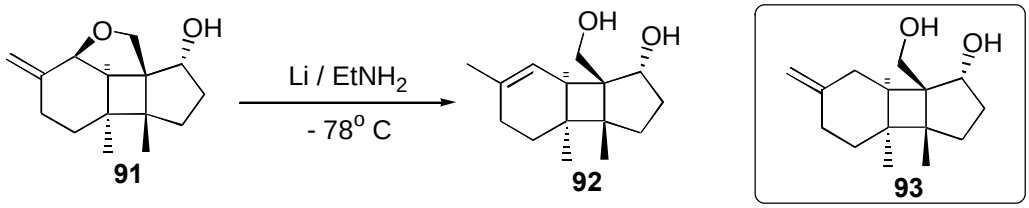

91 **92** **93**

The allylic ether in alcohol **91** was reduced at -78° C by lithium in liquid ethylamine. This two-electron reduction generated an allylic radical that, upon further

reduction, gave olefin **92** in 91% yield with the double bond in the more stable position. When the reaction was carried out using liquid ammonia, instead of ethylamine a mixture of the desired product was isolated along with the terminal di-substituted double bond side-product **93** at an approximate 1:1 ratio.

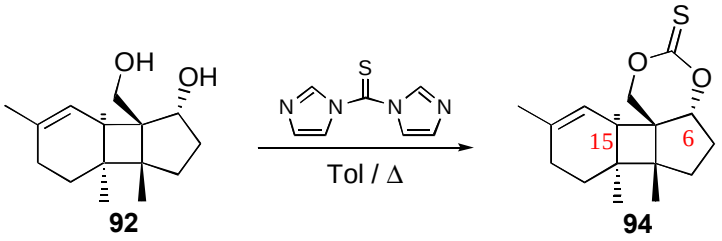

Preparation of the cyclic thionocarbonate **94** was carried out by reaction of diol **92** with thionocarbonyl diimidazole in toluene at reflux. More than one equivalent of the thionocarbonyl reagent was necessary for the reaction to go to completion, as the reagent apparently decomposed under these conditions. To prevent formation of the di-substituted product, a total of 2.3 equivalents of the reagent was added in three separate portions during the course of the reaction. The desired product **94** was obtained in 85% yield after it was separated from a small quantity of the di-substituted by-product. The absence of an NOE from H-6 to H-15 in the 1D-proton difference NOE experiments, compared to the results obtained for other compounds with similar structures, confirmed the R relative stereochemistry at C-6 for the cyclic carbonate portion of this fragmentation precursor (see Addendum I for details).

2. Model system 2

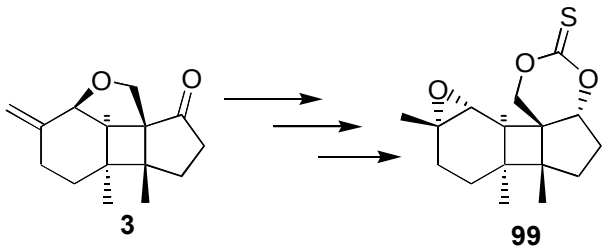

The second model system (epoxide **99**) represents a more advanced intermediate towards the synthesis of FS-2. The *trans* ring junction should once more induce formation of the primary radical upon C-O bond cleavage. The presence of the epoxide functionality enables an evaluation of the impact it may have on the system in terms of possible changes in the selectivity of the cyclobutylcarbinyl radical fragmentation.

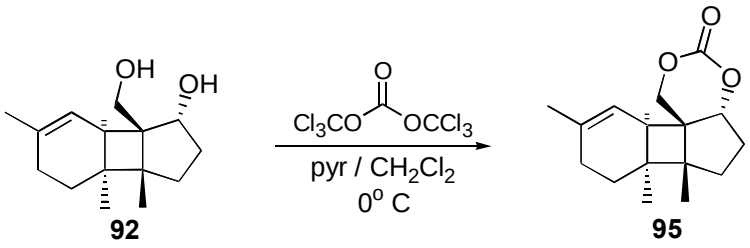

Carbonate **95** was prepared by reaction of the diol **92** with triphosgene (pyridine, CH_2Cl_2 at 0^o C) and it was isolated in 90% yield. Attempts to directly convert the carbonate into a thionocarbonate by reaction of compound **95** with Lawesson's reagent[154]

[154] Cava, M. P.; Levinson, M. J. *Tetrahedron* **1985**, *41*, 5061. Cherkasov, R. A. *Tetrahedron* **1985**, *41*, 2567. Clausen, K. *J. Chem. Soc., Perkin Trans. I* **1984**, 785. Jensen, O. E. *Tetrahedron* **1985**, *41*, 5595. Thomsen, I. *Org. Synth.* **1984**, *62*, 158.

(toluene, reflux) were only partially successful. The desired thionocarbonate product **94** was obtained, at best, in 30% yield and the remainder corresponded to base-line material.

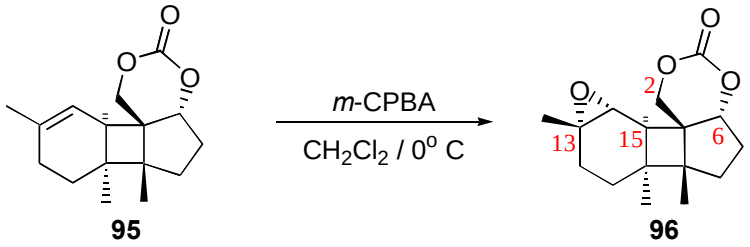

95 **96**

Diastereotopic face selective epoxidation of olefin-carbonate **95** was conducted by reaction with *meta*-chloroperbenzoic acid (*m*-CPBA) in CH_2Cl_2 at 0^o C and yielded epoxycarbonate **96** in 90 % yield. Oxidation occurred from the less hindered face to deliver the epoxide from the α-side of the molecule. 1D-proton difference NOE experiments were utilized to confirm the relative stereochemistry of the epoxide. An NOE observed between H-2α and H-14 confirmed the R relative stereochemistry at C-14. The absence of an NOE between H-6 and H-15 supported the assignment of the R relative stereochemistry for C-6 (see Addendum I for details). Since the attempts to directly convert the carbonate **95** into thionocarbonate **94** utilizing Lawesson's reagent were unsuccessful, it became necessary to investigate a new route to the installation of the thionocarbonate functionality *via* hydrolysis of the carbonate.

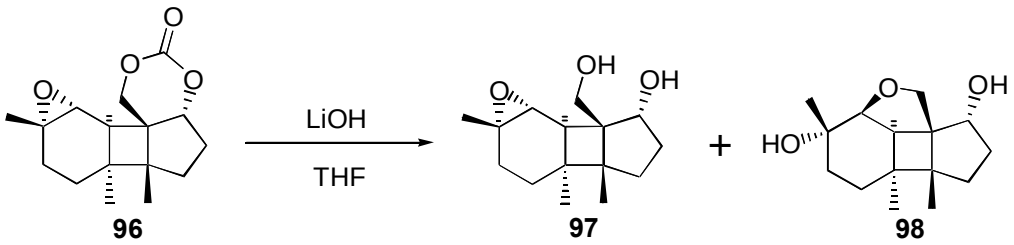

96 **97** **98**

Attempts to hydrolyze carbonate **96** under mild basic conditions (LiOH in THF at 0^{o} C) resulted in a mixture of products. The desired compound, diol **97**, was obtained in 16% yield while tetrahydrofuran **98,** a product of cyclization of the primary alcohol onto the epoxide, was isolated in 79 % yield. Attempts to perform this reaction under acidic conditions gave similar results.

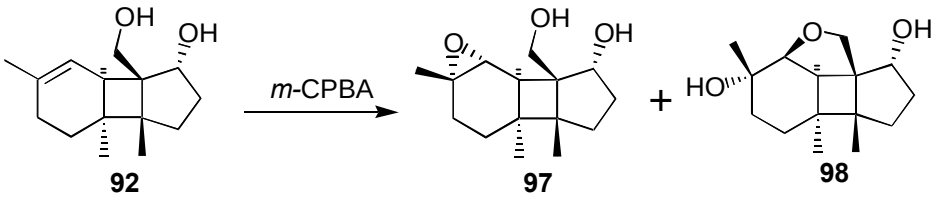

92 **97** **98**

Meta-chloroperbenzoic acid is usually thought of as a hydroxy-directed oxidizing agent due to formation of hydrogen bonds between a proximate hydroxyl and the reagent. Esters are generally used to prevent alcohols from directing the epoxidation,[155] which is why the epoxidation was originally carried out on the carbonate substrate **95**. Due to the problems associated with the hydrolysis of the carbonate and with the direct conversion to the thionocarbonate, the direct oxidation of diol **92** was attempted. Epoxidation of compound **92** with *m*-CPBA under buffered conditions ($NaHCO_3$, $CHCl_3$ and 0^{o} C) gave

compound **97** in 69% yield along with cyclic ether **98** in 17% yield. Oxidation occurred from the less hindered side of the molecule and no neighboring group effects were observed. The ^{1}H NMR spectrum of this epoxide product was identical to the ^{1}H NMR spectrum of the epoxide derived from hydrolysis of carbonate **96**, confirming that they had the same relative stereochemistry. Once diol **97** was isolated, it had to be used immediately to prevent cyclization to tetrahydrofuran **98**.

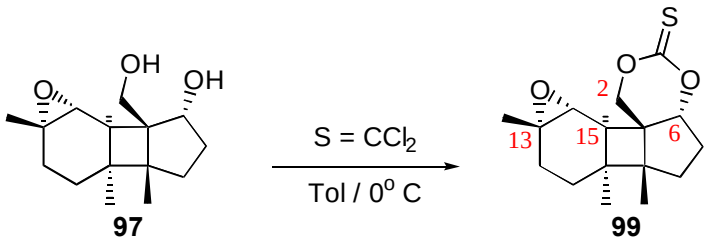

97 **99**

Reaction of diol **97** with thiophosgene (pyridine, toluene, 0° C) yielded the cyclic thionocarbonate **99** in 46 % yield. Attempts to perform the transformation with thionocarbonyl diimidazole at reflux temperature (as was done for compound **94**) failed, resulting in products derived from the opening of the epoxide. The ring opening was probably due to the high temperature necessary for the conversion; when the reaction was attempted at lower temperatures, only starting material was recovered. 1D-proton difference NOE experiments, along with 1D-proton decoupling experiments, confirmed the relative stereochemistry of the cyclic thionocarbonate and the epoxide. An NOE observed between H-2α and H-14 confirmed the R relative stereochemistry for the C-14

[155] Swern, D.; Dickel, G. B. *J. Am. Chem. Soc.* **1954**, *U*, 1957.

at the epoxide functionality. The absence of an NOE between H-6 and H-15 supported the R relative stereochemistry assignment at C-6 (see Addendum I for details).

3. Model system 3

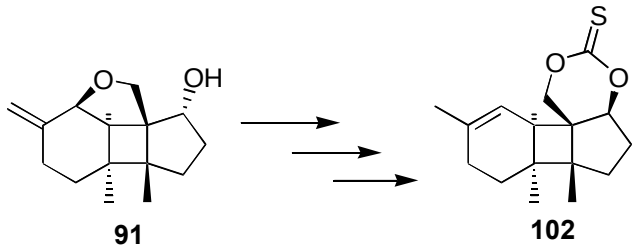

The third model system (cyclic-thionocarbonate **102**) enabled the examination of the selectivity of the fragmentation of the cyclic thionocarbonate in the environment of the *cis* ring junction. It also serves as a handle to determine if the fragmentation of the cyclobutyl carbinyl radical follows the same selectivity found in the first model system.

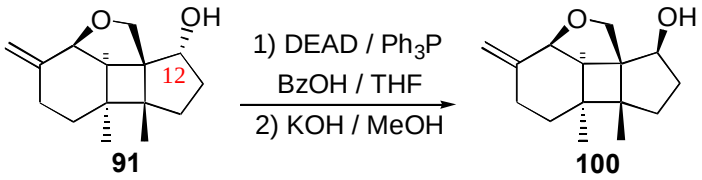

Mitsunobu inversion[156] of the hydroxyl group at C-12 was accomplished in two steps. First, reaction of α-alcohol **91** with triphenylphosphine and benzoic acid accompanied by slow addition of diethylazodicarboxylate (DEAD) generated the inverted

[156] Mitsunobu, O. *Synthesis* **1981**, 1.

benzoic ester at C-12 in 78% yield. Basic hydrolysis (KOH, MeOH at room temperature) of the newly generated ester gave alcohol **100** with the alcohol on the β-face of the molecule in 75% yield. 1D-proton difference NOE experiments were compared to those from α-alcohol **91**. An NOE observed between H-12 and H-13, which was absent on compound **91**, confirmed the S relative stereochemistry assignment for C-12 and agreed with the relative stereochemistry assignment shown for compound **100** (see Addendum I for details).

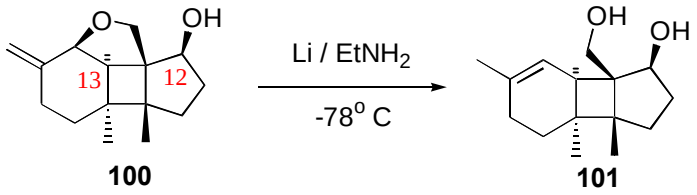

100 **101**

Reduction of the allylic ether portion of compound **100** followed the same procedure used for reduction of ether **91** (lithium in liquid ethylamine at -78° C), giving diol **101** in 97% yield.

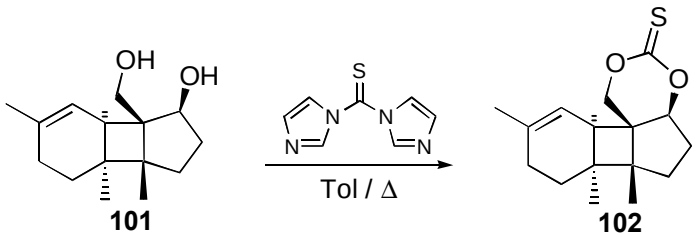

101 **102**

The final step for the assembly of thiocarbonate **102** required the transformation of the diol into a cyclic thionocarbonate. Reaction of diol **101** with thiocarbonyl diimidazole

in toluene at reflux yielded the desired product in 95% yield. No di-substituted by-product was observed because the formation of the desired product was rapid contrary to the results obtained for the *trans* ring-system.

4. Model system 4

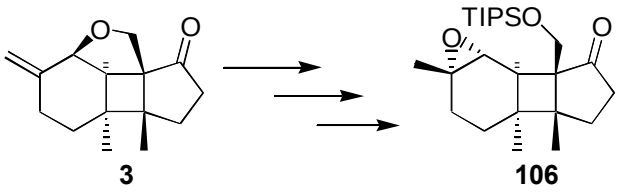

3 **106**

The concept for the fourth model system (ketone **106**) was to generate the secondary radical from a ketone by reaction with samarium diiodide. This study examines the importance of the thionocarbonate on the fragmentation. The cyclobutylcarbinyl radical is generated in the same position as if there were a *cis*-fused cyclic thionocarbonate in the molecule but through a different route.

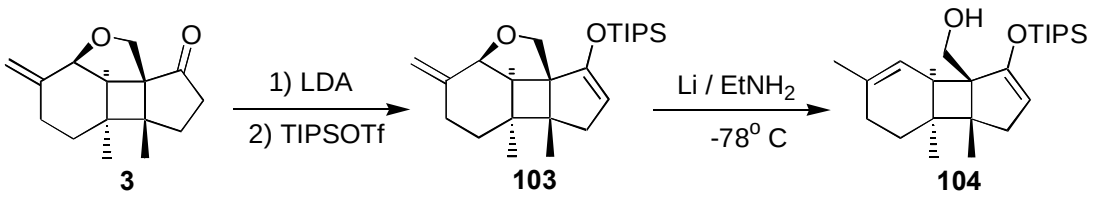

3 **103** **104**

Ketone **3** was protected by reaction with lithium diisopropylamide (LDA, THF, -78° C) then immediately treated with triisopropylsilyl triflate to form the TIPS enolether **103** in 87% yield. Reduction of the allylic ether was carried out with lithium wire in liquid ethylamine yielding silyl-enolether **104** in 95% yield. No reduction of the ketone was

observed under these conditions. Migration of the TIPS group to the primary alcohol was the major contaminant observed.

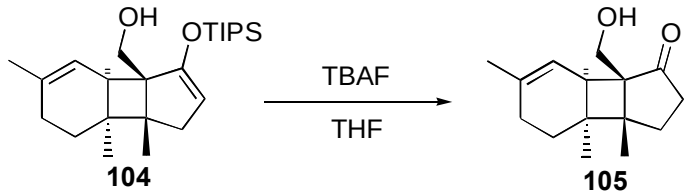

104 **105**

Deprotection of the ketone was accomplished by submitting silyl-enolether **104** to tetrabutyl ammonium fluoride in aqueous THF at 0^{o} C, giving keto-alcohol **105** in 73% yield.

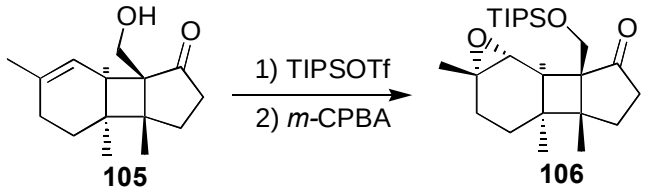

105 **106**

The primary alcohol in compound **105** was initially protected in the form of the tri isopropylsilyl ether (imidazole, DMAP, CH_2Cl_2, TIPSOTf) to prevent its participation during the epoxidation step. The reaction proceeded in 81% yield after purification of the product by silica gel flash chromatography. Epoxidation proceeded as desired (*m*-CPBA, $NaHCO_3$, CH_2Cl_2, 0^{o} C) with oxidation occurring from the less hindered side to give the epoxide on the α-face of the molecule. Keto-epoxide **106** was thus obtained in 62% yield.

- *Fragmentation of the model systems*

Radical fragmentation experiments were conducted under high dilution conditions (10^{-3} M), using the tributyltin hydride method.[118] Dry toluene was used as the solvent at reflux temperature and AIBN as the radical initiator. The reaction solution was degassed by freeze-pump-thaw technique prior to each experiment in order to suppress side products due to reaction with oxygen. A solution of the substrate dissolved in toluene was heated to reflux and a second solution containing Bu_3SnH and AIBN was added to the reaction mixture over a period of 6 hours.

The yields reported below are in percent of isolated products after purification by flash chromatography. The method chosen for the reaction work-up plays an important role on determining the amount and purity of the products. The oxidative work-up developed by Curran[157] was utilized with most success. The procedure consists of iodine oxidation to convert all tin by-products or excess tin hydride into tin halides, followed by treatment with DBU in wet ether to form a white solid which is then separated by filtering through a silica gel column using ether as the solvent.

[157] Curran, D. P.; Chang, C.-T. *J. Org. Chem.* **1989**, *54*, 3140.

1. Model system 1

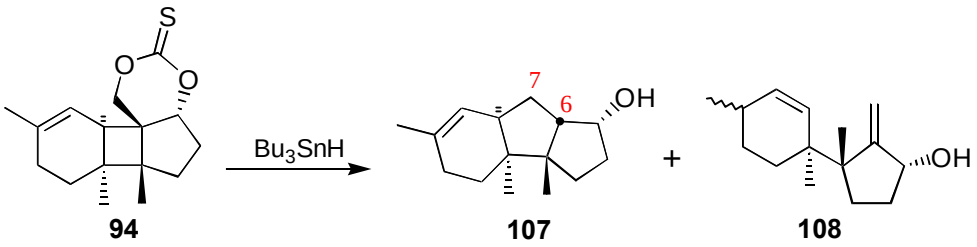

Fragmentation of *trans*-thionocarbonate **94** gave two products (**107** and **108**). Compound **107** was isolated in 47% yield and a ^{1}H NMR spectrum with 3 methyl singlet resonances at δ 0.79, 0.92 and 1.65 ppm (vinyl methyl) and one vinylic proton at δ 5.45 ppm was recorded. The structure was confirmed by conversion of the hydroxyl to acetate by treatment with excess acetic anhydride in pyridine. Observation of the shift of the ddd from δ 4.33 to 5.21 ppm (J = 6.5 Hz and 6.5 Hz) corresponding to the H-6, adjacent to the secondary alcohol, supports the structural assignment. Allylic alcohol **108** was isolated in 18% yield as a 3:1 mixture of diastereomers according to GC-MS analysis. The structure was confirmed by ^{1}H NMR which showed vinylic protons from δ 5.1 to 6.0 ppm corresponding to 4 protons (by integration) and a secondary hydroxyl at δ 4.41 ppm exchangeable with D_2O.

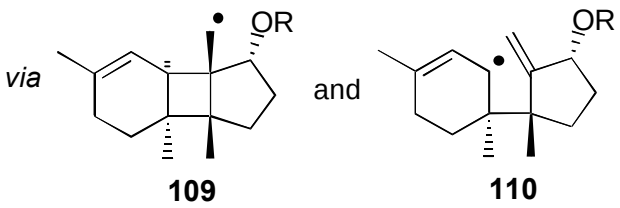

Both products **107** and **108** were derived from the fragmentation of the *trans* cyclic thionocarbonate to generate the radical at the primary center of intermediate **109** as expected. No product deriving from fragmentation to give the secondary radical was isolated or detected in the ^{1}H NMR spectra of the crude reaction mixture. The cyclobutylcarbinyl radical intermediate **109** fragmented further *via* cleavage of the exocyclic bond of the cyclobutane ring to give the more stable allylic radical **110**. No products deriving from ring expansion to give the tertiary radical were observed. The major product, tricyclo-dodecenol **107** derived from 1,5-cyclization of the allylic radical **110** with the terminal double bond generated after fragmentation of the four-membered ring. This hypothesis is corroborated by deuterium incorporation at C-6 when the fragmentation reaction was conducted with Bu_3SnD.

The results presented here for model system 1 were as predicted by Molecular Modeling calculations (see Addendum 4) and in agreement with previous examples studied in this lab. These results, however, are surprising in light of previous reports on four-membered ring fragmentations by Dowd[158] and Ziegler.[129] The ring expansion products were favored in both previous examples, rather than cleavage of the bond leading to the trichothecene skeleton.

[158] Zhang, W.; Dowd, P. *Tetrahedron*, **1993**, 49, 1965.

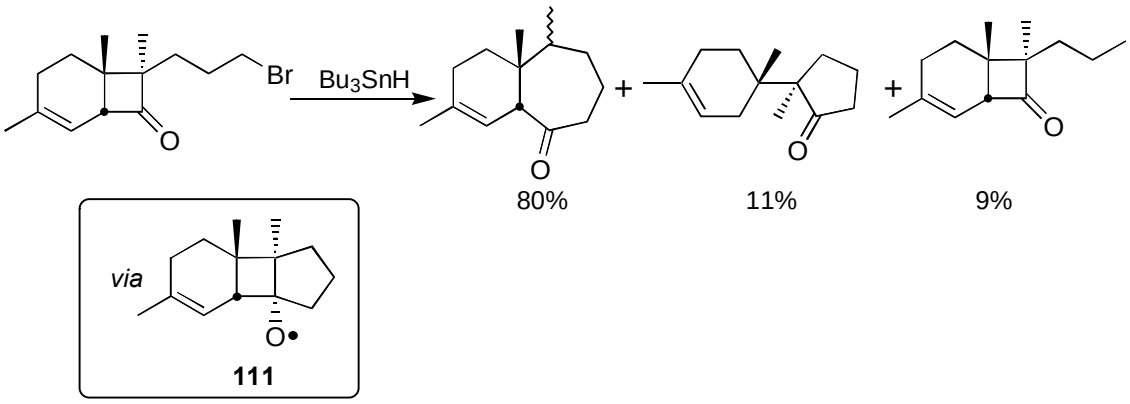

Dowd[158] studied 5-4-6 ring systems with an oxygen-centered radical, such as intermediate **111**, which is similar to intermediate **109** studied in the FS-2 synthesis. The cyclobutane ring can cleave to give a tertiary (ring expansion) or secondary allylic radical (trichothecene skeleton). For this oxygen-centered radical, the selectivity was found to favor the ring expansion product by an 8:1 ratio. He also studied the fragmentation of other related compounds.[159] The table below summarizes a comparison between other oxygen-centered radicals studied by Dowd (entries 1-5) and the carbon-centered radicals from the current study (entries 6 and 7).

[159] Dowd, P.; Zhang, W *J. Org. Chem.* **1992**, *57*, 7163. See also ref 158.

	Substrate	Radical Intermediate	Product Distribution: Ring Expansion	Exocyclic Fragmentation	Reduction
(1)	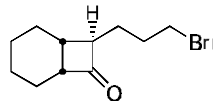	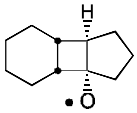	65%	16%	19%
(2)	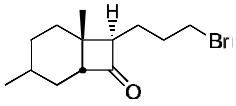	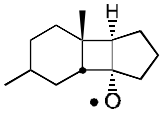	49%	14%	37%
(3)	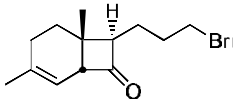	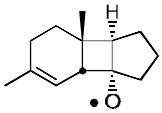	62%	X	38%
(4)	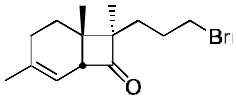	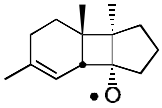	80%	11%	9%
(5)	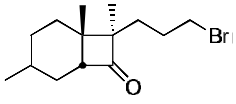	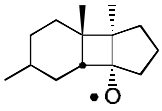	68%	22%	10%
(6)	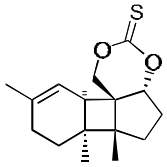	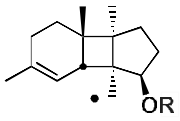	X	65%	X
(7)	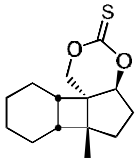	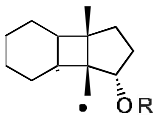	80%	X	X

Dowd demonstrated that the ring-expansion product is actually 1 Kcal/mol more strained than the trichothecene like product based on molecular mechanics calculations. Thus, it is not relief of strain that dictates the product distribution observed experimentally.

Comparison of the results obtained for entries 4 and 5 suggests that removal of the double bond in the six-membered ring favors cleavage of the bond leading to the trichothecene-like skeleton. Formation of the tertiary radical was favored over formation of the allylic radical in an 8:1 ratio (entry 4) while formation of the secondary radical was favored over formation of the allylic radical in a > 62:1 ratio (entry 3). Analysis of the results obtained for entries 3, 4 and 5 of the table indicates that the stability of the final radical does not determine the selectivity of the bond cleavage.

For the carbon-centered radicals, the product distribution suggests that the stability of the final radical determines the selectivity. Formation of the tertiary radical was favored over the secondary radical alternative in entry 7 and formation of the allylic radical was favored over the tertiary in entry 6. The possibility that the oxygen substituent, beta to the radical center, plays a role in deciding the selectivity was considered. However, the oxygen is adjacent to the radical at the starting point of the transformation and should not influence the final radical.

The release of strain is similar for both oxygen-centered radical **111** and carbon-centered radical **109**. The difference in the fragmentation selectivity for the two molecules may be a consequence of an early transition state for the oxygen-centered radical and a late transition state for the carbon-centered radical. If this is the case, bond overlap may play an important role for the oxygen-centered system while the stability of the product-radical may play an important role in determining the selectivity of the carbon-centered system.

Based on the result of the fragmentation of compound **94** into compound **107**, it was concluded that the lifetime of the allylic radical is long enough to allow 1,5 cyclization

to occur prior to termination. In competition with the cyclization is the reduction of the allylic radical generating compound **108**. The allylic radical favors the canonical structure with the more stable tertiary radical resulting in the product with the less stable di-substituted double bond.

2. Model system 2

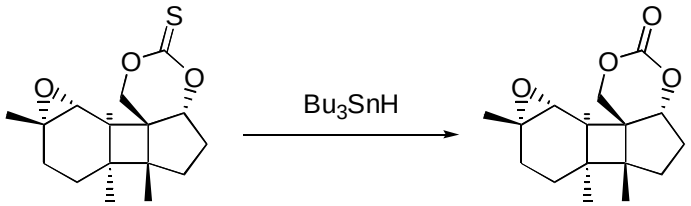

99 **96**

Isomerisation of the thionocarbonate **99** to the carbonate **96** was observed upon fragmentation of the second model system. The cyclic carbonate was isolated in 78% yield from the reaction mixture and was found to be identical to the product deriving from epoxidation of carbonate **95** with respect to TLC analysis, ^{1}H NMR and GC-MS trace. The fragmentation of compound **99** was carried out using the same stock solution used for compound **94**.

The isomerisation to compound **96** may be explained by postulating the formation of a 4-membered ring complex[160] in which the thiophilic tin atom changes its bonding

[160] Patroni, J. J.; Stick, R. V.; Tilbrook, D. M. G.; White, A. H.; Skelton, B. W. *Aust. J. Chem.* **1989**, 42, 2127.

partner with the carbon to form dibutyl tin sulfide. This transformation is driven by the conversion of the weak thionocarbonyl group into a stronger carbonyl group.

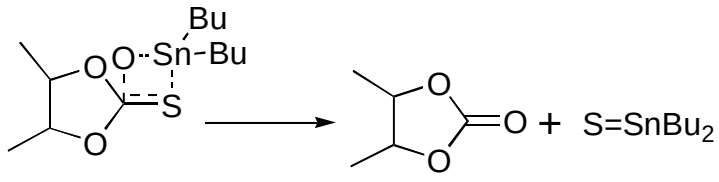

The other fragmentation reactions were not carried out due to lack of time or not enough material to characterize the reaction products.

- *Conclusion*

Starting from compound **3**, four model systems were built to test the selectivity of the radical fragmentation reaction proposed in the retrosynthetic analysis presented in chapter 1. Fragmentation experiments were conducted on two of the systems, model system 1 and 2. The results from model system 1 demonstrated that the stereochemistry at the ring junction between the six-membered cyclic thionocarbonate and the five-membered ring determined the selectivity of the cyclic thionocarbonate fragmentation. The *trans* stereochemistry led to formation of the primary radical (intermediate **109**). The resulting cyclobutylcarbinyl radical proceeded to cleave the bond leading to the more stable allylic radical, therefore unraveling the trichothecene-like skeleton. The results from model system 2 are unusual in that under these reaction conditions the thionocarbonate **99** isomerized into the carbonate **96**. This may suggest that there was some Bu_2SnO present

in the reaction mixture, either due to the presence of oxygen or air dissolved in the solution or due to aging of the Bu_3SnH reagent. Isomerisation to the carbonate was observed in two experiments, and in one case the reaction was run side by side to the fragmentation of the model system 1. No isomerisation of thionocarbonate **94** into carbonate **95** was observed which may suggest that the epoxide may play some role in the oxidation of the tin reagent. No other evidence for the oxidation was available since the experiment was not pursued.

This methodology offers a potential entry for the preparation of the family of trichothecene compounds *via* control of the stereochemistry at the ring junction of the cyclicthionocarbonates. The radical fragmentation of the cyclic thionocarbonate with the *cis* ring junction (Figure 3.19) can lead to the formation of trichothecenes with the FS-2 type skeleton *via* cleavage of the C-O bond leading to formation of the secondary radical. The radical fragmentation of the cyclic thionocarbonate with the *trans* ring junction (Figure 3.20) can lead to the formation of trichothecenes with the tricyclic type skeleton *via* cleavage of the C-O bond leading to formation of the primary radical followed by biomimetic cyclization[161] to assemble the final structure.

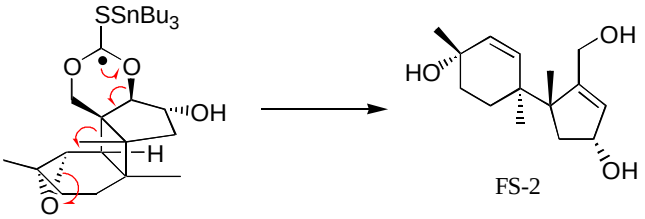

Figure 3.19

[161] (a) Masuoka, N.; Kamikawa, T. Tetrahedron Lett. 1976, 1691; (b) Masuoka, N.; Kanikawa, T.; Kubota, T. Chem. Lett. 1974, 751.

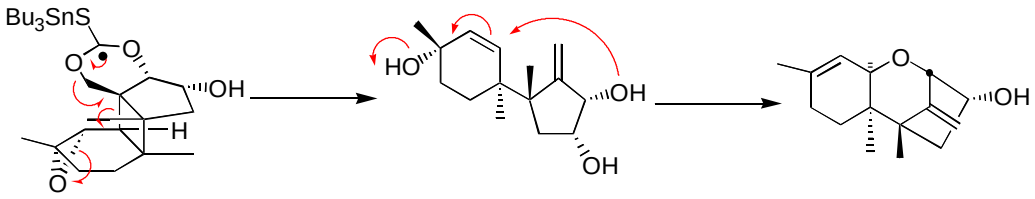

Figure 3.20

The selectivity observed for the fragmentation of model-system 1 encouraged the further development of intermediate **3** towards assemblage of the fragmentation precursor of FS-2. Work along this course is presented in detail in chapter 4.

CHAPTER IV: *ELABORATION OF THE FRAGMENTATION INTERMEDIATE.*

- *Introduction*

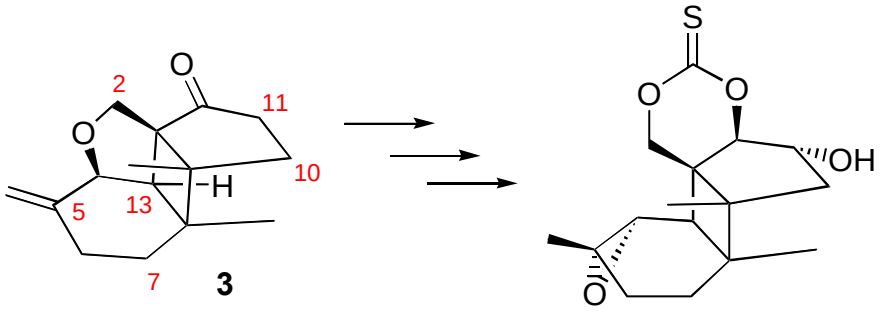

Once the tetracyclic structure of ketone **3** had been established (see chapter 2), its rigid structure could be coupled with face-selective reactions to introduce the remaining functionality for the preparation of the fragmentation precursor **1** (see chapter 1). The first goal was to introduce a hydroxy functionality in a stereoselective manner on the position alpha to the carbonyl (C-11). Subsequent elaboration of intermediate **3** would involve preparation of a *trans* diol (at C-11 and C-12), reduction of the allylic ether, introduction of an epoxide at C-4, C-5 and formation of the *cis*-fused cyclic thionocarbonate.

- *Functionalization alpha to the carbonyl:*

Introduction of the desired hydroxyl at C-11 required a way of placing this new functionality on the more hindered side of the molecule. Three strategies were investigated for this purpose.

1. Strategy I: α-Bromination

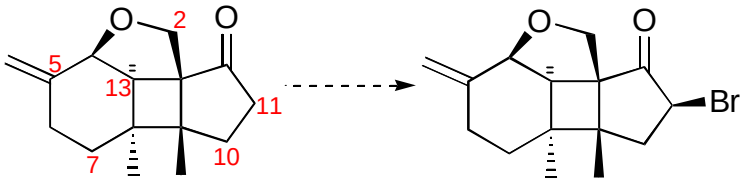

3 **112**

Bromination at the position activated by the carbonyl from the convex, less hindered side of the molecule would serve as a handle for nucleophilic attack and inversion of the configuration at that center. Once the bromine had been installed, intermolecular SN_2 displacement with an oxygen nucleophile would result in an alcohol with the desired α stereochemistry. Alternatively, one could set up for intramolecular displacement by reducing the ketone to an alcohol. Reduction would occur with hydride delivery from the less hindered, top side, of the bromoketone **112** yielding the alkoxide on the bottom face. Ideally, this alkoxide would displace the bromide prior to work-up to give an epoxide on the more hindered face of the compound. As a third option, a two step procedure could be used, with reduction of the carbonyl to an alcohol being followed by the displacement of the bromide in the formation of the same epoxide.

Bromination using standard reagents such as bromine or N-bromosuccinimide (NBS) gave only unreacted starting material. Reactions were attempted under basic or acidic conditions using stoichiometric or catalytic amounts of the reagents[162]. When the reaction was carried out in the presence of heat or under harsh conditions, base-line material was observed and no major product was isolated. The same was true when iodination was tried instead. Use of phenylselenium bromide[163] as the reagent solved the bromination problem. Taking advantage of solvent effects, one could select formation of the brominated product over the selenium derivative by carrying the reaction in a polar solvent, as was the case with ethyl acetate. The desired brominated product **112** was thus obtained in 72 % yield (PhSeBr, EtOAc, room temperature, 1h). 1D-proton difference NOE experiments aided on the relative stereochemistry assignment shown for the bromine at C-11 in compound **112**. An NOE observed between H-13 and H-11, which was not seen for compound **124**, confirms the S relative stereochemistry assignment for C-11. This assignment was further supported by the observation of NOEs between H-10α and H-13 and between H-10α and H-11 (see Addendum I for details).

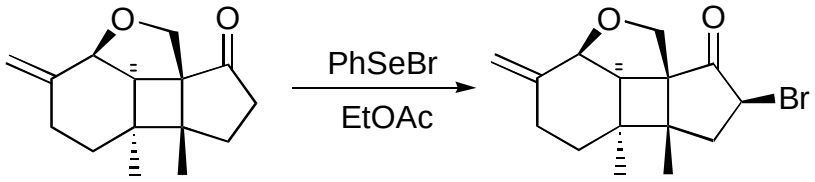

3 **112**

[162] Reaction with NBS was tried in the presence of H_2O_2 and/or UV light for initiation. Some of the reactions were tried in analogous substrates without the ether ring present as well. The results were the same as was observed for compound **3**.

[163] Abul-Haji, Y. J. *J. Org. Chem.* **1986**, 51, 3380.

Attempts to invert the bromine by direct displacement using KOH, benzoate and superoxide[164] were unsuccessful. For reactions where KOH and benzoate were used, the elimination product, enone **113**, was the major product. When superoxide was used, the oxidation product dienone **114** was obtained as the single product in 49% yield (KO_2, DMSO, 18-crown-6 ether, 3Å molecular sieves). Other minor side products included addition of hydroxide to the allylic ether and opening of the 5-membered ring to give a derivative of the type of compound **115**. Formation of the desired inverted product was not observed under SN_2 conditions.

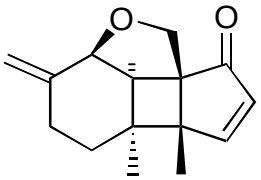

113

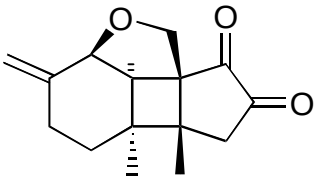

114

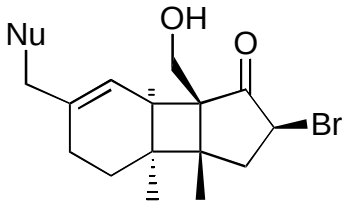

115

Reduction of the ketone in an attempt to prepare the epoxide in one step was also unsuccessful, but bromohydrin **116** was stable and could be isolated in 63% yield ($LiAlH_4$, Et_2O, 0^o C, 1h) along with product **91**, derived from over-reduction, where the bromide was removed.

[164] Corey, E. J.; Nicolaou, K. C.; Shibasaki, M.; Hachida, Y.; Shiner, C. S. *Tetrahedron Lett*. **1975**, 3183.

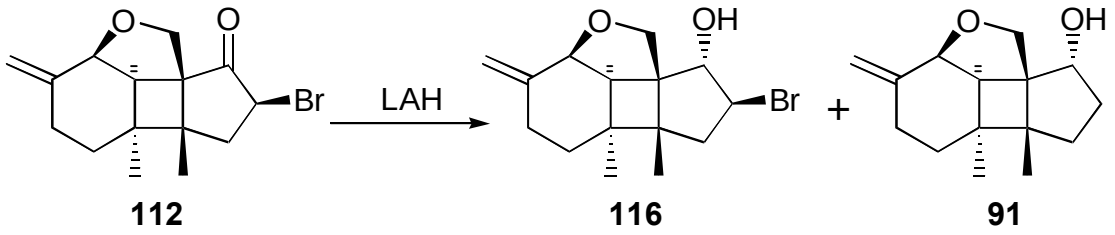

112 **116** **91**

Attempts to induce the formation of the epoxide by regenerating the alkoxide in compound **116** through the use of bases such as ^{t}BuOK, NaOMe or KOH or attempts to employ silver-assisted methods were unsuccessful. Mostly, recovery of unreacted bromohydrin along with elimination products evidenced by the increase of signal in the vinylic region of the ^{1}H NMR or decomposition of the starting material, as was the case for the silver assisted reactions, was observed. Alternative methods also involved reaction of bromoketone **112** with methoxide[165] or hydrazine[166] to attempt formation of the epoxide *via* a ketal or an aminal type intermediate, again with no success. This result can be attributed to the increase of ring strain upon formation of the epoxide thus disfavoring this pathway.

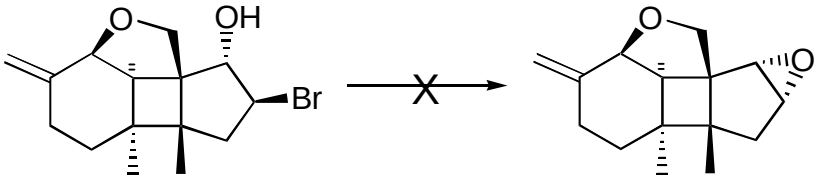

116 **117**

[165] Hassner, A.; Catsoulacos, P. *J. Org. Chem*. **1966**, 31, 3149.

[166] Catsoulacos, P.; Hassner, A. *J. Org. Chem.*, **1967**, 32, 3723 and Numazawa, M.; Nagaoka, M. *J. Org. Chem*. **1982**, 47, 4024.

Another attempt to reduce the carbonyl, this time using $NaBH_4$ (EtOH, R.T., 70 % yield), gave only one product (bromo-diol **118**) that was the result of reduction of the ketone along with reduction of the allylic ether.

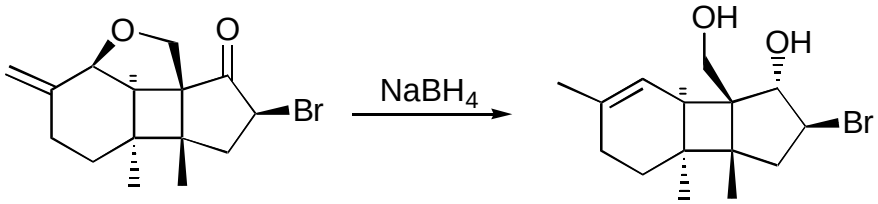

112 **118**

Bromo-diol **118** lacked the 5-membered ether ring, and should be less strained than the parent compound **116**, so it was possible that the epoxide would form in this system. Furthermore, reaction of this substrate would avoid the need to reduce the allylic ether in the presence of the epoxide in a later step, as would be the case in the original system.

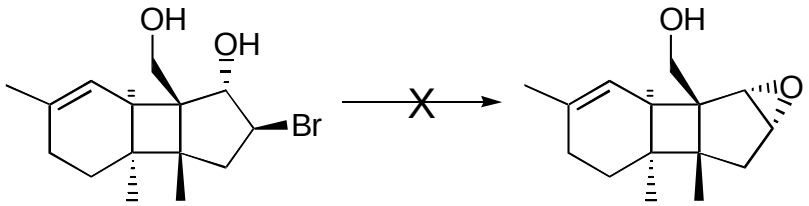

118 **119**

This approach was also unsuccessful, so the focus of the investigation was diverted to another strategy.

2. Strategy II: α-Oxidation

The second strategy involved preparation of a system at one oxidation-level higher (diketone), followed by reduction to a diol in a stereocontrolled manner.

Preparation of diketone **114** followed the procedure developed by Wasserman[167] where first the enamino-ketone **120** was prepared by treatment of ketone **3** with Brederick's reagent followed by singlet oxygen oxidation of the vinylogous amide.

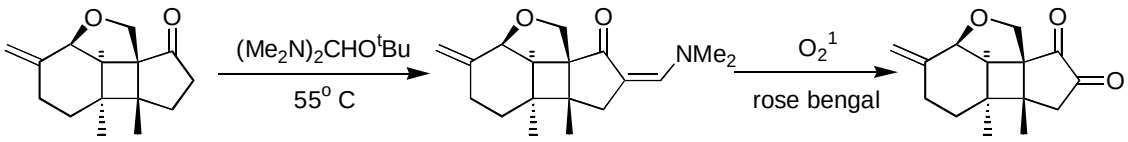

3 **120** **114**

The formation of the vinylogous amide **120** was performed in the presence of excess reagent with no solvent ($(Me_2N)_2CHO^tBu$, 55° C, 30 h) and the reaction progress could be monitored by ^1H NMR of the crude mixture in $CDCl_3$. One could follow the appearance of a signal at δ 8.00 ppm due to the proton on the enamine double bond and the N-methyls at δ 2.85 and 2.90 ppm. The infrared spectrum (CCl_4 solution) of a sample purified by flash chromatography with diethyl ether also showed peaks at 1685 and 1596 cm^{-1} associated with the vinylogous amide. The oxidation step followed without purification of the intermediate **120**, by dissolving the crude mixture in CH_2Cl_2, addition of a sensitizer (Rose Bengal) and irradiation with a sun lamp in the presence of a positive

[167] Wasserman, H. H.; Ives, J. L. *J. Am. Chem. Soc.* **1976**, 98, 7868.

pressure of oxygen for approximately 3h. The diketone **114** was thus obtained in 56% yield for the two steps.

Reduction (complete, not partial) of the diketone could have three possible results: formation of the alpha-*cis* diol, or the two possible *trans* diols. Reports in the literature[168] suggested that reduction of diketones tend to give *trans* products due to OH direction. Various reducing agents were used to determine the product distribution outcome. Elucidation of the relative stereochemistry of the diol products was done via NMR studies: 1D-proton difference NOE aided by 2D-proton COSY or selective single frequency decoupling experiments. Studies conducted using $LiAlH_4$, $NaBH_4$, $ZnBH_4$, selectride, Red-Al and other common reducing agents gave only the *cis* product **121** (^3J = 5.5 Hz between the diol methine hydrogens at C-11 and C-12). An NOE observed between H-11 and H-12 confirms the *cis* relative stereochemistry assigned for diol **121** and the absence of NOEs between H-13 and H-11 or between H-13 and H-12 supports the S* assignment for C-12 and the R* relative stereochemistry assignment for C-11. These assignments were further supported by comparison with the results for the NOE experiments conducted on the *trans* diol **126** (see Addendum I for details).

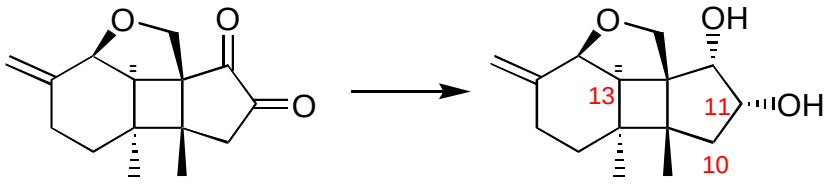

114 **121**

[168] Hashimoto, S.; Sakata, S.; Sonegawa, M.; Ikegami, S. *J. Am. Chem. Soc.* **1988**, *110*, 3670.

The relative stereochemistry of compound **121** was further confirmed by preparation of the rigid derivative **122**. This cyclic thionocarbonate was prepared by reaction of diol **121** with thiocarbonyl diimidazole, in toluene, at reflux. The desired product **122** was isolated, after purification, in 75% yield. Coupling constant of 6.8 Hz between the hydrogens at C-11 and C-12[169], along with 1D-proton difference NOE experiments results supported the *cis* relative stereochemistry assignment. An NOE observed between H-2 and H-12 confirmed the S relative stereochemistry assigned for C-12. The absence of NOEs between H-12 and H-13 and between H-11 and H-13 further supported the assignment (see Addendum I for details).

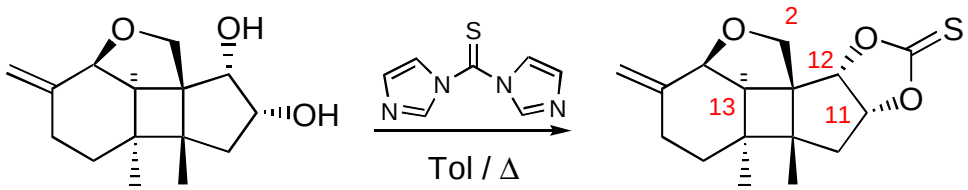

121 **122**

Compound **122** could be submitted to radical fragmentation conditions to verify if any selectivity would be achieved for the formation of one possible secondary radical over the other. For this molecule, strain release would be the only factor inducing selectivity. Unfortunately, the thiocarbonate was never prepared in large enough quantity for the experiment to be attempted.

[169] Predicted coupling constant for *cis* ring junction, based on molecular mechanics using MacroModel v4.5, was 6.6 Hz with a dihedral angle of 21.1°.

Further NMR analysis suggested that the stable form of diketone **114** is its enol-ketone tautomer as shown by the presence of proton signals at δ 8.53 ppm corresponding to the OH and a singlet at δ 6.59 ppm corresponding to the olefinic hydrogen. Monte Carlo simulations[170] of the two tautomeric forms of compound **114** favored the enol form by 20 Kcal/mol. The predominance of the enol-ketone tautomer was supported further by the infrared data with absorptions observed at 3602 cm^{-1} for the OH, and 1699 cm^{-1} for the enone.

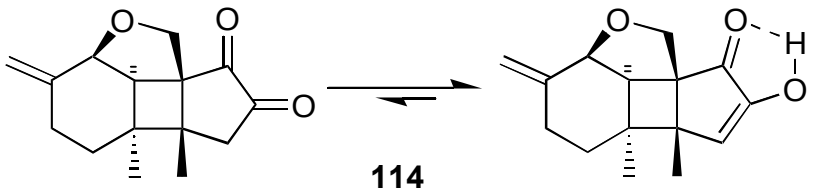

114

Another approach to synthesize the *trans* diol was to effect a Luche reduction[171] of compound **114**. The idea was to first perform a 1,2-reduction of the "enone portion" followed by reduction of the remaining ketone with $NaBH_4$ *via* complexation with the freshly prepared hydroxyl. This two-step reduction should force the system into a *trans* configuration. Attempts to isolate the Luche reduction intermediate were unsuccessful, probably due to equilibration of the keto-alcohol through its various tautomeric forms[170,172], and reduction of the crude Luche-reaction product afforded only *cis* diol **121**.

---

[170] Energy minimizations were carried out using MacroModel v4.5, developed by Prof. Clark Still at Columbia University. Conformational analysis were conducted using the Monte Carlo simulation package along with MM2 force fields.

[171] Gemal, A. L.; Luche, J.-L. *J. Am. Chem. Soc.* **1981**, 103, 5454.

[172] Molecular modeling using MacroModel placed all 5 tautomers within 1 Kcal/mol of each other.

Due to the difficulty in synthesizing the *trans* diol the new alternative focused on the preparation of the *cis* diol cleanly and use the primary alcohol, derived from reduction of the allylic ether, in compound **123** as a handle to invert the stereochemistry at C-3 of the triol. Dissolving metal reduction of the allylic ether **121** gave the desired triol **123** in 35% yield. This low yield was probably due to difficulties encountered during the purification of the highly polar final product.

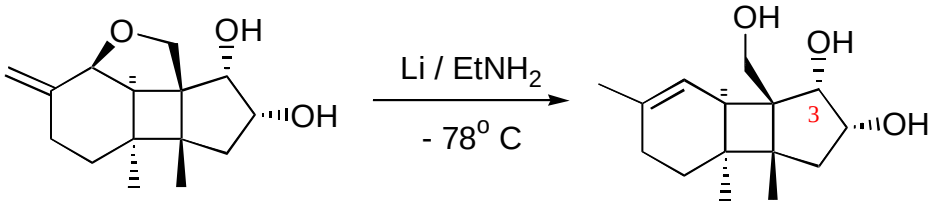

121 **123**

The first approach considered (see Figure 4.1) was to prepare the cyclic sulfite of the *cis* diol (an epoxide equivalent) and invert one of the hydroxyl centers (C-11 or C-12) by the intramolecular formation of a cyclic carbonate[173] or a phenylurethane[174]. Formation of the six-membered ring should be favored over formation of the seven-membered ring and inversion should occur at C-12 to give the desired stereochemical framework.

[173] Bartlett, P. A.; Meadows, J. D.; Brown, E. G.; Morimoto, A.; Jernstedt, K. K. *J. Org. Chem.* **1982**, 47, 4013.
[174] Roush, W. R.; Brown, R. J.; DiMare, M. *J. Org. Chem*. **1983**, 48, 5083.

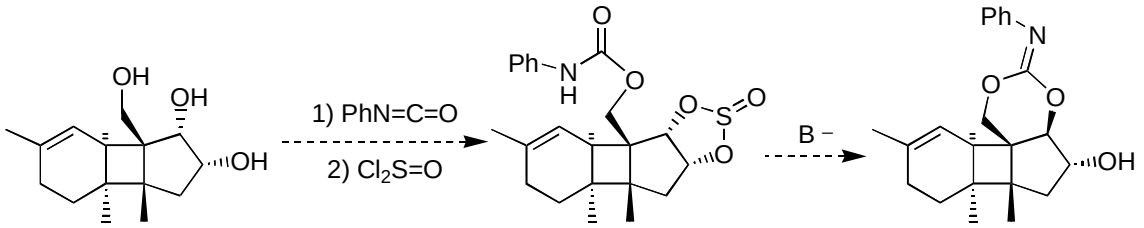

Figure 4.1

The second approach (see Figure 4.2) would be to activate the electrophile instead of the nucleophile. This could be accomplished by methylating the thionocarbonate and allowing a proximate pivaloate, or other ester group, to assist in the elimination.

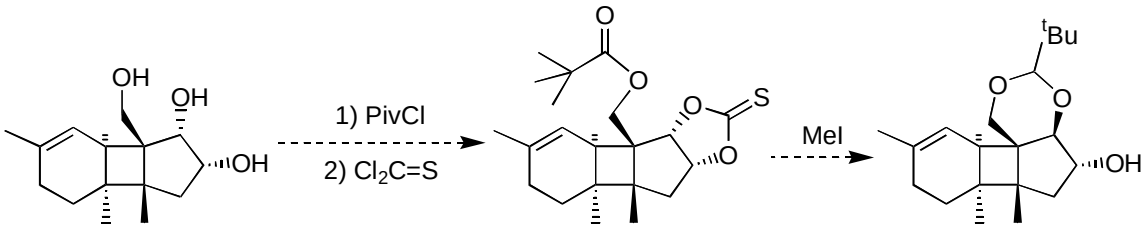

Figure 4.2

These ideas were not entertained for long because a more direct approach became available, the possibility of the direct installation of the hydroxy group in the concave face of the molecule.

3. Strategy III: The Moriarty Route

A solution to the need to install a hydroxyl in the concave face of the molecule was found in the work of Moriarty[175]. Treatment of ketone **3** with KOH, MeOH and iodoso benzene diacetate gave the alcohol-ketal **125**, which upon hydrolysis gave the desired compound **124** with the alcohol in the alpha face of the molecule.

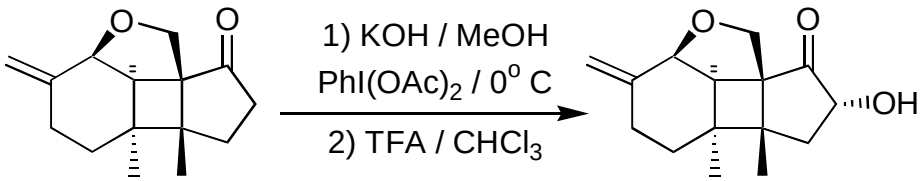

3 **124**

The procedure developed by Moriarty represents, in essence, an intramolecular double displacement in one step. More specifically, in this example, the enolate adds to the iodoso benzene from its least hindered face giving the β-substituted iodoso adduct. Methoxide attacks the carbonyl, again from the least hindered side of the molecule, resulting in an alkoxide in the opposite face that displaces the iodoso benzene substituent in an intramolecular SN_2 fashion. Another methoxide attacks the resulting methoxy-epoxide in the more electron rich site to give the hydroxy-ketal **125** (73% isolated yield). The new hydroxyl substituent is in the concave face of the molecule.

---

[175] Moriarty, R. M.; Gupta, S. C.; Hu, H.; Berenschot, D. R.; White, K. B. *J. Am. Chem. Soc*. **1981**, 103, 686; Moriarty, R. M.; Hu, H.; Gupta, S. C. *Tetrahedron Lett*. **1981**, 22, 1283; Moriarty, R. M.; Hu, H. *Tetrahedron Lett*. **1981**, 22, 2747; Moriarty, R. M.; Hou, K.-C. *Tetrahedron Lett*. **1984**, 25, 691; Moriarty, R. M.; Berglund, B. A.; Pen Masta, R. *Tetrahedron Lett.* **1992**, *33*, 6065.

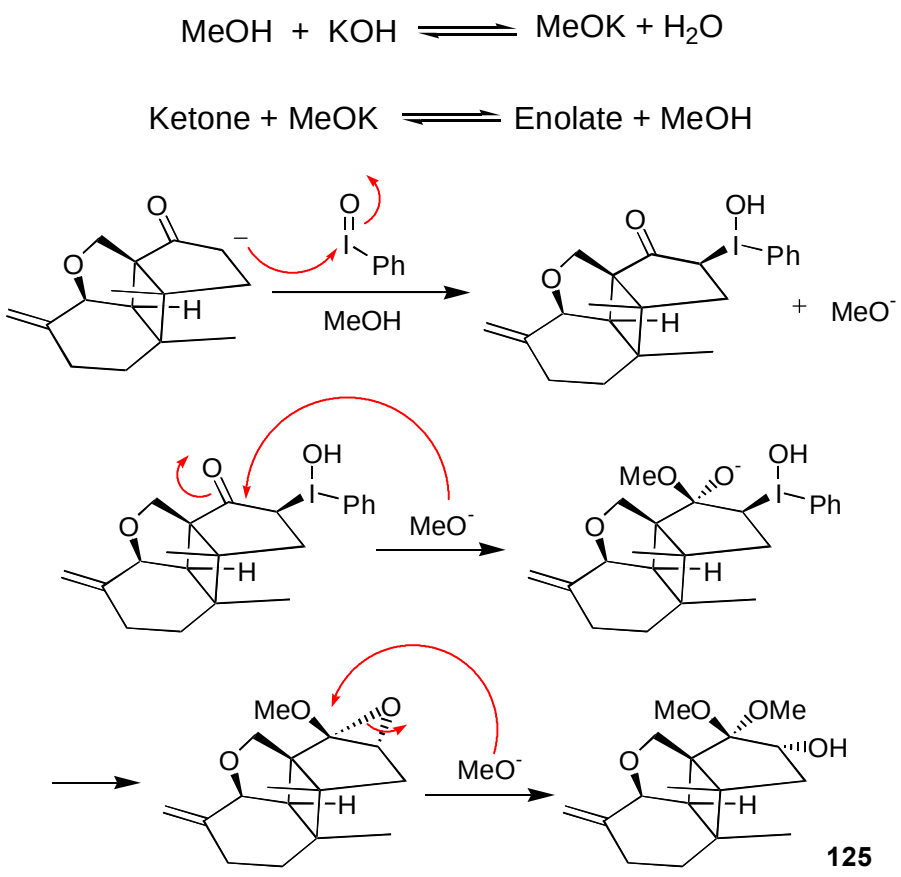

Hydrolysis of the ketal was a delicate issue because of the risk of equilibrating the hydroxy-ketone **124** into its tautomers. The best results[176] were obtained under cold acidic conditions[177] using trifluoroacetic acid in a water-chloroform mixture at 0° C.

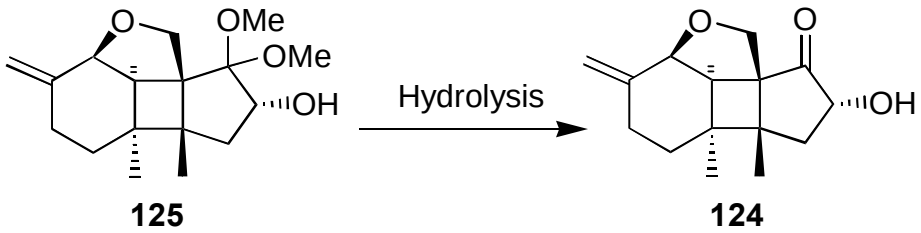

[176] Other reaction conditions attempted included dilute aqueous HCl, TsOH-MeOH and Acetic acid-THF-water.

[177] Ellison, R. A.; Lukenbach, E. R.; Chiu, C.-W. *Tetrahedron Lett.* **1975**, 16, 499.

The final product **124** was thus obtained in 62 % yield over the two steps. The stereochemistry assignment of the alcohol at C-11 was confirmed through a 2D-proton-proton NOESY experiment (see Addendum I for results).

- *Ketone Reduction:*

Once the relative stereochemistry of the hydroxyl group at C-11 was set, the next step was to convert the ketone into an alcohol with the beta configuration. To accomplish this transformation hydride delivery would have to occur from the concave side of the molecule.

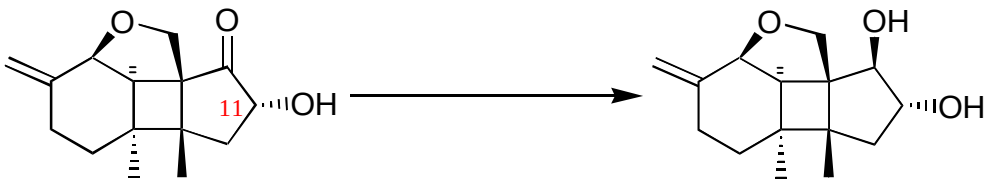

124 **126**

The objective was to use the hydroxyl as a handle for the reduction of the ketone. This transformation was attempted with various oxygen–complexing reducing agents such as $NaBH_4$, $ZnBH_4$, catechol borane[178], thexyl borane[179], cyclohexyl-borane[180], Alpine

[178] Kabalka, G. W.; Narayama, C.; Reddy, N. K. *Synth. Comm.* **1994**, *24*, 1019; *J. Chem. Soc. Chem. Comm*. **1993**, 1673.
[179] (a) Zweifel, G.; Pearson, N. R. *J. Am. Chem. Soc.* **1980**, *102*, 5919. (b) Negishi, E.; H.C.Brown *Synthesis* **1974**, 77.
[180] Brown, H. C.; Gupta, S. K. *J. Am. Chem. Soc.* **1971**, *93*, 4062.

borane[181] and Red-Al[182]. The reagents were expected to complex with the alcohol functionality and then reduce the ketone. In practice, however, most of these reagents lost some of their reducing potential once the complex was formed and more than one equivalent of reducing agent was needed for the reduction. In effect, it was the second equivalent that reduced the molecule while the first equivalent blocked the face of the molecule where it complexed. The reaction yields were low under all sets of conditions tried and the *cis* diol was the favored product.

Given the above results, a new strategy was designed to intentionally block the less hindered side of the molecule using Methylaluminum bis(2,6-di-tert-butyl-4-methylphenoxide) (MAD)[183], an aluminum complexing agent, followed by reduction of the ketone from the concave face with a small reducing agent such as NaH. The problem with sodium hydride was that it is a strong base and destroyed the starting material; the same was true for attempts using Clemmensen reduction (Zn(Hg)-HCl). Other reducing agents such as $LiBH_4$ and AlH_3[184] gave unreacted starting material and/or partial reduction of the olefin.

---

[181] (a) Ramachandran, P. V.; Gong, B. Q.; Teodorovic, A. V.; Brown, H. C. *Tetrahedron Asym.* **1994**, *5*, 1075. (b) Ramachandran, P. V.; Gong, B. Q.; Teodorovic, A. V.; Brown, H. C. *Tetrahedron Asym.* **1994**, *5*, 1061; (c) Masamune, S.; Kim, B.; Petersen, J. S.; Sato, T.; Veenstra, S. J.; Imai, T. *J. Am. Chem. Soc.* **1985**, *107*, 4549.

[182] Harashima, S.; Oda, O.; Amemiya, S. *Tetrahedron* **1991**, *47*, 2773.

[183] (a) Gerster, M.; Audergon, L.; Moufid, N.; Renaud, P. *Tetrahedron Lett*. **1996**, *37*, 6335; (b) Maruoka, K.; Nagahara, S.; Yamamoto, H. *Tetrahedron Lett.* **1990**, *31*, 5475; (c) Renaud, P.; Bourquard, T.; Carrupt, P.-A.; Gerster, M. *Helv. Chim. Acta* **1998**, *81*, 1048.

[184] Brown, H. C.; Hess, H. M. *J. Org. Chem*. **1969**, *34*, 2206.

Attempts to effect the reduction of the ketone using a modified version[185] of the Meerwein-Ponndorf-Verley reaction,[186] with SmI_2 and acetaldehyde (THF, -78° C) as part of the reduction scheme, was also unfruitful resulting in a 3:1 ratio of *cis*-*trans* diols.

A solution for the problem was found in the work of Evans[187] where he developed a borohydride reducing agent that provided a higher reducing potential once bound to the alcohol than the unbound species. Compound **124** was thus treated with tetramethylammonium triacetoxy-borohydride (AcOH, 0° C to room temperature) to yield upon isolation 75% of a 1:7 *cis*-*trans* mixture (NMR integration ratio) in favor of the desired *trans*-diol **126**.

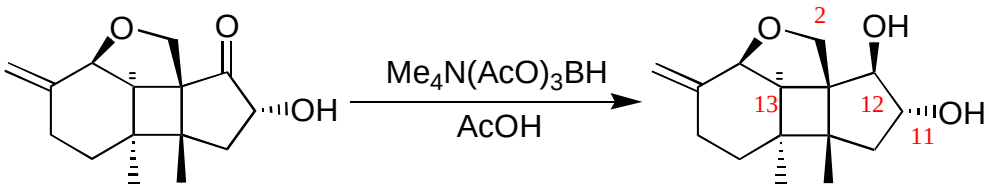

124 **126**

Compound **126** was separated from the *cis* diastereomer by flash chromatography to give the pure *trans* derivative. The reaction worked best when reduction was carried out soon after preparation of the keto-hydroxy intermediate **124** to minimize equilibration *via* tautomerization**.** Again the relative stereochemistry of the diol was confirmed through 1D-proton NOE difference experiments. An NOE observed between H-2β and H-11

---

[185] Evans, D. A.; Hoveyda, A. H. *J. Am. Chem. Soc.* **1990**, *112*, 6447.
[186] Wilds, A. L. *Org. Rxns.* **1944**, *2*, 178.
[187] Evans, D. A.; Chapman, K. T.; Carreira, E. M. *J. Am. Chem. Soc.* 1988, 110, 3560; Saksena, A. K.; Mangiaracina, P. *Tetrahedron Lett.* 1983, 24, 273.

confirmed the R relative stereochemistry assignment at C-11 and an NOE observed between H-12 and H-13 confirmed the R relative stereochemistry assignment at C-12. These assignments were further supported by comparison with the results obtained for compound **121** (see Addendum I for details).

- *Future developments:*

With the stereochemistry of the diol established, most of the chemistry necessary to transform intermediate **126** into the fragmentation precursor **1** had been developed during the preparation of the model systems (see chapter 3). Unfortunately, the amount of substrate available was too small to carry out the remaining reactions and the preparation of more material was lengthy and difficult. At this point work in the project was interrupted; nonetheless, the initial results were promising. The fragmentation of the cyclic thionocarbonate portion of the molecule could be controlled *via* manipulation at the ring junction and this system would probably serve as a versatile entry for the synthesis of the trichothecene class of compounds.

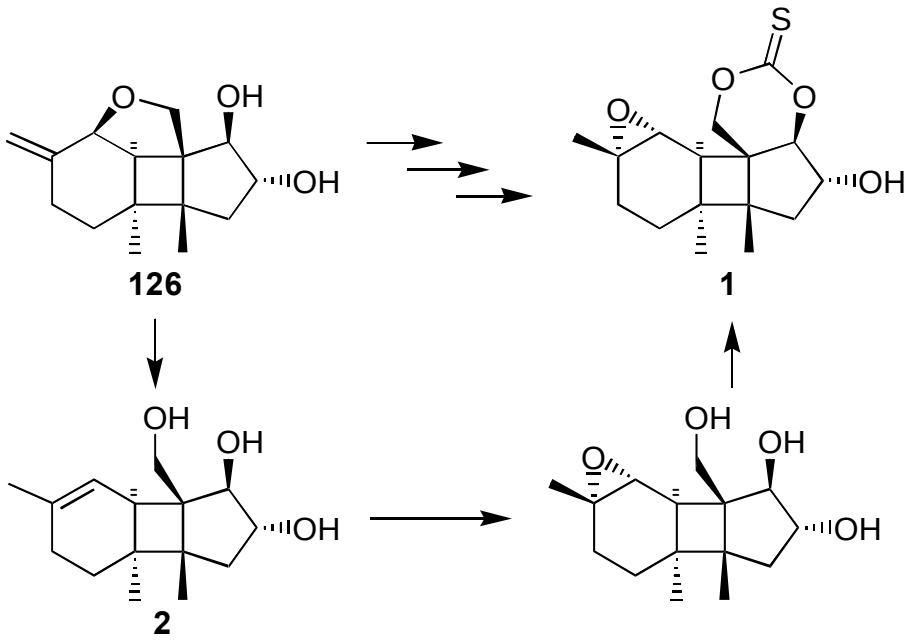

Future developments for this project would begin with reduction of the allylic ether in compound **126**. This conversion could be accomplished by dissolving metal reduction as it was used in the reduction of the analogous compound **123**. Next, epoxidation of the triol **2** with *m*-CPBA should install the desired epoxide at C-10 and C-11 (triol numbering), as was the result for diol **92**. Again, the delivery of the oxygen should occur from the less hindered (alpha) face, instead of directed oxidation by the primary alcohol. This triol-epoxide could be converted to the cyclic thionocarbonate **1** by reaction with thiophosgene (0^{o} C, slow addition of the reagent). The reaction should occur predominantly at the primary center followed by intramolecular cyclization. The cyclization step should favor formation of the six-membered ring over the seven-membered ring giving only the desired product required for the fragmentation step to unravel the trichothecene FS-2.

CHAPTER V: *EXPERIMENTAL PROCEDURES*

- *General*

Unless noted otherwise, materials were obtained from commercially available sources and used without further purification. Tetrahydrofuran (THF) and diethyl ether (Et_20) were distilled from sodium benzophenone ketyl under a nitrogen atmosphere. Benzene, toluene, dichloromethane (CH_2Cl_2), acetonitrile (CH_3CN) and pyridine were distilled from calcium hydride under a nitrogen atmosphere. Triethylamine (Et_3N) was distilled from barium oxide under an argon atmosphere and stored over potassium hydroxide. Chloroform ($CHCl_3$), carbon tetrachloride ($CC1_4$) and deuterated NMR solvents were dried over 1/16" bead 4Å molecular sieves. Alkyllithiums were titrated periodically employing 1,3-diphenylacetone-*p*-tosyl-hydrazone as described by Lipton.[188]

All operations involving moisture sensitive materials were conducted in oven and/or flame dried glassware under an atmosphere of anhydrous nitrogen. Hygroscopic solvents and liquid reagents were transferred using dry Gastight® syringes or cannulating needles. In cases where rigorous exclusion of dissolved oxygen was required, solvents were degassed via consecutive freeze, pump, thaw cycles. Photolyses were conducted in

---

[188] (a) Lipton, M. F.; Soresen C. M.; Sadler A. C.; Shapiro R. H. *J. Organomet. Chem.* **1980**, *186*, 155. (b) Suffert,J. *J. Org. Chem.* **1989**, *54*, 509.

Pyrex vessels employing a 450 W medium pressure Hanovia (ultraviolet) lamp. Ozonolyses were carried out using an OREC V10-0 ozonator.

Flash Chromatography was performed on EM Science (E. Merck) 230-400 mesh, Baker 40 μm (J. T. Baker Inc.) or SA 40 μm (Scientific Adsorbents Inc.) silica gel as described by Still.[189] Thin layer chromatography utilized EM Science (E. Merck) 250 μm 60 F_{254} Silica plates. Compounds which did not absorb ultraviolet light were visualized by dipping the TLC plate in vanillin[190] or ceric sulfate / ammonium molybdate[191] solution followed by heating.

Infrared spectra were obtained on either a Nicolet SX Nicolet Magna 550 or Midac Corporation M series FTIR using samples prepared, neat or in chloroform solution, as 0.5 mm thin films between NaCl plates. Low resolution mass spectra were acquired on a Hewlett-Packard HP-5989 MS Engine mass spectrometer equipped with a direct injection or Vacuometrics™ Inc. desorption chemical ionization probe. GC / MS analyses were performed with a Hewlett-Packard 5890 Series II gas chromatograph (Supelco SPB-5 column; 30m x 0.25mm I. D. capillary column) interfaced with an HP 5971A mass selective detector. High resolution mass spectra were performed at the University of Illinois, Urbana-Champaign, School of Chemical Sciences mass apectrometry laboratory.

Nuclear magnetic resonance (NMR) spectra were recorded on either a General Electric QEPlus 300 or Bruker AM-500 spectrometer. ^{1}H chemical shifts are given in parts per million (δ) downfield from tetramethylsilane using the residual solvent signal

---

[189] Still, W. C.; Kahn, M. *J. Org. Chem.* **1978**, *43*, 2923.

[190] Vanillin (27 g), dissolved in 20 mL H_2SO_4 (conc), 380 mL EtOH and 50 mL H_2O.

[191] $Ce(SO_4)_2$ (0.5-1.0 g) and $(NH_4)_6Mo_7O_{24}.4H_2O$ (24 g), dissolved in 500 mL of 10% aq. H_2SO_4.

($CHCl_3$ = δ 7.27, benzene = δ 7.15) as internal standard. Proton (^1H) NMR information is tabulated in the following format: multiplicity (s, singlet; d, doublet; t, triplet; q, quartet; m, multiplet), coupling constant(s) (*J*) in hertz and number of protons. The prefix *app.* is occasionally applied in cases where the true signal multiplicity is unresolved and *br* indicates that the signal in question is broadened. Proton decoupled ^{13}C NMR spectra are reported in ppm (δ) relative to $CDCl_3$ (δ 77.25) unless noted otherwise. Nuclear Overhauser Effect (NOE) difference spectroscopy measurements were made at 500 MHz in degassed $CDCl_3$ solution. Irradiation times were calculated based on measured T^1 relaxation time.

Melting points were measured on a Hoover Unimelt or Gallencamp digital apparatus and are uncorrected. Combustion Analyses were performed by Atlantic Microlab, Inc., Norcross, Georgia 30091. When possible, compound nomenclature follows I.U.P.A.C. rules wuth the aid of the program ACD/Name[192] or else it was provided based on analogies taken from *Chemical Abstracts* entries.

[192] ACD/Name, version 2.51 copyright 1994 - 97 by Advanced Chemistry Development Inc. *www.acdlabs.com.*

- *Specific Compounds*

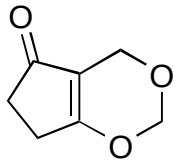

Compound 7:[193] 4, 5, 6, 7-Tetrahydrocyclopenta-[a]-[1, 3]-dioxin-5-one

1,3-Cyclopentadione (5.3 g, 0.05 mol) and 1,3,5-trioxane (16.0 g, 0.18 mol) were suspended in CH_2Cl_2 (260 mL) in a dry flask, under nitrogen. The heterogeneous mixture was cooled in an ice bath. $BF_3.Et_2O$ (20 mL, 0.16 mol) was added slowly, *via* syringe, as the white solid suspension becomes a homogeneous orange solution. After addition, the reaction mixture was kept at 0 ^oC for another two hours and then allowed to warm to room temperature. The solution was kept stirring at room temperature for 30 h and then it was quenched cold (in an ice bath) by addition of NaOH (10% aq, 100 mL) and ice (50 mL) with constant stirring for 10 min. The resulting two phases were separated and the organic layer was washed with brine (2 x 50 mL). The aqueous phase was saturated with NaCl and back-extracted with EtOAc (4 x 100 mL). The organic layers were reuned, washed with brine (1 x 100 mL) and dried over anhydrous Na_2SO_4. The solvent was evaporated *in vacuo* and the orange oily residue was recrystalized from an acetone-pentane solution to yield 6.72 g (96 %) of the enone as a white solid: mp (acetone/ pentane) 73.3-73.6 ^oC; IR ($CHCl_3$, cm^{-1}) 3000, 1690, 1640, 1430, 1310, 1205, 1180, 1090, 910; ^1H NMR (500 MHz, $CDCl_3$) δ 5.21 (s, 2H); 4.44 (t, J = 2.0 Hz, 2H), 2.63 -

2.60 (m, 2H), 2.39 - 2.37 (m, 2H); ^{13}C NMR (125 MHz, $CDCl_3$) ppm 201.08, 181.95, 114.66, 92.68, 62.99, 32.56, 26.41; HRMS (EI) *m/z* (M^+) calcd 140.0473, obsd 140.0482.

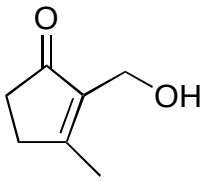

Compound 5:[193] 2-(Hydroxymethyl)-3-methyl-2-cyclopenten-1-one

Compound **7** (14 g, 0.1 mol) was dissolved in THF (250 mL) in a dry flask, under nitrogen, and the solution was cooled to -78 ^oC. A MeLi solution (250 mL, 0.225 mol, 0.9 M in diethyl ether) was added *via* syringe over 30 min. The reaction mixture turned yellow and was kept cold for another 1h. The solution was allowed to warm to 0 ^oC and ice cold HCl (4% aq., 440 mL) was added dropwise to the mixture. Hydrolysis was allowed to proceed at 0 ^oC for 1.5 h and at room temperature for another 2 h (reaction mixture turned dark orange). Reaction was quenched by addition of $NaHCO_3$ solid until pH neutral and saturated with NaCl. The layers were separated; the aqueous layer was acidified with a couple of drops of HCl (conc.) and extracted with EtOAc (3 x 100 mL). The organic layers were reuned and dried over anhydrous $MgSO_4$. Concentration and purification by flash chromatography using EtOAc as the eluent gave 9.93 g (79 %) of ketoalcohol **5** as a white needle-like solid: mp 52 - 53.5 ^oC; IR (CCl_4, cm^{-1}) 3453, 2917,

[193] Modification of procedure developed by Smith III, A. B.; Dorsey, B. D.; Ohba, M.; Lupo Jr., A. T.; Malames, M. S. *J. Org. Chem.* **1988**, *53*, 4314.

2862, 1696, 1664, 1488, 1387, 1337, 1011; ^{1}H NMR (300 MHz, $CDCl_3$) δ 4.31, (*br* s, 2H), 3.07 (*br* s, 1H, exchange with D_2O), 2.56 - 2.53 (m, 2H), 2.39 - 2.36, (m 2H), 2.10 (s, 3H); ^{13}C NMR (75 MHz, $CDCl_3$) ppm 210.02, 173.29, 138.46, 54.58, 34.19, 31.79, 16.98; HRMS (EI) *m/z* (M^+) calcd 126.0681, obsd 126.0672.

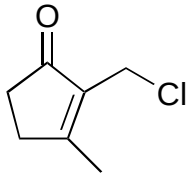

Compound 18: 2-(Chloromethyl)-3-methyl-2-cyclopenten-1-one

Compound **5** (4.5 g, 36 mmol) was dissolved in chloroform (45 mL) and the solution was cooled to 0 ^{o}C. Thionyl chloride (6.75 mL, 92 mmol) was added neat, dropwise, *via* syringe. The reaction mixture turned yellow. Solution was kept cold for another 20 min when there was no more starting material present in the medium. The reaction mixture was quenched by slow addition of $NaHCO_3$ (solid) and $NaHCO_3$ (sat., aq.) until pH neutral. Phases were separated; the organic layer was dried over anhydrous $MgSO_4$ and concentrated. The residue was purified by flash chromatography using methylene chloride as the eluent to give 5.02 g (96%) of chloride **18** as a pale yellow oil: IR ($CDCl_3$, cm^{-1}) 2964, 2917, 2858, 1698, 1650, 1438, 1385, 1346, 1263, 1178, 1078; ^{1}H NMR (300 MHz, $CDCl_3$) δ 4.19 (s, 2H), 2.62 - 2.60 (m, 2H), 2.46 - 2.43 (m, 2H), 2.21 (s, 3H); ^{13}C NMR (75 MHz, $CDCl_3$) ppm 206.51, 175.95, 136.72, 34.09, 32.77, 31.78, 17.40; HRMS (EI) *m/z* (M^+) calcd 144.0342, obsd 144.0351.

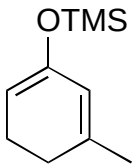

Compound 8:[194] 3-Trimethylsilyloxy-1-methyl-1, 3-cyclohexadiene

Lithium diisopropyl amide (LDA) was prepared at -78 ^{o}C by dissolving diisopropylamine (14 mL, 100 mmol) in THF (150 mL) and then adding butyllithium (10.6 mL, 106 mmol, 10 M in hexanes) slowly, to the cooled solution. 3-Methylcyclohexen-2-one (10 g, 91 mmol) was added to the cold base to afford a light yellow solution that was kept at -78 ^{o}C for 20 min. After that time, a solution of TMSCl (12.5 mL, 98 mmol) in THF (15 mL) was also added dropwise and set to react for another 20 min. The reaction mixture was then allowed to warm to room temperature and the THF was evaporated *in vacuo*. The residue was ressuspended in hexanes and washed with half saturated sodium bicarbonate (aqueous, 100 mL) and brine (2 x 200 mL), dried over anhydrous sodium sulfate and concentrated to give 16.2 g (98 %) of the enol ether **8** as a pale yellow oil, carried on with no further purification: ^{1}H NMR (300 MHz, $CDCl_3$) δ 5.44 (t, J = 1.5Hz, 1H), 4.73 (*br* s, 1H), 2.19 - 2.15 (m, 2H), 2.05 - 1.99 (m, 2H), 1.79 (s, 3H), 0.19 (s, 9H).

[194] (a) Iwata, C.; Takemoto, Y.; Nakamura, A.; Imanish, T. *Tetrahedron Lett.*, **1985**, *26*, 3227 . (b) Rubboton, G. M.; Gruber, J. M. *J. Org. Chem.* **1978**, 43, 1599.

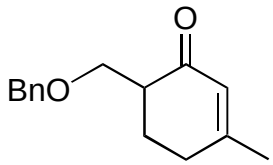

Compound 9: 6-(Benzyloxymethyl)-3-methyl-2-cyclohexen-1-one

Method A (small scale): Compound **8** (510 mg, 2.8 mmol), benzyl-(chloromethyl)-ether (80%, 670 mg, 3.4 mmol) and methylene chloride (4 mL) were combined in a dry flask, under nitrogen, resulting in a yellow solution which was cooled to 0 ^{o}C. Freshly sublimed (flame heated, under 1 mm Hg) zinc bromide (68 mg, 0.3 mmol, 10 % eq.) was added to the reaction mixture in one portion. The solution turned orange-red, then brown and was kept stirring at 0 ^{o}C for 3 hours. At this point very little starting material was left but a second product started to form so the reaction was quenched, while the mixture was still cold, by the addition of $NaHCO_3$ (sat., aq., 2 mL). The layers were separated, the aqueous was extracted with more methylene chloride (2 x 5 mL) and the combined organic phase was dried over anhydrous $MgSO_4$ and concentrated. The residue was purified *via* flash chromatography using 1 % diethyl ether in methylene chloride to give 303 mg (49 %) of the enone **9**.

Method B (large scale): Zinc dust (12.3 g, 188 mmol) and cuprous chloride (2.6 g, 26 mmol) were suspended in methylene chloride (60 mL), in a dry flask, under nitrogen. The reaction mixture was heated to reflux for 30 min, then cooled to room temperature. Diiodo methane (8.3 mL, 102 mmol) was added neat and the new mixture was heated to reflux for another 1 h then cooled to 0 ^{o}C. Compound **8** (16.2 g, 89 mmol) was dissolved in CH_2Cl_2 (12 mL) and added to the reaction media, followed by slow addition of benzyl-

(chloromethyl)-ether (90%, 20 mL, 136 mmol) in methylene chloride (24 mL). The mixture was allowed to warm to room temperature over 2 h and then it was refluxed overnight. The reaction was quenched at 0 ^{o}C by addition of diethyl ether (300 mL) followed by sulfuric acid (10% aq., 300 mL, 0 ^{o}C). The phases were separated. The aqueous layer was extracted with diethyl ether (3 x 80 mL) and the combined organic layer was washed first with sodium bicarbonate (aq., sat.) until pH neutral and then with brine (2 x 100 mL). The final organic layer was filtered over a plug of silica gel and concentrated. The enone was isolated using dry chromatography[195] (solvent: hexanes to methylene chloride, 10% increments, 200 mL of each), 12 g (58%) of the enone **9** was purified as a pale yellow oil.

Compound **9**: IR (CCl_4, cm^{-1}) 3083, 3059, 3024, 2917, 2865, 1673, 1619, 1453, 1417, 1380, 1345, 1205, 1104; ^{1}H NMR (300 MHz, C_6D_6) δ 7.28 - 7.08 (m, 5H), 5.85 (s, 1H), 4.34 (s, 2H), 3.91 (dd, *J* = 9.3 Hz, 3.9 Hz, 1H), 3.66 (dd, *J* = 9.3 Hz, 7.8 Hz, 1H), 2.31 - 2.27 (m, 1H), 1.98 - 1.92 (m, 1H), 1.68 - 1.59 (m, 2H), 1.64 (s, 1H), 1.29 (s, 3H); ^{13}C NMR (75MHz, $CDCl_3$) ppm 198.93, 162.16, 138.35, 128.20, 127.45, 127.39, 126.45, 73.13, 69.28, 45.90, 30.27, 25.83, 24.11; HRMS (EI) *m/z* (M^+) calcd 230.1307, obsd 230.1310.

[195] Dry chromatography technique: *Aldrichimica Acta* **1985,** 18, 1.

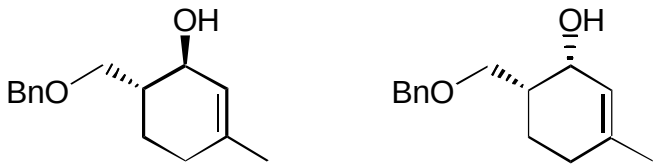

Compounds 6a and 6b: (1R*, 6S*)-6-(Benzyloxymethyl)-3-methyl-2-cyclohex-2-ene-1-ol and (1R*, 6R*)-6-(Benzyloxymethyl)-3-methyl-2-cyclohex-2-ene-1-ol

Compound **9** (12 g, 52 mmol) was dissolved in diethyl ether (200 mL) in a dry flask, under nitrogen. The solution was cooled to -10 ^{o}C (ice, salt, EtOH). $LiAlH_4$ (0.65 g, 19.2 mmol) was added to this mixture in 3 portions of about 200 mg each, at 45 min intervals. The conversion from starting material was complete in 3 h and the reaction was quenched, cold, by slow addition of sodium sulfate (aq., sat). The reaction mixture was dried over anhydrous $MgSO_4$, filtered and concentrated. Crude ^{1}H NMR ($CDCl_3$) indicated a *trans*/*cis* ratio of 7.1: 1 by integration. Flash Chromatography in 1 % benzene and 5% diethyl ether in methylene chloride gave 9.22 g (76%) of pure *trans* alcohol **6a** and 1.1 g (9%) of the *cis* product **6b** as colorless oils. *Trans* alcohol **6a**: IR (CCl_4, cm^{-1}) 3613, 3523, 3085, 3060, 3031, 2914, 2858, 1484, 1444, 1369, 1364 1242, 1204, 1153 1089, 1075; ^{1}H NMR (300 MHz, $CDCl_3$) δ 7.48 - 7.23 (m, 5H), 5.38 (s, 1H), 4.56 (s, 2H), 4.14 (*br* d, *J* = 8.4 Hz, 1H), 3.60 (dd, *J* = 5.4 Hz, 3 Hz, 1H), 3.50 (dd, *J* = 5.7 Hz, 5.4 Hz, 1 H), 3.27 (*br* s, 1H, exchange with D_2O), 2.09 - 1.98 (m, 1H), 1.91 - 1.79 (m, 2H), 1.71 (s, 3H), 1.70 - 1.60 (m, 1H), 1.33 - 1.22 (m, 1H, 8 lines); ^{13}C NMR (75 MHz, $CDCl_3$) ppm 137.81, 136.25, 128.37, 127.64, 127.51, 124.30, 75.27, 73.36, 71.87, 41.53, 29.36, 23.42, 23.04; HRMS (EI) *m/z* (M^+) calcd 232.1463, obsd 232.1451. *Cis* alcohol **6b**: IR ($CDCl_3$, cm^{-1}) 3611, 3478, 3102, 3066, 3033, 2917, 2863, 1668, 1602, 1497, 1453, 1423, 1369, 1365 1077, 1027; ^{1}H NMR (500 MHz, $CDCl_3$) δ 7.38 - 7.28 (m, 5H),

5.62 (s, 1H), 4.56 (s, 2H), 4.24 (t, *J* = 4.0 Hz, 1H), 3.64 (dd, *J* = 9.1 Hz, 8 Hz, 1H), 3.52 (dd, *J* = 9.1 Hz, 6.0 Hz, 1H), 1.98 (*br* t, *J* = 6.0 Hz, 2H), 1.91 - 1.83 (m, 2H), 1.71 (s, 3H), 1.57 - 1.52 (m, 2H); ^{13}C NMR (125 MHz, $CDCl_3$) ppm 139.66, 138.73, 128.70, 127.89, 123.38, 73.17, 72.02, 65.09, 38.75, 29.89, 23.18, 20.07; HRMS (EI) *m/z* (M^+) calcd 232.1463, obsd 232.1443.

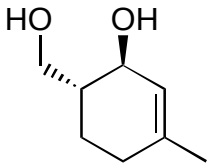

Compound 10: 6-Hydroxymethyl-3-methyl-(1R*, 6S*)-2-cyclohexen-1-ol

A two-neck flask equipped with a dry ice condenser was flame dried and flushed with dry nitrogen. Ethylamine (4 mL, excess) was condensed onto the flask at -78 ^oC followed by addition of a solution of alcohol **6a** (200 mg, 0.86 mmol) in 4 mL of diethyl ether. Lithium wire (120 mg, 17.3 mmol), was cut in small pieces, and added to the reaction flask. The suspension of lithium pieces in ethereal ethylamine was stirred at -78 ^oC until a persistent dark blue color was observed (about 30 min). The suspension was allowed to stir at -78 ^oC for an additional 15 min before the blue color was discharged by addition of a few drops of 1-octyne. The remaining lithium pieces were removed with a spatula and the color of the resulting yellow solution was discharged by addition of methanol, dropwise. The mixture was allowed to warm to room temperature and was concentrated in a rotatory evaporator. The residue was resuspended in diethyl ether, dried over anhydrous $MgSO_4$ and filtered over a plug of silica gel. After that, the clear solution

was again concentrated followed by purification of the residue by flash chromatography using 1:1 solution of diethyl ether and methylene chloride as the eluent. Obtained 119 mg (97%) of *trans* diol **10** as a white solid: mp 68.5 - 69 ^{o}C; IR ($CDCl_3$, cm^{-1}) 3614, 3500, 2928, 2886, 2837, 1678, 1444, 1374, 1262; ^{1}H NMR (500 MHz, $CDCl_3$) δ 5.32 (s, 1H), 4.12 (d, *J* = 7.5 Hz, 1H), 3.71 (dd, *J* = 10.5 Hz, 4.3 Hz, 1H), 3.63 (dd, *J* = 10.5 Hz, 8.5 Hz, 1H), 3.51 (*br* s, 1.5H, exchange with D_2O), 2.03 - 2.00 (m, 1H), 1.87 (dd, *J* = 12 Hz, 5.5 Hz, 1H), 1.68 - 1.59 (m, 2H), 1.66 (s, 3H), 1.30 - 1.21 (m, 1H); ^{13}C NMR (125 MHz, $CDCl_3$) ppm 136.75, 124.62, 72.36, 67.50, 43.29, 29.54, 23.39, 22.98.

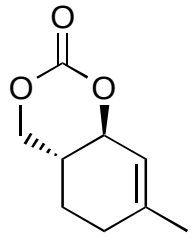

Compound 11: 7-Methyl-(4aR*, 8aR*)-5H, 6H-benzo[a][1, 3]dioxin-2-one

A solution of compound **10** (50 mg, 0.352 mmol), pyridine (285 μL, 3.52 mmol) and DMAP (4 mg, 0.32 mmol) in 2.0 mL of THF was stirred at 0 ^{o}C in a dry flask, under nitrogen. A solution of triphosgene (52.0 mg, 0.176 mmol) in 0.8 mL of diethyl ether was added to the reaction mixture, *via* syringe pump, over 20 min. A white precipitate formed as addition of the reagent progressed. After addition was complete, the reaction mixture was kept at 0 ^{o}C for 1 h and at room temperature for 6 h. After this, the solvent was evaporated and the residue was suspended in 10 mL of water. The aqueous layer was extracted with methylene chloride (3 x 15 mL). The combined organic layers were dried

over anhydrous $MgSO_4$ and concentrated. Purification of the residue by flash chromatography was done using 10% diethyl ether in methylene chloride as the eluent and it afforded 56.2 mg (93%) of the *trans* cyclic carbonate **11** as a clear oil: IR ($CDCl_3$, cm^{-1}) 2976, 2928, 2869, 1749, 1667, 1480, 1406, 1353, 1308, 1237, 1203, 1154 1086; ^1H NMR (500 MHz, $CDCl_3$) δ 5.49 (s, 1H), 4.67 (d, *J* = 9.5 Hz, 1H), 4.43 (dd, *J* = 10.5 Hz, 5 Hz, 1H), 4.12 (dd, *J* = 12 Hz, 10.5 Hz, 1H), 2.23 - 2.16 (m, 1H), 2.10 - 2.01 (m, 2H), 1.89 - 1.84 (m, 1H), 1.74 (s, 3H), 1.43 - 1.34 (m, 1H); ^{13}C NMR (125 MHz, $CDCl_3$) ppm 149.26, 139.04, 119.09, 78.41, 73.06, 34.28, 29.29, 22.83, 21.37; HRMS (EI) *m/z* (M^+) calcd 168.0786, obsd 168.0795.

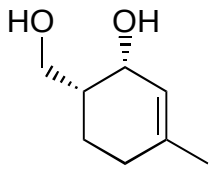

Compound 12: 6-Hydroxymethyl-3-methyl-(1R*, 6R*)-2-cyclohexen-1-ol

A two-neck flask equipped with a dry ice condenser was flame dried and flushed with dry nitrogen. Ethylamine (4 mL, excess) was condensed onto the flask at -78 °C. A solution of alcohol **6b** (100 mg, 0.43 mmol) in 4 mL of diethyl ether was added to the reaction media. Lithium wire (120 mg, 17.3 mmol), was cut in small pieces, and added to the flask. The suspension of lithium pieces in ethereal ethylamine was stirred at -78 °C until the presence of a persistent dark blue color was observed (about 30 min). The suspension was allowed to stir at -78 °C for an additional 15 min before the blue color was discharged by addition of a few drops of 1-octyne. The remaining lithium pieces were

removed with a spatula and the color of the resulting yellow solution was discharged by addition of methanol, dropwise. The mixture was allowed to warm to room temperature and was concentrated in a rotatory evaporator. The residue was resuspended in ether, dried over anhydrous $MgSO_4$ and filtered over a plug of silica gel. After that the clear solution was concentrated followed by purification of the residue by flash chromatography, using 1:1 solution of diethyl ether and methylene chloride as the eluent. Obtained 56 mg (90%) of the *cis* diol **12** as a white solid: mp 63 – 65 ^oC; IR ($CDCl_3$, cm^{-1}) 3609, 3509, 2933, 2885, 2833, 1670, 1601, 1448, 1430, 1382; ^1H NMR (300 MHz, $CDCl_3$) δ 5.61 (s, 1H), 4.28 (s, 1H), 3.86 - 3.73 (m, 2H), 2.04 - 2.02 (m, 1H), 1.86 (*br* s, 2H, exchange with D_2O), 1.73 (s, 3H), 1.76 - 1.54 (m, 4H); ^{13}C NMR (125 MHz, $CDCl_3$) ppm 140.57, 123.18, 66.72, 65.24, 40.11, 30.02, 23.19, 19.7.

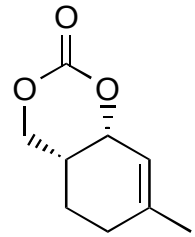

Compound 13: 7-Methyl-(4aR*, 8aS*)-5H, 6H-benzo[a][1, 3]dioxin-2-one

A solution of compound **12** (55 mg, 0.387 mmol) and pyridine (285 μL, 3.52 mmol) in 2.0 mL of THF was placed in a dry flask, under nitrogen, and was stirred at 0 ^oC. A solution of triphosgene (52.0 mg, 0.176 mmol) in 1 mL of THF was added to the reaction mixture, *via* syringe pump, over a period of 160 min. Observed formation of a white precipitate as the addition progressed. After addition was complete, the reaction

mixture was kept at 0 ^{o}C for 1 h and at room temperature for another 3 h. Reaction was quenched while mixture was still cold by addition of 5 mL of methanol. The solvent was evaporated and the residue was purified immediately by flash chromatography using 10% diethyl ether in methylene chloride as the eluent. Isolated 58 mg (89%) of the *cis* cyclic carbonate **13** as a clear colorless oil: IR ($CDCl_3$, cm^{-1}) 2937, 2918, 1743, 1672, 1476, 1405, 1386, 1216, 1184, 1140, 1118; ^{1}H NMR (500 MHz, $CDCl_3$) δ 5.60 (d, *J* = 2.5 Hz, 1H), 4.93 (dd, *J* = 4.3 Hz, 2.5 Hz, 1H), 4.47 (dd, *J* = 11 Hz, 3.5 Hz, 1H), 4.23 (dd, *J* = 11 Hz, 3.5 Hz, 1H), 2.15 - 2.08 (m, 3H), 1.86 - 1.72 (m, 2H), 1.77 (s, 3H); ^{13}C NMR (125 MHz, $CDCl_3$) ppm 149.16, 142.73, 118.44, 75.65, 69.99, 29.52, 28.51, 23.03, 20.20; HRMS (EI) *m/z* (M^{+}) calcd 168.0786, obsd 168.0809.

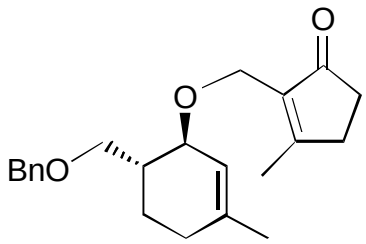

Compound 4: 2-(6-Benzyloxymethyl-3-methyl-(1R*, 6S*)-2-cyclohexenyloxymethyl)-3-methyl-2-cyclopenten-1-one

Reaction was set up in a flame-dried flask, under nitrogen atmosphere, containing about 2 g of activated molecular sieves 4Å. Alcohol **6a** (300 mg, 1.28 mmol) was dissolved in methylene chloride (3.0 mL), along with 2,6-di-tert-butylpyridine (850 μL, 3.84 mmol) and the clear solution was stirred for 30 min. Silver trifluoromethanesulfonate (1.0 g, 3.85 mmol) was added and the reaction flask was protected from light. Chloride **18** (185 mg, 1.28 mmol) was dissolved in 500 μL of methylene chloride and added to the

reaction mixture, *via* syringe pump, over a period of eight hours. The reaction was conducted at room temperature, protected from light, over 12 h. The reaction was quenched by addition of brine (25 mL), ammonium chloride (sat., aq., 7 mL) and stirred for 1 h. The reaction mixture was filtered over celite to give a dark yellow organic phase accompanied by a clear aqueous phase. The layers were separated and the aqueous was back-extracted with CH_2Cl_2 (2 x 10 mL) and EtOAc (2 x 5 mL). Organic phases were reuned, dried over anhydrous $MgSO_4$ and concentrated. (Brown residue). Flash Chromatography with 3% diethyl ether in methylene chloride gave 247 mg (57%) of the ether **4** as a clear oil: IR ($CDCl_3$, cm^{-1}) 3089, 3063, 3025, 2922, 2860, 1695, 1649, 1496, 1453, 1430, 1373, 1041; ^{1}H NMR (300 MHz, $CDCl_3$) δ 7.37 - 7.26 (m, 5H), 5.55 (s, 1H), 4.53 (s, 2H), 4.22 (d, *J* = 10.7 Hz, 1H), 4.10 (d, *J* = 10.7 Hz, 1H), 3.8 (*br* d, *J* = 5.7 Hz, 1H), 3.56 (dd, *J* = 8.9 Hz, 4.3 Hz, 1H), 3.44 (dd, *J* = 8.9 Hz, 6.6 Hz, 1H), 2.51 - 2.49 (m, 2H), 2.39 - 2.36 (m, 2H), 2.13 (s, 3H), 1.98 -1.90 (m, 4H), 1.69 (s, 3H), 1.62 - 1.51 (m, 1H); ^{13}C NMR (75 MHz, $CDCl_3$) ppm 208.16, 175.74, 138.76, 138.32, 137.34, 128.26, 127.50, 127.46, 121.05, 75.20, 73.02, 71.30, 58.59, 38.75, 34.37, 31.87, 28.91, 23.65, 23.45, 17.58; HRMS (EI) *m/z* (M^+) calcd 340.2038, obsd 340.2051; UV π-π* 210 – 250 nm, η-π* 310 – 330 nm. Some of starting material **6a** was also recovered (30%).

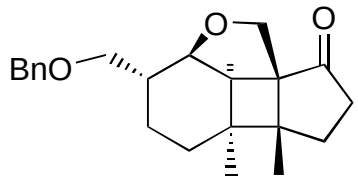

Compound 17: 3-[(Benzyloxy)-methyl]-5a, 5b-dimethyl-(2aR*, 3S*, 5aR*, 5bS*, 8aR*, 8bS*)-perhydro-2-xacyclopenta[4, 1]cyclobuta[c, d]-inden-8-one

A solution prepared by dissolving compound **4** (1.19 g, 3.5 mmol) in 400 mL of benzene (photrex), was deoxygenated by flushing argon through the solution for 1 h. Photoaddition of this solution was conducted at room temperature, for 2 h, by irradiation with a 450 Watt, Hanovia, medium pressure mercury arc lamp until 50% conversion of the substrate. Solvent was evaporated under reduced pressure. Flash chromatography of the residue was conducted in 5% diethyl ether in methylene chloride and gave the photoadduct product, which was reserved, along with 2.18 g of unreacted starting material that was resubmited to the reaction conditions. The process was repeated 3 times. After 3 cycles, 928 mg (78%) of the photoadduct **17** was obtained as a clear oil: IR ($CDCl_3$, cm^{-1}) 3103, 3077, 3039, 2961, 2928, 2865, 1721, 1529, 1454, 1368, 1265 1104, 1059; ^1H NMR (300 MHz, $CDCl_3$) δ 7.26 - 7.16 (m, 5H), 4.38 (s, 2H), 3.76 (d, *J* = 9.9 Hz, 1H), 3.69 (d, *J* = 6.0 Hz, 1H), 3.64 (d, *J* = 9.9 Hz, 1H), 3.25 (dd, *J* = 9.0 Hz, 5.6 Hz, 1H), 3.18 (dd, *J* = 9.0 Hz, 6.3 Hz, 1H), 2.67 - 2.53 (m, 1H), 2.34 - 2.17 (m, 2H), 2.14 (d, *J* = 6Hz, 1H), 1.98 (td, *J* = 13 Hz, 3.1 Hz, 1H), 1.71 - 1.62 (m, 1H), 1.48 - 1.41 (m, 1H), 1.16 - 0.81 (m, 3H), 1.11 (s, 3H), 1.09 (s, 3H); ^{13}C NMR (75 MHz, $CDCl_3$) ppm 218.66, 138.68, 128.62, 127.79, 78.63, 73.33, 73.00, 66.29, 61.07, 51.54, 46.05,

39.05, 36.40, 36.17, 31.31, 27.29, 23.81, 20.91, 19.43; HRMS (EI) *m/z* (M^+) calcd 340.2038, obsd 340.2002.

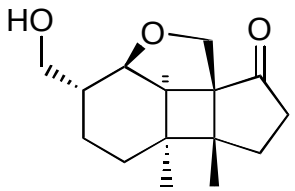

Compound 39: 3-Hydroxymethyl-5a, 5b-dimethyl-(2aR*, 3S*, 5aR*, 5bS*, 8aR*, 8bS*)-perhydro-2-oxacyclopenta[4, 1]cyclobuta[c, d]-inden-8-one

Compound **17** (827 mg, 2.43 mmol) was dissolved in absolute ethanol (70 mL), in a dry Parr shaker flask, under nitrogen. The catalyst, activated 10% palladium on carbon (50 mg, 6% w/w), was added to the solution. The suspension was then stirred at room temperature in a Parr Shaker Hydrogenator apparatus, under 40 psi of hydrogen, for 6 h, until there was no more starting material according to TLC analysis. The reaction mixture was filtered through a 1g SiO_2 plug. The filtrate was dried over anhydrous $MgSO_4$ and concentrated to give 600 mg (98 %) of alcohol **39** as a colorless oil: IR (CCl_4, cm^{-1}) 3640, 2969, 2928, 2865, 1729, 1462, 1454, 1405, 1216, 1132; ^1H NMR (300 MHz, $CDCl_3$) δ 3.76 (d, *J* = 9.9 Hz, 1H), 3.71 (d, *J* = 5.8 Hz, 1H), 3.63 (d, *J* = 9.9 Hz, 1H), 3.44 (dd, *J* = 10.5 Hz, 6.0 Hz, 1H), 3.32 (dd, *J* = 10.5 Hz, 6.9 Hz, 1H), 2.69 - 2.55 (m, 1H), 2.35 - 2.25 (m, 2H), 2.17 (d, *J* = 5.8 Hz, 1H), 2.12 - 1.95 (m, 2H), 1.72 - 1.62 (m, 1H), 1.51 - 1.39 (m, 1H), 1.12 (s, 3H), 1.06 (s, 3H), 1.14 - 0.85 (m, 3H); ^{13}C NMR (75 MHz, $CDCl_3$) ppm 218.31, 77.84, 65.80, 65.09, 60.64, 50.93, 45.78, 38.61, 38.41, 35.91, 30.90, 26.84, 23.34, 20.22, 19.01; HRMS (EI) *m/z* (M^+) calcd 250.1569, obsd 250.1551.

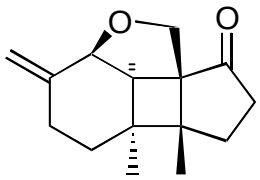

Compound 3: 5a, 5b-Dimethyl-3-methylene-(2aR*, 5aR*, 5bS*, 8aR*, 8bS*) perhydro-2-oxacyclopenta[4, 1]cyclobuta[c, d]inden-8-one

Alcohol **39** (240 mg, 0.96 mmol) and ortho-nitrophenylselenium cyanide (97% pure, 400 mg, 1.7 mmol) were dissolved in THF (6 mL) in a dry flask, under nitrogen. The dark yellow solution was cooled to 0^{o} C and then tri-*n*-butylphosphine (340 μL, 1.36 mmol) was added *via* syringe. The reaction mixture turned to a darker color while it was allowed to stir at 0^{o} C for 2 h and at room temperature for another 8 h. At that point all starting material had been consumed so the THF was evaporated in a rotatory evaporator. The residue was diluted with CH_2Cl_2 (100 mL) and transferred to a 3-neck flask. Diisopropyl amine (3 mL, 21 mmol) was added to the reaction mixture and the resulting solution was cooled to -78^{o} C and submitted to ozonolysis until a pale green color persisted. A stream of nitrogen was bubbled through this solution at -78^{o} C for 2 h to remove excess ozone, and another 5 mL of diisopropyl amine was added before it was allowed to warm to room temperature. The mixture was stirred at room temperature for 10 h. The solvent was evaporated and the residue was resuspended in diethyl ether (50 mL), washed with KOH (2M, 3 x 10 mL) and brine (2 x 10 mL). The organic layer was dried over anhydrous $MgSO_4$ and concentrated. Purification of the residue by flash chromatography, using 5% Et_2O in CH_2Cl_2 as the eluent afforded 167 mg (75 %) of keto-

olefin **3** as a colorless oil: IR ($CDCl_3$, cm^{-1}) 2967, 2932, 2869, 1722, 1515, 1455, 1451, 1373, 1263, 1143, 1051, 1027; ^1H NMR (300 MHz, $CDCl_3$) δ 5.11 (*br* s, 1H), 5.06 (*br* s, 1H), 4.14 (d, *J* = 5.8 Hz, 1H), 3.95 (d, *J* = 10.2 Hz, 1H), 3.88 (d, *J* = 10.2 Hz, 1H), 2.76 - 2.64 (m, 1H), 2.55 - 2.27 (m, 3H), 2.41 (d, *J* = 5.8 Hz, 1H), 2.19 - 2.08 (m, 1H), 1.66 - 1.54 (m, 1H), 1.28 - 1.05 (m, 2H), 1.13 (s, 3H), 1.12 (s, 3H); ^{13}C NMR (75 MHz, $CDCl_3$) ppm 217.60, 142.13, 115.60, 79.71, 67.00, 61.39, 53.63, 46.06, 38.43, 35.77, 30.53, 28.05, 25.38, 22.79, 18.71; HRMS (EI) *m/z* (M^+) calcd 232.1463, obsd 232.1470.

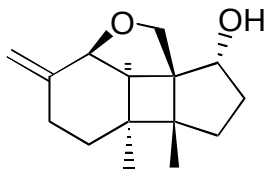

Compound 91: 5a, 5b-Dimethyl-3-methylene-(2aR*, 5aR*, 5bS*, 8S*, 8aR*, 8bS*) perhydro-2-oxacyclopenta [4, 1] cyclobuta [c, d] inden-8-ol

A solution of ketone **3** (142 mg, 0.61 mmol) in 15 mL of diethyl ether was stirred at 0° C as $LiAlH_4$ (22 mg, 0.66 mmol) was added in small portions. The reaction mixture was kept at 0° C for 20 min. The suspension was diluted with 10 mL of diethyl ether, and the reaction was quenched at 0° C by dropwise addition of Na_2SO_4 (aq., sat.) until there was no more evolution of H_2. The suspension was filtered through a mixture of celite and anhydrous $MgSO_4$. Concentration of the filtrate and purification by flash chromatography using 10 % diethyl ether in methylene chloride as the eluent gave 127 mg (89 %) of alcohol **91** as a white solid: mp 115 - 116° C; IR ($CDCl_3$, cm^{-1}) 3615, 3443, 2956, 2928, 2867, 1645, 1602, 1450, 1374, 1327, 1301, 1282, 1244, 1208; ^1H NMR (300 MHz, $CDCl_3$) δ 5.09 (*br* s, 1H), 5.05 (*br* s, 1H), 4.02 (d, *J* = 5.1 Hz, 1H), 3.95 (d, *J* = 9.8 Hz,

1H), 3.88 (dd, *J* = 10.2 Hz, 6.1 Hz, 1H), 3.57 (d, *J* = 9.8 Hz, 1H), 2.46 - 2.39 (m, 1H), 2.29 (td, *J* = 9.8 Hz, 3.5 Hz, 1H), 2.21 - 2.00 (m, 3H), 1.80 - 1.62 (m, 2H), 1.31 - 1.19 (m, 1H), 1.08 - 0.93 (m, 2H), 0.99 (s, 3H), 0.95 (s, 3H); ^{13}C NMR (75 MHz, $CDCl_3$) ppm 143.17, 115.45, 80.38, 72.81, 68.05, 60.39, 46.81, 44.25, 34.89, 34.50, 32.81, 27.22, 25.38, 19.90, 18.67; HRMS (EI) *m/z* (M^+) calcd 234.1619, obsd 234.1615.

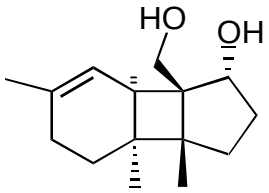

Compound 92: 7b-(Hydroxymethyl)-3a, 3b, 6-trimethyl-(1R*, 3aR*, 3bS*, 7aR*, 7bS*)-2, 3, 3a, 3b, 4, 5, 7a, 7b-octahydro-1*H*-cyclopenta[3, 4] cyclobuta[a]benzen-1-ol

A solution of alcohol **91** (29 mg, 0.12 mmol) in 3 mL of diethyl ether was added to a 2-neck flask containing 3 mL of ethylamine, at -78^o C, and equipped with a dry ice condenser. The resulting clear solution was kept at -78^o C as lithium wire (20 mg, 2.88 mmol) was added. The reaction mixture was vigorously stirred for about 1 h until a stable dark blue color was observed and another 20 min after that. Reaction was then quenched, still cold, by addition of solid NH_4Cl until the blue color disappeared. The excess lithium pieces were removed with the aid of a spatula and a few drops of MeOH were added. Anhydrous $MgSO_4$ was added to the resulting suspension and it was allowed to warm to room temperature. The ethylamine was evaporated and the residue was resuspended in EtOAc, filtered and concentrated in a rotatory evaporator. Purification of the residue by flash chromatography using EtOAc as the eluent gave 26 mg (91%) of diol **92** as a white

solid: mp 104.2 - 105° C; IR ($CDCl_3$, cm^{-1}) 3568, 3434, 2952, 2917, 2871, 1747, 1596, 1467, 1445, 1371, 1295, 1211, 1077, 983; ^1H NMR (300 MHz, $CDCl_3$) δ 5.41 (*br* s, 1H), 4.23 (dd, *J* = 10 Hz, 6.4 Hz, 1H), 4.14 (d, *J* = 10.3 Hz, 1H), 3.73 (d, *J* = 10.3 Hz, 1H), 2.57 (*br* s, 1H), 2.42 (*br* s, 1H), 2.05 - 1.61 (m, 6H), 1.73 (s, 3H), 1.36 - 1.25 (m, 3H), 0.90 (s, 3H), 0.85 (s, 3H); ^{13}C NMR (75 MHz, $CDCl_3$) ppm 136.82, 120.59, 78.96, 66.72, 52.90, 46.83, 39.40, 35.75, 33.43, 31.56, 30.93, 26.27, 24.13, 19.38, 18.22; HRMS (EI) *m/z* (M^+) calcd 236.1776, obsd 236.1782.

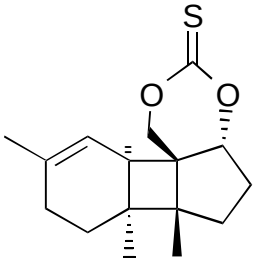

Compound 94: 6a, 6b, 9-Trimethyl-(4aR*, 6aR*, 6bS*, 10aR*, 10bS*)-4a, 5, 6, 6a, 6b, 7, 8, 10a-octahydrobenzo[3', 4']cyclobuta[2, 3]cyclopenta[d][1, 3]dioxin-3-thione

Diol **92** (20 mg, 0.084 mmol) and thionocarbonyl diimidazole (23 mg, 0.13 mmol) were dissolved in 2.5 mL of toluene in a dry flask, under nitrogen. The reaction mixture was heated to reflux for 10 h. Analysis by TLC showed that there was still some starting material present so an additional 11mg (0.065 mmol) of thionocarbonyl diimidazole was added and the reaction mixture was refluxed for another 8 h. At this point there was no more starting material left. The solvent was evaporated and the residue was immediately purified by flash chromatography using 10% EtOAc in hexanes as the eluent. Obtained 19.8 mg (85%) of the cyclic thionocarbonate **94** as a light yellow oil: IR (CCl_4, cm^{-1})

2973, 2957, 2914, 1549, 1253, 1216, 1067, 1005, 979; ^{1}H NMR (300 MHz, $CDCl_3$) δ 5.17 (*br* s, 1H), 4.82 (d, *J* = 9.9 Hz, 1H), 4.52, (d, *J* = 9.9 Hz, 1H), 4.35 (dd, *J* = 10.2 Hz, 6.9 Hz, 1H), 2.39 (*br* s, 1H), 2.33 - 2.14 (m, 3H), 1.96 - 1.83 (m, 2H), 1.72 (s, 3H), 1.58 - 1.38 (m, 3H), 0.93 (s, 3H), 0.92 (s, 3H); ^{13}C NMR (75MHz, $CDCl_3$) ppm 191.26, 139.56, 117.69, 81.95, 79.43, 47.90, 47.19, 40.21, 36.94, 33.16, 30.92, 27.81, 26.00, 23.99, 19.17, 17.53; HRMS (EI) *m/z* (M^+) calcd 278.1341, obsd 278.1334.

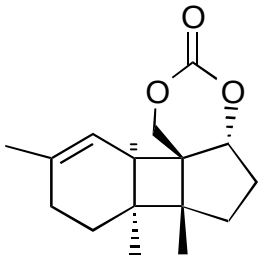

Compound 95: 6a, 6b, 9-Trimethyl-(4aR*, 6aR*, 6bS*, 10aR*, 10bS*)-4a, 5, 6, 6a, 6b, 7, 8, 10a-octahydrobenzo[3', 4']-cyclobuta[2, 3]cyclopenta[d][1, 3]-dioxin-3-one

Compound **92** (26 mg, 0.11 mmol), and pyridine (50 μL, 0.61 mmol) were dissolved in methylene chloride (1.0 mL), in a dry flask, under nitrogen atmosphere. The transparent solution was cooled to 0^{o} C. A solution of triphosgene (12 mg, 0.04 mmol) in 1.6 mL of methylene chloride was added to the cold reaction mixture, *via* syringe, over a 20 min period. After addition, the reaction was allowed to proceed at 0^{o} C for another 150 min. Once there was no more starting material left, according to TLC analysis, the reaction was quenched by addition of brine (5 mL). The organic mixture was extracted with CH_2Cl_2, dried over anhydrous Na_2SO_4 and concentrated. Purification by flash chromatography using 30% EtOAc in CH_2Cl_2 as the eluent gave 26 mg (90 %) of

carbonate **95** as a clear oil: IR ($CDCl_3$, cm^{-1}) 2956, 2931, 2870, 1744, 1606, 1456, 1447, 1396, 1372, 1202, 1167, 1171; ^1H NMR (500 MHz, $CDCl_3$) δ 5.19 (*br* s, 1H), 4.67 (d, *J* = 9.5 Hz, 1H), 4.43 (dd, *J* = 10.5 Hz, 7.0 Hz, 1H), 4.40 (d, *J* = 9.5 Hz, 1H), 2.43 (*br* s, 1H), 2.28 (dd, *J* = 14 Hz, 7 Hz, 1H), 2.18 - 2.10 (m, 2H), 1.97 (*br* t, *J* = 14 Hz, 1H), 1.86 (dt, *J* = 16.5 Hz, 3.5 Hz, 1H), 1.73 (*br* s, 3H), 1.58 - 1.46 (m, 2H), 1.41 (dt, *J* = 12.5 Hz, 3.5 Hz, 1H), 0.97 (s, 3H), 0.94 (s, 3H); ^{13}C NMR (125 MHz, $CDCl_3$) ppm 149.95, 139.24, 118.18, 81.76, 75.24, 47.09, 40.00, 36.87, 33.62, 30.91, 29.66, 27.79, 26.01, 23.94, 19.20, 17.61; HRMS (EI) *m/z* (M^+) calcd 262.1569, obsd 262.1558.

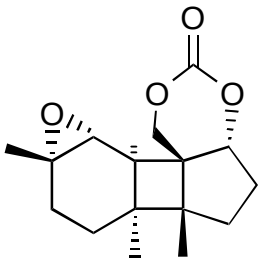

Compound 96: 1a, 3a, 3b-Trimethyl-(1aR*, 3aS*, 3bR*, 5aR*, 9aS*, 9bS*, 9cR*)-perhydrooxireno[2''', 3''':3'', 4'']benzo[3', 4']cyclobuta[2, 3]cyclopenta[d][1, 3] dioxin-7-one

Compound **95** (20 mg, 0.076 mmol) was dissolved in CH_2Cl_2 (2 mL), in a dry flask, under nitrogen, and the clear solution was cooled to 0^o C. *m*-CPBA (75% pure, 24 mg, 0.1 mmol) was dissolved in CH_2Cl_2 and this oxidizing solution was added dropwise to the reaction mixture. After addition was complete, the reaction mixture was stirred at 0^o C for 30 min (until no more starting material was detected by TLC analysis). The reaction was quenched by addition of 4 mL of $NaHCO_3$ (aqueous, sat.). The organic was extracted with diethyl ether, dried over anhydrous Na_2SO_4 and concentrated. Purification

of the residue with flash chromatography, using 10 % EtOAc in hexanes as the eluent yielded 19 mg (90 %) of the pure epoxy-carbonate **96** as white needle-like crystals: mp 108 – 110° C; IR ($CDCl_3$, cm^{-1}) 2974, 2927, 2829, 2252, 1751, 1602, 1474, 1441, 1386, 1369, 1193, 1170, 1111; ^{1}H NMR (500 MHz, C_6D_6) δ 4.01 (d, *J* = 10 Hz, 1H), 3.64 (d, *J* = 10. Hz, 1H), 3.33 (dd, *J* = 10 Hz, 7 Hz, 1H), 2.83 (d, *J* = 3 Hz, 1H), 2.25 (d, *J* = 3 Hz, 1H), 1.56 - 1.45 (m, 3 H), 1.26 (dd, *J* = 10 Hz, 4.5 Hz, 1H), 1.23 (t, *J* = 3.5 Hz, 1H), 1.19 (dd, *J* = 10 Hz, 4.5 Hz, 1H), 1.03 (s, 3H), 0.97 - 0.92 (m, 1 H), 0.67 - 0.58 (m, 1H), 0.57 (s, 3H), 0.30 (s, 3H); ^{13}C NMR (125 MHz, C_6D_6) ppm 148.84, 81.37, 73.87, 57.23, 56.60, 45.55, 44.13, 38.77, 35.01, 33.67, 28.78, 27.36, 27.29, 22.59, 22.33, 16.63; HRMS (EI) *m/z* (M^+) calcd 278.1518, obsd 278.1509.

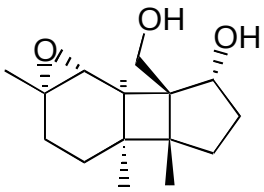

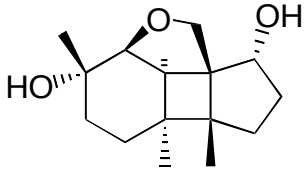

Compounds 97 and 98: 6a-Hydroxymethyl-1a, 3a, 3b-trimethyl-(1aR*, 3aR*, 3bS*, 6S*, 6aR*, 6bS*, 6cS*)perhydrocyclopenta[3 , 4]cyclobuta[3, 4]benzo[b]oxiren-6-ol and 3, 5a, 5b-Trimethyl-(2aR*, 3R*, 5aR*, 5bS*, 8S*, 8aR*, 8bS*)-perhydro-2-oxacyclopenta[4, 1]cyclobuta[c, d]indene-3, 8-diol

Method A: Compound **96** (40 mg, 0.146 mmol) was dissolved in THF (800 μL) and the solution was cooled to 0° C. A solution of LiOH (0.11M, aqueous, 800 μL) was added and the mixture was stirred at 4° C for 6h. The THF was removed in the rotatory evaporator and the residue was ressuspended in diethyl ether. The organic layer was washed with NH_4Cl (aqueous, sat.), until pH neutral, and then it was washed once with

brine. The combined aqueous phase was back-extracted with ethyl acetate. The organic layers were reuned, dried over anhydrous Na_2SO_4 and concentrated. Purification *via* flash chromatography using 60 % EtOAc in CH_2Cl_2 as the eluent gave 6 mg of the diol epoxide **97** (0.024 mmol, 16 % yield) as a clear oil as well as 29 mg of the cyclic ether **98** (0.115 mmol, 79 % yield) as a white solid.

Method B: Sodium bicarbonate (20 mg, 0.24 mmol) was suspended in a solution of compound **92** (26 mg, 0.11 mmol) in chloroform (2 mL). The heterogeneous mixture was cooled to 0^o C. A solution of *m*-CPBA (75 % pure, 28 mg, 0.12 mmol) dissolved in 2 mL of chloroform was added dropwise to the reaction mixture. The mixture was kept at 0^o C for 20 min, and then the reaction was quenched by addition of 3 mL of Na_2CO_3 (sat., aqueous). The phases were separated and the aqueous was extracted with diethyl ether (3 x 5 mL). The combined organic layers were washed once with $NaHSO_3$ (aqueous, 10 %) and once with $NaHCO_3$ (aqueous, sat.) and then dried over anhydrous Na_2SO_4. Purification *via* flash chromatography using 40 % diethyl ether in methylene chloride as the eluent gave 19.2 mg (69 %) of epoxide **97** as a clear oil and 4.7 mg (17 %) of the cyclic ether **98** as a white solid.

Compound **97**: IR (CCl_4, cm^{-1}) 3560, 2958, 2935, 2880, 1468, 1452, 1374, 1370, 1296, 1073, 985; ^{1}H NMR (500 MHz, C_6D_6) δ 4.63 (d, *J* = 11 Hz, 1H), 4.08 (dd, *J* = 10 Hz, 6.5 Hz, 1 H), 3.62 (d, *J* = 11 Hz, 1H), 2.82 (*br* s, 1H), 2.79 (d, *J* = 4.5 Hz, 1H), 2.23 (d, *J* = 4.5 Hz, 1H), 2.19 (*br* s, 1H), 2.01 - 1.95 (m, 2H), 1.81 - 1.72 (m, 1H), 1.67 (dd, *J* = 13.5 Hz, 8 Hz, 1H), 1.57 (dt, *J* = 14.5 Hz, 3.5 Hz, 1H), 1.44 (td, *J* = 14.5 Hz, 3.5 Hz, 1H), 1.10 (s, 3H), 1.01 (td, *J* = 13.5 Hz, 6.5 Hz, 1H), 0.73 - 0.68 (m, 1H), 0.66 (s, 3H), 0.62 (s, 3H); ^{13}C NMR (125 MHz, C_6D_6) ppm 80.70, 67.02, 58.97, 56.00, 54.86, 47.48,

36.16, 34.46, 33.18, 31.48, 26.57, 26.20, 22.04, 18.78, 17.07; HRMS (EI) *m/z* (M^+) calcd 252.1726, obsd 252.1742.

Compound **98**: mp 129.6 - 131.8° C; IR (CCl_4, cm^{-1}) 3626, 2950, 2908, 2856, 1733, 1457, 1371, 1058, 914; ^1H NMR (500 MHz, $CDCl_3$) δ 3.92 (d, *J* = 9.5 Hz, 1H), 3.84 (dd, *J* = 10 Hz, 7 Hz, 1H), 3.53 (d, *J* = 9.5 Hz, 1H), 3.51 (d, *J* = 6.5 Hz, 1H), 2.66 (*br* s, 2H), 2.41 (d, *J* = 6.5 Hz, 1H), 2.11 (m, 1H, 5 lines), 1.94 (dd, *J* = 14 Hz, 8 Hz, 1H), 1.88 - 1.80 (m, 2H), 1.78 - 1.73 (m, 1H), 1.42 - 1.34 (m, 1H), 1.34 (s, 3H), 1.21 - 1.08 (m, 2 H), 1.06 (s, 3H), 0.94 (s, 3H); ^{13}C NMR (125 MHz, $CDCl_3$) ppm 84.55, 73.16, 70.14, 68.80, 58.92, 46.21, 42.35, 34.85, 32.93, 32.62, 29.36, 28.12, 26.77, 22.41, 18.26; HRMS (EI) *m/z* (M^+) calcd 252.1726, obsd 252.1735.

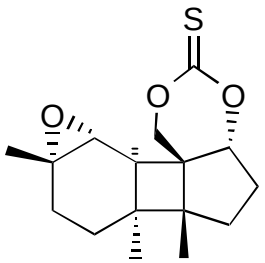

Compound 99: 1a, 3a, 3b-Trimethyl-(1aR*, 3aS*, 3bR*, 5aR*, 9aS*, 9bS*, 9cR*)-perhydrooxireno [2''', 3''':3'', 4''] benzo [3', 4'] cyclobuta [2, 3] cyclopenta[d][1, 3] dioxin-7-thione

Compound **97** (24 mg, 0.095 mmol) and pyridine (80 μL, 0.99 mmol) were dissolved in toluene (10 mL). The solution was cooled to 0° C and to it, a solution of thiophosgene (95 % pure, 16 μL, 0.2 mmol) in 2 mL of toluene was added over a period of 1 h. After addition, the reaction mixture was stirred at 0° C for another 1 h and then was quenched by addition of 20 mL of brine. The aqueous phase was extracted with

EtOAc and the organic was dried over anhydrous Na_2SO_4 and concentrated. Purification of the residue by flash chromatography using 10 % diethyl ether in CH_2Cl_2 as the eluent gave 12.8 mg (46 %) of thionocarbonate **99** as a light yellow oil: IR ($CDCl_3$, cm^{-1}) 2969, 2925, 2867, 2252, 1721, 1601, 1467, 1447, 1389, 1273; ^{1}H NMR (300 MHz, $CDCl_3$) δ 5.67 (d, *J* = 9.5 Hz, 1H), 4.51 (d, *J* = 9.5 Hz, 1H), 4.30 (dd, *J* = 11 Hz, 6 Hz, 1H), 2.93 (d, *J* = 4.5 Hz, 1H), 2.27 - 2.16 (m, 3H), 2.12 - 2.05 (m, 1H), 1.96 (td, *J* = 13 Hz, 4 Hz, 1H), 1.86 (dt, *J* = 14.5 Hz, 3.5 Hz, 1H), 1.77 (td, *J* = 14 Hz, 3.5 Hz, 1H), 1.41 (td, *J* = 13.5 Hz, 7 Hz, 1H), 1.32 (s, 3H), 1.03 (*br* d, *J* = 13.5 Hz, 1H), 0.98 (s, 3H), 0.96 (s, 3H); ^{13}C NMR (75MHz, $CDCl_3$) ppm 191.65, 83.11, 79.38, 56.84, 51.29, 48.37, 48.00, 37.45, 36.50, 33.20, 27.69, 26.08, 25.84, 21.87, 19.26, 16.83; HRMS (EI) *m/z* (M^+) calcd 294.1290, obsd 294.1286.

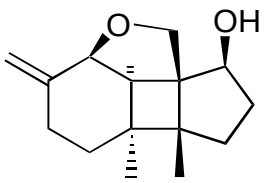

Compound 100: 5a, 5b-Dimethyl-3-methylene-(2aR*, 5aR*, 5bS*, 8R*, 8aR*, 8bS*) perhydro-2-oxacyclopenta[4, 1]cyclobuta[c, d]inden-8-ol

Compound **91** (127 mg, 0.54 mmol), triphenyl phosphine (147 mg, 0.56 mmol) and benzoic acid (134 mg, 1.09 mmol) were dissolved in THF (2 mL) in a dry flask, under nitrogen. DEAD (95 μL, 0.60 mmol) was dissolved in 2 mL of THF and this solution was added to the reaction mixture, at room temperature, over a period of 100 min. The solution turned yellow. Reaction was allowed to proceed at room temperature for another

8h. TLC analysis showed no more change, but conversion was not complete. The solvent was evaporated and the residue was purified by flash chromatography using 30 % EtOAc in hexanes as the eluent to give 142 mg (78 %) of the benzoate and 19.8 mg (16 %) of unreacted starting material **91**. Hydrolysis of the ester was conducted by dissolving the benzoate (142 mg, 0.42 mmol) in 4 mL of methanol and adding this solution to KOH (aqueous, 3.6 M, 2 mL). The yellow color disappeared, and a precipitate formed. The reaction mixture was stirred for 8 h, at room temperature, and once the conversion was complete, according to TLC analysis, the methanol was evaporated. The remaining aqueous phase was extracted with CH_2Cl_2 (3 x 5 mL) and the combined organic layer was washed with brine, dried over anhydrous $MgSO_4$ and concentrated. Purification of the residue using flash chromatography with 30 % EtOAc in hexanes as the eluent gave 75 mg (75 %) of the inverted alcohol **100** as a white solid: mp 102 - 103.5^{o} C; IR (CCl_4, cm^{-1}) 3626, 2948, 2925, 2858, 1742, 1453, 1372, 1264, 1051, 1006, 942; ^{1}H NMR (500 MHz, $CDCl_3$) δ 5.09 (*br* s, 1H), 5.04 (*br* s, 1H), 4.10 - 4.04 (m, 3H), 3.69 (d, *J* = 10 Hz, 1H), 2.42 (*br* d, *J* = 17 Hz, 1H), 2.31 (td, *J* = 13.5 Hz, 3.7 Hz, 1H), 2.13 - 2.10 (m, 2H), 2.08 - 1.97 (m, 1H), 1.83 (dd, *J* = 13.5 Hz, 7.5 Hz, 1H), 1.75 - 1.68 (m, 2H), 1.25 (*br* s, 1H), 1.07 (s, 3H), 1.02 (dt, *J* = 13.0 Hz, 3.7 Hz, 1H), 0.95 (s, 3H); ^{13}C NMR (125 MHz, $CDCl_3$) ppm 143.36, 115.70, 80.06, 79.10, 68.79, 61.68, 47.97, 47.88, 35.62, 34.49, 33.58, 26.89, 25.02, 20.68, 18.75; HRMS (EI) *m/z* (M^+) calcd 234.1619, obsd 234.1611.

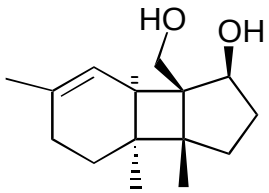

Compound 101: 7b-(Hydroxymethyl)-3a, 3b, 6-trimethyl-(1R*, 3aS*, 3bR*, 7aS*, 7bR*)-2, 3, 3a, 3b, 4, 5, 7a, 7b-octahydro-1*H*-cyclopenta [3, 4] cyclobuta [a] benzen-1-ol

A solution of alcohol **100** (40 mg, 0.171 mmol) in 6 mL of diethyl ether was added to a 2-neck flask containing 6 mL of ethylamine, at -78^{o} C, and equipped with a dry ice condenser. The resulting clear solution was kept at -78^{o} C as lithium wire (20 mg, 2.88 mmol) was added. The reaction mixture was vigorously stirred for about 1 h until a stable dark blue color was observed and another 20 min after that. Reaction was then quenched, still cold, by addition of solid NH_4Cl until the blue color disappeared. The excess lithium pieces were removed with the aid of a spatula and a few drops of MeOH were added. Anhydrous $MgSO_4$ was added to the resulting suspension and it was allowed to warm to room temperature. The ethylamine was evaporated and the residue was resuspended in EtOAc, filtered and concentrated. Purification of the residue by flash chromatography using 5 % diethyl ether in methylene chloride as the eluent gave 39 mg (97%) of diol **101** as a clear oil: IR (CCl_4, cm^{-1}) 3625, 3524, 2954, 2926, 2884, 1731, 1449, 1436, 1370, 1263, 1032, 953; ^{1}H NMR (300 MHz, $CDCl_3$) δ 5.35 (s, 1H), 4.18 (d, J = 8.0 Hz, 1 H), 3.95 (s, 2H), 2.70 (*br* s, 1H, exchange with D_2O), 2.30 (*br* s, 1H, exchange with D_2O), 2.15 – 1.95 (m, 2H), 1.90 – 1.70 (m, 5H), 1.75 (s, 3H), 1.38 – 1.24 (m, 2H), 1.05 (s, 3H), 0.85 (s, 3H); ^{13}C NMR (75 MHz, $CDCl_3$) ppm 137.40, 119.11, 80.71, 63.46, 55.80,

48.21, 44.11, 35.78, 35.05, 33.78, 30.96, 26.49, 24.24, 20.69, 19.13; HRMS (EI) *m/z* (M^+) calcd 236.1776, obsd 236.1792.

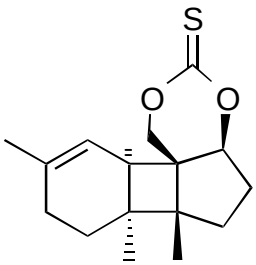

Compound 102: 6a, 6b, 9-Trimethyl-(4aR*, 6aS*, 6bR*, 10aS*, 10bR*)-4a, 5, 6, 6a, 6b, 7, 8, 10a-octahydrobenzo[3', 4']-cyclobuta[2, 3] cyclopenta[d][1, 3]-dioxin-3-thione

Diol **101** (7.0 mg, 0.03 mmol) and thiocarbonyl diimidazole (8 mg, 0.05 mmol) was dissolved in 2 mL of toluene in a dry flask, under nitrogen. The reaction mixture was heated to reflux for 10 h. At this point there was no more starting material left. The solvent was evaporated and the residue was immediately purified by flash chromatography using 10% EtOAc in hexanes as the eluent. Obtained 8 mg (95 %) of cyclic thionocarbonate **102** as a light yellow oil: IR (CCl_4, cm^{-1}) 2957, 2288, 1589, 1247, 1223, 1048, 1012, 979, 774; ^{1}H NMR (300 MHz, $CDCl_3$) δ 5.09 (s, 1H), 4.67 (d, *J* = 9.5 Hz, 1H), 4.33 (d, *J* = 9.5 Hz, 1H), 4.18 (*br* s, 1H), 2.09 (s, 1H), 2.01 – 1.82 (m, 3H), 1.67 – 1.49 (m, 2H), 1.38 (s, 3H), 1.24 – 1.03 (m, 4 H), 0.58 (s, 3H), 0.51 (s, 3H); HRMS (EI) *m/z* (M^+) calcd 278.1341, obsd 278.1328.

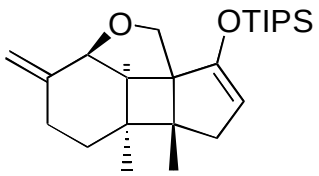

Compound 103: 5a, 5b-dimethyl-3-methylene-(2aR*, 5aR*, 5bS*, 8aR*, 8bS*)-[(2a, 3, 4, 5, 5a, 5b, 6, 8b-octahydro-2-oxacyclopenta[4, 1]cyclobuta[c, d]inden-8-yl)oxy](triisopropyl)silane

LDA was prepared at -78° C, in a dry flask, under nitrogen, by slow addition of BuLi (1.4M in hexanes, 1.5 mL, 2.1 mmol) to a solution of diisopropylamine (280 μL, 2.0 mmol) in THF (5 mL). Compound **3** (38 mg, 0.16 mmol) was dissolved in 1 mL of THF and this solution was cooled to -78° C. The freshly prepared LDA (800 μL, 0.24 mmol) was added *via cannula* and enolization was allowed to proceed for 30 min. The enol was trapped by addition of TIPSOTf (73 μL, 0.27 mmol) in one portion and the reaction mixture was stirred for 2 h. The reaction was quenched by addition of 1 mL of H_2O and the solution was allowed to warm to room temperature. The THF was evaporated under reduced pressure and the residue was extracted with diethyl ether. The organic phase was dried over anhydrous $MgSO_4$, concentrated and the residue was purified by flash chromatography using 30 % CH_2Cl_2 in hexanes as the eluent to give 54 mg (87 %) of the TIPS enol ether **103** as a clear oil: IR (CCl_4, cm^{-1}) 3071, 2953, 2869, 1638, 1465, 1370, 1325, 1251, 1178, 1026; ^{1}H NMR (500 MHz, $CDCl_3$) δ 5.03 (*br* s, 1H), 4.95 (*br* s, 1H), 4.63, (*br* s, 1H), 4.18 (d, *J* = 6.5 Hz, 1H), 3.93 (d, *J* = 9.0 Hz, 1H), 3.70 (d, *J* = 9.0 Hz, 1H), 2.65 - 2.58 (m, 2H), 2.4 (d, *J* = 6.5 Hz, 1H), 2.07 - 1.99 (m, 2H), 1.85 (dd, *J* = 16Hz, 1.5 Hz, 1H), 1.26 (s, 3H), 1.25 - 1.06 (m, 4H), 1.12 (s, 3H), 1.08 (d, *J* = 9.0 Hz,

18H); ^{13}C NMR (75MHz, $CDCl_3$) ppm 153.49, 145.93, 112.86, 102.31, 80.61, 68.34, 60.87, 53.66, 44.92, 38.79, 34.71, 32.52, 27.66, 27.36, 18.24, 17.68, 17.61, 12.01.

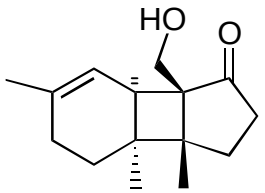

Compound 105: 7b-(Hydroxymethyl)-3a, 3b, 6-trimethyl-(3aR*, 3bS*, 7aR*, 7bS*)-2, 3, 3a, 3b, 4, 5, 7a, 7b-octahydro-1*H*-cyclopenta[3, 4]cyclobuta[a]benzen-1-one

A solution of compound **103** (54 mg, 0.14 mmol) in 6 mL of diethyl ether was added to a 2-neck flask containing 6 mL of ethylamine, at -78° C, and equipped with a dry ice condenser. The resulting clear solution was kept at -78° C as lithium wire (10 mg, 1.45 mmol) was added. The reaction mixture was vigorously stirred for about 30 min until a stable dark blue color was observed and another 25 min after that. Reaction was then quenched, still cold, by addition of solid NH_4Cl until the blue color disappeared. The excess lithium pieces were removed with the aid of a spatula and MeOH (2 mL) was added. The suspension was allowed to warm to room temperature, the ethylamine was allowed to evaporate and the residue was resuspended in EtOAc, washed with brine, dried over anhydrous $MgSO_4$ and concentrated. Obtained 52 mg (95%) of alcohol **104** as a light oil. This intermediate could be purified by flash chromatography using 5 % ethyl acetate in hexanes as the eluent for characterization, but for most cases it was carried on crude to the next step. The deprotection was carried out by addition of TBAF (1.0 M in THF, 1 mL) to the crude reduced product **104** at 0° C, allowing the mixture to warm to

room temperature, and stirring it for 24 h. The reaction was quenched by addition of NH_4Cl (aqueous, sat., 3 mL). The mixture was extracted with diethyl ether (3 x 5 mL) and dried over anhydrous $MgSO_4$. Concentration and purification via flash chromatography using 5 % diethyl ether in CH_2Cl_2 as the eluent gave 24 mg (73 % overall) of keto-alcohol **105** as a light viscous oil: IR ($CDCl_3$, cm^{-1}) 3606, 3501, 2960, 2927, 2877, 1713, 1601, 1446, 1405, 1373, 1299, 1152, 1021; ^1H NMR (500 MHz, $CDCl_3$) δ 5.33 (*br* s, 1H), 3.95 (d, *J* = 12 Hz, 1H), 3.84 (d, *J* = 12 Hz, 1H), 2.73 - 2.66 (m, 1H, 5 lines), 2.42 - 2.31 (m, 2H), 2.29 (*br* s, 1H), 1.94 - 1.84 (m, 2H), 1.72 (s, 3H), 1.68 - 1.61 (m, 2H), 1.45 - 1.42 (m, 1H), 1.26 (*br* s, 1H), 1.10 (s, 3H), 1.03 (s, 3H); ^{13}C NMR (125 MHz, $CDCl_3$) ppm 224.19, 138.60, 117.85, 61.65, 57.22, 46.08, 44.53, 37.46, 37.17, 30.47, 29.95, 25.99, 23.80, 21.11, 18.20; HRMS (EI) *m/z* (M^+) calcd 234.1620, obsd 234.1602.

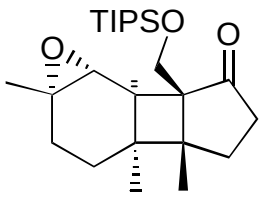

Compound 106: 1a, 3a, 3b-trimethyl-6a-{[(1, 1, 1-trimethylsilyl)oxy]methyl}-(1aR*, 3aR*, 3bS*, 6aR*, 6bS*, 6cS*)-perhydrocyclopenta[3 , 4]cyclobuta[3, 4] benzo[b]oxiren-6-one

Compound **105** (30 mg, 0.13 mmol), imidazole (20 mg, 0.29 mmol) and DMAP (4 mg, 0.03 mmol) were dissolved in 0.5 mL of dichloromethane, in a dry flask, under nitrogen. The reaction system was cooled to 0^oC and a solution of TIPSOTf (75 μL, 0.28

mmol) in 0.5 mL of CH_2Cl_2 was added *via* syringe. The reaction mixture was kept at 0^o C for 2 h until no more substrate was left. The reaction was quenched by addition of 2 mL of water followed by extraction with methylene chloride (3 x 3 mL). The organic layers were combined, washed once with NH_4Cl (sat., aqueous), dried over Na_2SO_4 and concentrated. Purification *via* flash chromatography using 1:1 ethyl acetate in hexanes gave 41.6 mg (81.5 %) of the TIPS protected hydroxy ketone intermediate. The protected intermediate (41.6 mg, 0.106 mmol) was dissolved in 1 mL of CH_2Cl_2, in a dry flask, under nitrogen. $NaHCO_3$ (15 mg, 0.178 mmol) was added and the suspension was cooled to 0^o C. A solution of *m*-CPBA (75 % pure, 30 mg, 0.130 mmol) dissolved in 1 mL of CH_2Cl_2 was added dropwise, *via* syringe, and the reaction mixture was stirred at 0^o C for 2 h. Reaction was quenched by addition of brine (1 mL) and Na_2CO_3 (solid). The layers were separated, and the aqueous was extracted with dichloromethane. The combined organic phase was dried over Na_2SO_4 and concentrated. Purification of the residue using flash chromatography with 5 % Et_2O in CH_2Cl_2 as the eluent gave 27 mg (62 %) of epoxide **106** as a light yellow oil: ^{1}H NMR (300 MHz, $CDCl_3$) δ 4.22 (d, J = 8.0 Hz, 1H), 3.94 (d, J = 8.0 Hz, 1H), 2.80 (d, J = 4.0 Hz, 1H), 2.65 – 2.45 (m, 2H), 2.42 – 2.25 (m, 1H), 2.24 – 2.05 (m, 1H), 2.21 (d, J = 4.0 Hz, 1H), 2.04 – 1.88 (m, 1H) 1.73 – 1.50 (m, 3H), 1.60 (s, 3H), 1.45 – 1.18 (m, 2H), 1.35 (s, 3H), 1.32 (s, 3H), 1.15 –0.80 (m, 18 H); ^{13}C NMR (125MHz, $CDCl_3$) ppm 221, 62.8, 60.8, 57.5, 55.6, 47.2, 42.6, 37.4, 35.3, 31.7, 29.4, 28.1, 25.5, 22.5, 19.4, 17.5, 11.7; HRMS (EI) *m/z* (M^+) calcd 406.2903, obsd 406.2933.

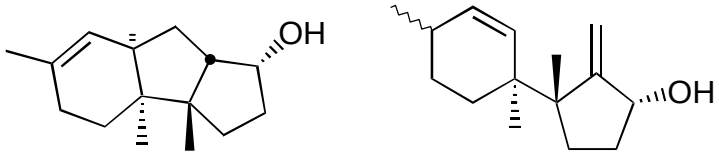

Compounds 107 and 108: 3a, 3b, 6-Trimethyl-(1R*, 3aS*, 3bS*, 7aR*, 8aS*)-1, 2, 3, 3a, 3b, 4, 5, 7a, 8, 8a-decahydrocyclopenta[a]inden-1-ol and 3(1, 4-Dimethyl-(1R*)-2-cyclohexenyl)-3-methyl-2-methylene-(1R*, 3R*)-cyclopentan-1-ol

Toluene used in this reaction was first deoxygenated using the freeze-pump-thaw technique (3 cycles). A standard solution of Bu_3SnH / AIBN in toluene was prepared by dissolving Bu_3SnH (125 μL, 0.46 mmol) and AIBN (8 mg, 0.095 mmol) in toluene (10 mL). A solution of cyclic thionocarbonate **94** (24 mg, 0.09 mmol) in 28 mL of toluene was heated to reflux as 2.5 mL of the above standard solution was added *via* syringe pump over 6 h. After addition, the reaction mixture was allowed to reflux for an additional 60 min and it was then set to cool to room temperature. Solvent was evaporated *in vacuo*. The residue was ressuspended in 2.0 mL of wet ether and titrated with a saturated solution of iodine in ether until the orange color persisted.[196] A suspension of 1,8-diazabicyclo [5.4.0] undec-7-ene (60 mg, 0.39 mmol) in diethyl ether (4.0 mL) was added. Some white precipitate formed first and disappeared later. After this reaction mixture was stirred at room temperature for 1 h, water (40 mL) was added and the aqueous layer was extracted with diethyl ether (3 x 20 mL). The combined organic layers were dried over anhydrous Na_2SO_4 and concentrated. Purification of the residue by flash chromatography using 10 % diethyl ether in methylene chloride gave 9.0

[196] Curran, D. P.; Chang, C-T. *J. Org. Chem.* **1989**, 54, 3140.

mg (47%) of the tricyclic alcohol **107** and 3.5 mg (18%) of the diene-ol **108** as colorless oils.

Tricyclic alcohol **107**: IR (CCl_4, cm^{-1}) 3631, 2959, 2926, 2854, 1771, 1455,1369, 1115; ^1H NMR (500 MHz, $CDCl_3$) δ 5.46 (*br* d, *J* = 4.5 Hz, 1H), 4.34 (q, *J* = 6.5Hz, 1H), 2.19 - 2.15 (m, 1H), 2.07 - 2.04 (m, 1H), 2.02 - 1.90 (m, 3H), 1.87 - 1.79 (m, 2H), 1.65 (s, 3H), 1.61 - 1.54 (m, 1H), 1.44 - 1.26 (m, 4H), 1.15 - 1.10 (m, 1H), 0.92 (s, 3H), 0.79 (s, 3H); ^{13}C NMR (75MHz, $CDCl_3$) ppm 131.22, 124.14, 74.87, 52.64, 45.18, 43.55, 41.04, 33.64, 33.03, 31.85, 27.87, 27.63, 23.32, 21.66, 16.92; HRMS (EI) *m/z* (M^+) calcd 220.1827, obsd 220.1811.

Diene-ol **108** (3:1 mixture of diastereomers by GC-MS analysis): IR ($CHCl_3$, cm^{-1}) 3387, 3353, 1467, 1446, 1066, 1032; ^1H NMR (500 MHz, $CDCl_3$) δ 5.98 and 5.84 (d, *J* = 10.8 Hz, 1H), 5.57 and 5.53 (d, *J* = 10.8 Hz, 1H), 5.29 and 5.28 (s, 1H), 5.14 and 5.10 (s, 1H), 4.42 and 4.41 (s, 1H), 2.38–2.32 (m, 1H), 2.20–2.10 (m, 1H), 1.99–1.95 and 1.92–1.87 (m, 1H), 1.84 – 1.78 (m, 1H), 1.73 – 1.60 (m, 2H), 1.57 – 1.53 (m, 2H), 1.47, 1.43 (m, 1H), 1.37 and 1.36 (s, 3H), 1.16 –1.06 (m, 6 lines, 6H); HRMS (EI) *m/z* (M^+) calcd 220.1827, obsd 220.1793.

Fragmentation of compound 99

Toluene used in this reaction was first deoxygenated using the freeze-pump-thaw technique (3 cycles). A standard solution of Bu_3SnH / AIBN in toluene was prepared by dissolving Bu_3SnH (125 μL, 0.46 mmol) and AIBN (6.5 mg, 0.05 mmol) in toluene (10 mL). A solution of cyclic thionocarbonate **99** (7.7 mg, 0.026 mmol) in 10 mL of toluene

was heated to reflux as 735 μL of the above standard solution was added *via* syringe pump over 6 h. After addition, the reaction mixture was allowed to reflux for an additional 1 h and it was then cooled to room temperature. Solvent was evaporated *in vacuo*. The residue was ressuspended in 10 mL of wet diethyl ether and titrated with a saturated solution of iodine in ether until the orange color persisted.[196] A suspension of DBU (23 mg , 0.15 mmol) in diethyl ether (1 mL) was added. Some white precipitate formed first and disappeared later. After this reaction mixture was stirred at room temperature for 1 h, water (10 mL) was added and the aqueous layer was extracted with diethyl ether (3 x 8 mL). The combined organic layers were dried over anhydrous Na_2SO_4 and concentrated. Purification of the residue by flash chromatography using 10 % diethyl ether in methylene chloride gave 5.7 mg (78 %) of compound **96** as a colorless oil.

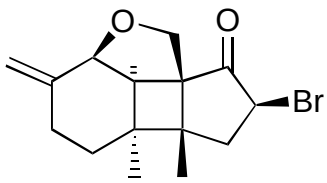

Compound 112: 7-Bromo-5a, 5b-dimethyl-3-methylene-(2aR*, 5aR*, 5bS*, 7R*, 8aR*, 8bS*)perhydro-2-oxacyclopenta[4, 1]cyclobuta[c, d]inden-8-one

Compound **3** (31 mg, 0.13 mmol) was dissolved in 5 mL of ethyl acetate, in a dry flask, under nitrogen. PhSeBr (80 mg, 0.34 mmol) was added to the reaction mixture and was let stir for 1 h. The solvent was removed in the rotatory evaporator and the dark brown residue was immediately purified by flash chromatography using 1:1 CH_2Cl_2 and hexanes as the eluent, 29mg (72 %) of the bromo-ketone **112** was obtained as a light

yellow oil: IR ($CDCl_3$, cm^{-1}) 3077, 2950, 2930, 2866, 1749, 1737, 1449, 1378, 1294, 1267, 1066,1027, 907; ^1H NMR (500 MHz, $CDCl_3$) δ 5.14 (s, 1H), 5.12 (s, 1H), 4.83 (t, *J* = 9.0 Hz, 1H), 4.16 (d, *J* = 6.0 Hz, 1H), 4.05 (d, *J* = 10.0 Hz, 1H), 3.95 (d, *J* = 10.0 Hz, 1H), 3.06 (dd, *J* = 15 Hz, 9 Hz, 1H), 2.51 (*br* d, *J* = 16.5 Hz, 1H), 2.39 (d, *J* = 6.0 Hz, 1H), 2.34 (td, *J* = 13.0, 8.0 Hz, 1H), 2.13 (*br* t, *J* = 13 Hz, 1H), 1.98 (dd, *J* = 15.0, 9.0 Hz, 1H), 1.23 (s, 3H), 1.19 (*br* t, *J* = 8.5 Hz, 1H), 1.15 (s, 3H); ^{13}C NMR (75MHz, $CDCl_3$) ppm 209.32, 141.85, 116.75, 79.90, 67.57, 58.88, 53.45, 48.88, 45.83, 41.57, 36.00, 27.39, 24.97, 22.75, 18.55; HRMS (EI) *m/z* (M^+) calcd 310.0568, obsd 310.0557.

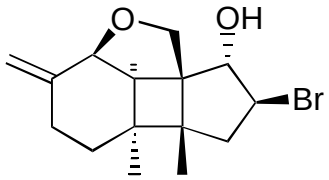

Compound 116: 7-Bromo-5a, 5b-dimethyl-3-methylene-(2aR*, 5aR*, 5bS*, 7S*, 8S*, 8aR*, 8bS*)perhydro-2-oxacyclopenta[4, 1]cyclobuta[c, d]inden-8-ol

Compound **112** (15 mg, 0.05 mmol) was dissolved in 2 mL of diethyl ether, in a dry flask, under nitrogen and the resulting light yellow solution was cooled to 0^o C. $LiAlH_4$ (2 mg, 0.06 mmol) was added to the reaction mixture in one portion. The reaction mixture was allowed to warm to room temperature and was let stir for 30 min. The suspension was cooled to 0^o C, diluted with 5 mL of diethyl ether, and the reaction was quenched by dropwise addition of Na_2SO_4 (aqueous, sat.) until there was no more evolution of H_2. The suspension was filtered through a mixture of celite and anhydrous $MgSO_4$. Concentration of the filtrate and purification by flash chromatography using 20

% diethyl ether in methylene chloride as the eluent gave 9.9 mg (63 %) of bromo-alcohol **116** as a clear oil: IR ($CDCl_3$, cm^{-1}) 3692, 3605, 2950, 2928, 2861, 2253, 1603, 1455, 1016; ^1H NMR (500 MHz, $CDCl_3$) δ 5.12 (s, 1H), 5.07 (s, 1H), 4.26 - 4.20 (m, 1H), 4.05 (d, *J* = 5.5 Hz, 1H), 3.99 (d, *J* = 9.5 Hz, 1H), 3.89 (*br* d, *J* = 9.0 Hz, 1H), 3.60 (d, *J* = 9.5 Hz, 1H), 2.62 (dd, *J* = 14.0, 7.0 Hz, 1H), 2.44 (*br* d, *J* = 16.5 Hz, 1H), 2.28 (d, *J* = 13.5, 4.0 Hz, 1H), 2.23 (d, *J* = 5.5 Hz, 1H), 2.17 - 2.08 (m, 1H), 1.76 (dd, *J* = 14.0, 12.0 Hz, 1H), 1.06 - 1.01 (m, 1H), 1.02 (s, 3H), 1.01 (s, 3H); ^{13}C NMR (75MHz, $CDCl_3$) ppm 142.87, 116.22, 80.41, 78.72, 67.72, 57.63, 54.56, 46.67, 44.31, 43.50, 34.83, 26.70, 24.95, 20.34, 18.01; HRMS (EI) *m/z* (M^+) calcd 312.0725, obsd 312.0720.

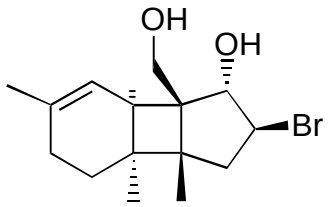

Compound 118: 7b-(Hydroxymethyl)-3a, 3b, 6-trimethyl-(1R*, 2R*, 3aR*, 3bS*, 7aR*, 7bS*)-2, 3, 3a, 3b, 4, 5, 7a, 7b-octahydro-1*H*-2-bromo-cyclopenta[3, 4] cyclobuta[a]benzen-1-ol

Compound **112** (15 mg, 0.05 mmol) was dissolved in 3 mL of ethanol, in a dry flask, under nitrogen. Sodium borohydride (3 mg, 0.08 mmol) was added to the reaction mixture in one portion and allowed to react for 4 h. Once there was no more starting material left the reaction was quenched by addition of half saturated solution of NaCl. The ethanol was evaporated and the residue was extracted with EtOAc (3 x 5 mL). The combined organic extracts were dried over $MgSO_4$ and the solvent was evaporated.

Purification by flash chromatography followed using 20 % diethyl ether in methylene chloride as the eluent to give 11 mg (70 %) of alcohol **118** as a light yellow oil: IR ($CDCl_3$, cm^{-1}) 3691, 3607, 3552, 2957, 2927, 2874, 1726, 1600, 1447, 1372, 1293, 1076; ^1H NMR (500 MHz, $CDCl_3$) δ 5.38 (*br* s, 1H), 4.32 – 4.29 (m, 1H), 4.22 (d, *J* = 8.5 Hz, 1H), 4.05 (d, *J* = 10.5 Hz, 1H), 3.78 (d, *J* = 10.5 Hz, 1H), 2.73 (*br* s, 1H), 2.58 (dd, *J* = 14.0, 7.0 Hz, 1H), 2.33 (*br* s, 1H), 1.89 – 1.82 (m, 3H), 1-77 – 1.71 (m, 2H), 1.57 (s, 3H), 1.37 – 1.33 (m, 1H), 0.96 (s, 3H), 0.92 (s, 3H); ^{13}C NMR (75MHz, $CDCl_3$) ppm 138, 119.5, 85, 65, 53, 52.5, 47, 45, 40.5, 36.5, 31, 26.5, 24.5, 20, 18; HRMS (EI) *m/z* (M^+) calcd 314.0881, obsd 314.0889.

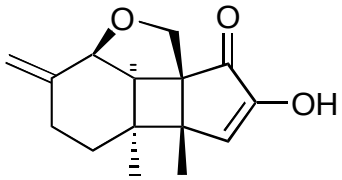

Compound 114: 7-Hydroxy-5a, 5b-dimethyl-3-methylene-(2aR*, 5aR*, 5bS*, 8aR*, 8bS*)-2a, 3, 4, 5, 5a, 5b, 8, 8b-octahydro-2-oxacyclopenta[4, 1] cyclobuta[c, d]inden-8-one

Brederick's reagent (900 μL, 4.4 mmol) and compound **3** (75 mg, 0.32 mmol) were heated, neat, to 55° C, for 30 h. At this point, NMR of the crude mixture indicated formation of the enamine. The reaction mixture was let cool to room temperature and was diluted in 20 mL of dichloromethane. A tip of a spatula of rose bengal was added to the solution which was submitted to photolysis with a sun lamp, at -78° C, while oxygen was bubbled through the reaction mixture. After 5 h the photolysis was stopped, the solvent was evaporated and the residue was ressuspended in ethyl acetate (20 mL).

Work-up followed by washing the organic mixture with brine (1 x 10 mL), drying it over anhydrous $MgSO_4$ and concentrating it in the rota-vapor. Purification of the residue by flash chromatography using 20 % EtOAc in hexanes as the eluent gave 44 mg (56 %) of diketone **114** in its keto enol form: IR ($CDCl_3$, cm^{-1}) 3602, 3501, 2928, 2859, 1699, 1651, 1602, 1396, 1250; ^1H NMR (300 MHz, $CDCl_3$) δ 8.53 (*br* s, exchange with D_2O), 6.59 (s, 1H), 5.17 (*br* s, 1H), 5.12 (*br* s, 1H), 4.30 (d, *J* = 5.5 Hz, 1H), 3.97 (d, *J* = 10 Hz, 1H), 3.90 (d, *J* = 10 Hz, 1H), 2.51 (dt, *J* = 16 Hz, 4.3 Hz, 1H), 2.38 - 2.28 (m, 2H), 2.19 (d, *J* = 5.5 Hz, 1H), 2.16 - 2.09 (m, 1H), 1.72 - 1.57 (m, 1H), 1.13 (s, 3H), 0.95 (s, 3H); ^{13}C NMR (125 MHz, $CDCl_3$) ppm 217.53, 203.02, 142.37, 135.45, 116.53, 80.10, 67.08, 59.73, 50.52, 36.88, 33.0, 27.59, 25.07, 23.47, 14.40; HRMS (EI) *m/z* (M^+) calcd 246.1256, obsd 246.1274.

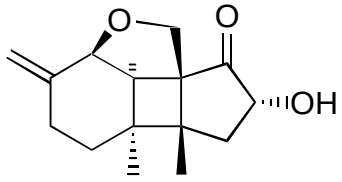

Compound 124: 5a, 5b-dimethyl-3-methylene-(2aR*, 5aR*, 5bS*, 7S*, 8aR*, 8bS*)-perhydro-2-oxacyclopenta[4, 1]cyclobuta[c, d]inden-7-ol-8-one

Compound **3** (30 mg, 0.13 mmol) was dissolved in 2.5 mL of methanol, in a dry flask, under nitrogen and this solution was cooled to 0^o C. A pre-cooled solution of KOH (52.5 mg, 0.94 mmol) in 1.2 mL of methanol was added to the cold reaction mixture and was let stir for 30 min. After this time, still at 0^o C, the $PhI(OAc)_2$ (83 mg, 0.26 mmol) was added in one portion and the reaction was allowed to proceed for another 3h. Once

there was no more starting material left the methanol was evaporated, the residue was resuspended in water (3 mL) and extracted with dichloromethane (3 x 5 mL). The organic layers were combined and washed with brine (1 x 5 mL), dried over anhydrous Na_2SO_4 and concentrated. Purification by flash chromatography using CH_2Cl_2 as the eluent gave 28 mg (73 %) of ketal-alcohol **125**. Hydrolysis of the ketal was conducted by dissolving the product in chloroform (2.0 mL) and adding trifluoroacetic acid (50%, aqueous, 750 μL). Reaction was conducted at 0^o C for 90 min and then it was diluted in chloroform (5 mL) and washed with $NaHCO_3$ (aqueous, sat.) until pH neutral. The organic phase was dried in anhydrous Na_2SO_4, concentrated and purified by flash chromatography using 10% diethyl ether in CH_2Cl_2 as the eluent to give 20 mg (62 % overall) of hydroxy ketone **124** as a light yellow oil: IR ($CDCl_3$, cm^{-1}) 3240, 2985, 2979, 1730, 1375, 1267, 1249, 1046; ^{1}H NMR (500 MHz, $CDCl_3$) δ 5.12 (*br* s, 1H), 5.04 (*br* s, 1H), 4.26 - 4.20 (m, 2H), 4.10 (d, J = 9.5 Hz, 1H), 3.79 (d, J = 9.5 Hz, 1H), 2.74 (*br* s, 1H), 2.64 (d, J = 5.5 Hz, 1H), 2.53 (*br* d, J = 17.5 Hz, 1H), 2.43 (td, J = 13 Hz, 5 Hz, 1H), 2.27 - 2.15 (m, 3H), 1.18 - 1.13 (m, 1H), 1.11 (s, 3H), 1.06 (s, 3H); HRMS (EI) *m/z* (M^+) calcd 248.1413, obsd 248.1415.

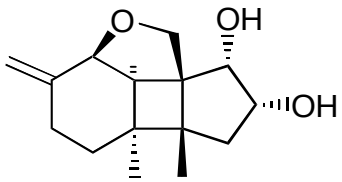

Compound 121: 5a, 5b-Dimethyl-3-methylene-(2aR*, 5aR*, 5bS*, 7S*, 8S*, 8aR*, 8bS*)-perhydro-2-oxacyclopenta[4, 1]cyclobuta[c, d]inden-7, 8-diol

Method A: Compound **114** (15 mg, 0.06 mmol) and a tip of a spatula of anhydrous potassium carbonate were suspended in ethanol (2.0 mL). $NaBH_4$ (20 mg, 0.52 mmol) was added to the reaction mixture in 4 portions, over a period of 18 h. One hour after the addition of the last portion of the reducing agent all the starting material had reacted, so the reagent was quenched by slow addition of water (1 mL) until no more gas evolution was observed. The ethanol was removed in the rota-vapor and the residue was ressuspended in EtOAc (5 mL). The layers were separated, the organic phase was washed with brine (1 x 2 mL), dried over anhydrous $MgSO_4$ and concentrated. Purification of the residue by flash chromatography afforded 13 mg (87 %) of *cis* diol **121** as a white solid.

Method B: Compound **124** (10 mg, 0.04 mmol) was dissolved in ethanol (1.0 mL) and $NaBH_4$ (10 mg, 0.26 mmol) was added to the solution, at 0^o C, in three portions, over 1h. After the addition was complete the reaction mixture was allowed to warm to room temperature and was stirred for another 1 h until reaction completion. Once all the starting material was consumed the ethanol was removed *in vacuo* and the residue was resuspended in EtOAc (5 mL), washed with brine, dried over anhydrous $MgSO_4$ and concentrated. Purification of the residue by flash chromatography using 30 % diethyl

ether in methylene chloride as the eluent gave 8 mg (80 %) of the *cis* diol **121** as a white solid.

Compound **121**: mp 131-133^{o} C; IR ($CDCl_3$, cm^{-1}) 3627, 3552, 2976, 2927, 2869, 1730, 1644, 1602, 1446, 1381, 1207, 1112, 1039, 994; ^{1}H NMR (500 MHz, $CDCl_3$) δ 5.09 (*br* s, 1H), 5.03 (*br* s, 1H), 4.21 (td, *J* = 5.5 Hz, 1.5 Hz, 1H), 4.03 (d, *J* = 5.0 Hz, 1H), 4.01 (d, *J* = 10 Hz, 1H), 3.86 (d, *J* = 5.5 Hz, 1H), 3.58 (d, *J* = 10 Hz, 1H), 2.64 (d, *J* = 5.0 Hz, 1H), 2.51 (*br* d, *J* = 15 Hz, 1H), 2.43 (*br* d, *J* = 15 Hz, 1H), 2.32 (td, *J* = 13.5 Hz, 4 Hz, 1H), 2.18 (*br* t, *J* = 15 Hz, 1H), 1.58 (dd, *J* = 15 Hz, 5.5 Hz, 1H), 1.23 (*br* s, 2H), 1.14 (s, 3H), 1.01 (*br* d, *J* = 13.5 Hz, 1H), 0.95 (s, 3H); ^{13}C NMR (125 MHz, $CDCl_3$) ppm 143.48, 115.43, 81.26, 76.70, 73.25, 69.20, 59.00, 46.73, 44.34, 41.84, 34.29, 26.89, 24.88, 21.51, 18.66; HRMS (EI) *m/z* (M^{+}) calcd 250.1569, obsd 250.1536.

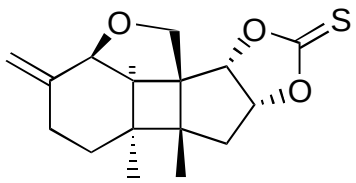

Compound 122: 5a, 5b-dimethyl-methylene-(2aR*, 5aR*, 5bS*, 6aS*, 9aR*, 9bR*, 9cS*)-perhydro[1]benzoxolo[3'', 4'':2', 3', 4']cyclobuta[4, 5] cyclopenta[d][1,3]dioxole-8-thione

Compound **121** (8 mg, 0.032 mmol) and thiocarbonyl diimidazole (15 mg, 0.084 mmol) were dissolved in dry toluene, in a dry flask, under nitrogen atmosphere and the yellow reaction mixture was heated to reflux for 24 h. The toluene was removed under reduced pressure and the residue was immediately purified by flash chromatography using 10 % EtOAc in hexanes as the eluent to give 7 mg (75 %) of the cyclic thionocarbonate

122 as a yellow oil: IR ($CDCl_3$, cm^{-1}) 2957, 2927, 2854, 1804, 1601, 1460, 1368, 1319, 1168, 1137, 1085, 1052; ^1H NMR (300 MHz, $CDCl_3$) δ 5.18 (s, 1H), 5.13 – 5.08 (m, 2H), 4.81 (d, *J* = 6.8 Hz, 1H), 4.15 – 4.10 (m, 2H), 3.42 (d, *J* = 11.2 Hz, 1H), 2.94 (d, *J* = 15.6 Hz, 1H), 2.45 (*br* d, *J* = 16.9 Hz, 1H), 2.31 (d, *J* = 6.0 Hz, 1H), 2.6 (td, *J* = 12.5, 3.1 Hz, 1H), 2.20 – 2.10 (m, 1H), 1.85 (dd, J = 15.6, 6.3 Hz, 1H), 1.12 (s, 3H), 1.11 – 1.06 (m, 1H), 1.05 (s, 3H); ^{13}C NMR (123 MHz, $CDCl_3$) ppm 156.30, 142.63, 117.01, 84.07, 83.48, 80.87, 69.43, 60.11, 49.86, 44.73, 40.32, 33.39, 28.95, 26.13, 24.51, 22.71, 18.32; HRMS (EI) *m/z* (M^+) calcd 292.1133, obsd 292.1139.

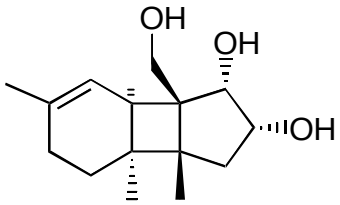

Compound 123: 7b-(Hydroxymethyl)-3a, 3b, 6-trimethyl-(1R*, 2S*, 3aR*, 3bS*, 7aR*, 7bS*)-2, 3, 3a, 3b, 4, 5, 7a, 7b-octahydro-1*H*-cyclopenta[3, 4] cyclobuta[a]benzen-1, 2-diol

A two-neck flask equipped with a dry ice condenser was flame dried and flushed with dry nitrogen. Ethylamine (3 mL, excess) was condensed onto the flask at -78° C. A solution of diol **121** (12 mg, 0.048 mmol) in 3 mL of diethyl ether was added to the reaction media. Lithium wire (10 mg, 1.4 mmol), was cut in small pieces, and added to the flask. The suspension of lithium pieces in ethereal ethylamine was stirred at -78° C until a persistent dark blue color was observed (about 30 min). The suspension was allowed to stir at -78° C for an additional 30 min before the blue color was discharged by

addition of a few drops of 1-octyne. The remaining lithium pieces were removed with a spatula and the color of the resulting yellow solution was discharged by addition of methanol, dropwise. The mixture was allowed to warm to room temperature and was concentrated in a rotatory evaporator. The residue was resuspended in ether, dried over anhydrous $MgSO_4$ and filtered over a plug of silica gel. The clear solution was again concentrated followed by purification of the residue by flash chromatography, using a solution of 1:1 diethyl ether and methylene chloride as the eluent. Obtained 4 mg (35 %) of triol **123** as a clear oil: IR (CCl_4, cm^{-1}) 3691, 3607, 3552, 2952, 2926, 2871, 1726,1622, 1436,1372, 1276, 1055.

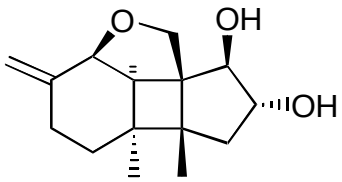

Compound 126: 5a, 5b-Dimethyl-3-methylene-(2aR*, 5aR*, 5bS*, 7S*, 8R*, 8aR*, 8bS*)-perhydro-2-oxacyclopenta[4, 1]cyclobuta[c, d]inden-7, 8-diol

Compound **124** (15 mg, 0.06 mmol) was dissolved in acetic acid (glacial, 3 mL) and the solution was cooled to 0^o C. Tetramethylammonium triacetoxi-borohydride (42 mg, 0.15 mmol) was added in one portion. Reaction was allowed to warm to room temperature over 1 hour and them it was kept stirring for another 5h. Once there was no more starting material according to TLC analysis, the reaction mixture was diluted with brine (10 mL) and the aqueous phase was extracted with ethyl acetate (6 x 10 mL). The combined organic layers was dried over anhydrous $MgSO_4$, concentrated and the residue was purified using flash chromatography with a 1:1 solution of ethyl acetate and hexanes

used as the eluent. Obtained 11.3 mg (75 %) of *trans*-diol **126** along with 1.5 g (15 %) of the *cis*-diol **121**. Trans diol **126**: IR ($CDCl_3$, cm^{-1}) 3691, 3611, 2974, 2928, 2869, 1603, 1448, 1382, 1209, 1118, 1072, 1013; ^1H NMR (500 MHz, $CDCl_3$) δ 5.09 (*br* s, 1H), 5.03 (*br* s, 1H), 4.20 - 4.18 (m, 1H), 4.09 - 4.01 (m, 3H, 5 lines), 3.73 (d, *J* = 10 Hz, 1H), 2.51 (d, *J* = 5.5 Hz, 1H), 2.46 (*br* d, *J* = 18 Hz, 1H), 2.39 - 2.32 (m, 2H), 2.18 (*br* t, *J* = 14 Hz, 1H), 1.88 (dd, *J* = 15.0 Hz, 6.5 Hz, 1H), 1.56 (*br* s, 2H), 1.07 (s, 3H), 1.05 (s, 3H), 1.04 - 1.00 (m, 1H); ^{13}C NMR (125 MHz, $CDCl_3$) ppm 143.42, 115.31, 84.57, 80.75, 80.16, 68.52, 59.00, 49.44, 48.03, 42.59, 33.76, 26.91, 24.89, 21.40, 19.37; HRMS (EI) *m/z* (M^+) calcd 250.1569, obsd 250.1550.

ADDENDUM I: *SELECTED ^1H NMR SPECTRA*

Note:

^{1}H NMR data was processed with *Felix* version 95.0 NMR data processing program, from Biosym Technologies Inc., on a Silicon Graphics *Indigo* R3000 workstation, running Irix version 5.3 as the operating system.

X-Axis = *ppm* downfield from TMS

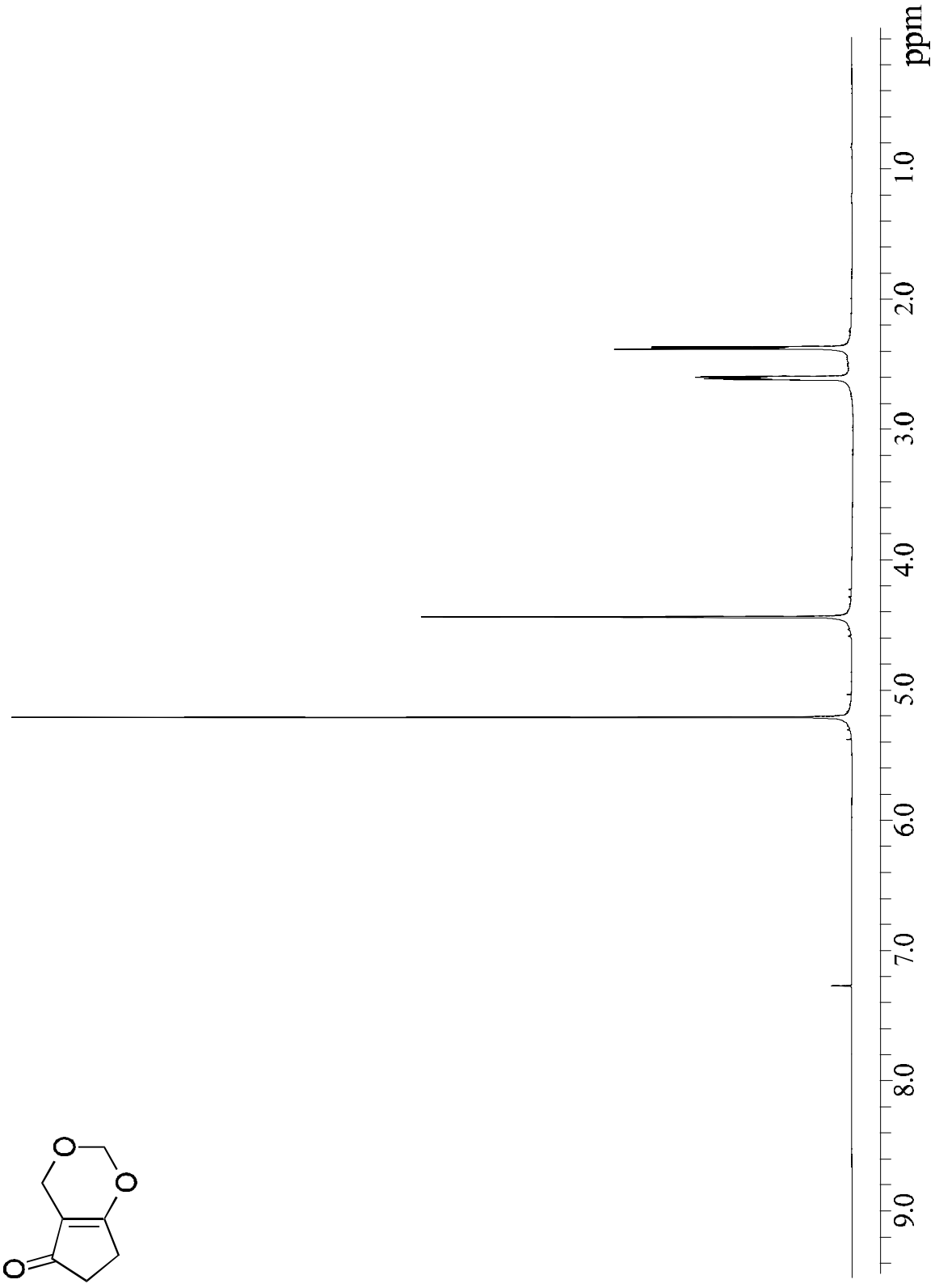
ppm
1.0
2.0
3.0
4.0
5.0
6.0
7.0
8.0
9.0
O
O
O

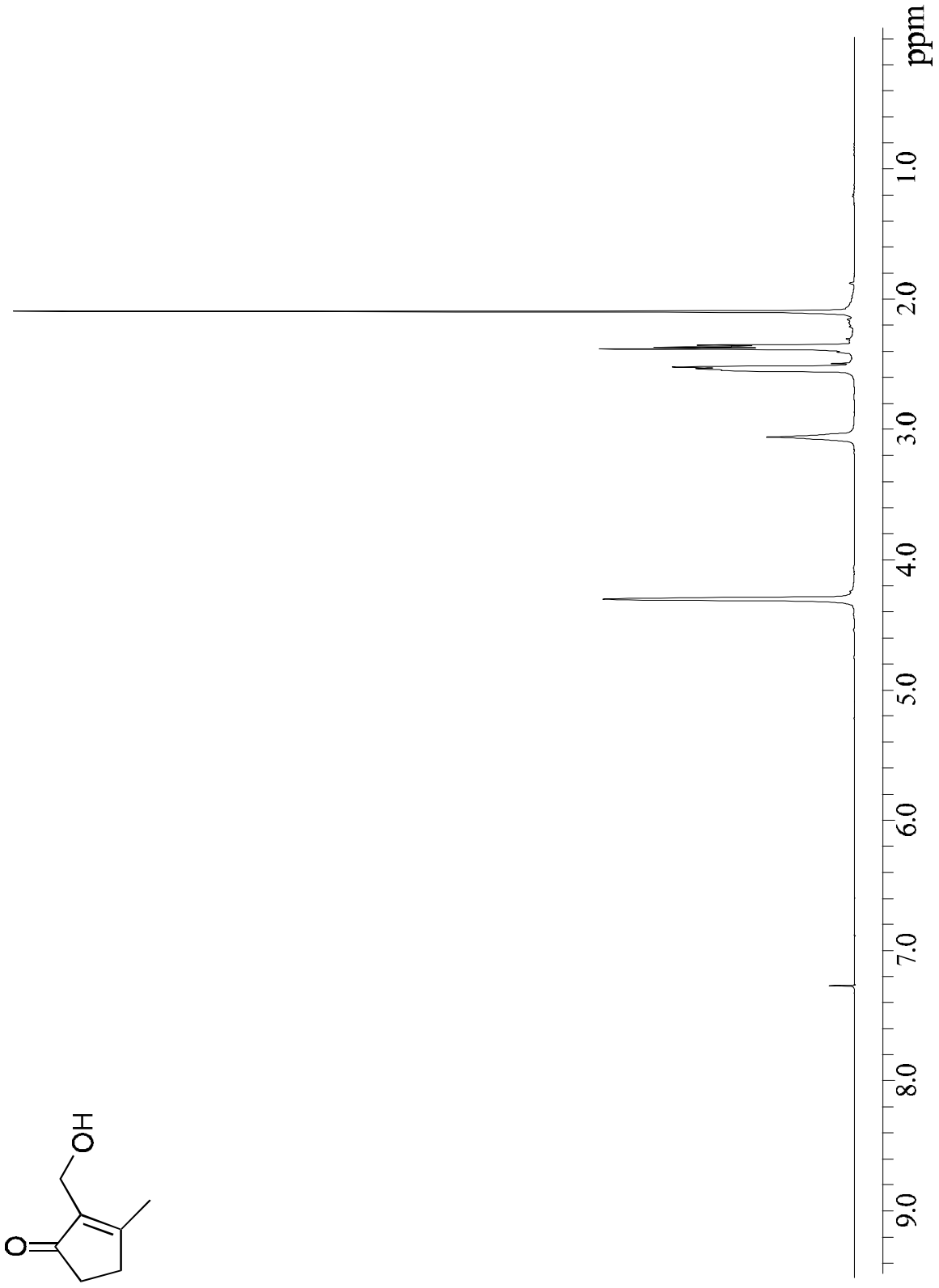
ppm
1.0
2.0
3.0
4.0
5.0
6.0
7.0
8.0
9.0
OH
O

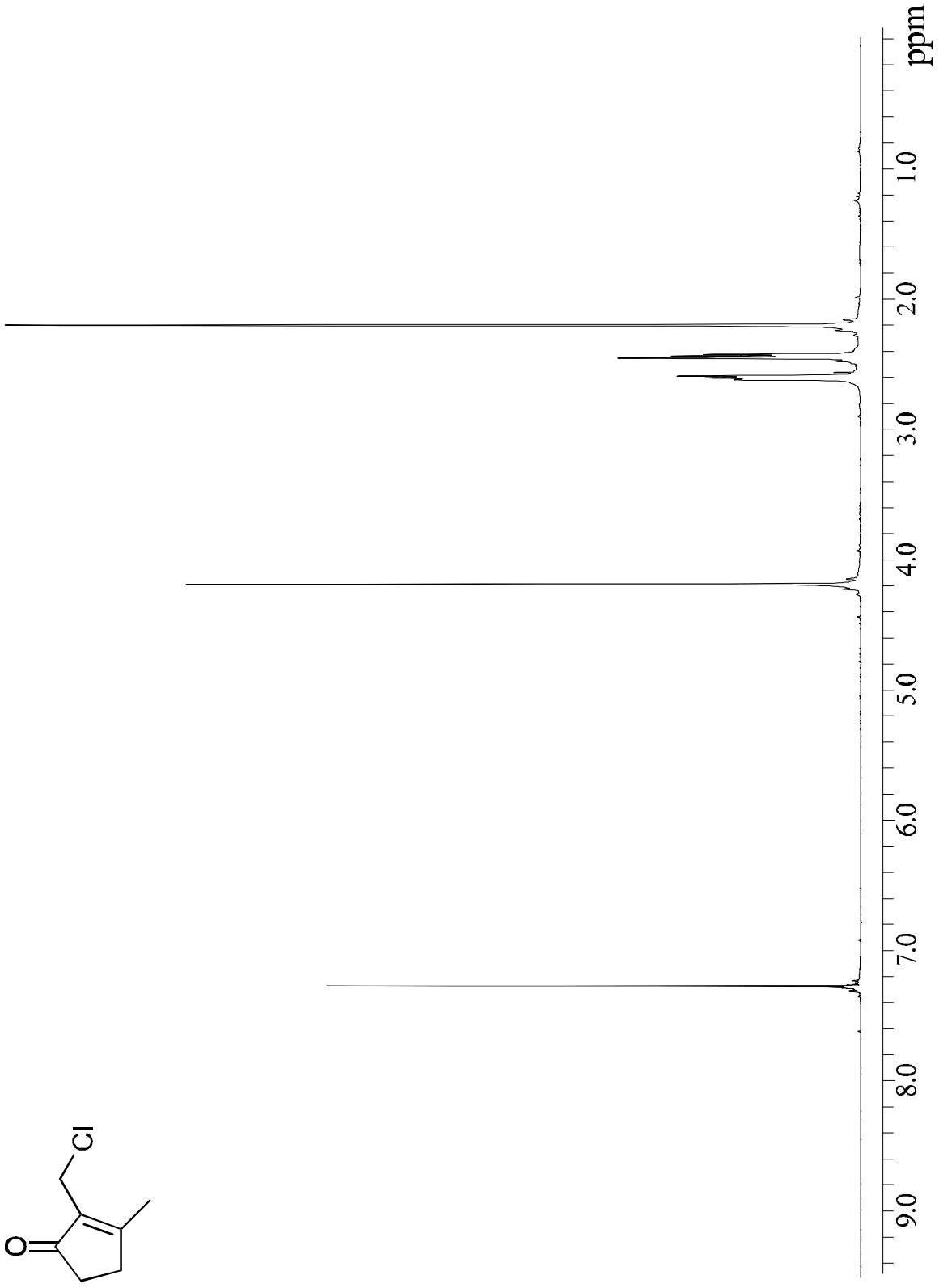
ppm
1.0
2.0
3.0
4.0
5.0
6.0
7.0
8.0
9.0
Cl
O

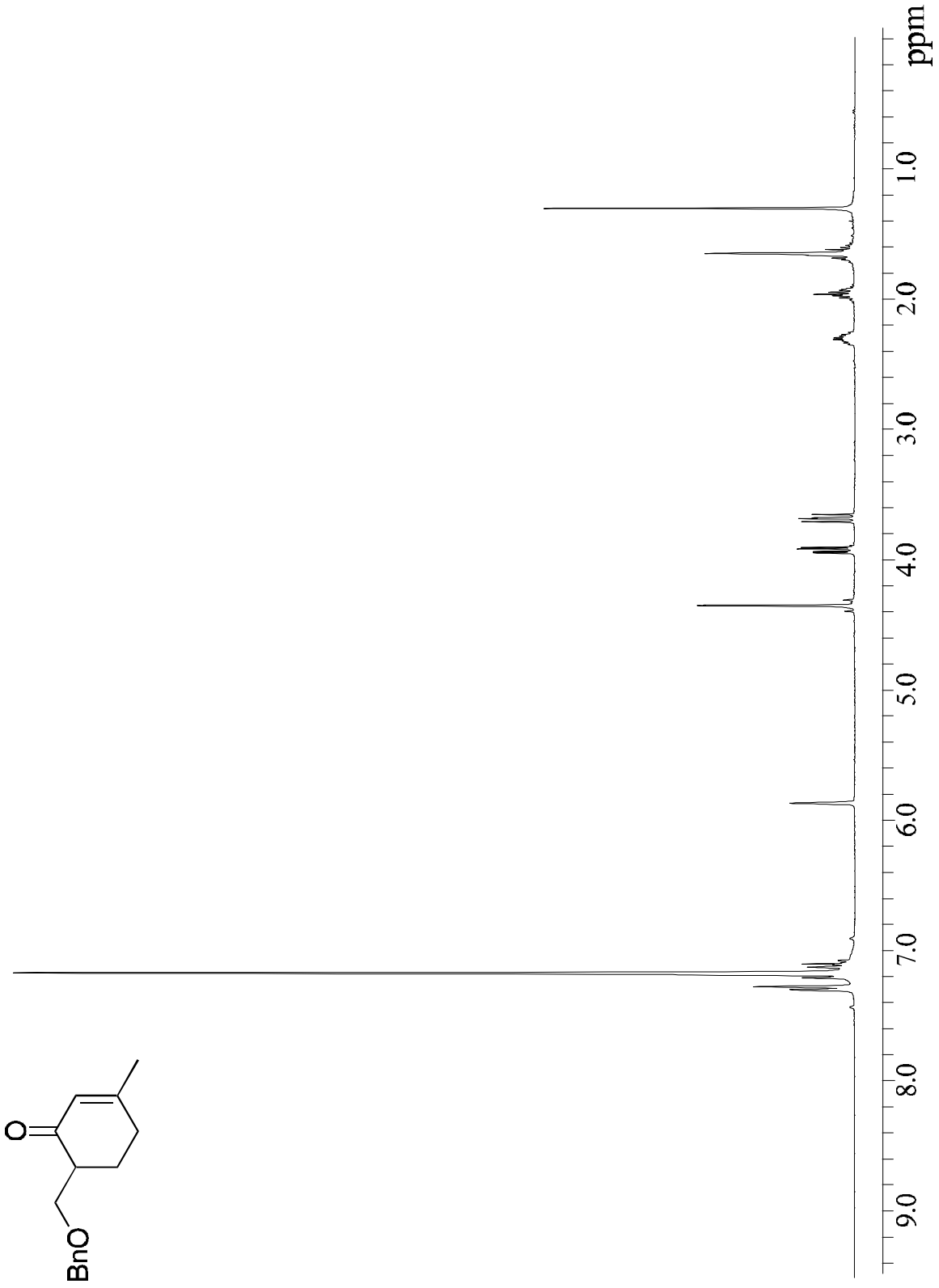
ppm
1.0
2.0
3.0
4.0
5.0
6.0
7.0
8.0
9.0
O
BnO

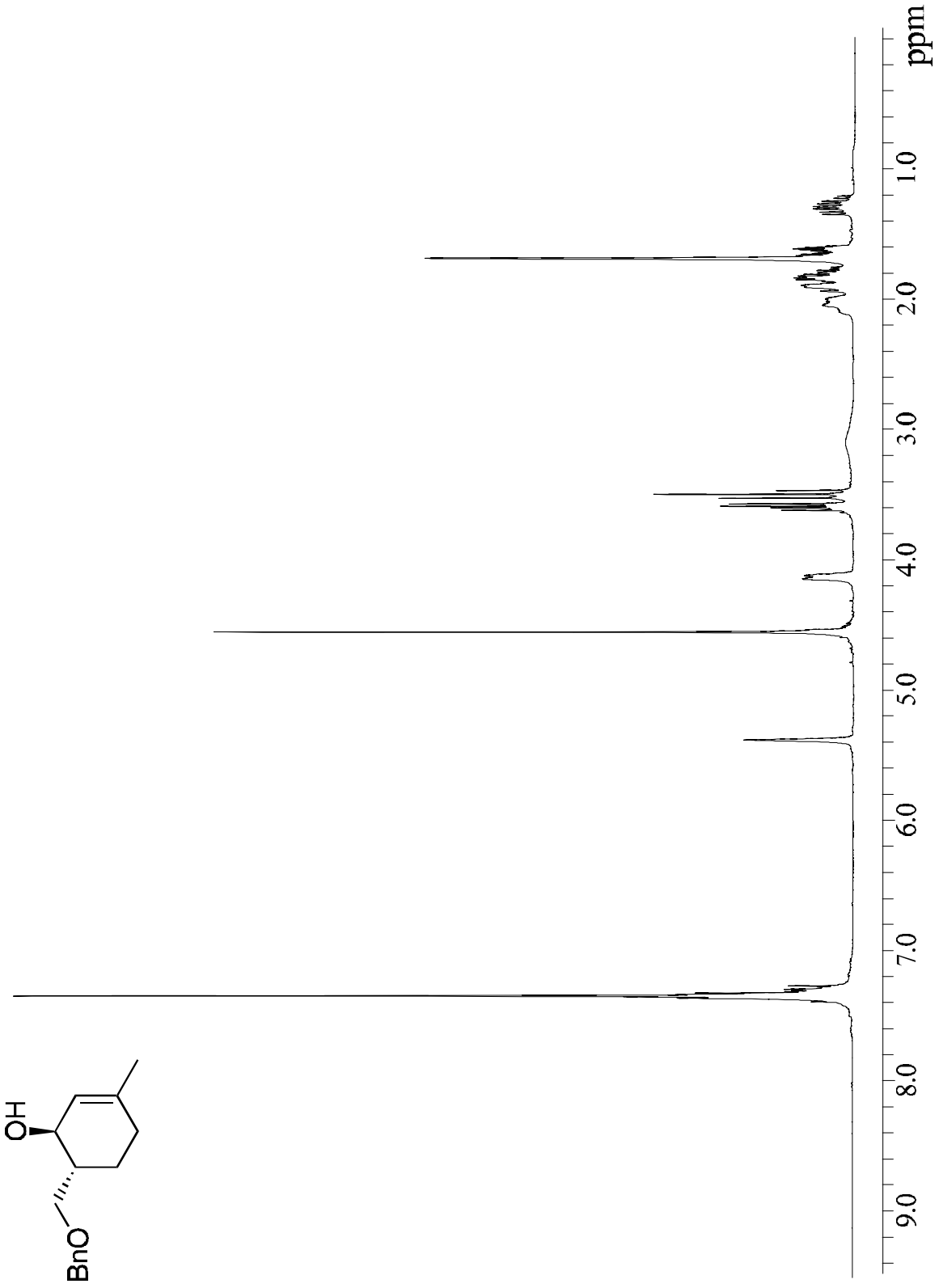
ppm
1.0
2.0
3.0
4.0
5.0
6.0
7.0
8.0
9.0
OH
BnO

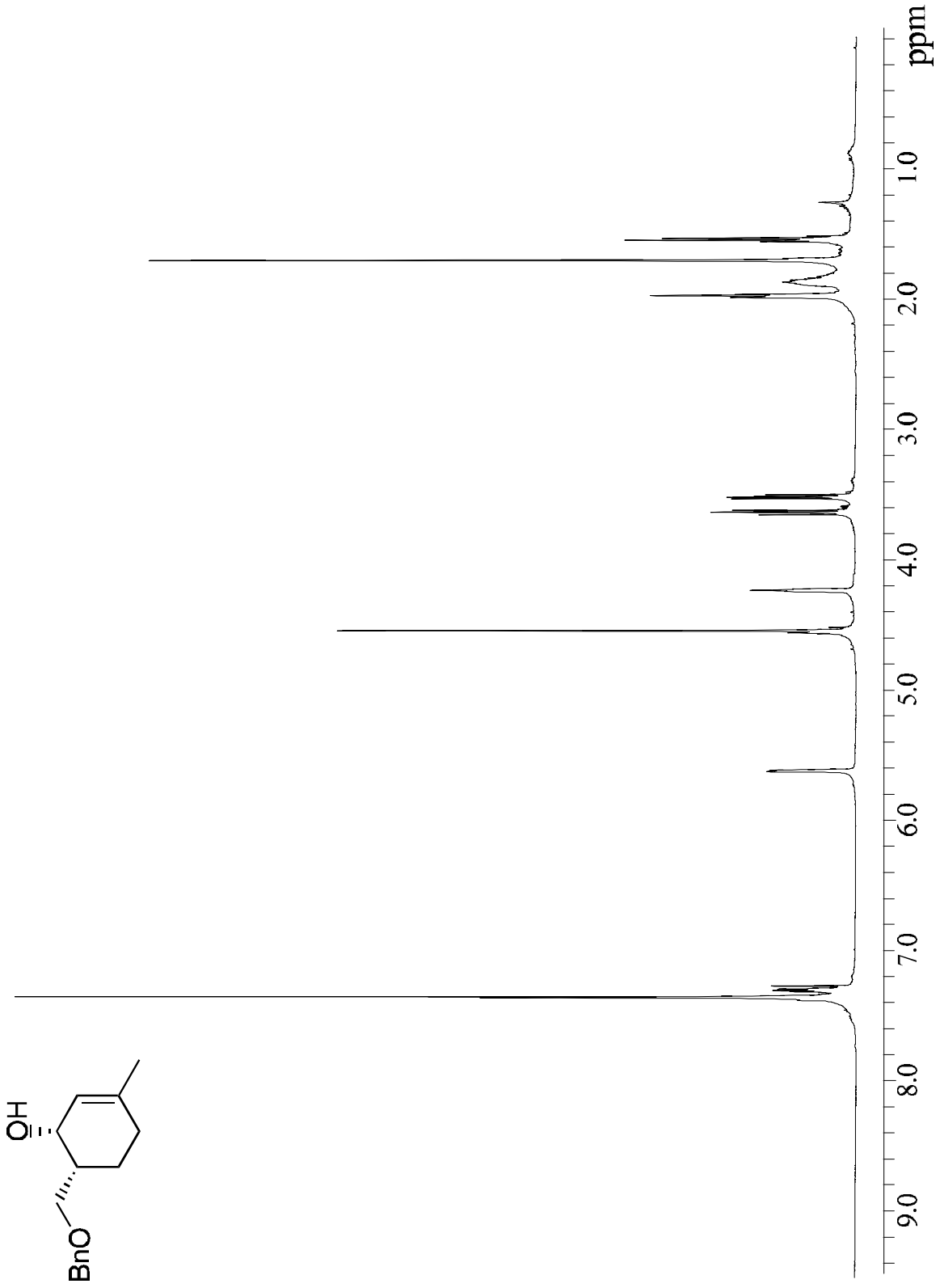
ppm
1.0
2.0
3.0
4.0
5.0
6.0
7.0
8.0
9.0
OH
BnO

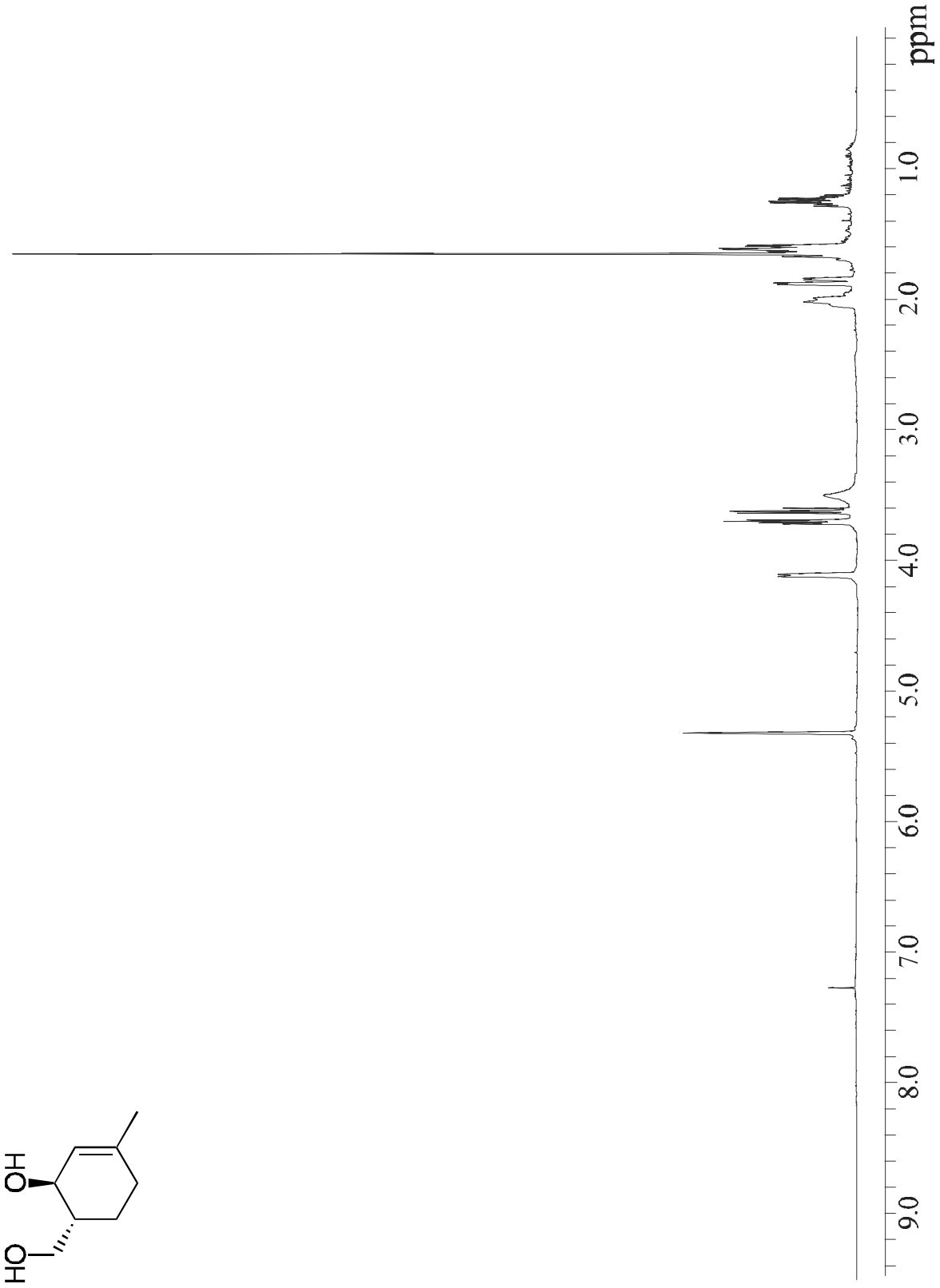
ppm
1.0
2.0
3.0
4.0
5.0
6.0
7.0
8.0
9.0
OH
HO

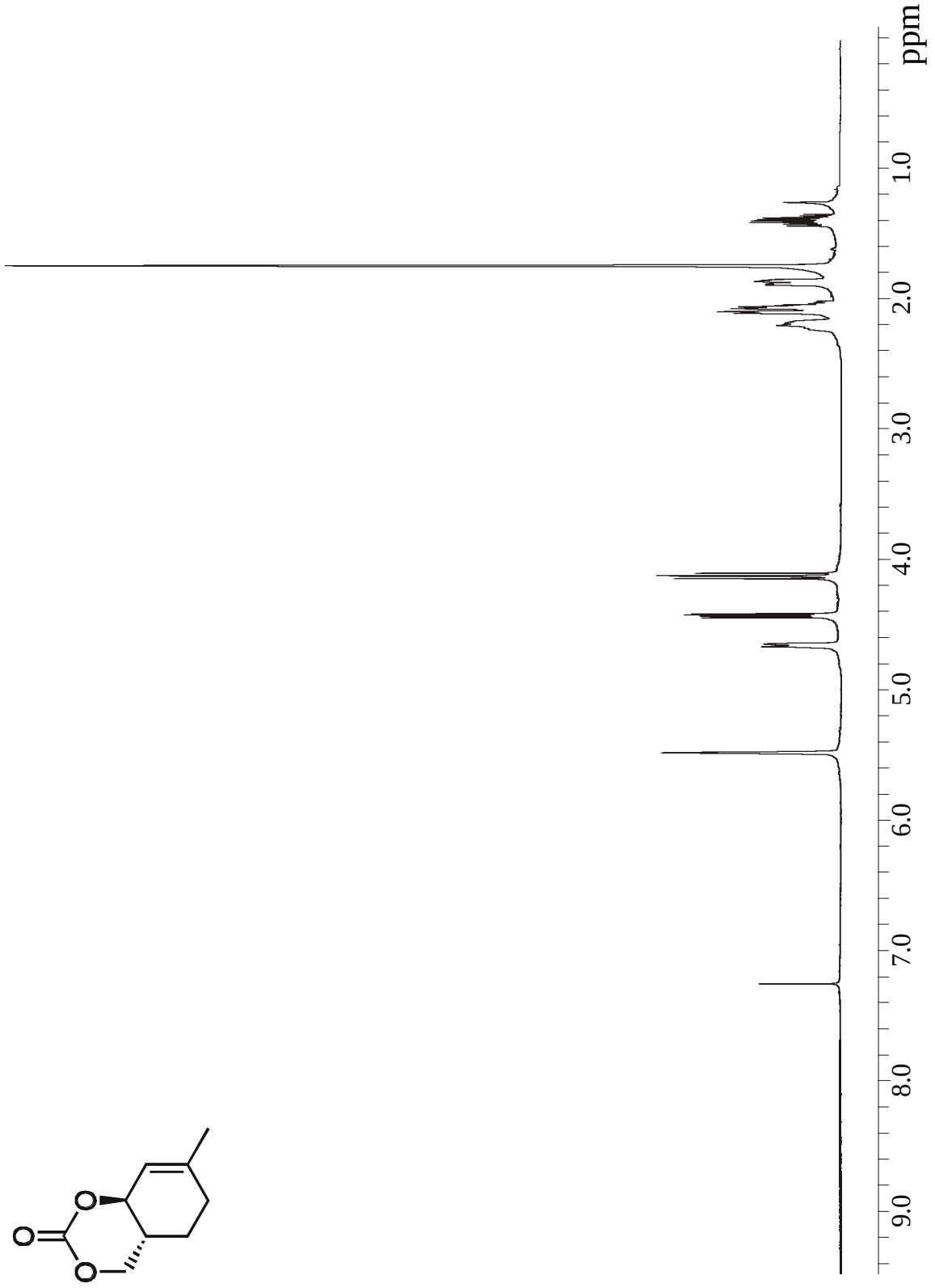
ppm
1.0
2.0
3.0
4.0
5.0
6.0
7.0
8.0
9.0

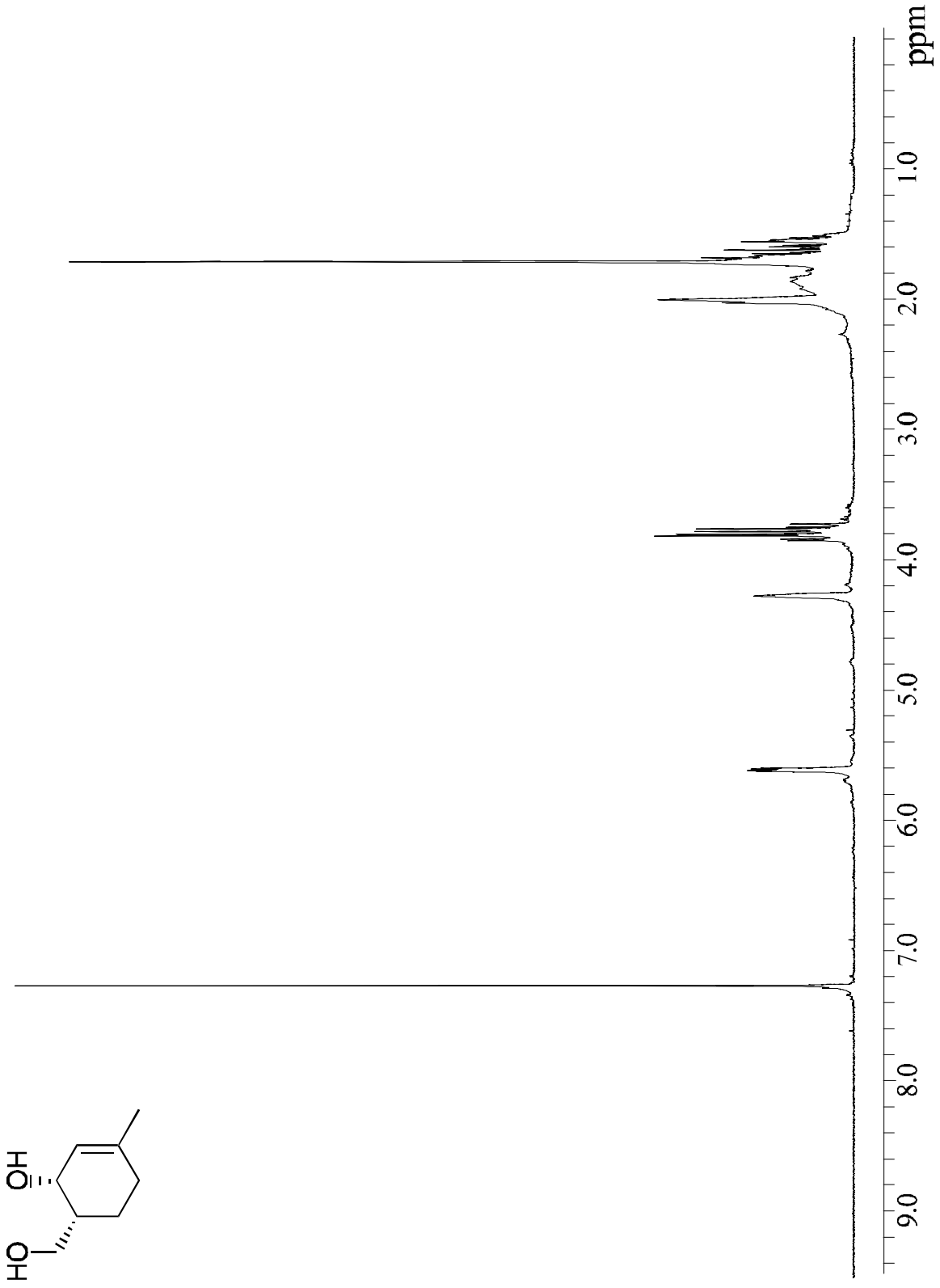
ppm
1.0
2.0
3.0
4.0
5.0
6.0
7.0
8.0
9.0
OH
HO

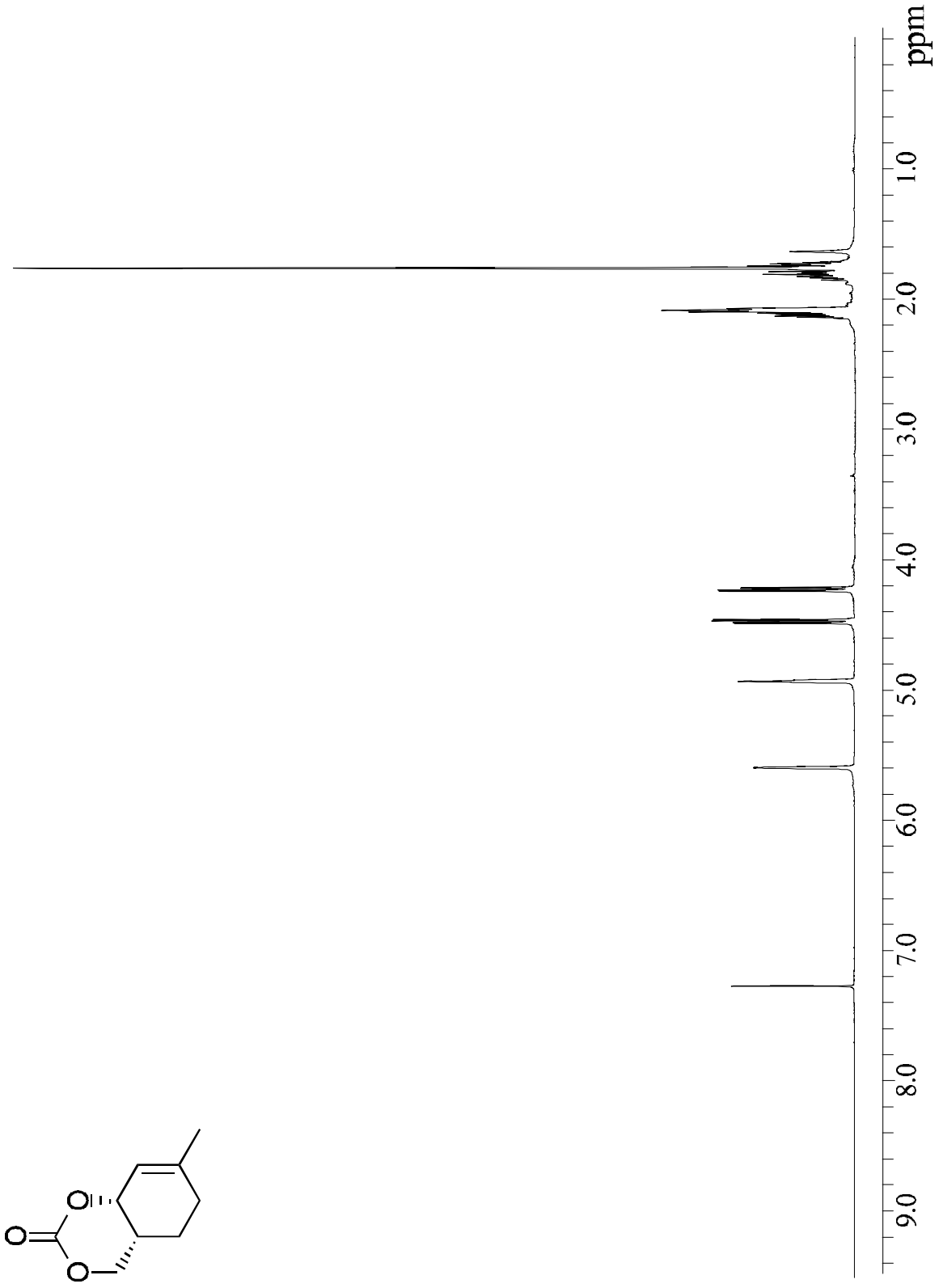
ppm
1.0
2.0
3.0
4.0
5.0
6.0
7.0
8.0
9.0

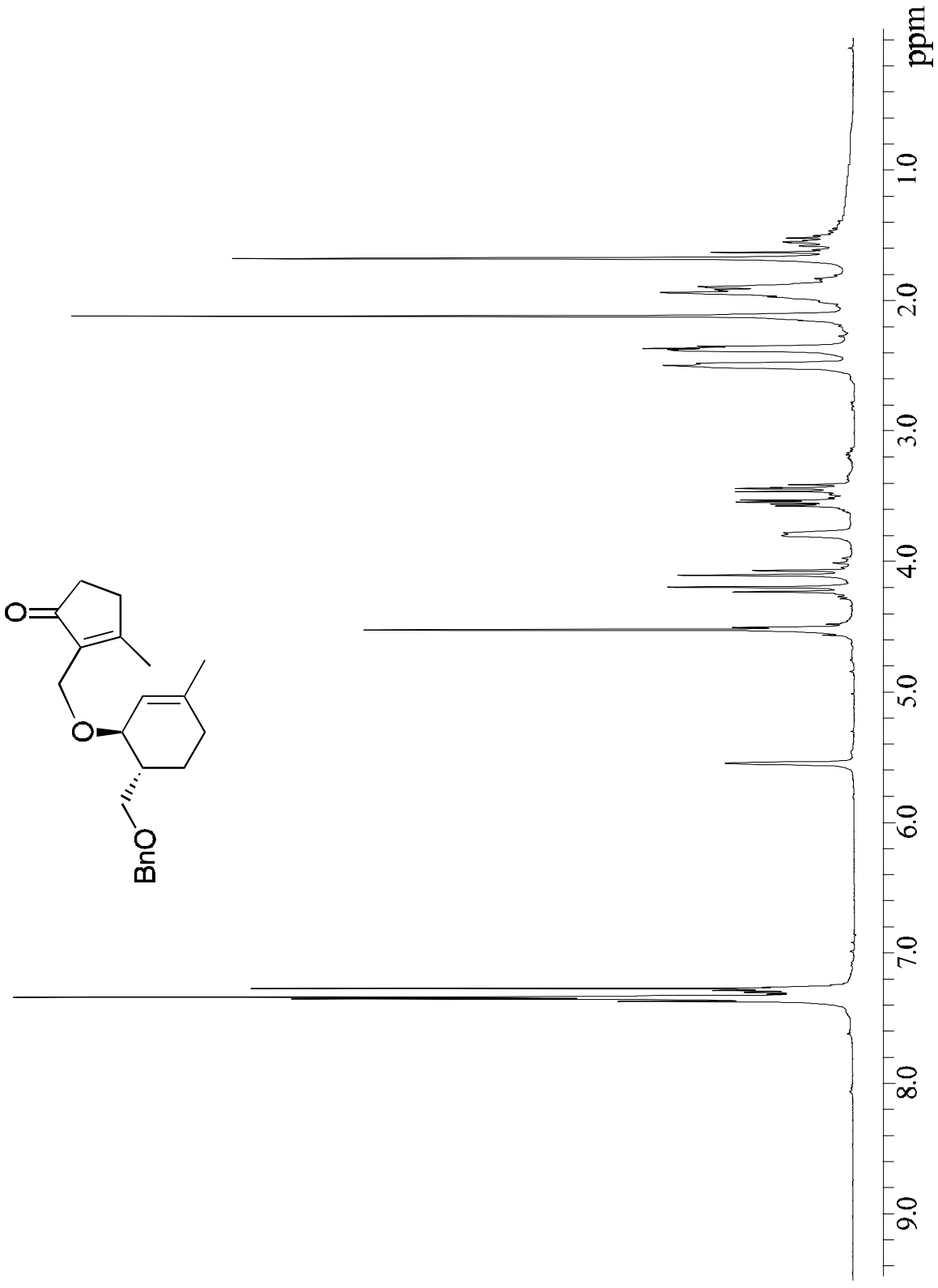
ppm
1.0
2.0
3.0
4.0
5.0
6.0
7.0
8.0
9.0
O
O
BnO

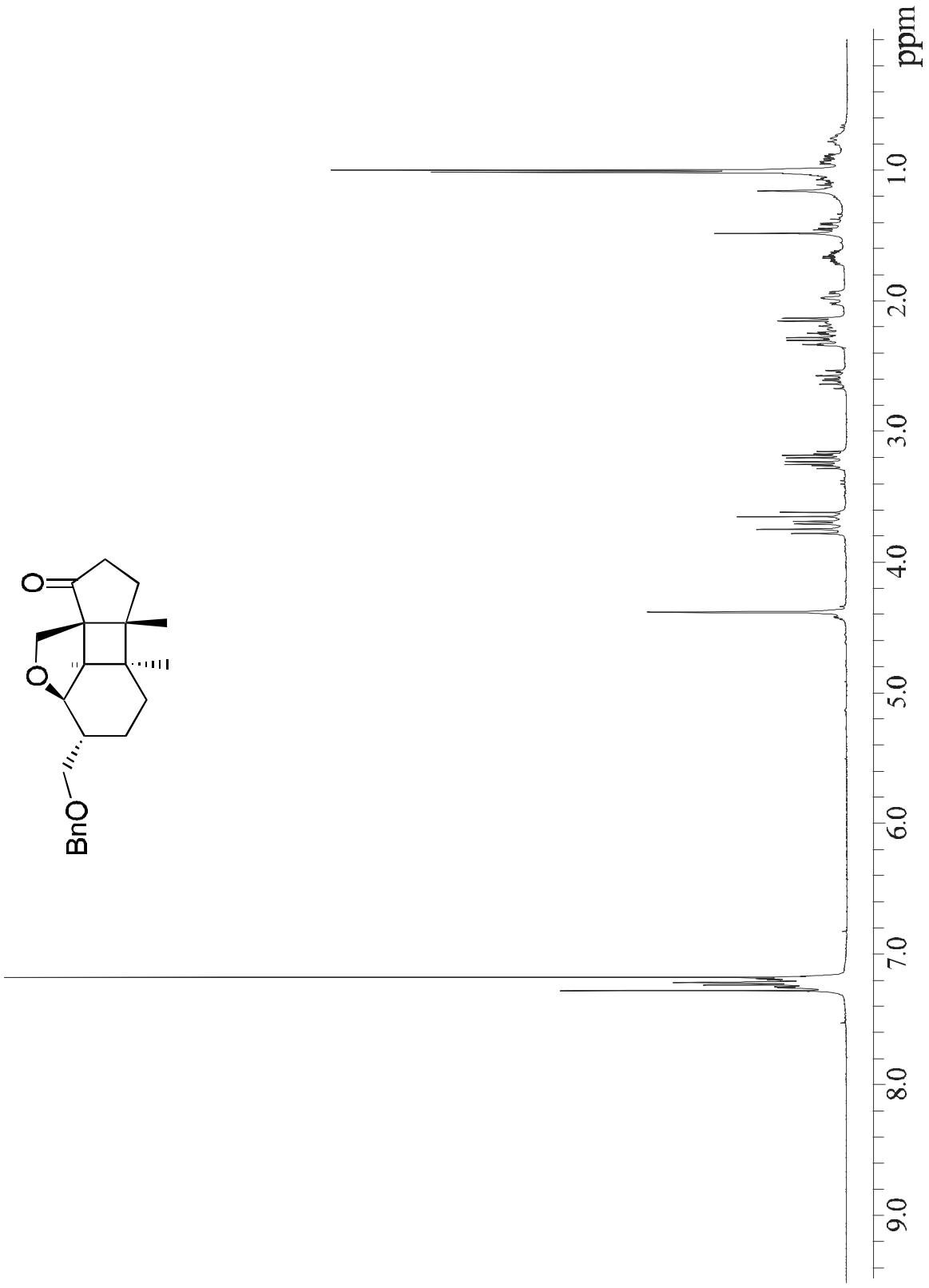
O
O
BnO
ppm
1.0
2.0
3.0
4.0
5.0
6.0
7.0
8.0
9.0

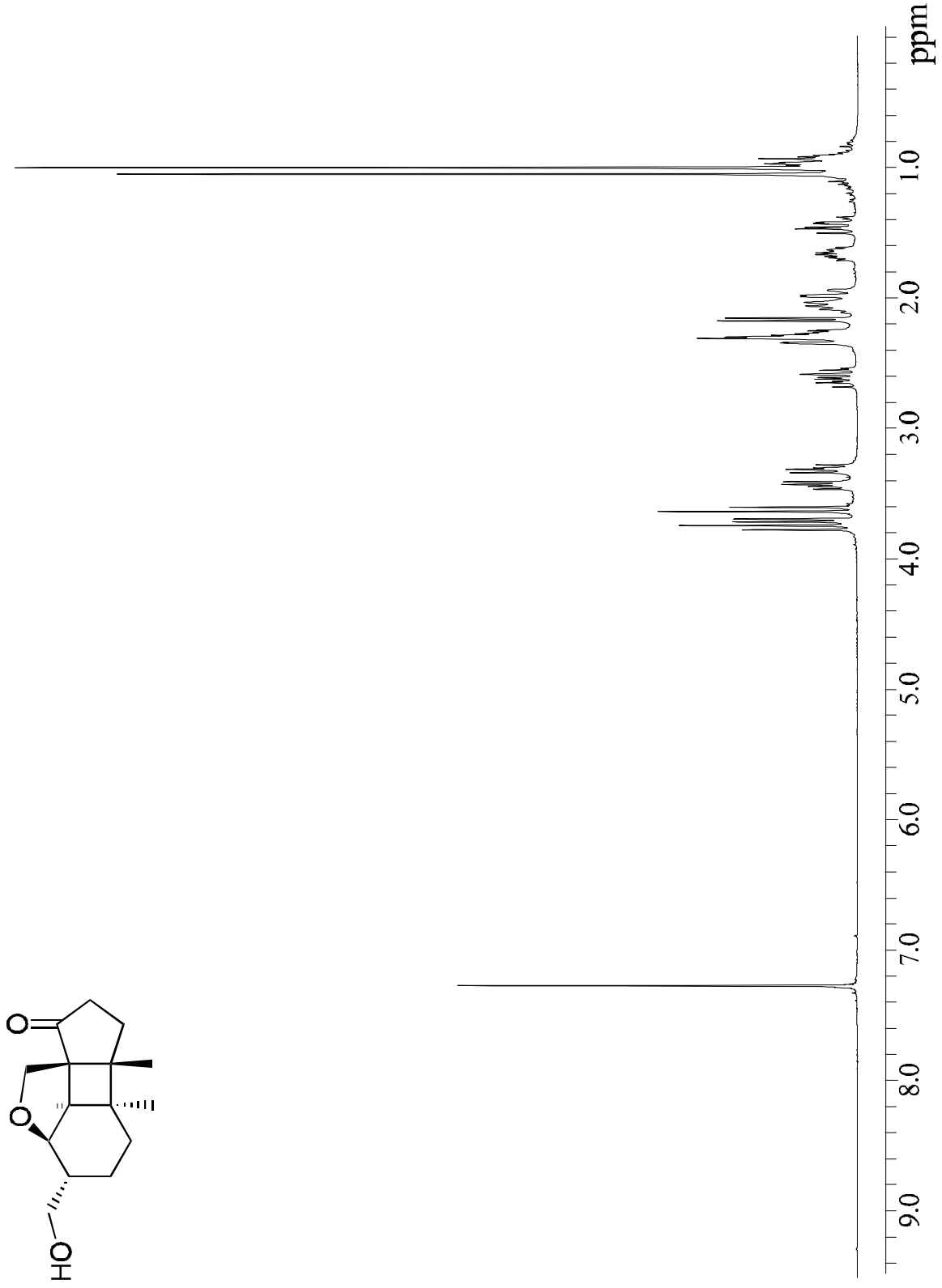
ppm
1.0
2.0
3.0
4.0
5.0
6.0
7.0
8.0
9.0
O
O
HO

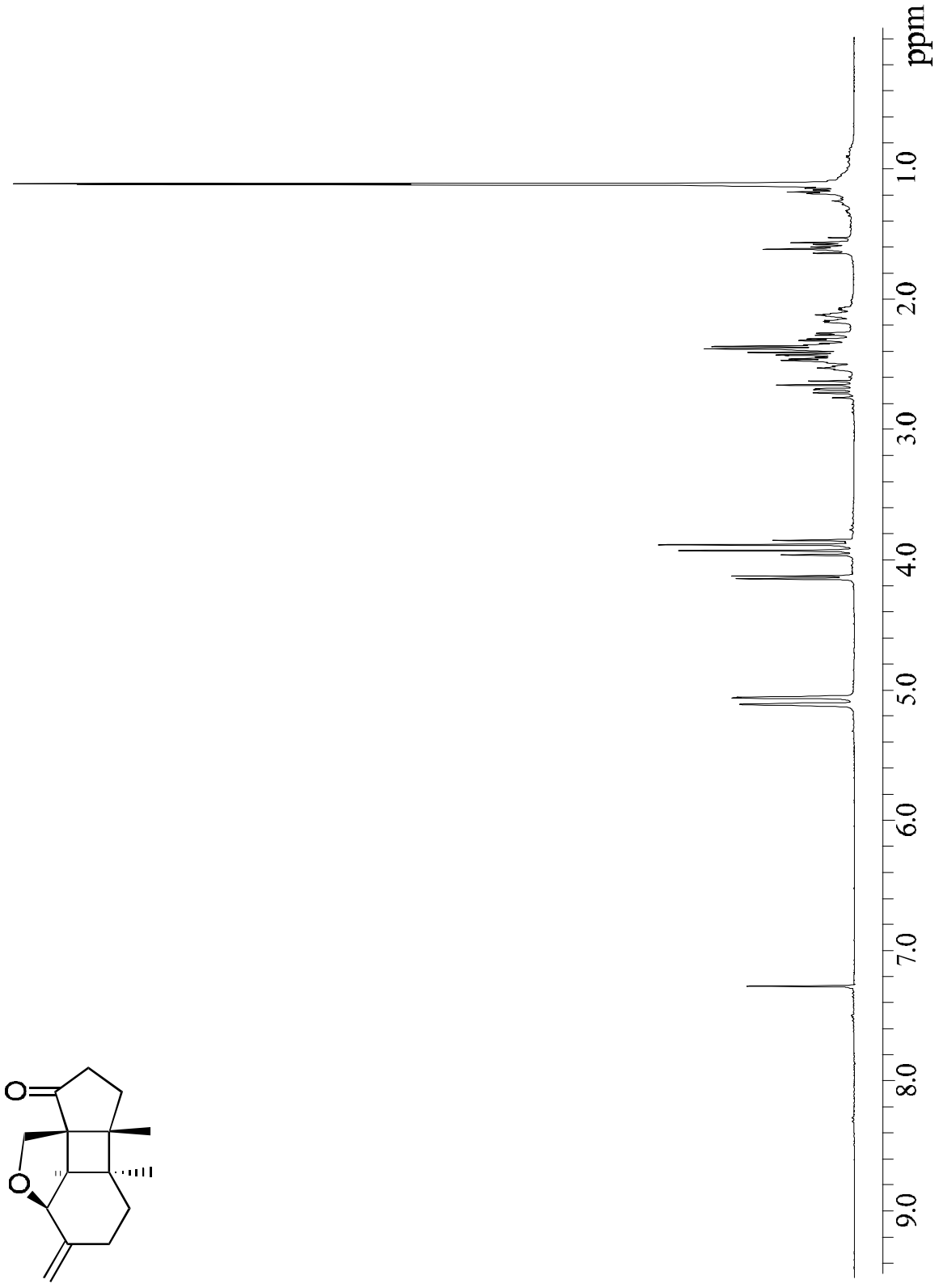
ppm
1.0
2.0
3.0
4.0
5.0
6.0
7.0
8.0
9.0

O
O

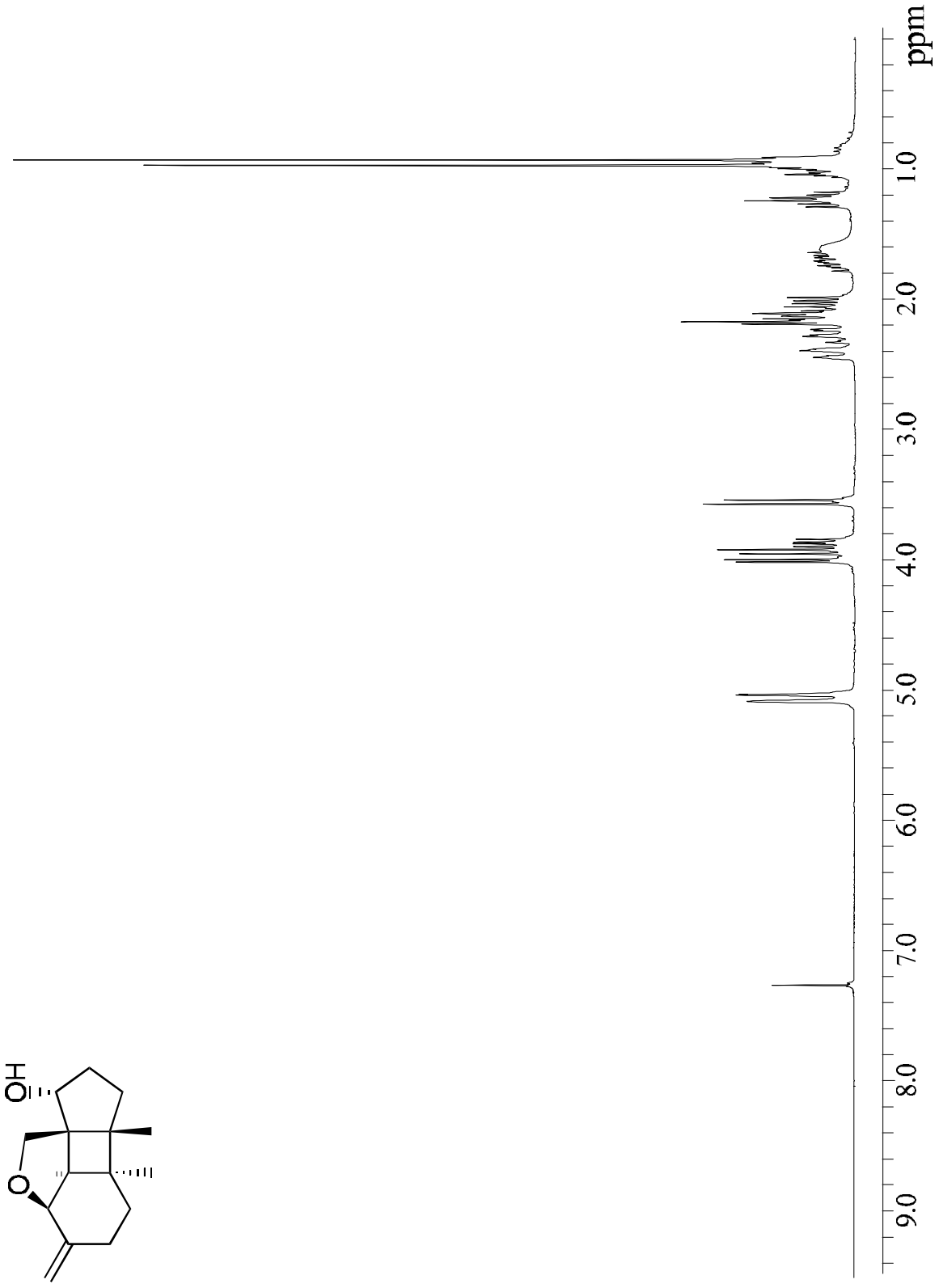
ppm
1.0
2.0
3.0
4.0
5.0
6.0
7.0
8.0
9.0
OH
O

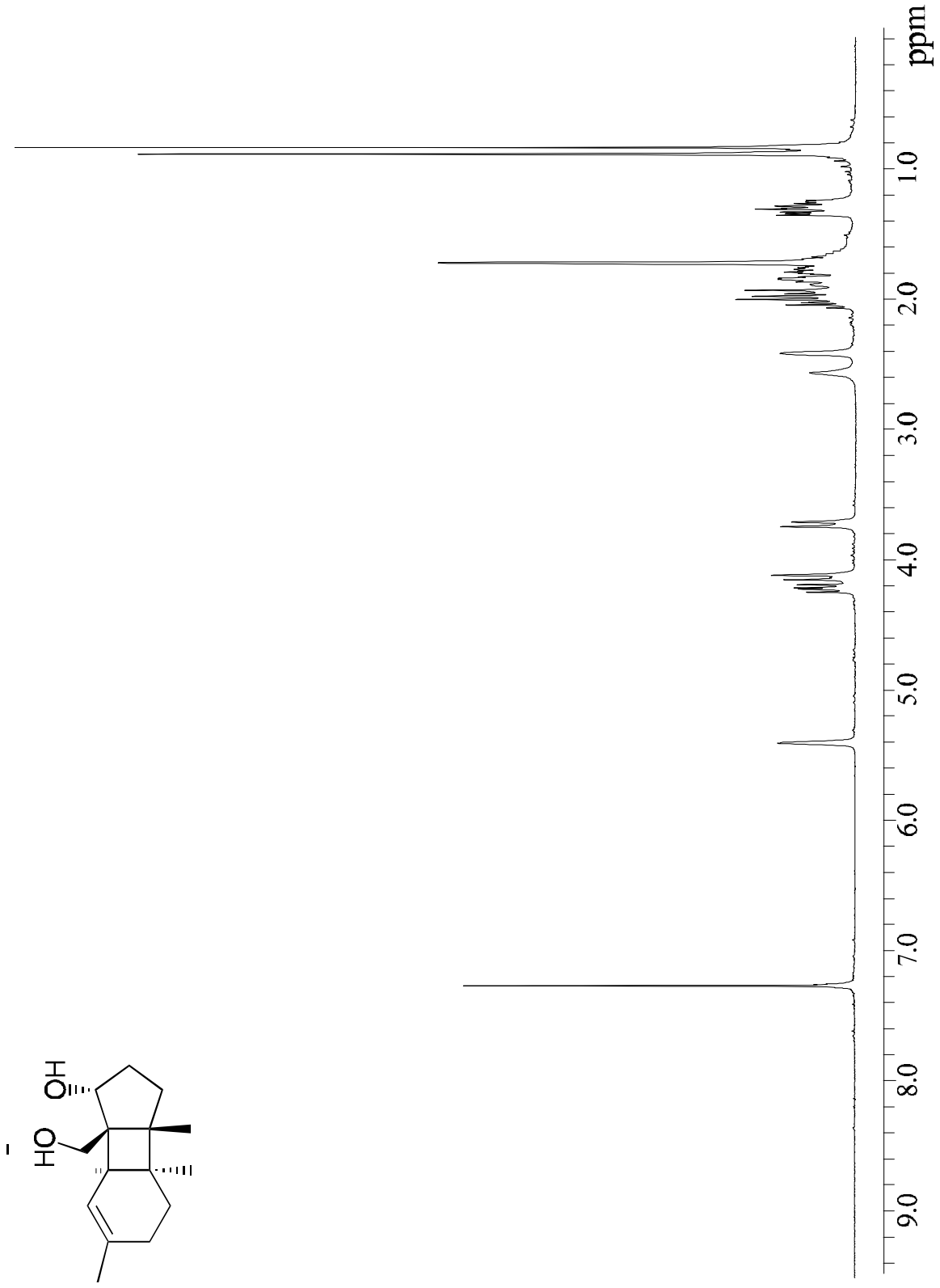
ppm
1.0
2.0
3.0
4.0
5.0
6.0
7.0
8.0
9.0
OH
HO

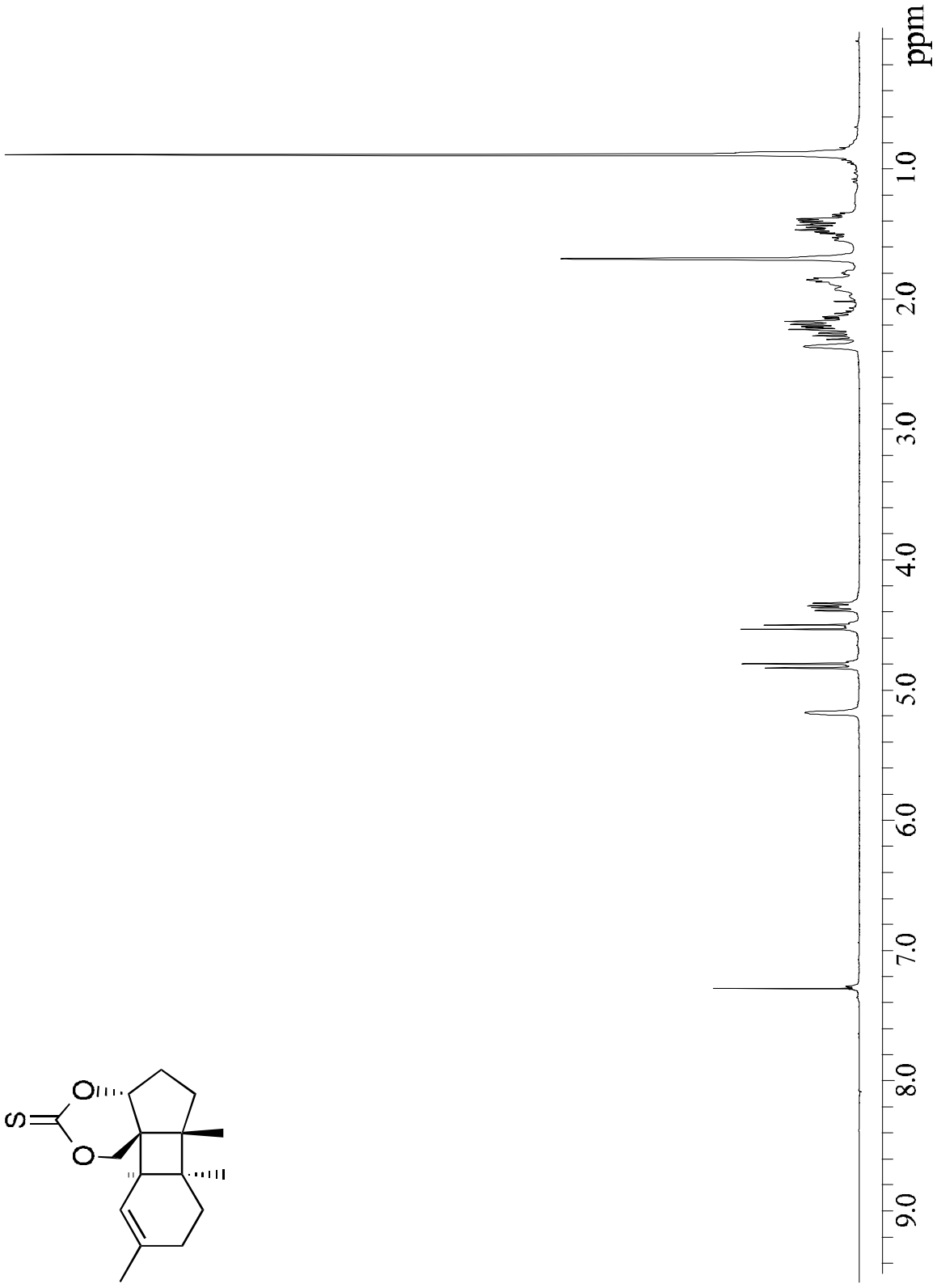
ppm
1.0
2.0
3.0
4.0
5.0
6.0
7.0
8.0
9.0
S
O
O

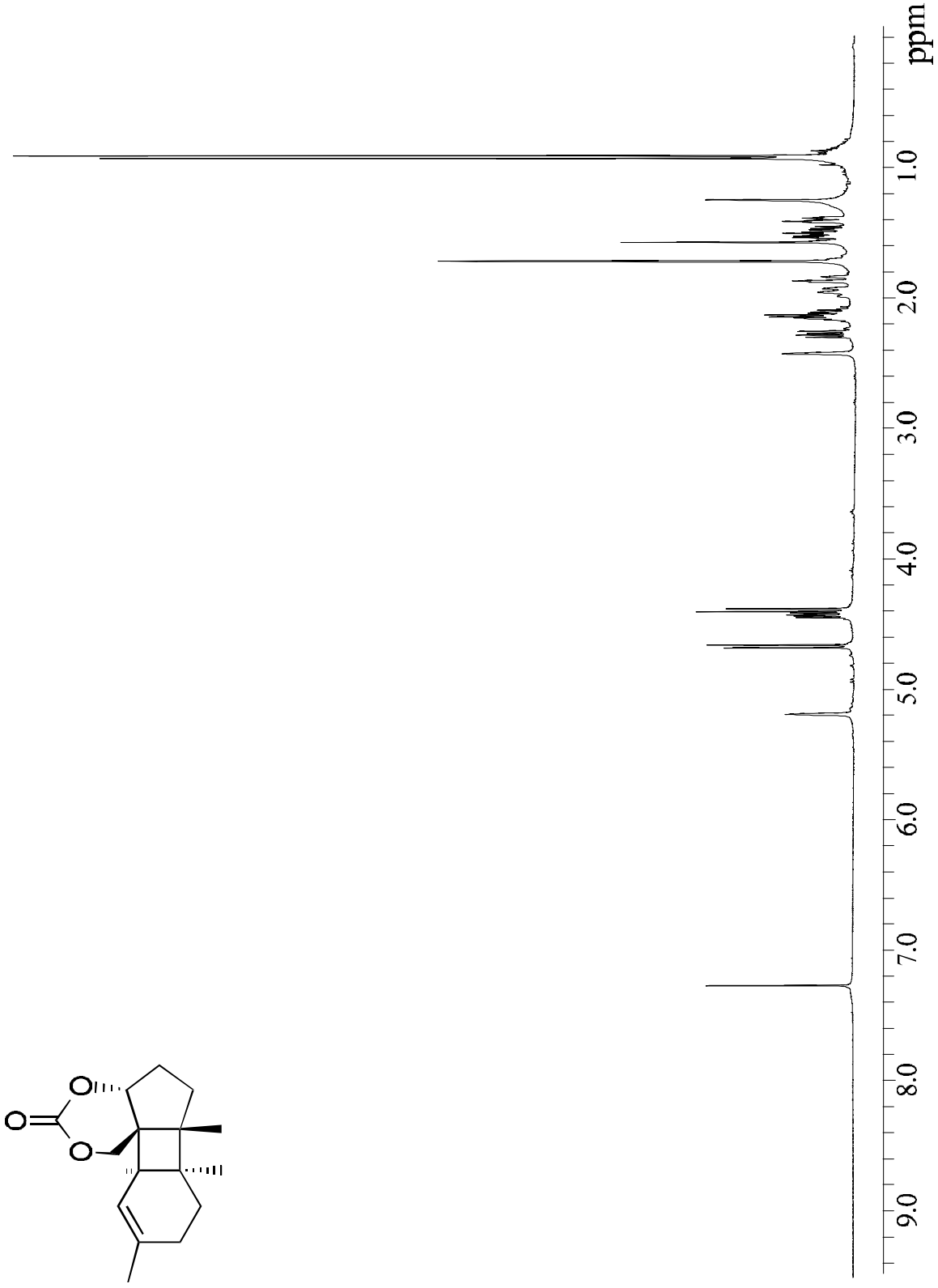
ppm
1.0
2.0
3.0
4.0
5.0
6.0
7.0
8.0
9.0
O
O
O

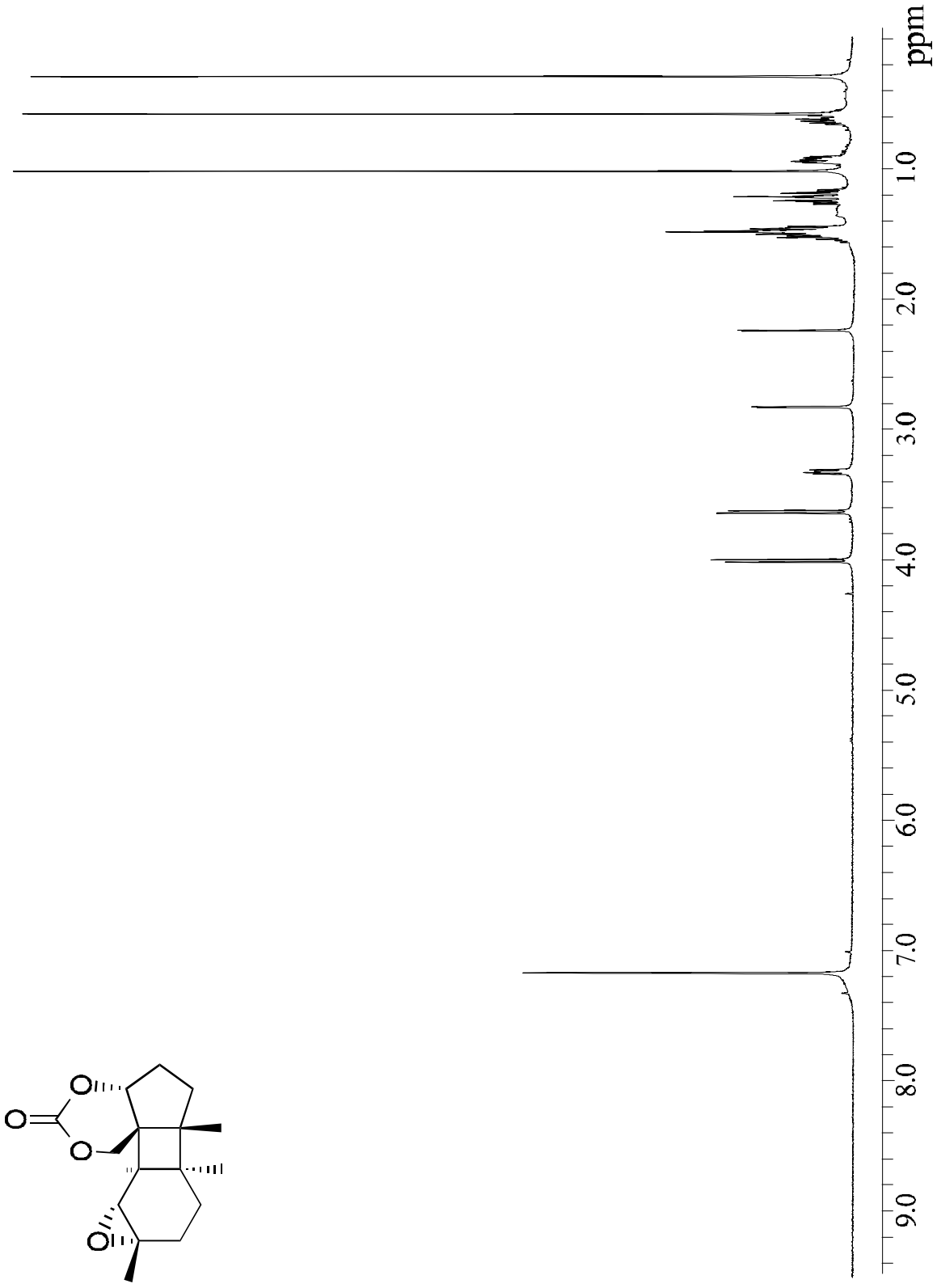
ppm
1.0
2.0
3.0
4.0
5.0
6.0
7.0
8.0
9.0

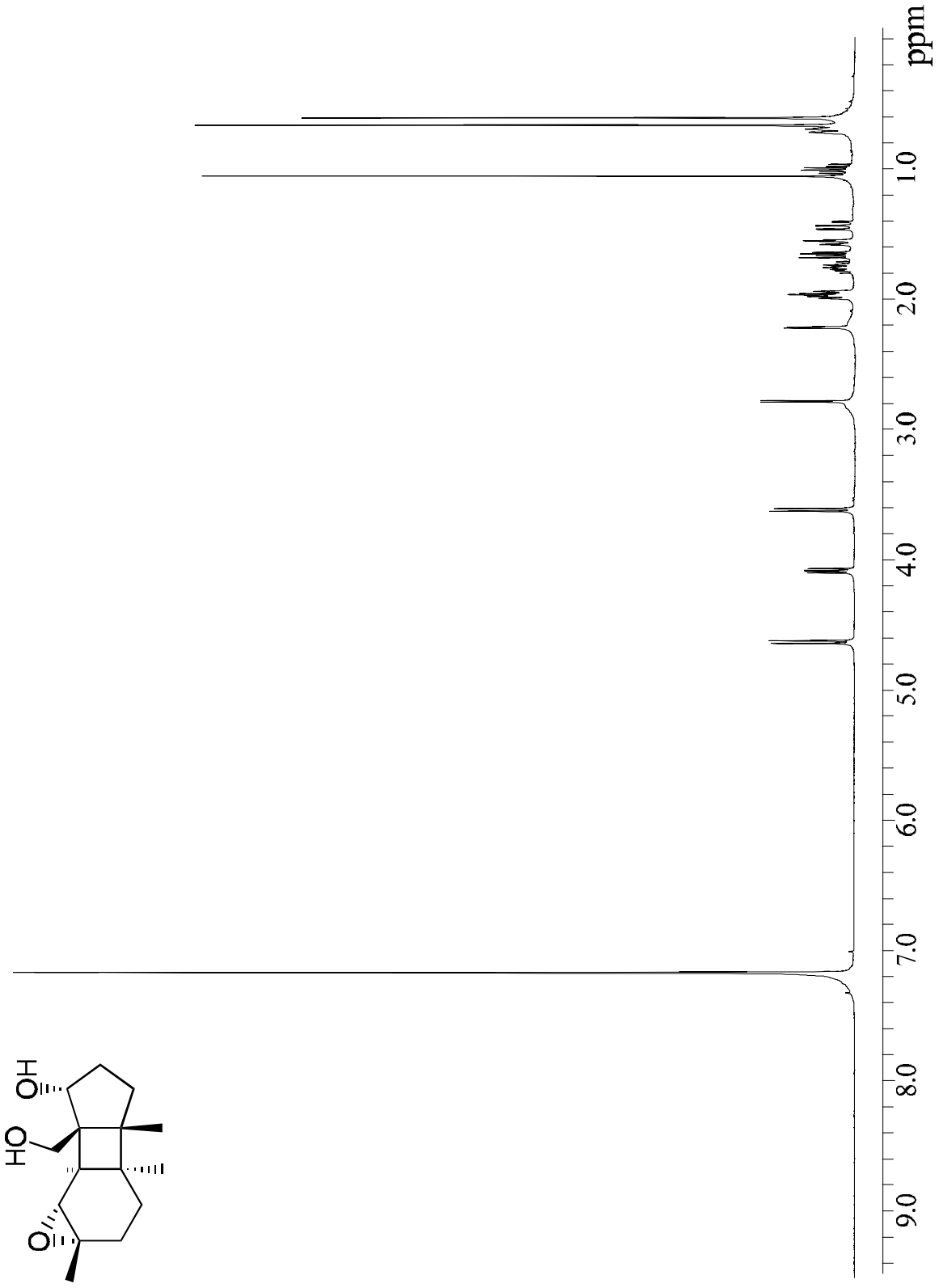
ppm
1.0
2.0
3.0
4.0
5.0
6.0
7.0
8.0
9.0
HO
OH
O

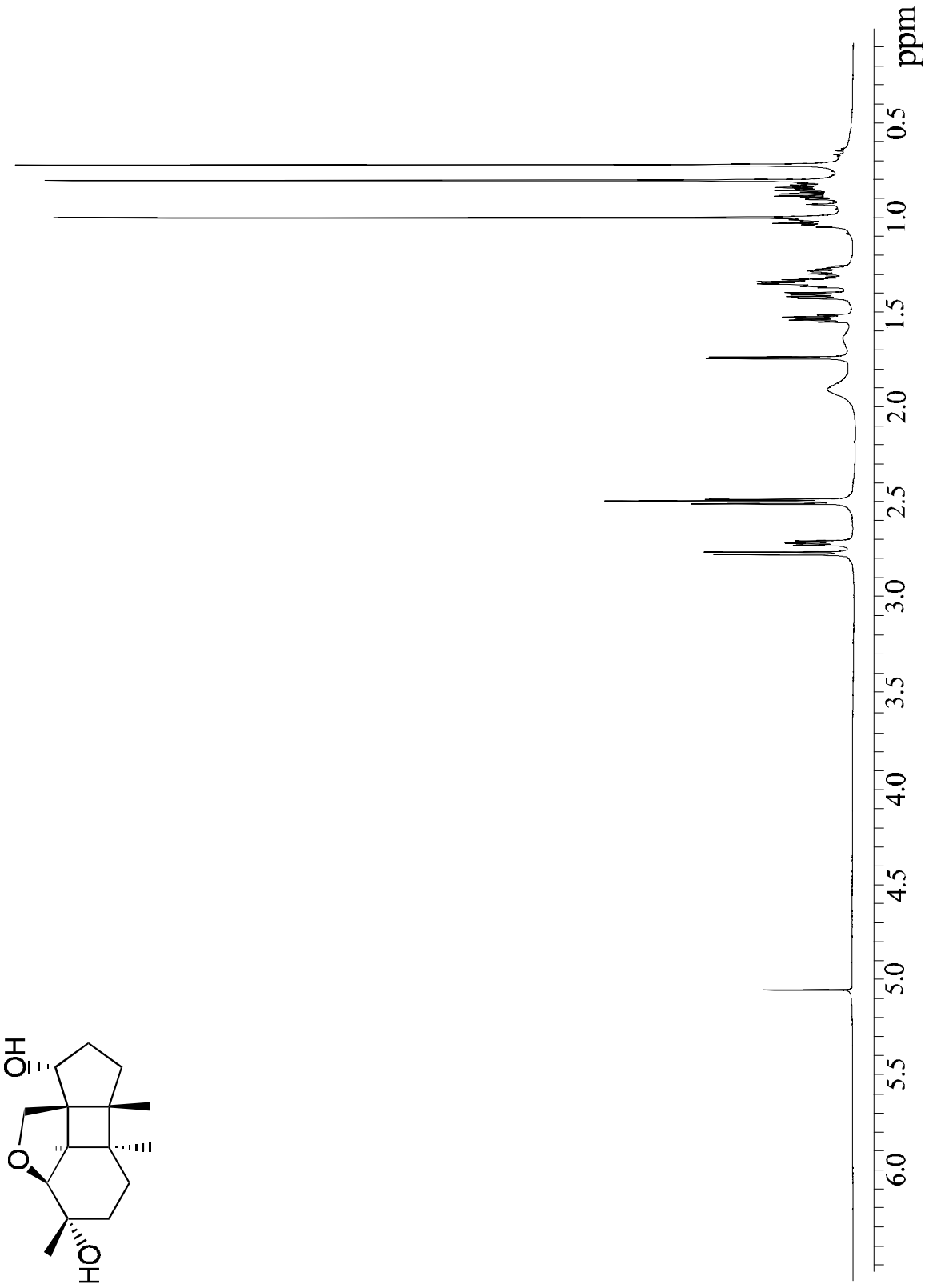
ppm
0.5
1.0
1.5
2.0
2.5
3.0
3.5
4.0
4.5
5.0
5.5
6.0
OH
O
HO

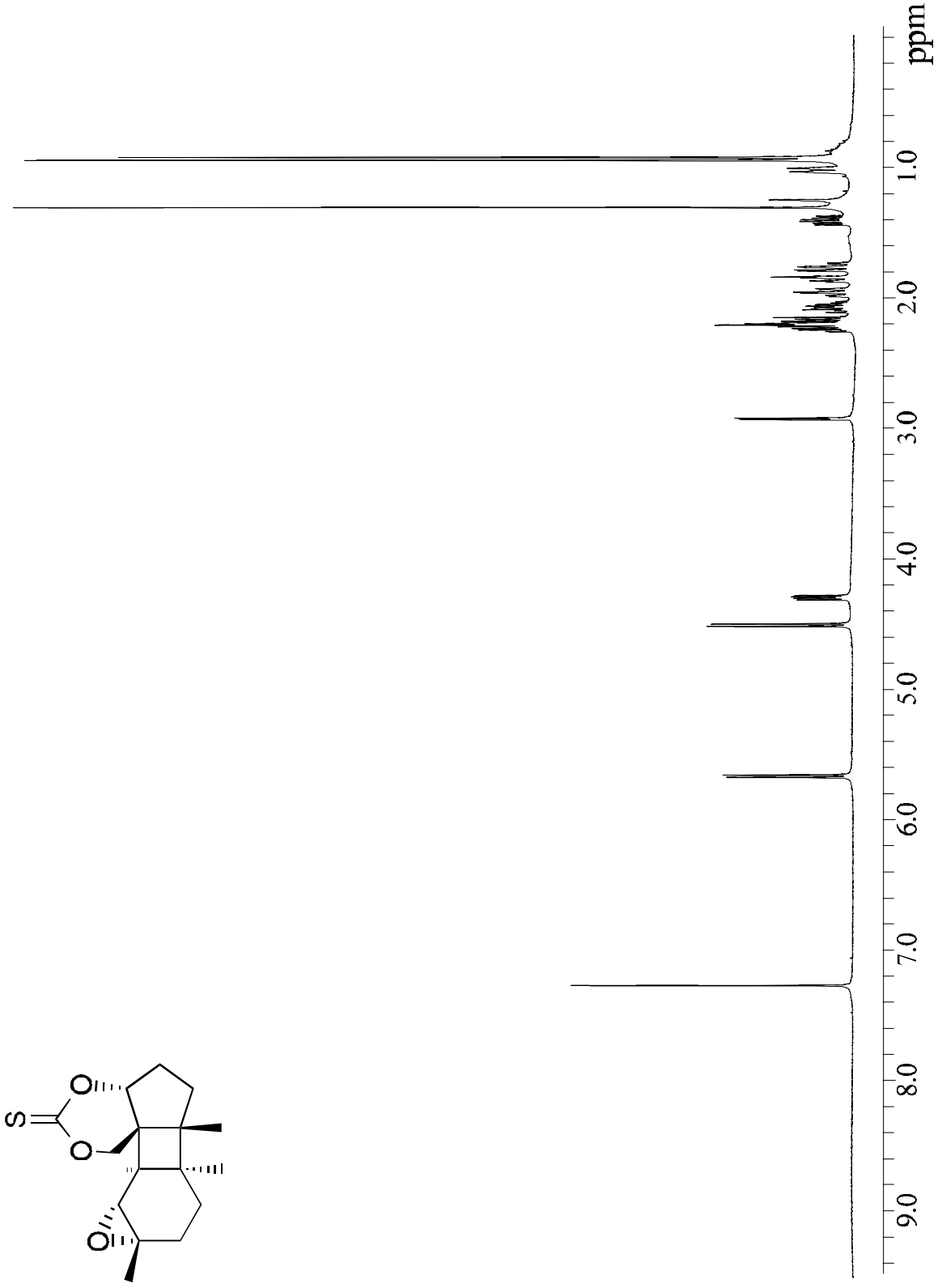
ppm
1.0
2.0
3.0
4.0
5.0
6.0
7.0
8.0
9.0
S
O
O
O

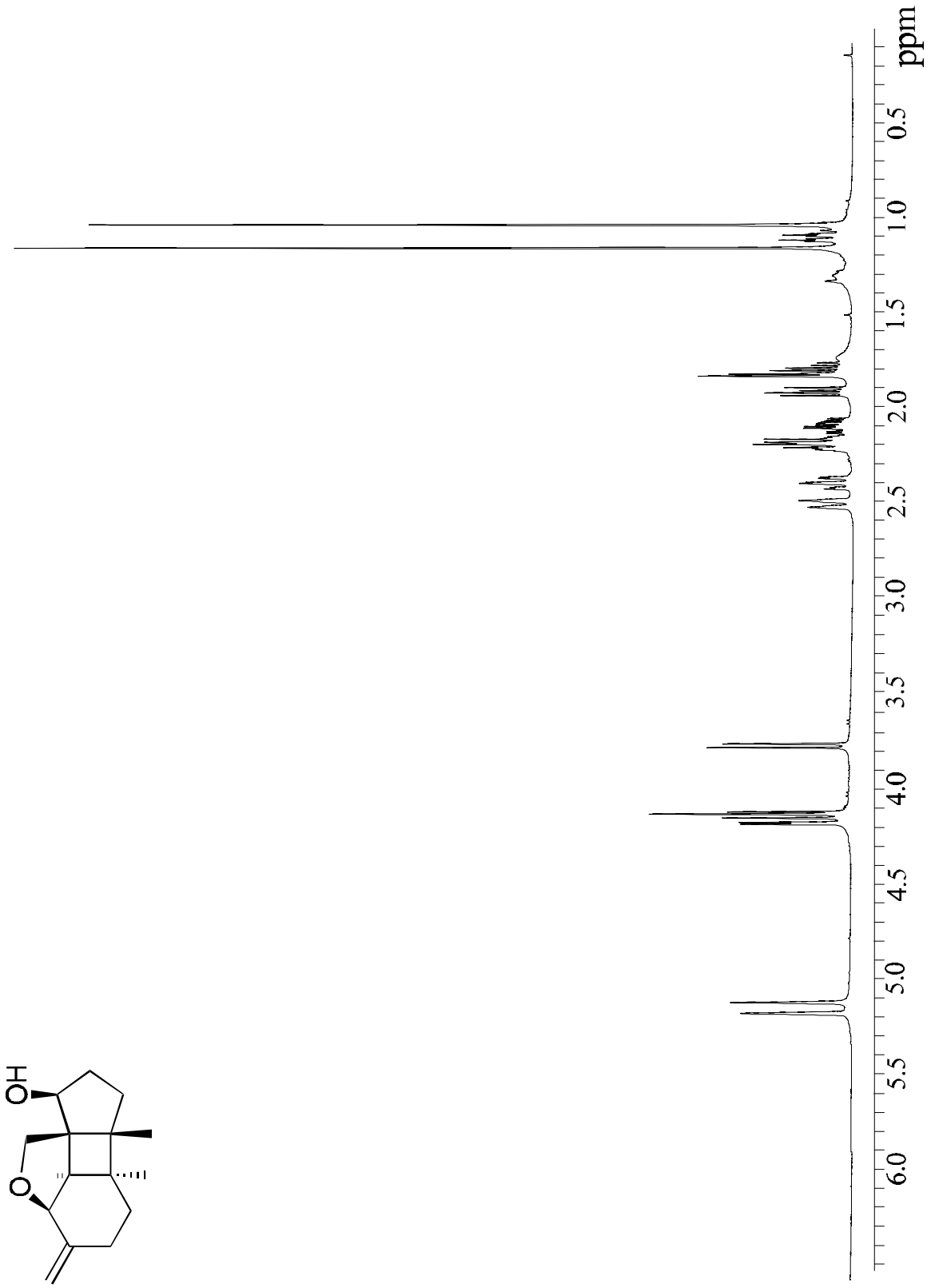
ppm
0.5
1.0
1.5
2.0
2.5
3.0
3.5
4.0
4.5
5.0
5.5
6.0
OH
O

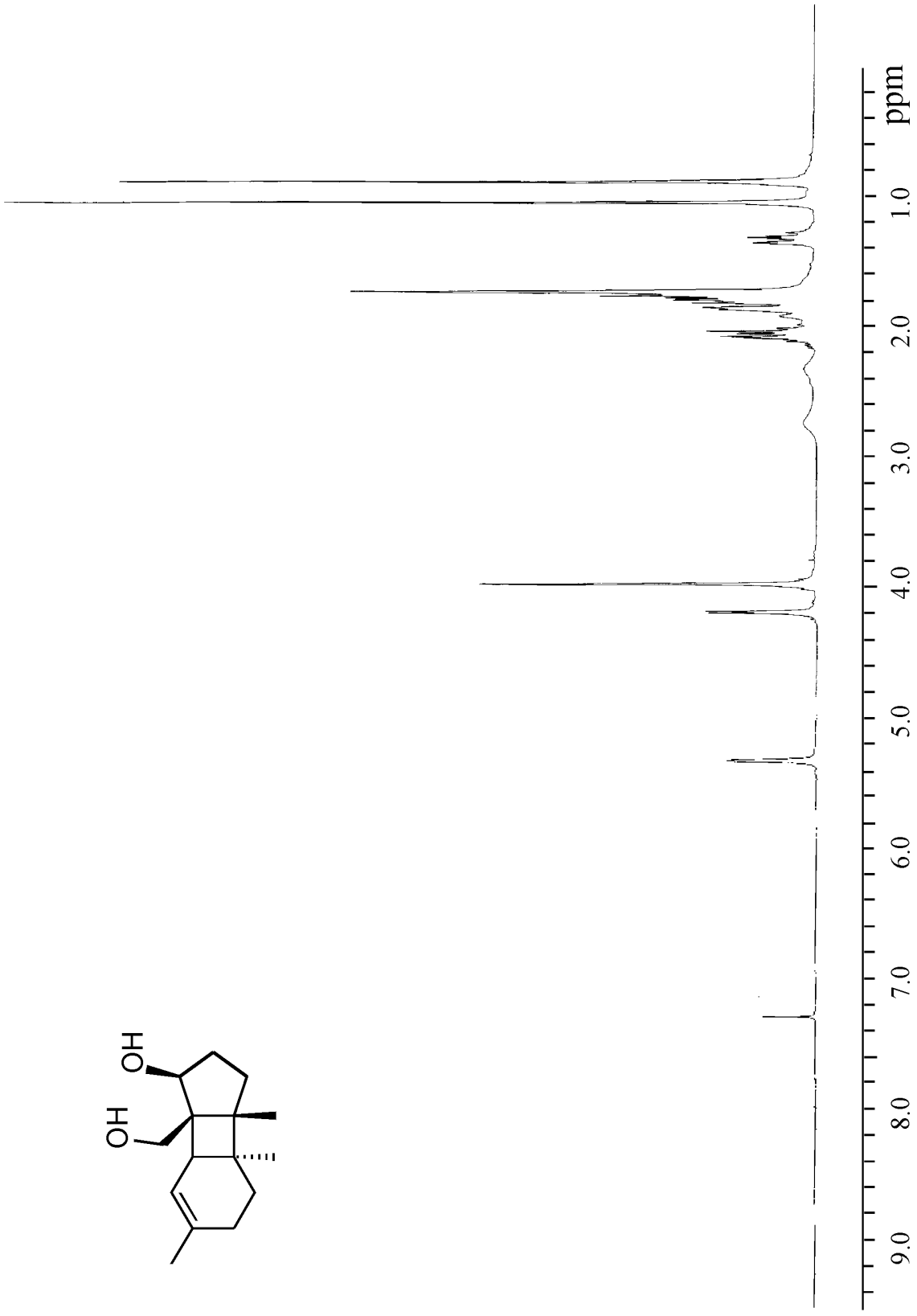
ppm
1.0
2.0
3.0
4.0
5.0
6.0
7.0
8.0
9.0
OH
OH

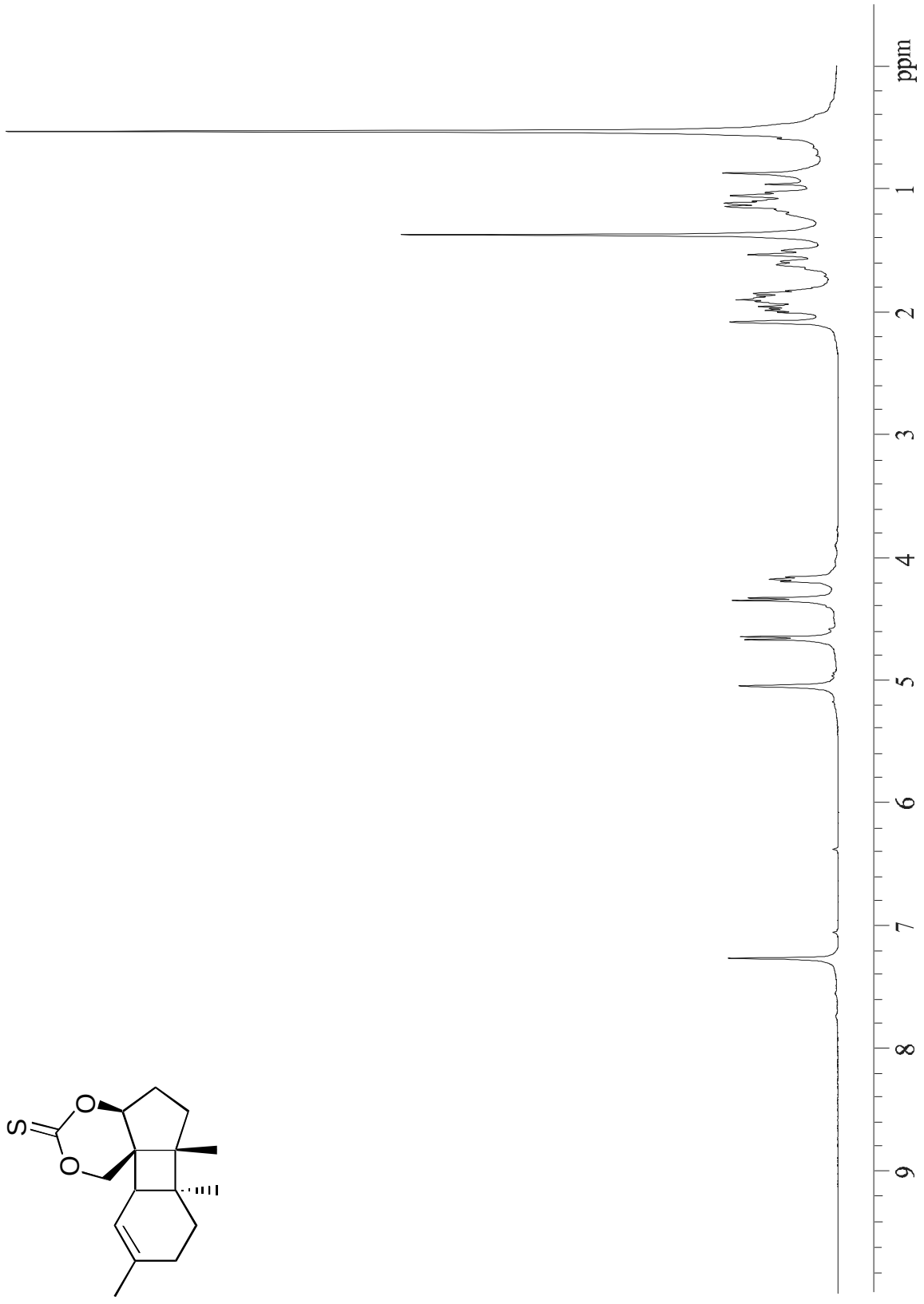
ppm
1
2
3
4
5
6
7
8
9
S
O
O

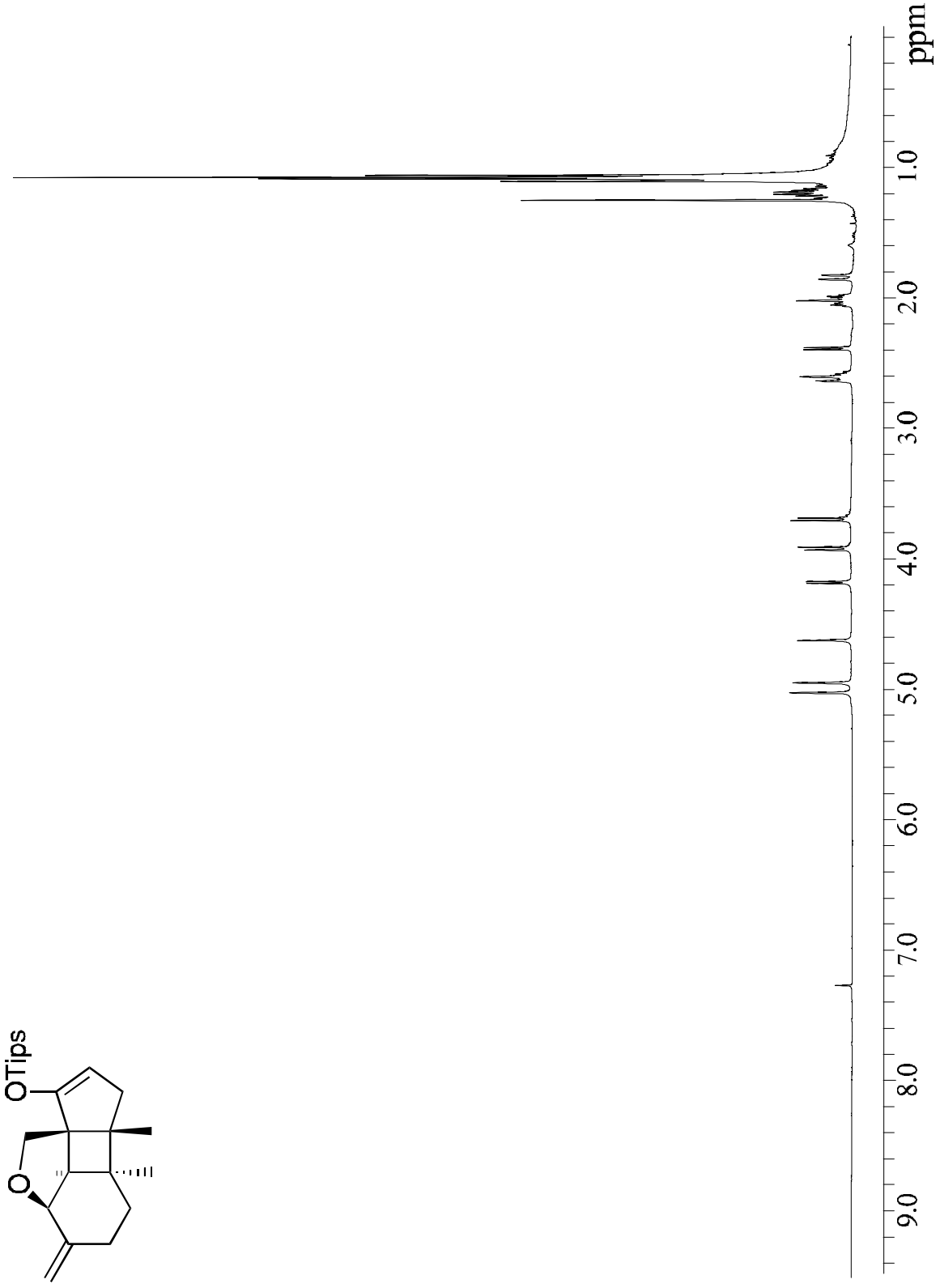
ppm
1.0
2.0
3.0
4.0
5.0
6.0
7.0
8.0
9.0
OTips
O

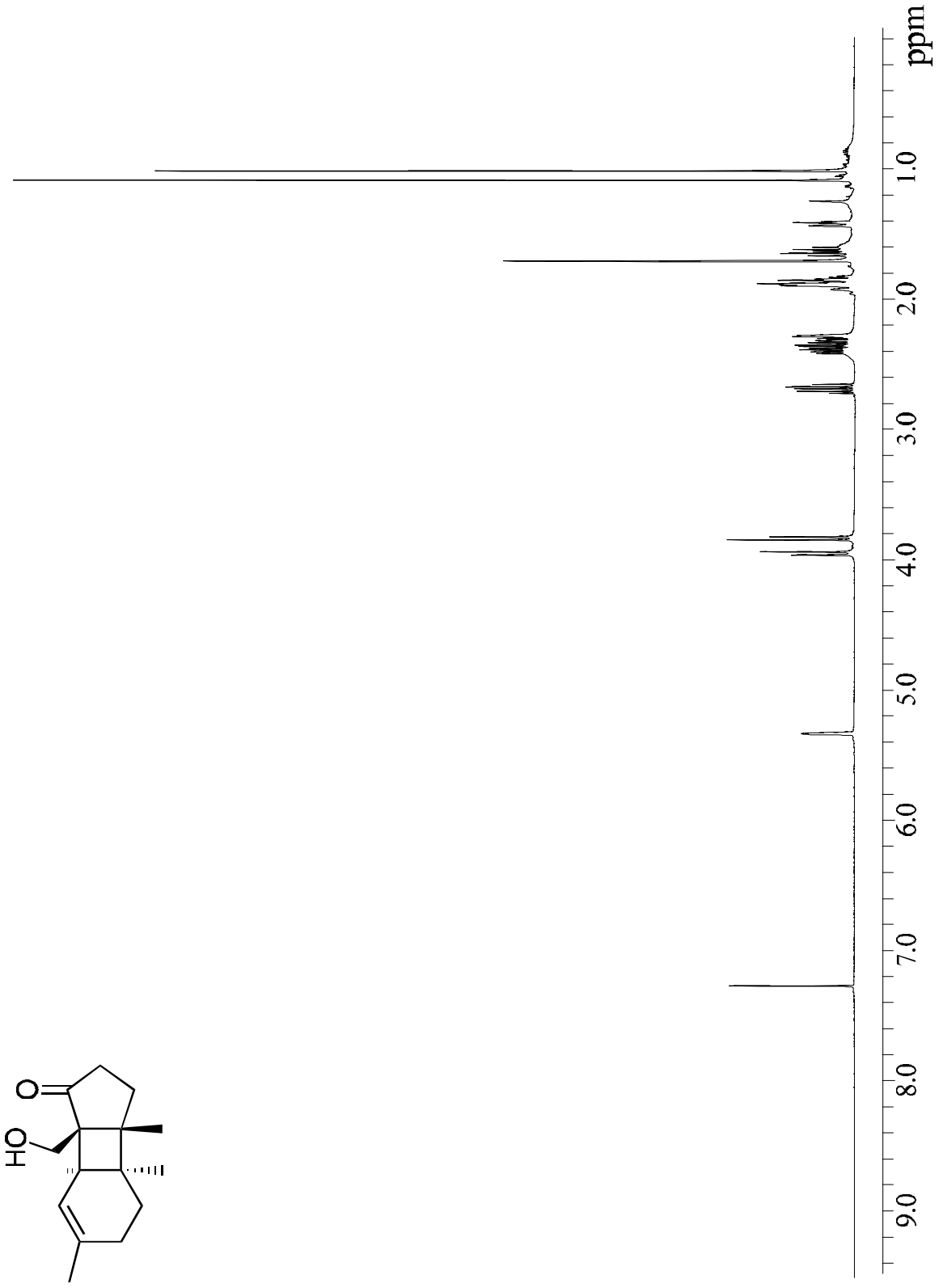
ppm
1.0
2.0
3.0
4.0
5.0
6.0
7.0
8.0
9.0
O
HO

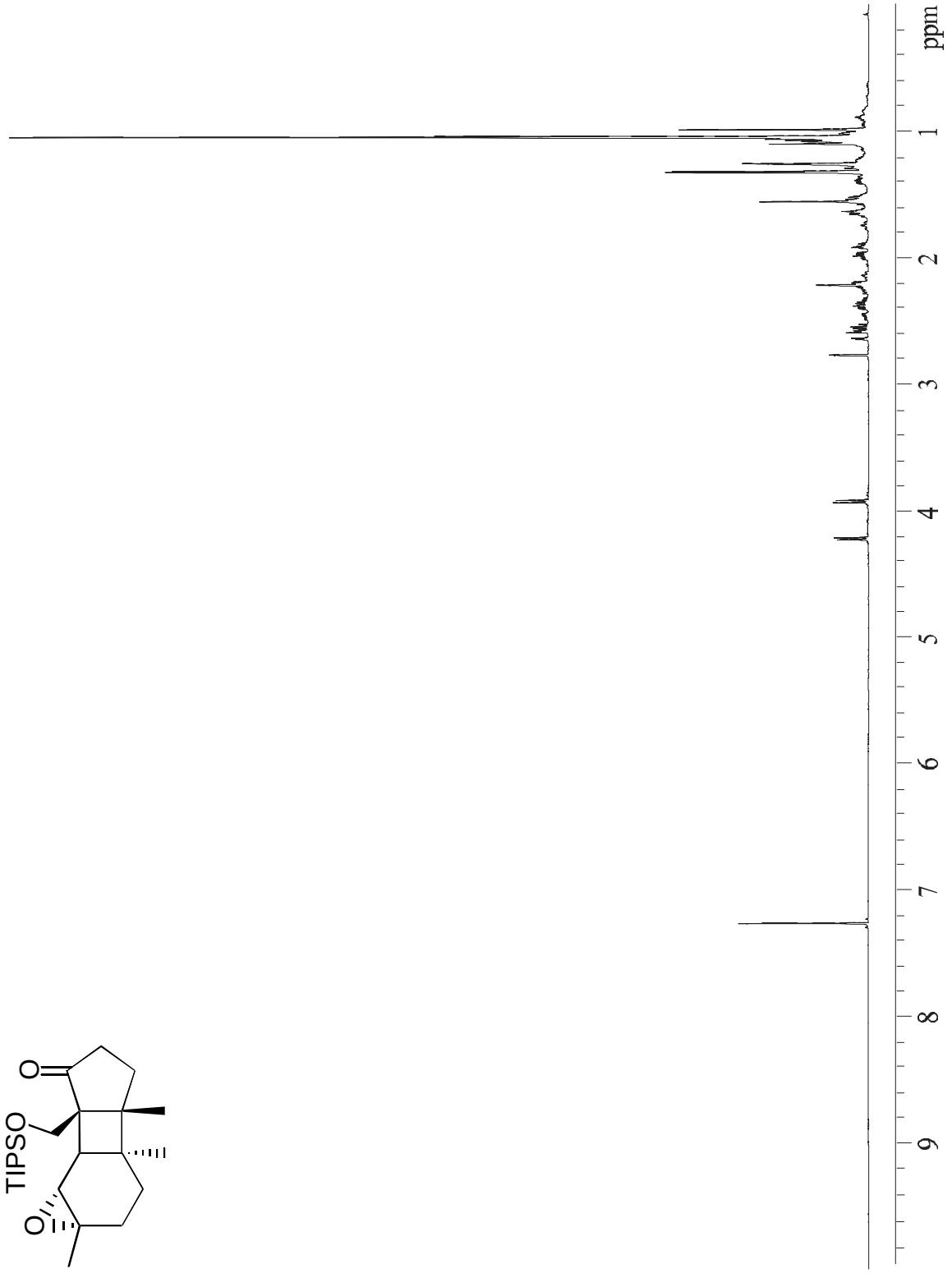
ppm
1
2
3
4
5
6
7
8
9
TIPSO
O
O

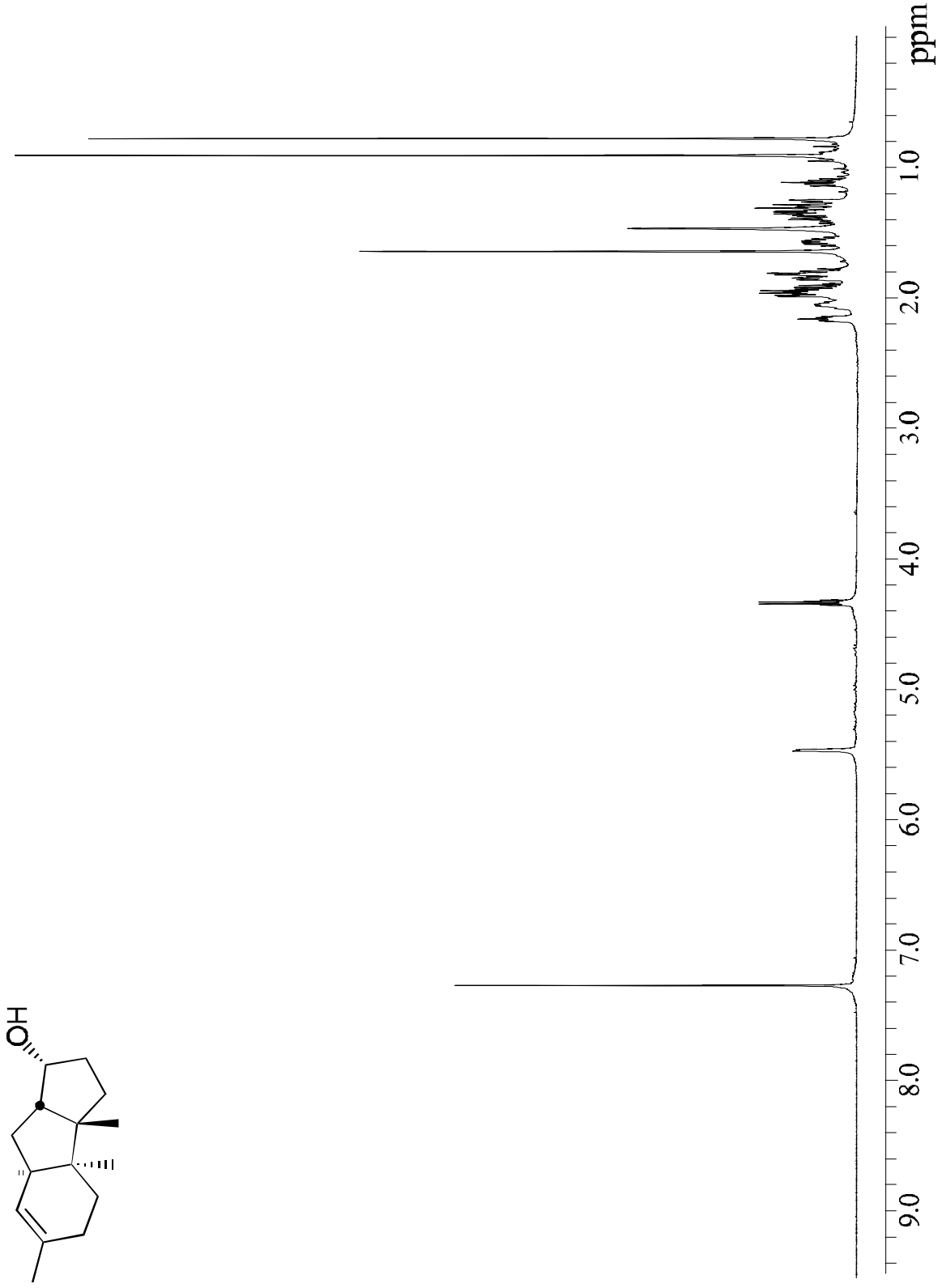
ppm
1.0
2.0
3.0
4.0
5.0
6.0
7.0
8.0
9.0
OH

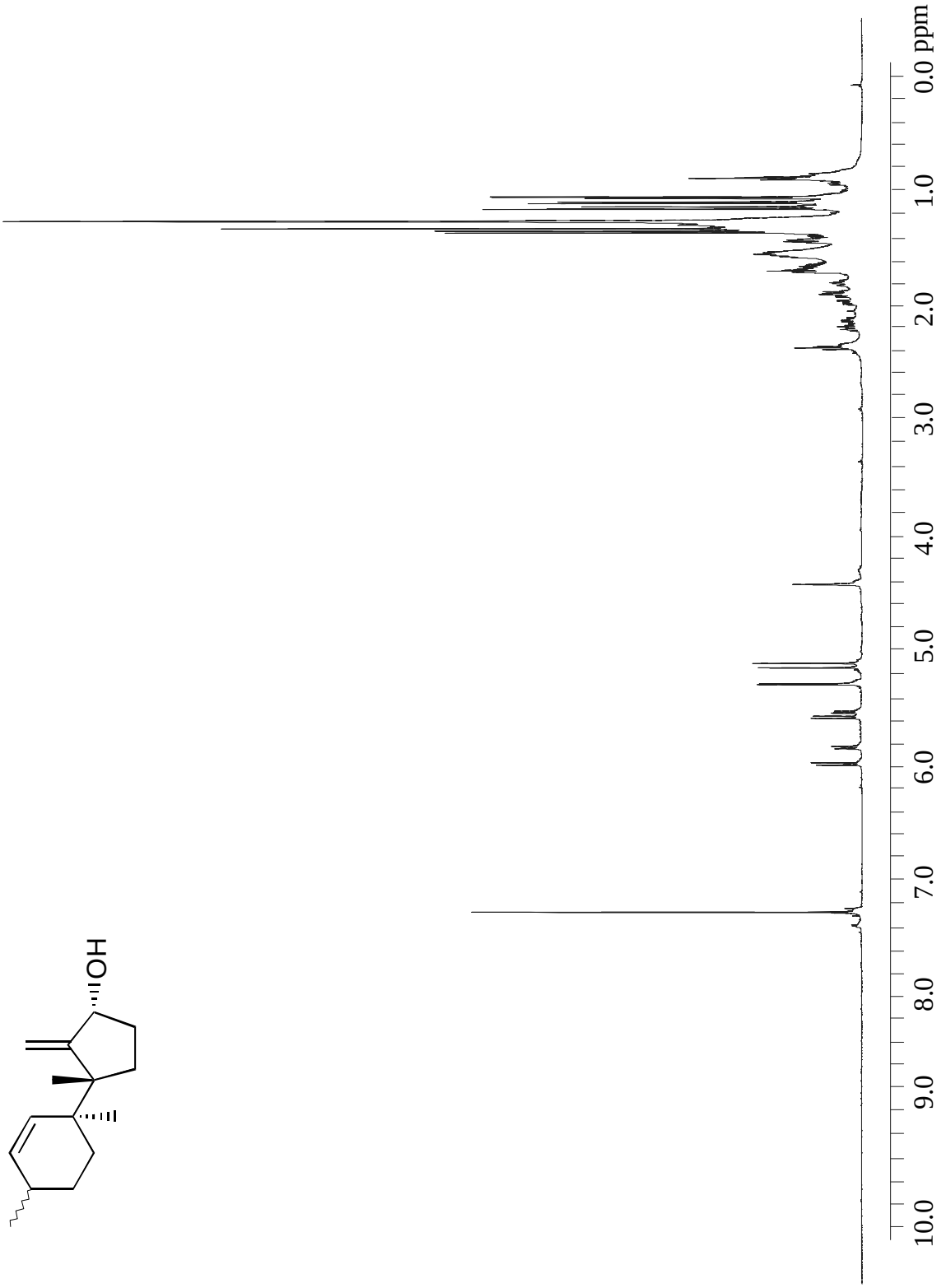
0.0 ppm
1.0
2.0
3.0
4.0
5.0
6.0
7.0
8.0
9.0
10.0
HO

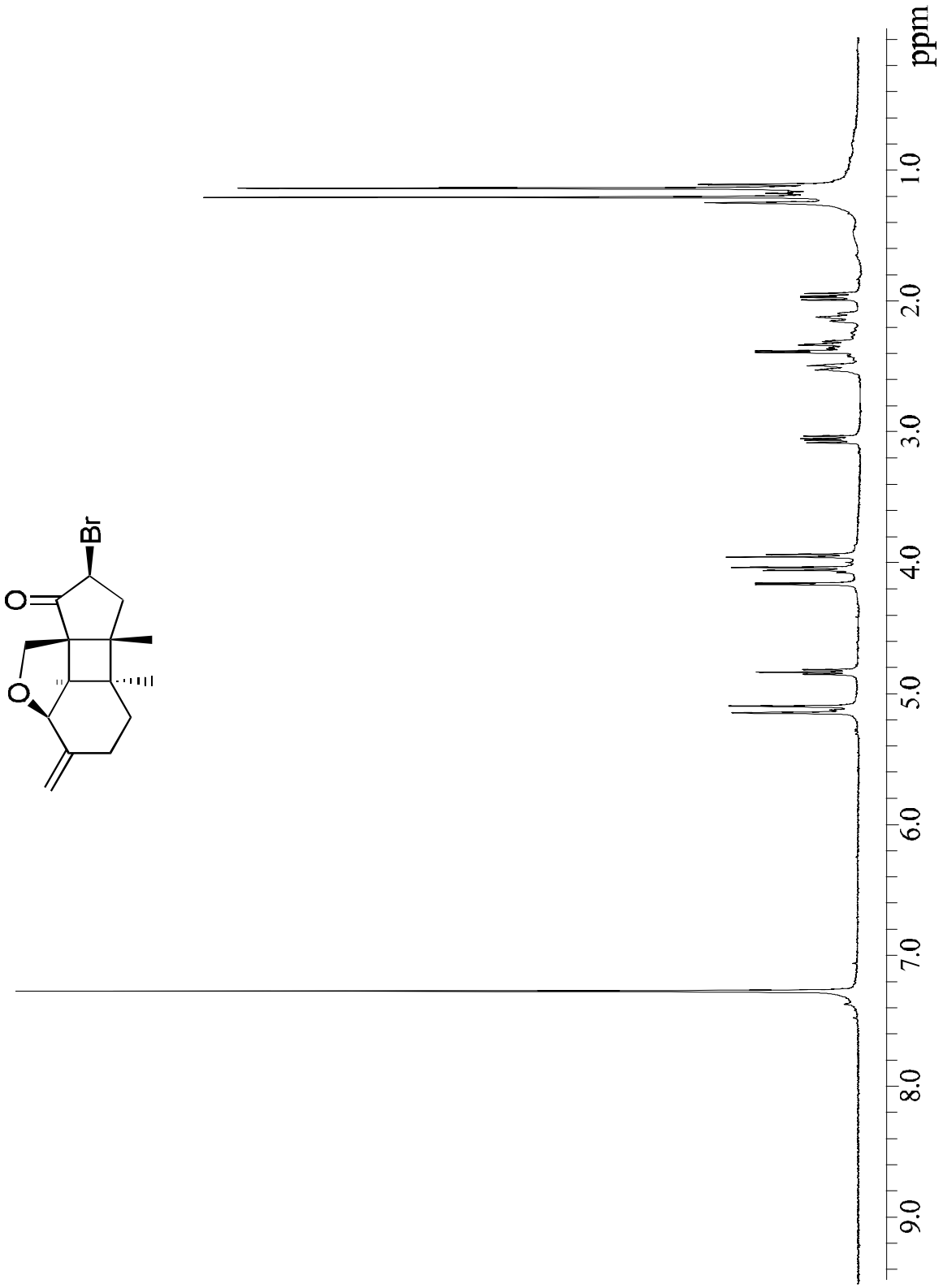
Br
O
O
ppm
1.0
2.0
3.0
4.0
5.0
6.0
7.0
8.0
9.0

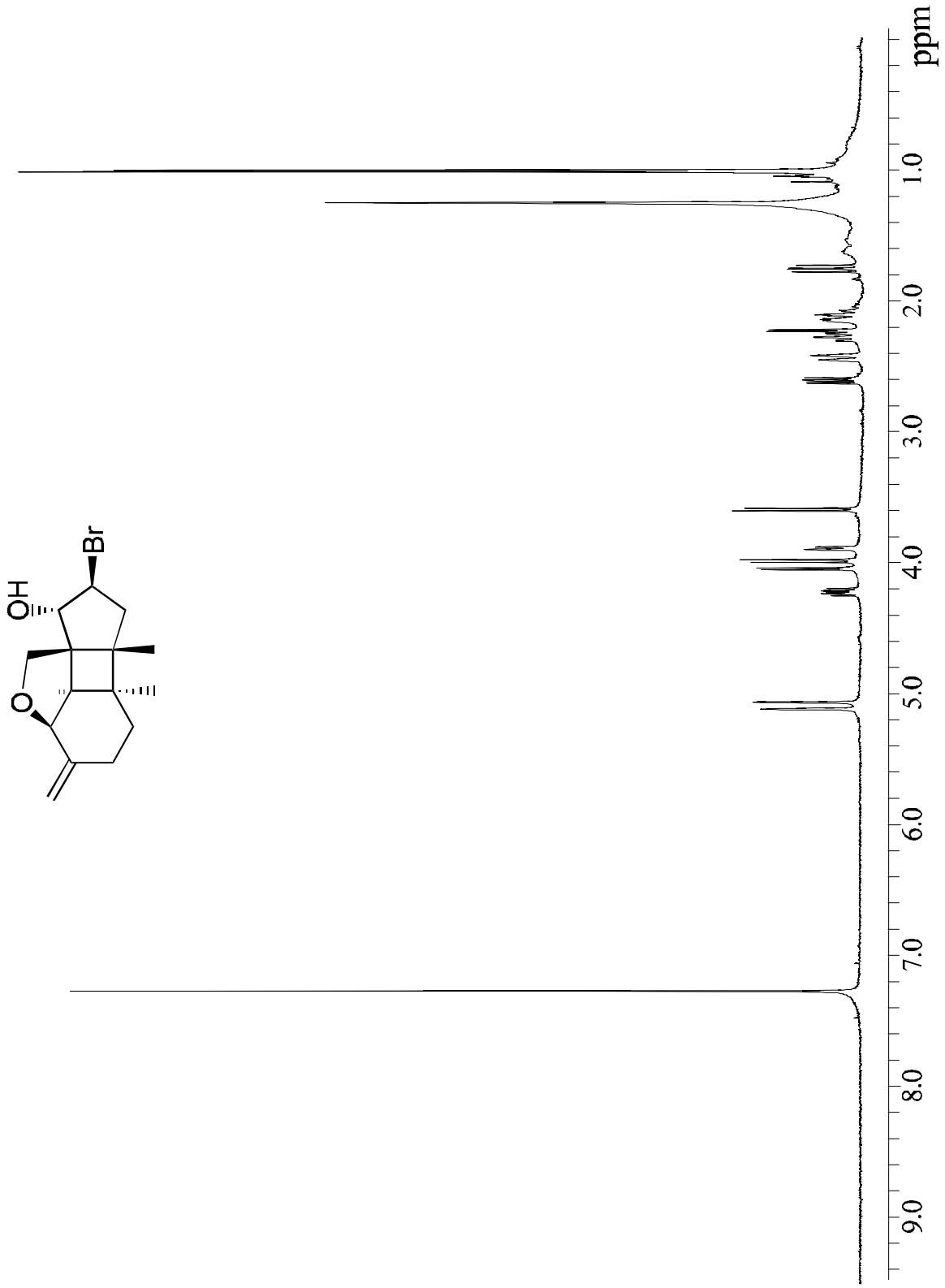
ppm
1.0
2.0
3.0
4.0
5.0
6.0
7.0
8.0
9.0
Br
OH
O

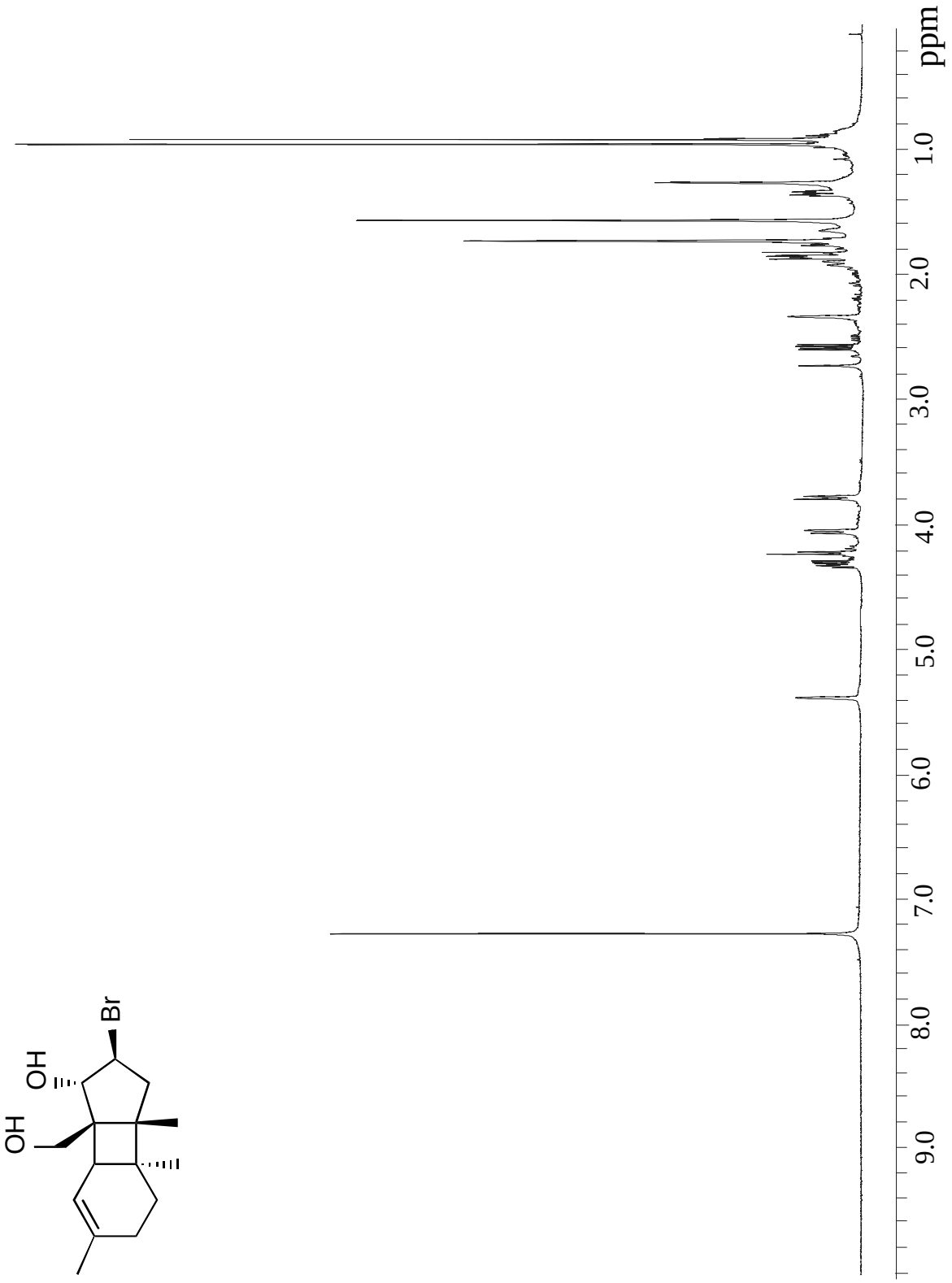
ppm
1.0
2.0
3.0
4.0
5.0
6.0
7.0
8.0
9.0
Br
OH
OH

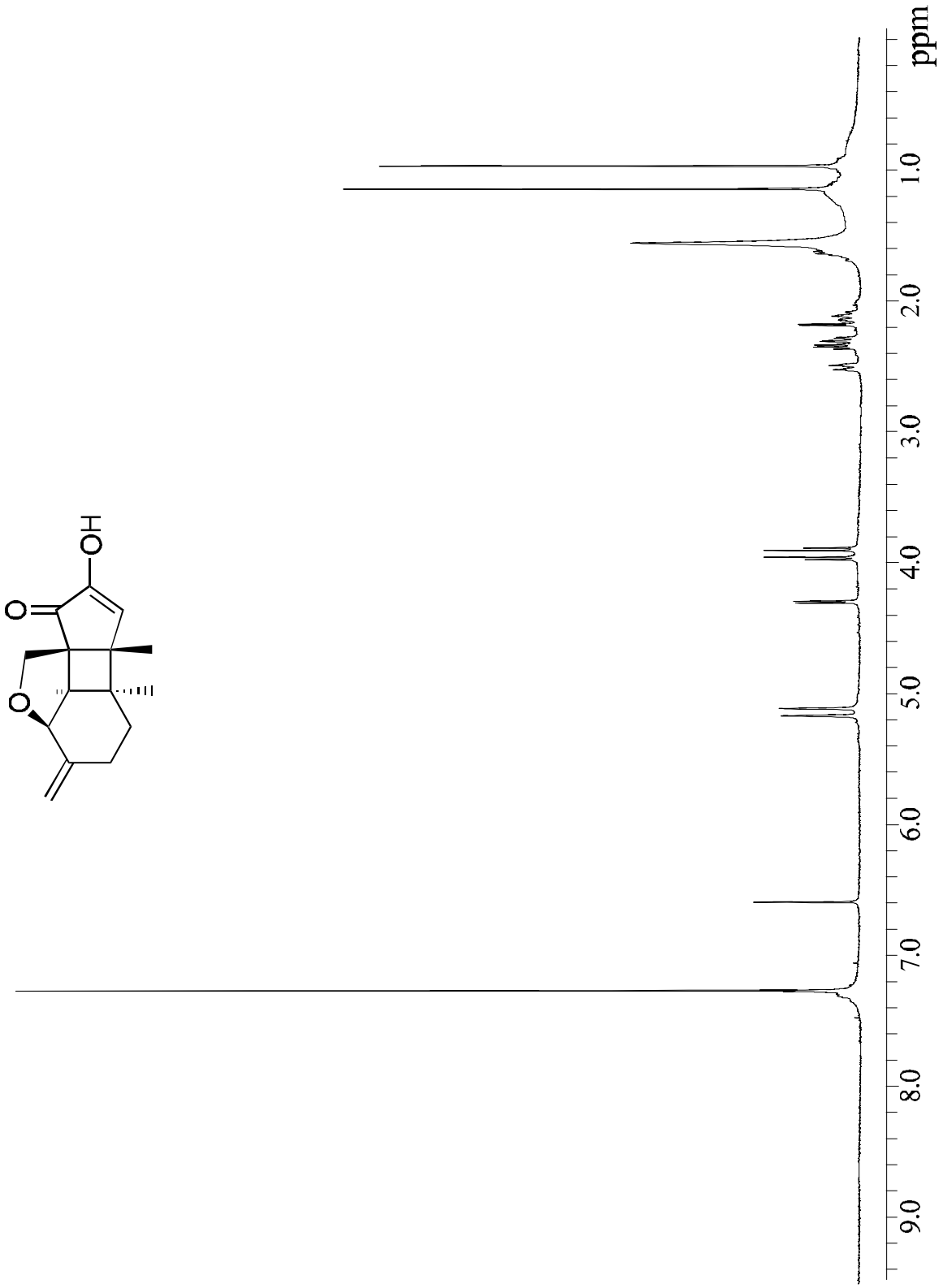
OH
O
O
ppm
1.0
2.0
3.0
4.0
5.0
6.0
7.0
8.0
9.0

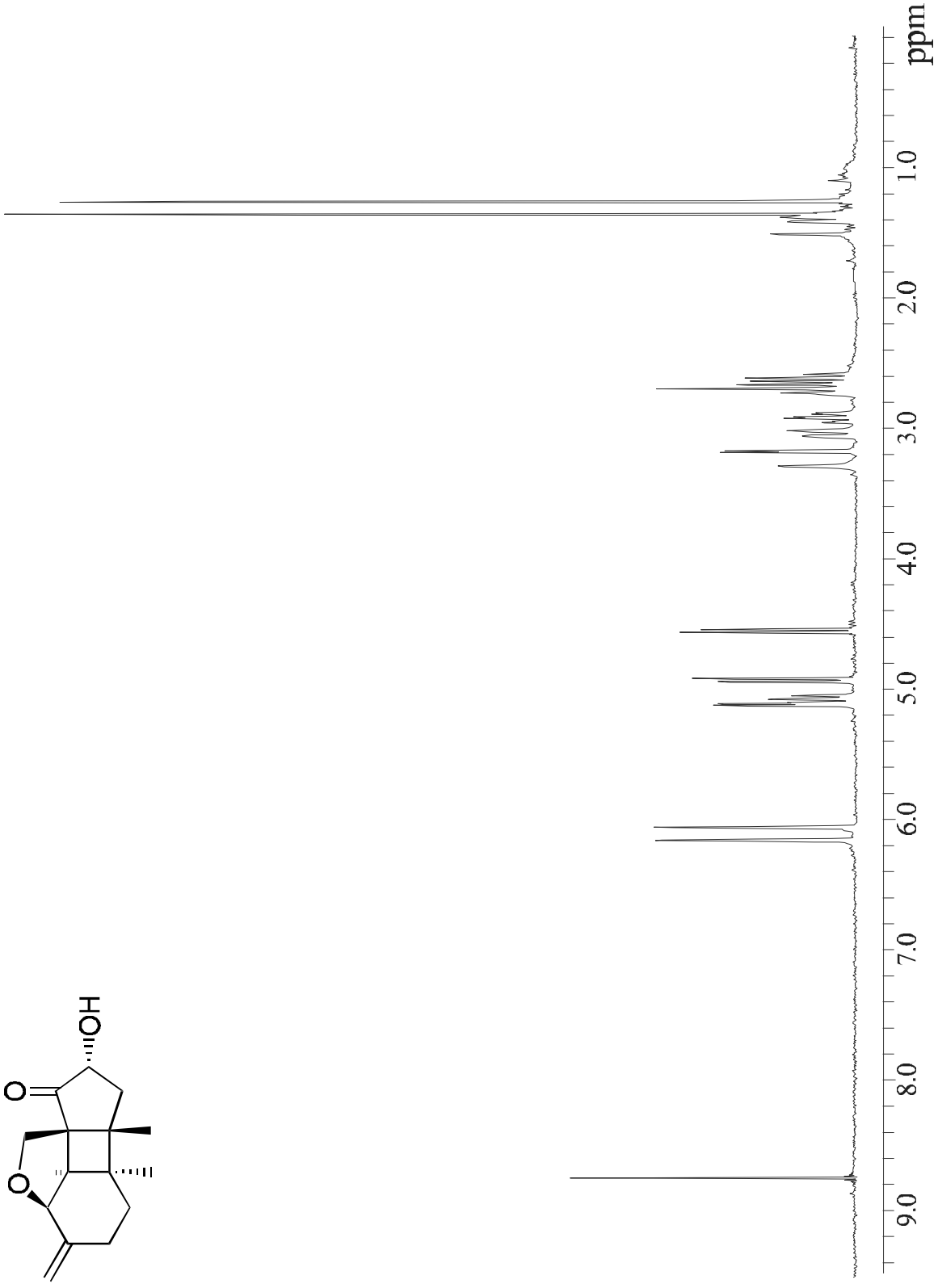
ppm
1.0
2.0
3.0
4.0
5.0
6.0
7.0
8.0
9.0
OH
O
O

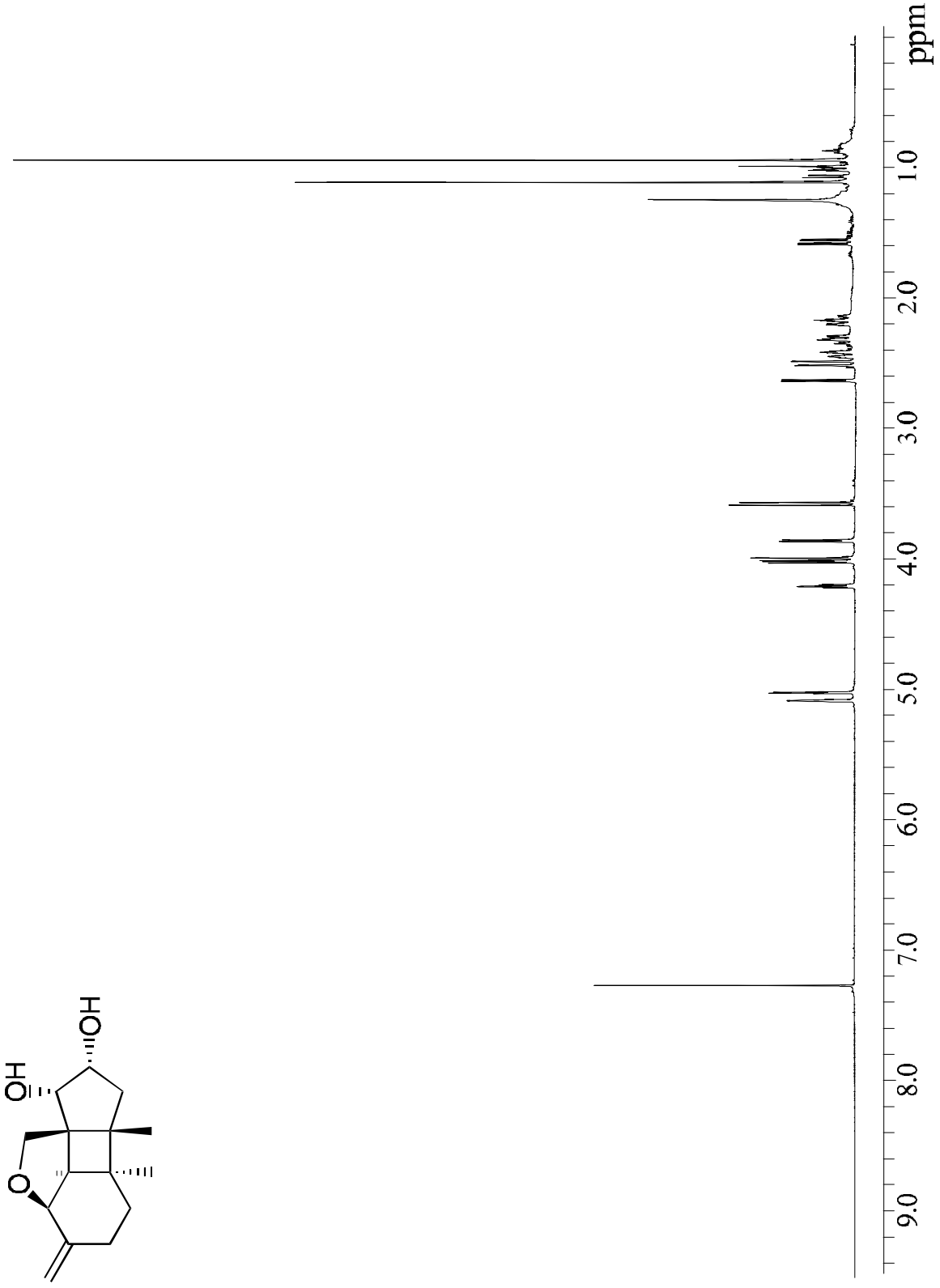
ppm
1.0
2.0
3.0
4.0
5.0
6.0
7.0
8.0
9.0
OH
OH
O

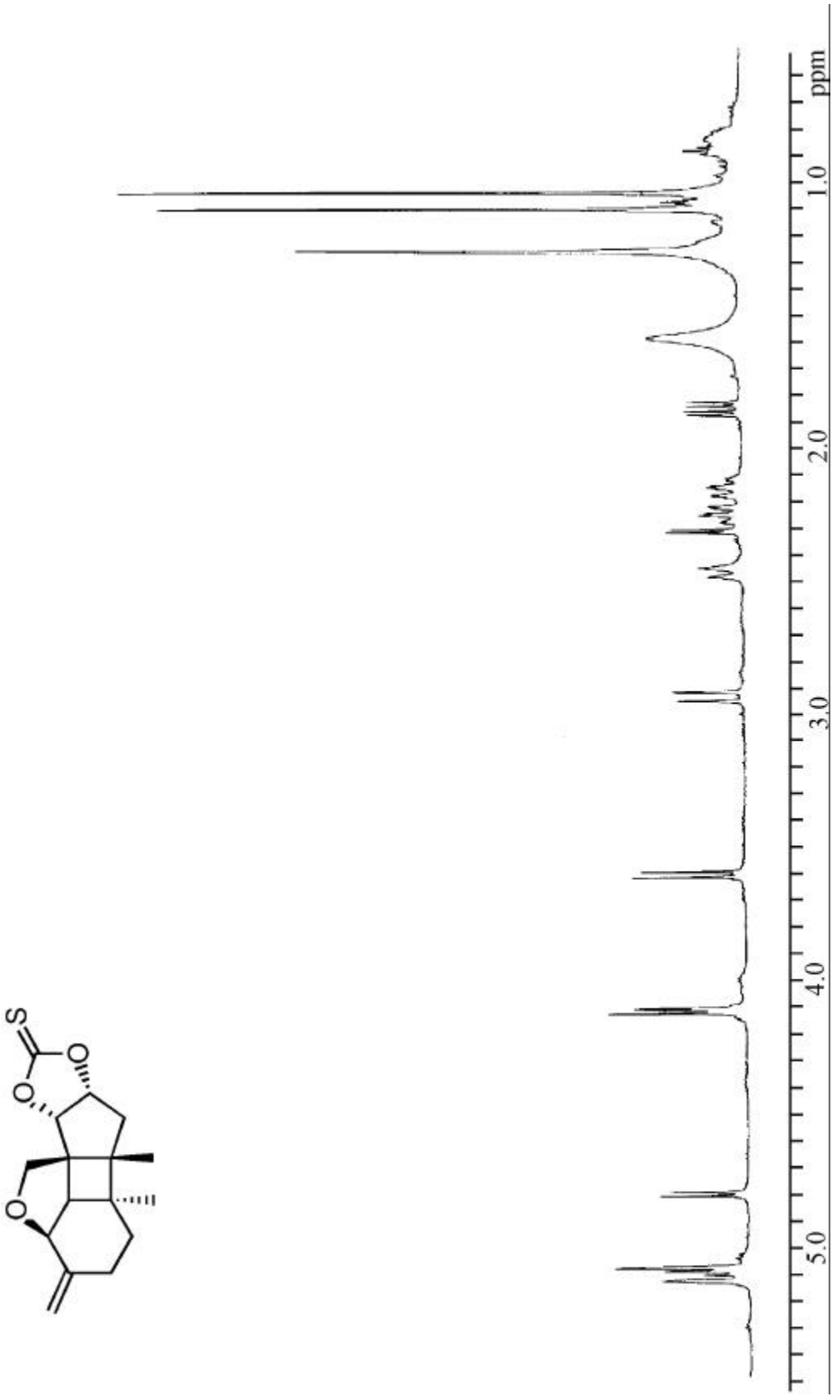
ppm
1.0
2.0
3.0
4.0
5.0
S
O
O
O
O

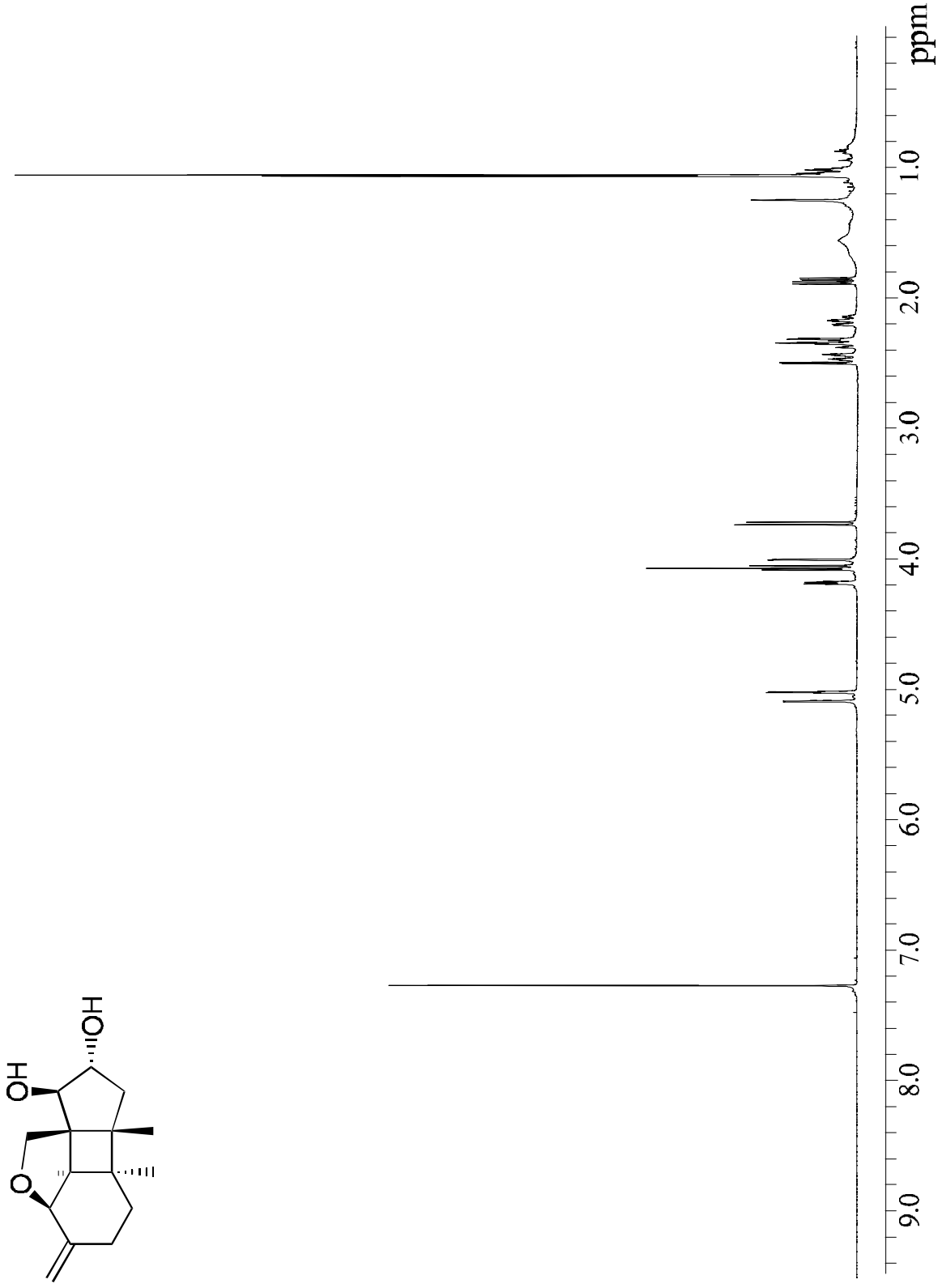
ppm
1.0
2.0
3.0
4.0
5.0
6.0
7.0
8.0
9.0
OH
OH
O

- *Results of NOE experiments Chapter 3*

1. Compound 91

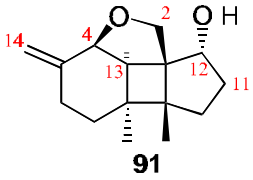

91

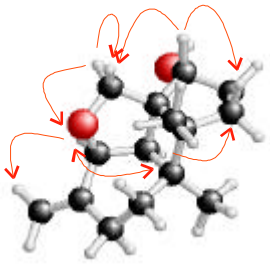

1D-proton difference NOE experiments were conducted. The T^1 relaxation times for the protons involved in the experiment were calculate via inverse recovery experiments. The mixing times for the NOE experiments were maximized in other to observe maximum NOE to about 2/3 of the T^1 relaxation measured.

NOEs observed: H-2α (δ 3.95 ppm) to H-2β (δ 3.57 ppm), H-2α (δ 3.95 ppm) to H-4 (δ 4.02 ppm), H-4 (δ 4.02 ppm) to H-14 (δ 5.09 ppm), H-4 (δ 4.02 ppm) to H-13 (δ 2.20 ppm), H-13 (δ 2.20 ppm) to H-4 (δ 4.02 ppm), H-13 (δ 2.20 ppm) to H-11 (δ 2.15 ppm), H-12 (δ 3.88 ppm) to H-11 (δ 2.15 ppm), H-12 (δ 3.88 ppm) to H-2β (δ 3.57 ppm).

The absence of an NOE between H-12 and H-13, which was seen for compound **100**, confirms the R relative stereochemistry of the hydroxyl at C-12.

2. Compound 94

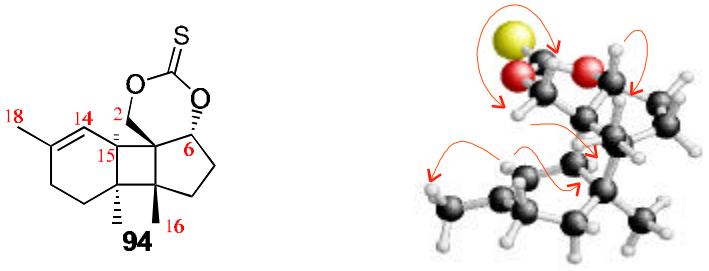

1D-proton difference NOE experiments were conducted. The T^1 relaxation times for the protons involved in the experiment were calculate via inverse recovery experiments. The mixing times for the NOE experiments were maximized in other to observe maximum NOE to about 2/3 of the T^1 relaxation measured.

NOEs observed: H-2α (δ 4.82 ppm) to H-2β (δ 4.52 ppm), H-2β (δ 4.52 ppm) to H-2α (δ 4.82 ppm), H-2α (δ 4.82 ppm) to H-15 (δ 2.39 ppm), H-14 (δ 5.17 ppm) to H-15 (δ 2.39 ppm), H-14 (δ 5.17 ppm) to H-18 (δ 1.72 ppm), H-6 (δ 4.35 ppm) to H-16 (δ 0.92 ppm).

The absence of an NOE from H-6 to H-15 confirms the R relative stereochemistry at C-6.

3. Compound 96

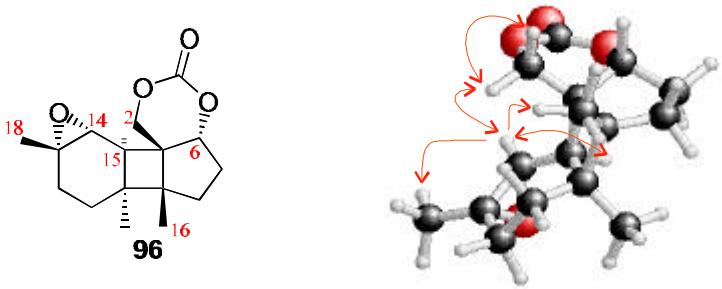

1D-proton difference NOE experiments were conducted. The T^1 relaxation times for the protons involved in the experiment were calculate via inverse recovery experiments. The mixing times for the NOE experiments were maximized in other to observe maximum NOE to about 2/3 of the T^1 relaxation measured.

NOEs observed: H-2α (δ 4.01 ppm) to H-2β (δ 3.64 ppm), H-2β (δ 3.64 ppm) to H-2α (δ 4.01 ppm), H-2α (δ 4.01 ppm) to H-14 (δ 2.83 ppm), H-14 (δ 2.83 ppm) to H-2α (δ 4.01 ppm), H-14 (δ 2.83 ppm) to H-15 (δ 2.25 ppm), H-15 (δ 2.25 ppm) to H-14 (δ 2.83 ppm), H-14 (δ 2.83 ppm) to H-18 (δ 1.03 ppm), H-14 (δ 2.83 ppm) to H-16 (δ 0.57 ppm).

An NOE observed between H-2α and H-14 confirms the R relative stereochemistry at C-14. The absence of an NOE between H-6 and H-15 supports the assignment of the R relative stereochemistry for C-6.

4. Compound 99

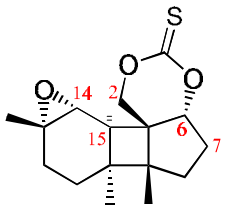

99

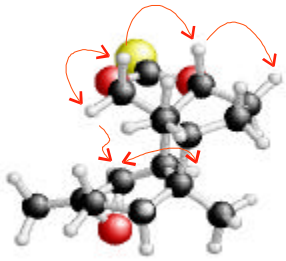

1D-proton difference NOE experiments were conducted. The T^1 relaxation times for the protons involved in the experiment were calculate via inverse recovery experiments. The mixing times for the NOE experiments were maximized in other to observe maximum NOE to about 2/3 of the T^1 relaxation measured.

NOEs observed: H-2α (δ 5.67 ppm) to H-2β (δ 4.51 ppm), H-2β (δ 4.51 ppm) to H-2α (δ 5.67 ppm), H-2β (δ 4.51 ppm) to H-6 (δ 4.30 ppm), H-6 (δ 4.30 ppm) to H-7β (δ 1.41 ppm), H-2α (δ 5.67 ppm) to H-14 (δ 2.93 ppm), H-14 (δ 2.93 ppm) to H-15 (δ 2.20 ppm), H-15 (δ 2.20 ppm) to H-14 (δ 2.93 ppm).

An NOE observed between H-2α and H-14 confirms the R relative stereochemistry for the C-14 at the epoxide functionality. The absence of an NOE between H-6 and H-15 supports the R relative stereochemistry assignment at C-6.

5. Compound 100

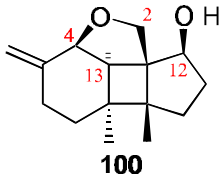

100

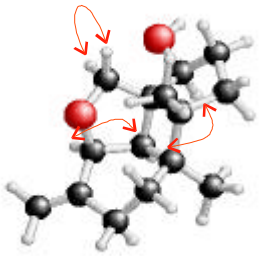

1D-proton difference NOE experiments were conducted. The T^1 relaxation times for the protons involved in the experiment were calculate via inverse recovery experiments. The mixing times for the NOE experiments were maximized in other to observe maximum NOE to about 2/3 of the T^1 relaxation measured.

Observed NOEs: H-2α (δ 4.05 ppm) to H-2β (δ 3.69 ppm), H-2β (δ 3.69 ppm) to H-2α (δ 4.05 ppm), H-4 (δ 4.10 ppm) to H-13 (δ 2.11 ppm), H-13 (δ 2.11 ppm) to H-4 (δ 4.10 ppm), H-12 (δ 4.08 ppm) to H-13 (δ 2.11 ppm), H-13 (δ 2.11 ppm) to H-12 (δ 4.08 ppm).

An NOE observed between H-12 and H-13, which was absent on compound **91**, confirms the S relative stereochemistry assignment for C-12.

- *Results of NOE experiments Chapter 4*

1. Compound 112

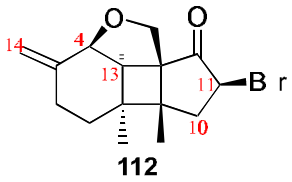

112

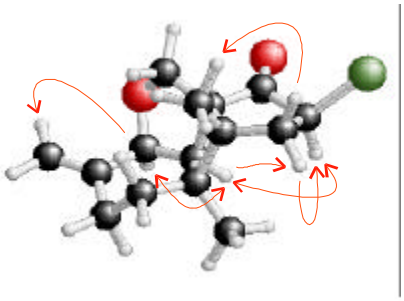

1D-proton difference NOE experiments were conducted. The T^1 relaxation times for the protons involved in the experiment were calculate via inverse recovery experiments. The mixing times for the NOE experiments were maximized in other to observe maximum NOE to about 2/3 of the T^1 relaxation measured.

Observed NOEs: H-4 (δ 4.16 ppm) to H-14 (δ 5.14 ppm), H-4 (δ 4.16 ppm) to H-13 (δ 2.39 ppm), H-13 (δ 2.39 ppm) to H-4 (δ 4.16 ppm), H-13 (δ 2.39 ppm) to H-10α (δ 1.98 ppm), H-13 (δ 2.39 ppm) to H-11 (δ 4.83 ppm), H-11 (δ 4.83 ppm) to H-13 (δ 2.39 ppm), H-10α (δ 1.98 ppm) to H-11 (δ 4.83 ppm), H-10β (δ 3.06 ppm) to H-16 (δ 1.23 ppm).

An NOE observed between H-3 and H-11, which was not seen for compound **124**, confirms the S relative stereochemistry assignment for C-11. This assignment is further supported by the observation of NOEs between H-10α and H-13 and between H-10α and H-11.

2. Compound 121

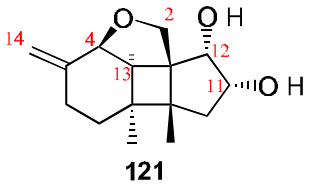

121

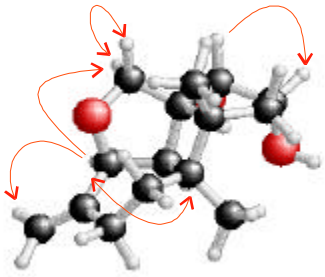

1D-proton difference NOE experiments were conducted. The T^1 relaxation times for the protons involved in the experiment were calculate via inverse recovery experiments. The mixing times for the NOE experiments were maximized in other to observe maximum NOE to about 2/3 of the T^1 relaxation measured.

NOEs observed: H-2α (δ 4.01 ppm) to H-2β (δ 3.58 ppm), H-2β (δ 3.58 ppm) to H-2α (δ 4.01 ppm), H-4 (δ 4.03 ppm) to H-2α (δ 4.01 ppm), H-4 (δ 4.03 ppm) to H-14 (δ 5.09 ppm), H-4 (δ 4.03 ppm) to H-13 (δ 2.64 ppm), H-13 (δ 2.64 ppm) to H-4 (δ 4.03 ppm), H-12 (δ 3.86 ppm) to H-11 (δ 4.21 ppm).

An NOE observed between H-11 and H-12 confirms the *cis* relative stereochemistry assigned for the diol and the absence of NOEs between H-13 and H-11 or between H-13 and H-12 supports the S* assignment for C-12 and the R* relative stereochemistry assignment for C-11. These assignments are further supported by comparison with the results for the NOE experiments conducted on the *trans* diol **126**.

3. Compound 122

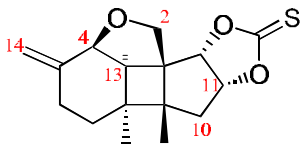

122

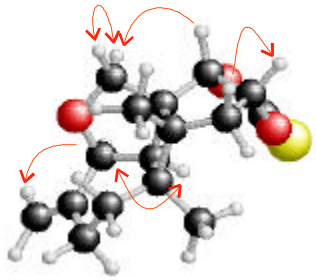

1D-proton difference NOE experiments were conducted. The T^1 relaxation times for the protons involved in the experiment were calculate via inverse recovery experiments. The mixing times for the NOE experiments were maximized in other to observe maximum NOE to about 2/3 of the T^1 relaxation measured.

NOEs observed: H-2α (δ 4.12 ppm) to H-2β (δ 3.42 ppm), H-2β (δ 3.42 ppm) to H-2α (δ 4.12 ppm), H-4 (δ 4.14 ppm) to H-14 (δ 5.18 ppm), H-4 (δ 4.14 ppm) to H-13 (δ 2.31 ppm), H-13 (δ 2.31 ppm) to H-4 (δ 4.14 ppm), H-10β (δ 1.85 ppm) to H-11 (δ 5.10 ppm), H-12 (δ 4.81 ppm) to H-2α (δ 4.12 ppm).

An NOE observed between H-2 and H-12 confirms the S relative stereochemistry assigned for C-12. The absence of NOEs between H-12 and H-13 and between H-11 and H-13 further supports the assignment.

4. Compound 124

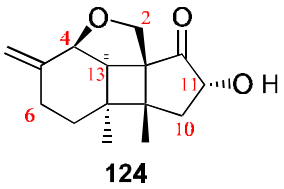

124

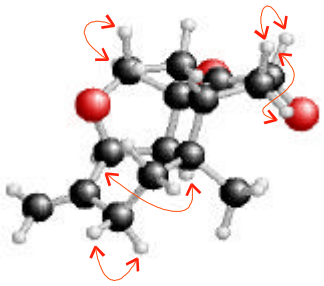

A 2D-proton-proton NOESY experiment was conducted on compound **124**. NOEs reported are those corresponding to the cross peaks observed on the 2D-experiment.

NOEs observed (cross peaks): H-2α (δ 4.10 ppm) to H-2β (δ 3.79 ppm), H-4 (δ 4.25 ppm) to H-13 (δ 2.64 ppm), H-6α (δ 2.25 ppm) to H-6β (δ 2.53 ppm), H-10β (δ 2.17 ppm) to H-11 (δ 4.23 ppm), H-10α (δ 2.20 ppm) to H-10β (δ 2.17 ppm).

The absence of a cross peak between H-11 and H-13 supports the R relative stereochemistry assignment at C-11. This assignment was further supported by comparison with the results obtained for compound **112**.

5. Compound 126

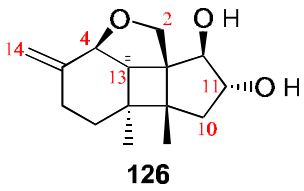

126

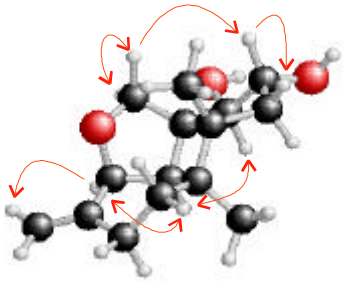

1D-proton difference NOE experiments were conducted. The T^1 relaxation times for the protons involved in the experiment were calculate via inverse recovery experiments. The mixing times for the NOE experiments were maximized in other to observe maximum NOE to about 2/3 of the T^1 relaxation measured.

Observed NOEs: H-2α (δ 3.73 ppm) to H-2β (δ 4.05 ppm), H-2β (δ 4.05 ppm) to H-2α (δ 3.73 ppm), H-2β (δ 4.05 ppm) to H-11 (δ 4.19 ppm), H-4 (δ 4.07 ppm) to H-13 (δ 2.51 ppm), H-13 (δ 2.51 ppm) to H-4 (δ 4.07 ppm), H-11 (δ 4.19 ppm) to H-10β (δ 1.88 ppm), H-12 (δ 4.03 ppm) to H-13 (δ 2.51 ppm), H-13 (δ 2.51 ppm) to H-12 (δ 4.03 ppm), H-4 (δ 4.07 ppm) to H-14 (δ 5.09 ppm).

An NOE observed between H-2β and H-11 confirms the R relative stereochemistry assignment at C-11 and an NOE observed between H-12 and H-13 confirms the R relative stereochemistry assignment at C-12. These assignments are further supported by comparison with the results obtained for compound **121**.

ADDENDUM II: SELECTED ^{13}C NMR SPECTRA

Note:

^{13}C NMR data was processed with *Felix* version 95.0 NMR data processing program, from Biosym Technologies Inc., on a Silicon Graphics *Indigo* R3000 workstation, running Irix version 5.3 as the operating system.

X-Axis = *ppm* downfield from TMS

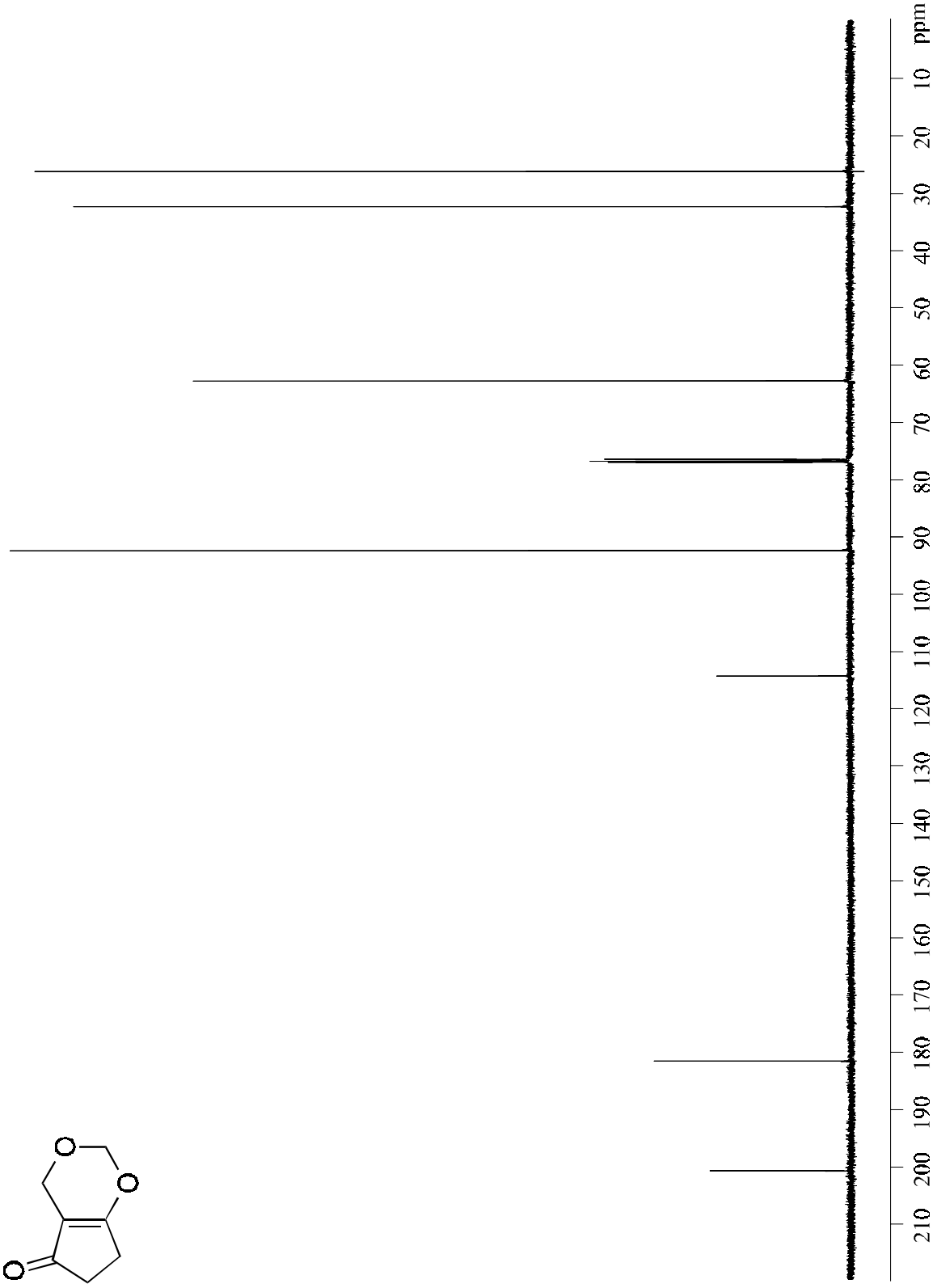
ppm
10
20
30
40
50
60
70
80
90
100
110
120
130
140
150
160
170
180
190
200
210

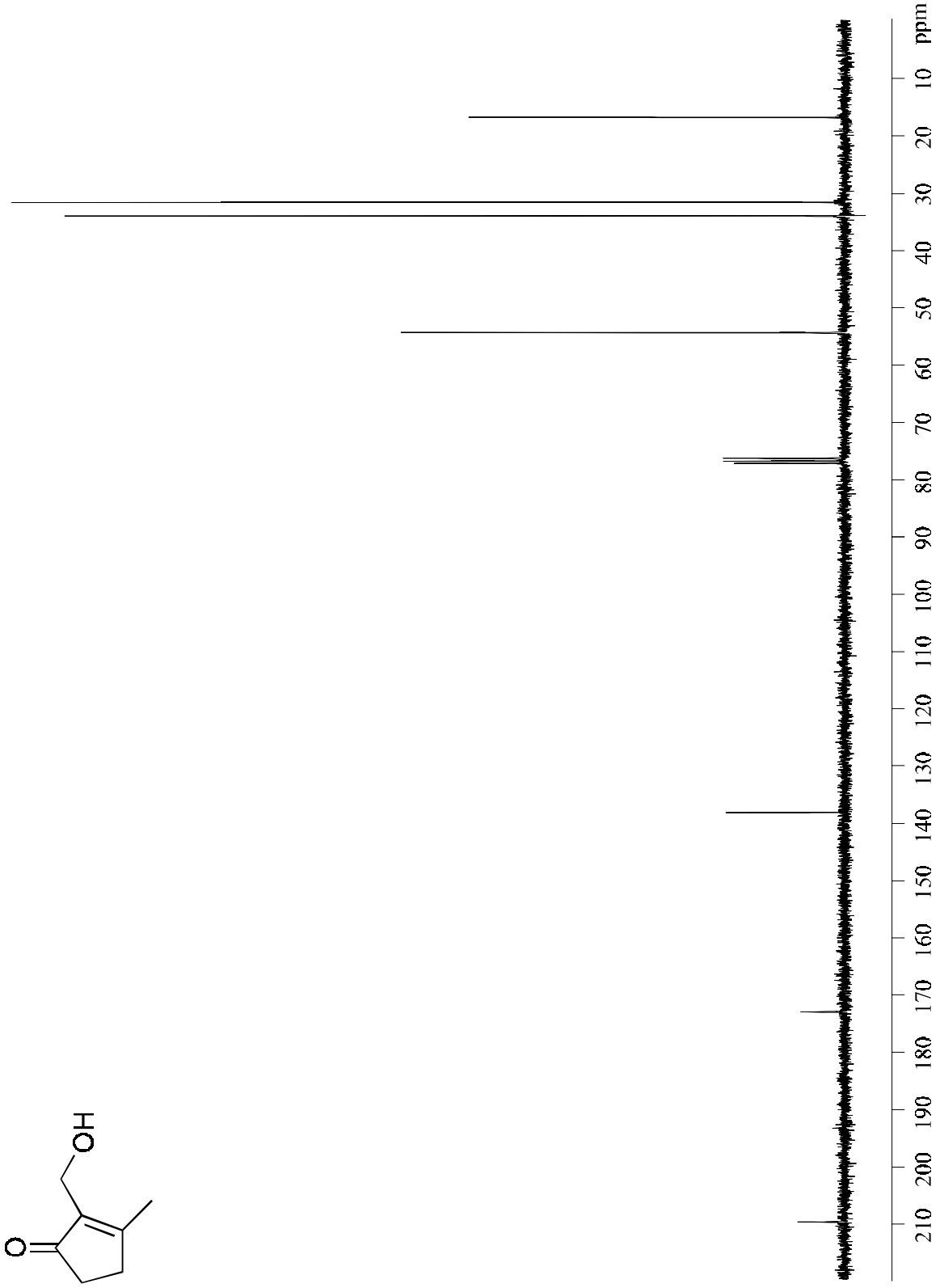
ppm
10
20
30
40
50
60
70
80
90
100
110
120
130
140
150
160
170
180
190
200
210
OH
O

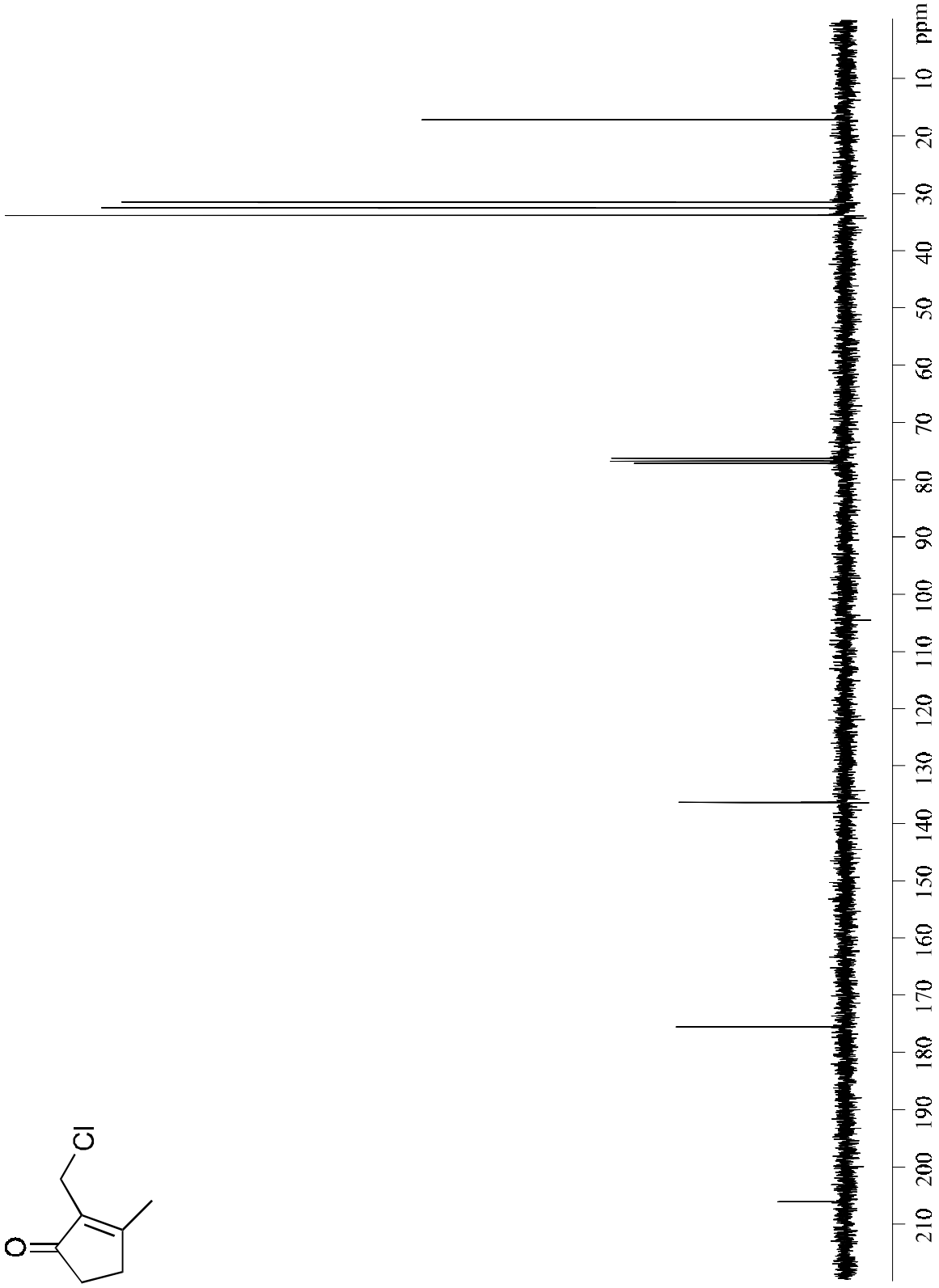
ppm
10
20
30
40
50
60
70
80
90
100
110
120
130
140
150
160
170
180
190
200
210
Cl
O

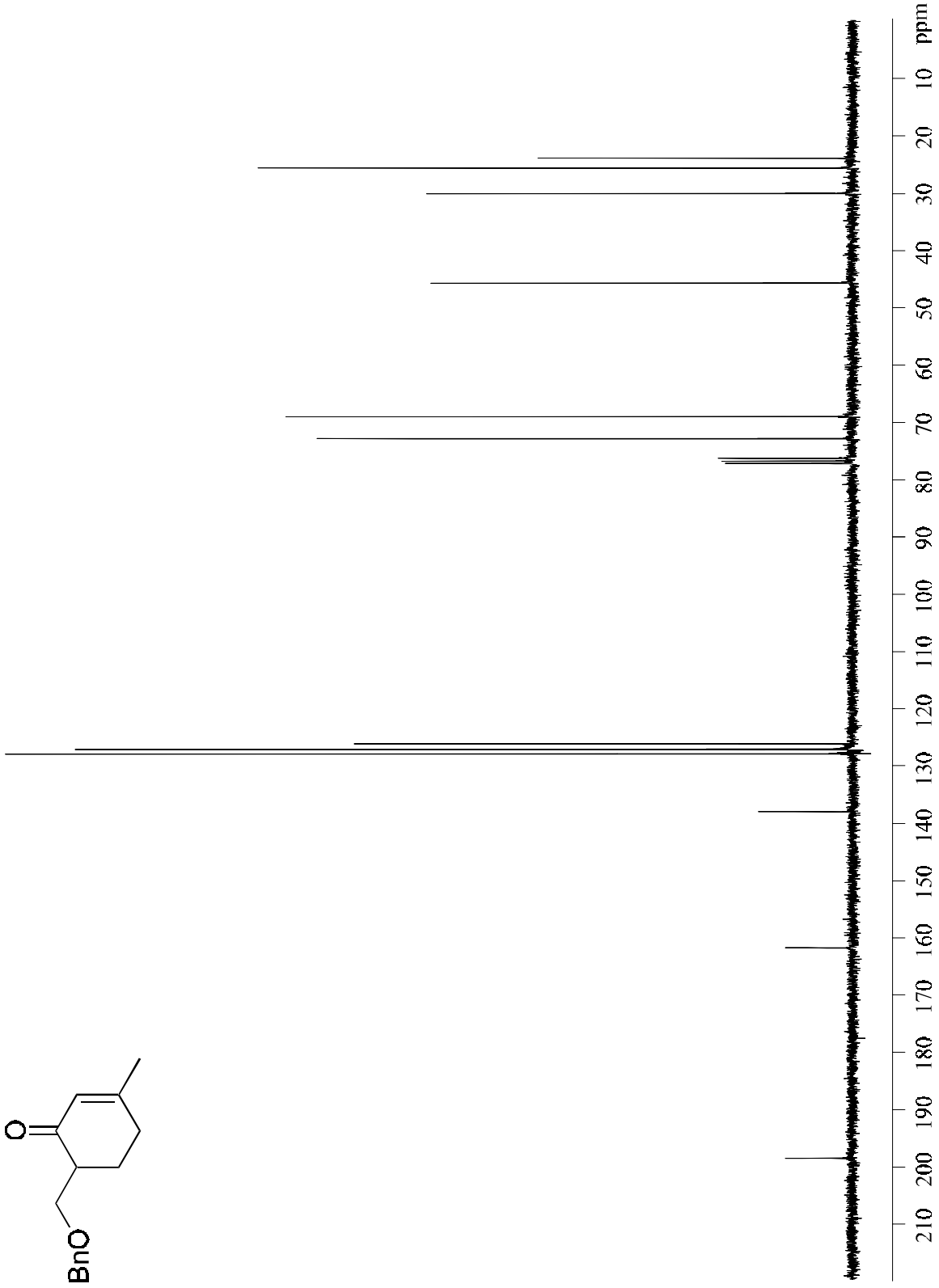
ppm
10
20
30
40
50
60
70
80
90
100
110
120
130
140
150
160
170
180
190
200
210
O
BnO

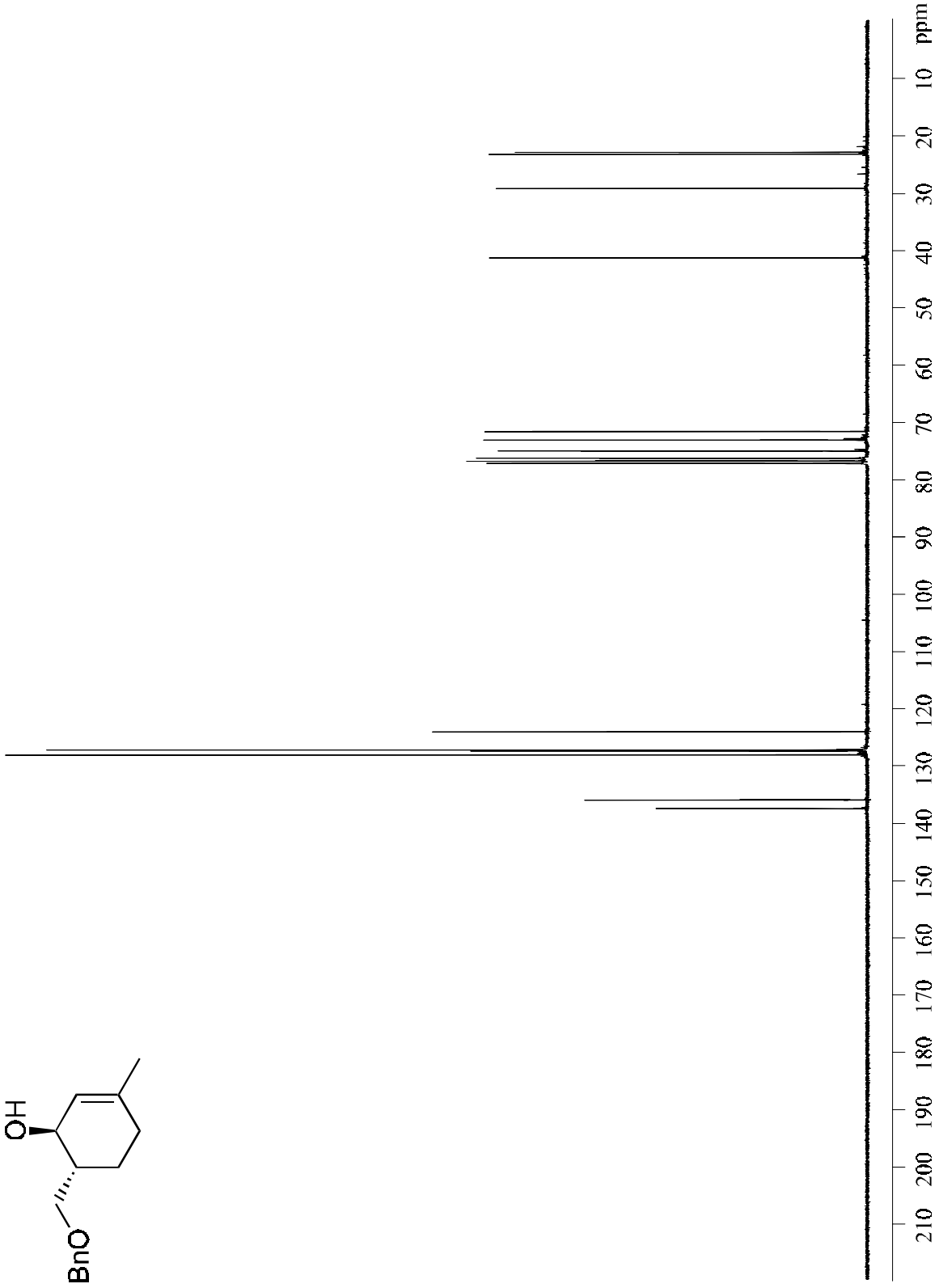
ppm
10
20
30
40
50
60
70
80
90
100
110
120
130
140
150
160
170
180
190
200
210
OH
BnO

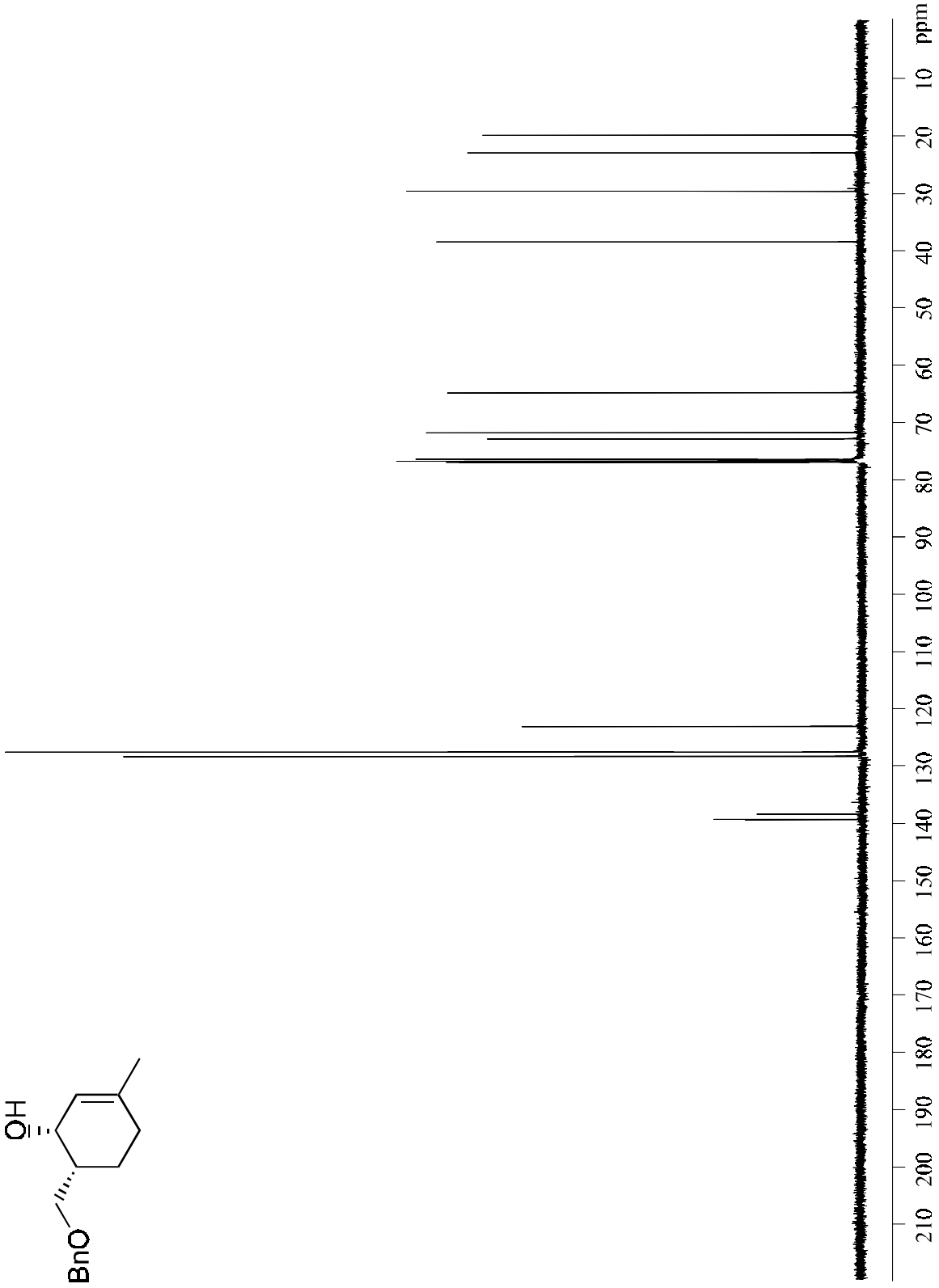
OH
BnO
ppm
10
20
30
40
50
60
70
80
90
100
110
120
130
140
150
160
170
180
190
200
210

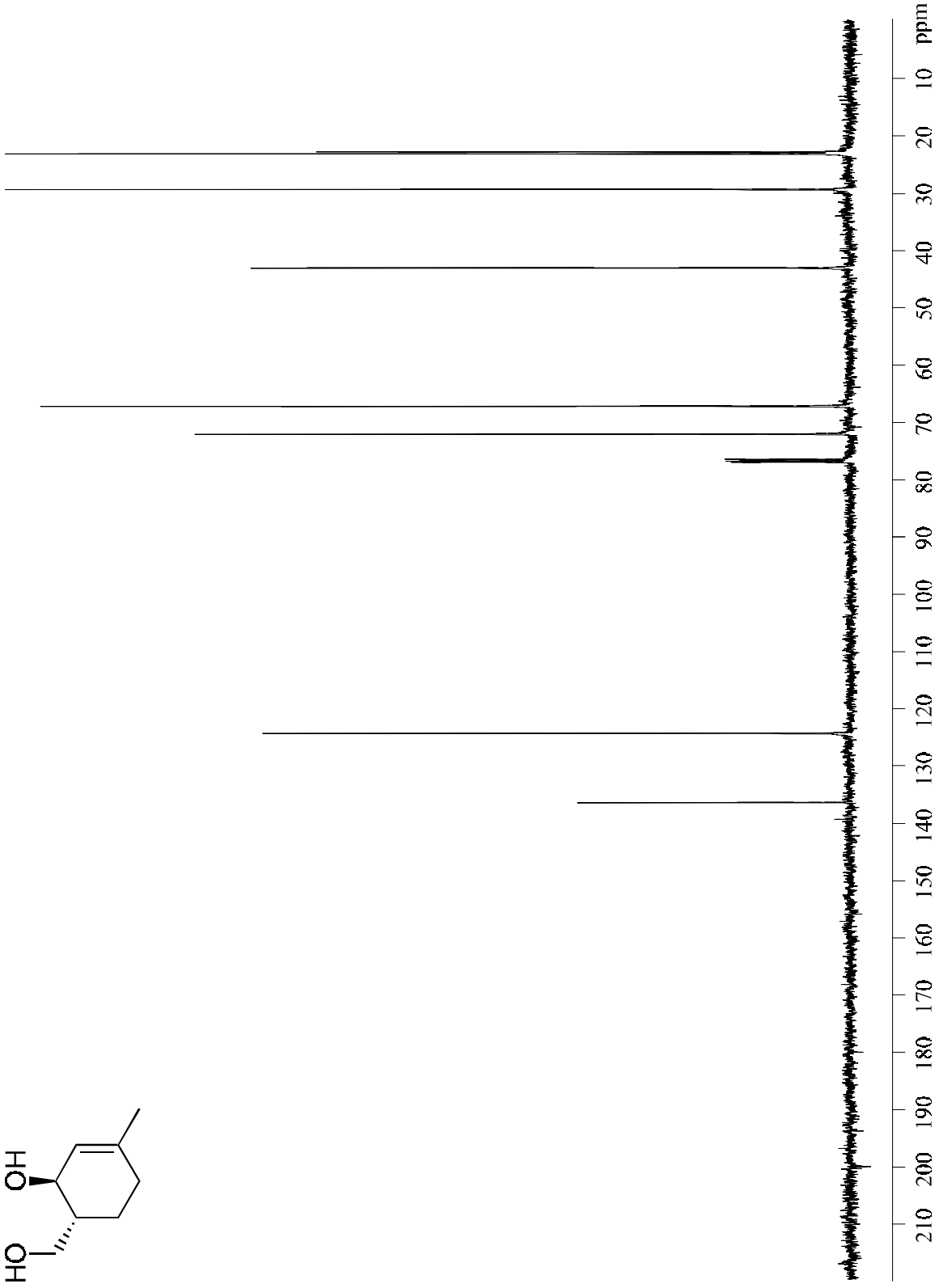
ppm
10
20
30
40
50
60
70
80
90
100
110
120
130
140
150
160
170
180
190
200
210
OH
HO

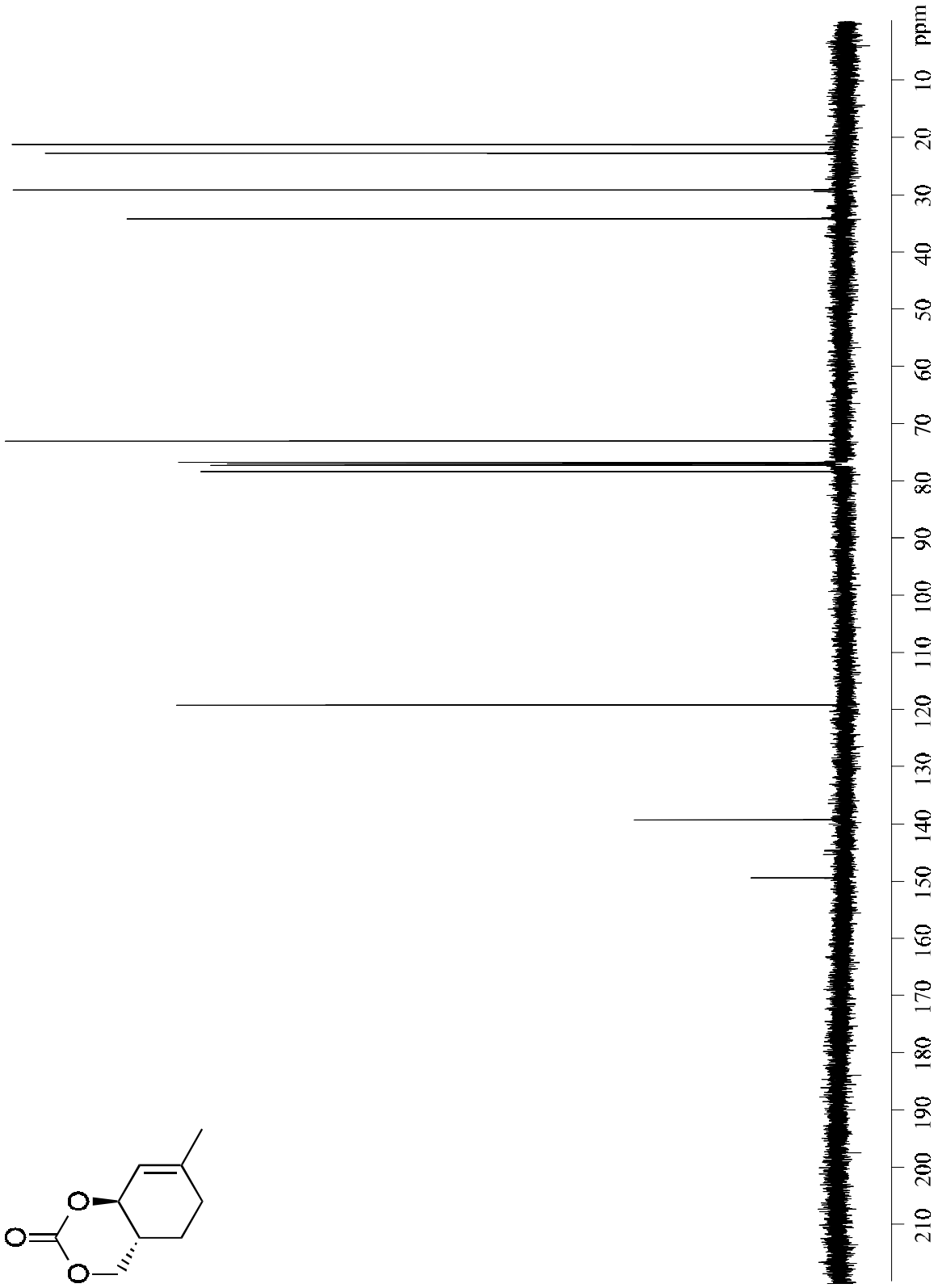
ppm
10
20
30
40
50
60
70
80
90
100
110
120
130
140
150
160
170
180
190
200
210

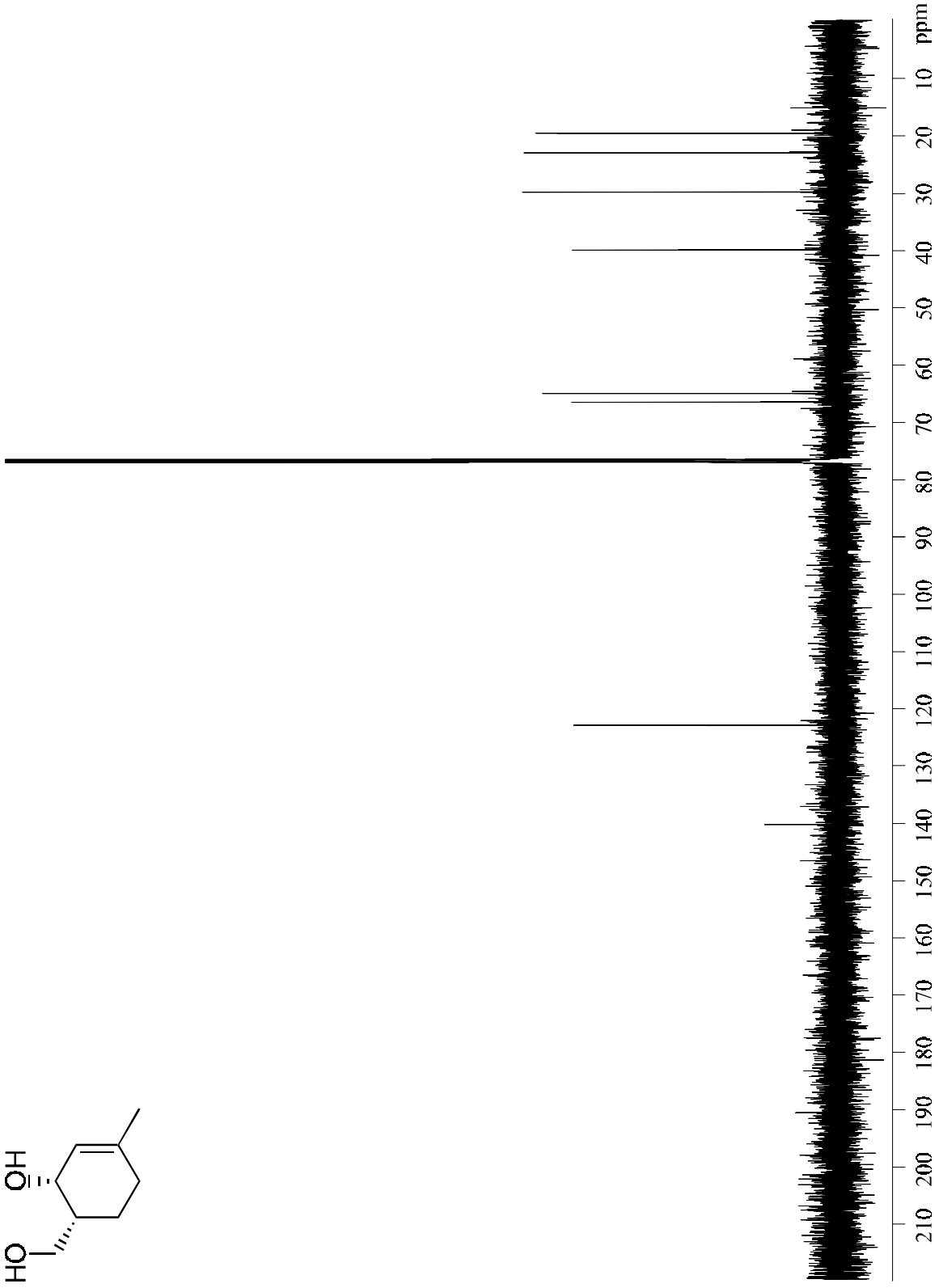
ppm
10
20
30
40
50
60
70
80
90
100
110
120
130
140
150
160
170
180
190
200
210
OH
HO

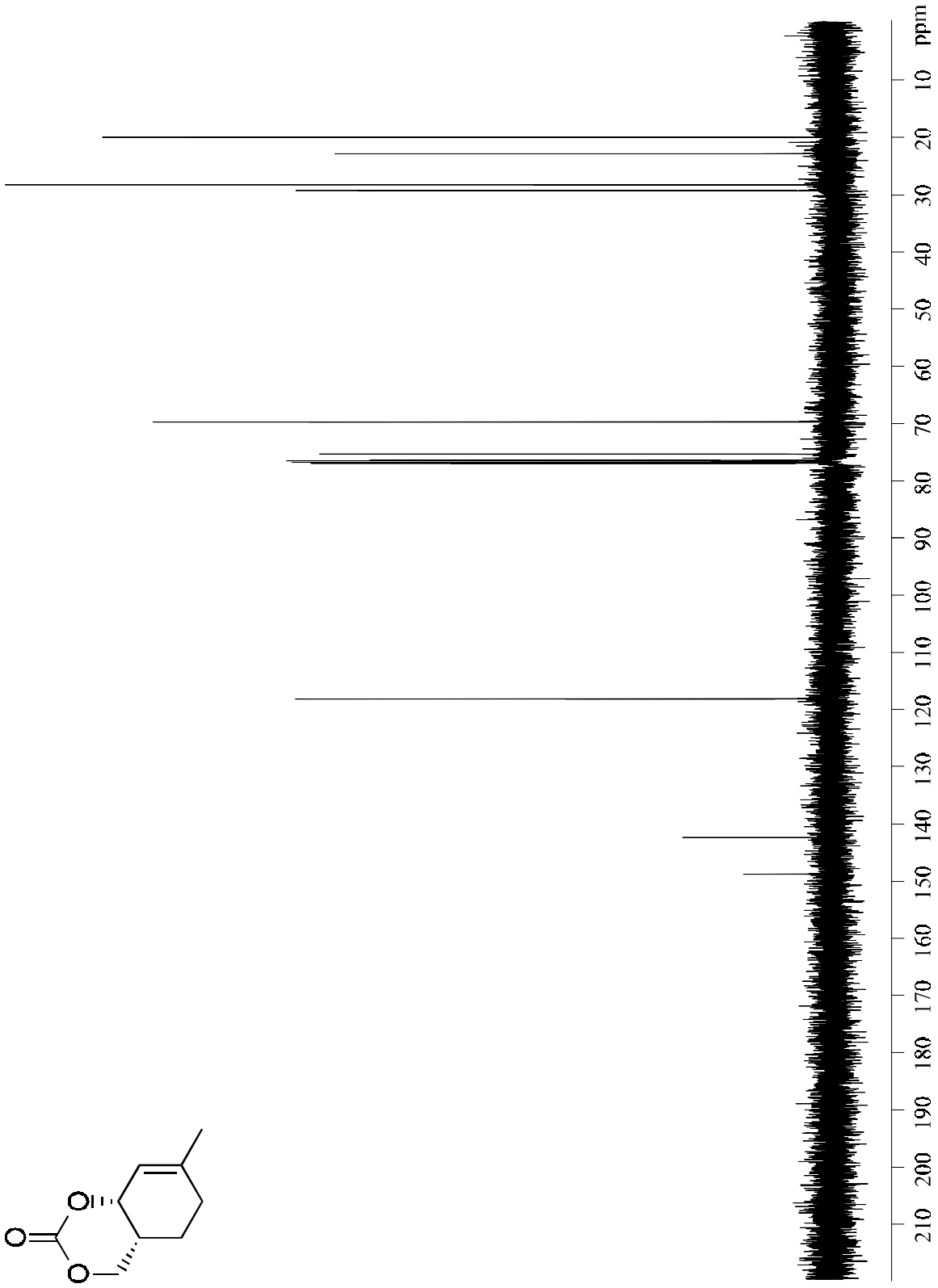
ppm
10
20
30
40
50
60
70
80
90
100
110
120
130
140
150
160
170
180
190
200
210

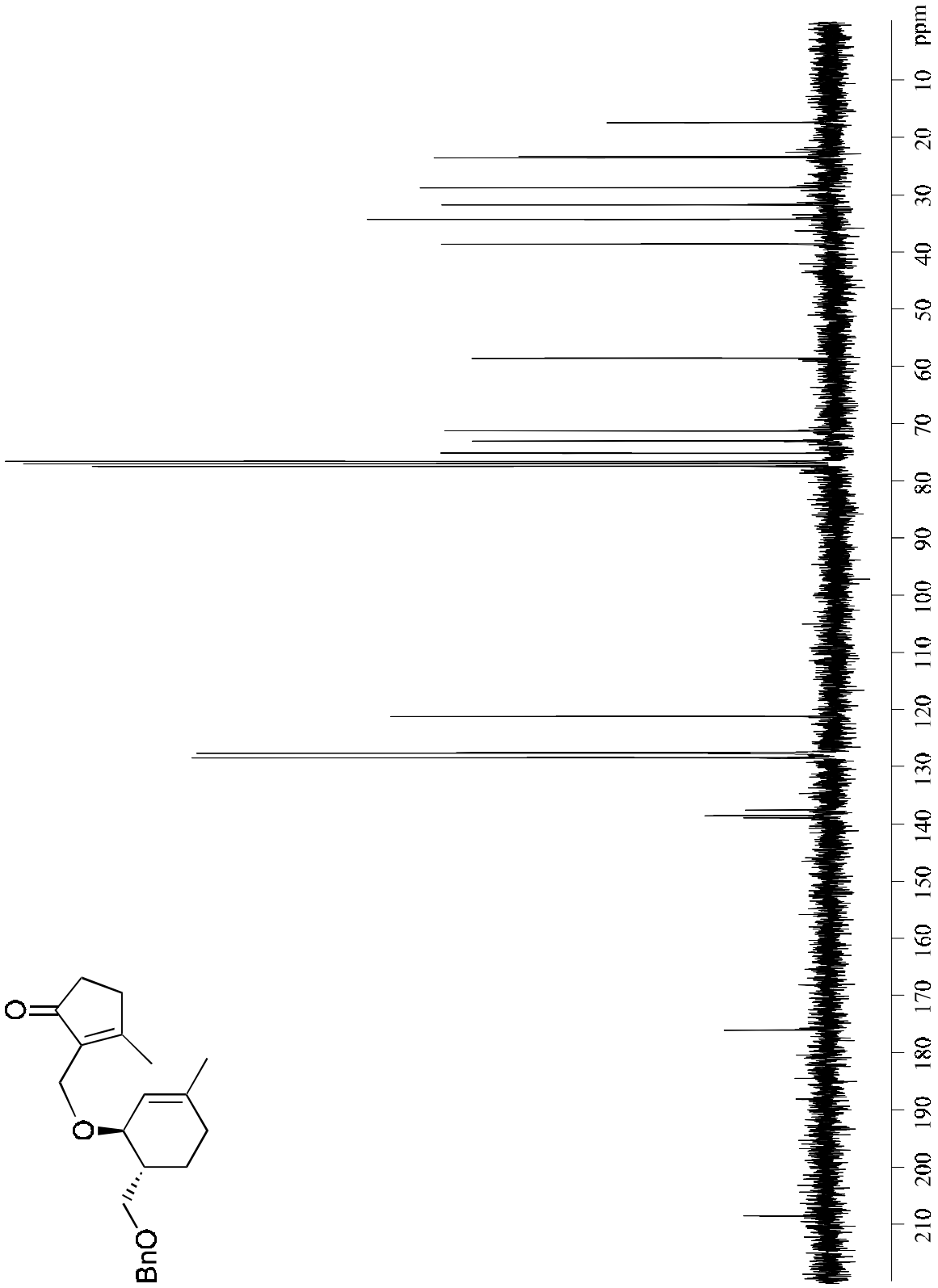
ppm
10
20
30
40
50
60
70
80
90
100
110
120
130
140
150
160
170
180
190
200
210
O
O
BnO

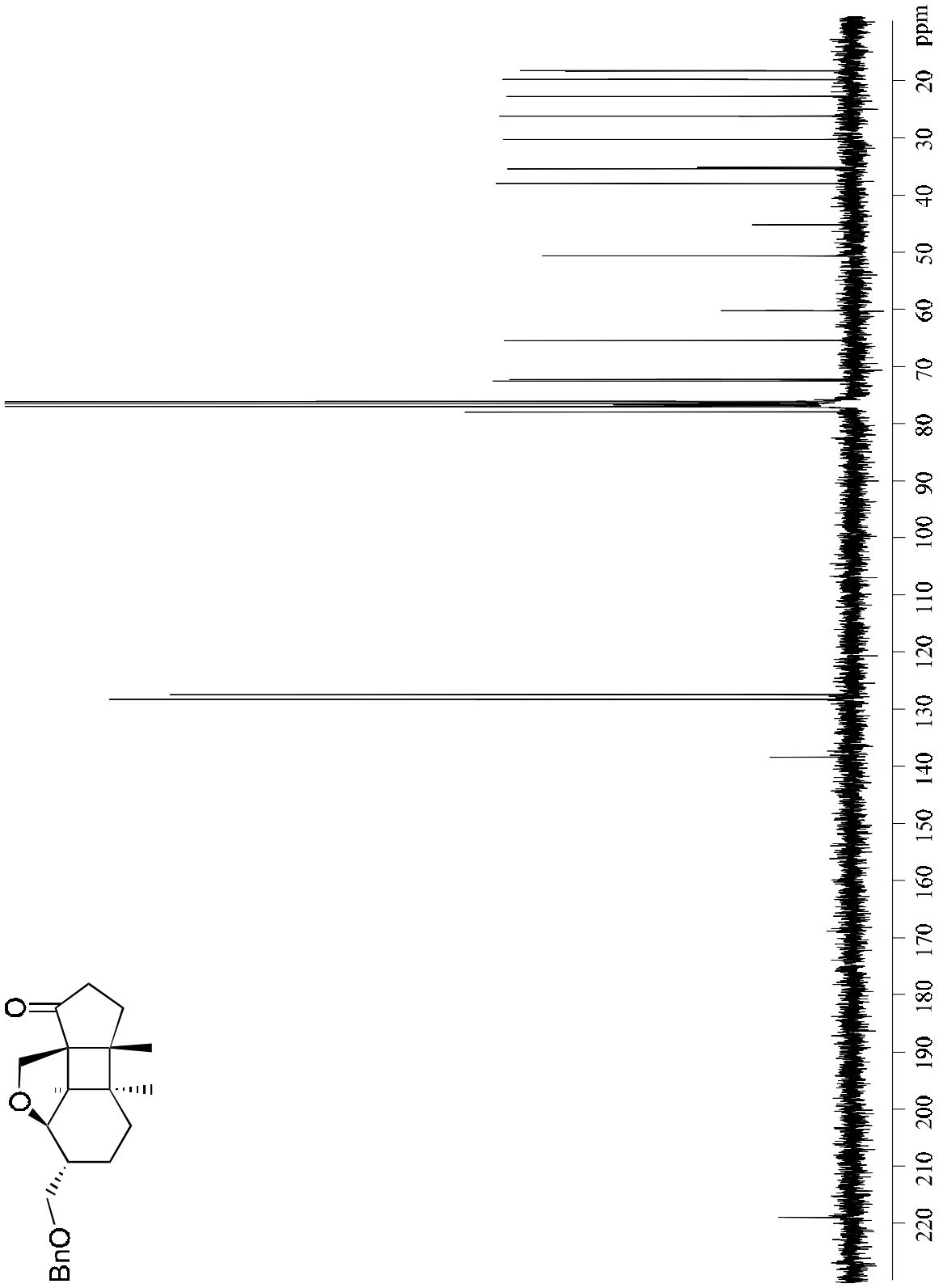
ppm
20
30
40
50
60
70
80
90
100
110
120
130
140
150
160
170
180
190
200
210
220
O
O
BnO

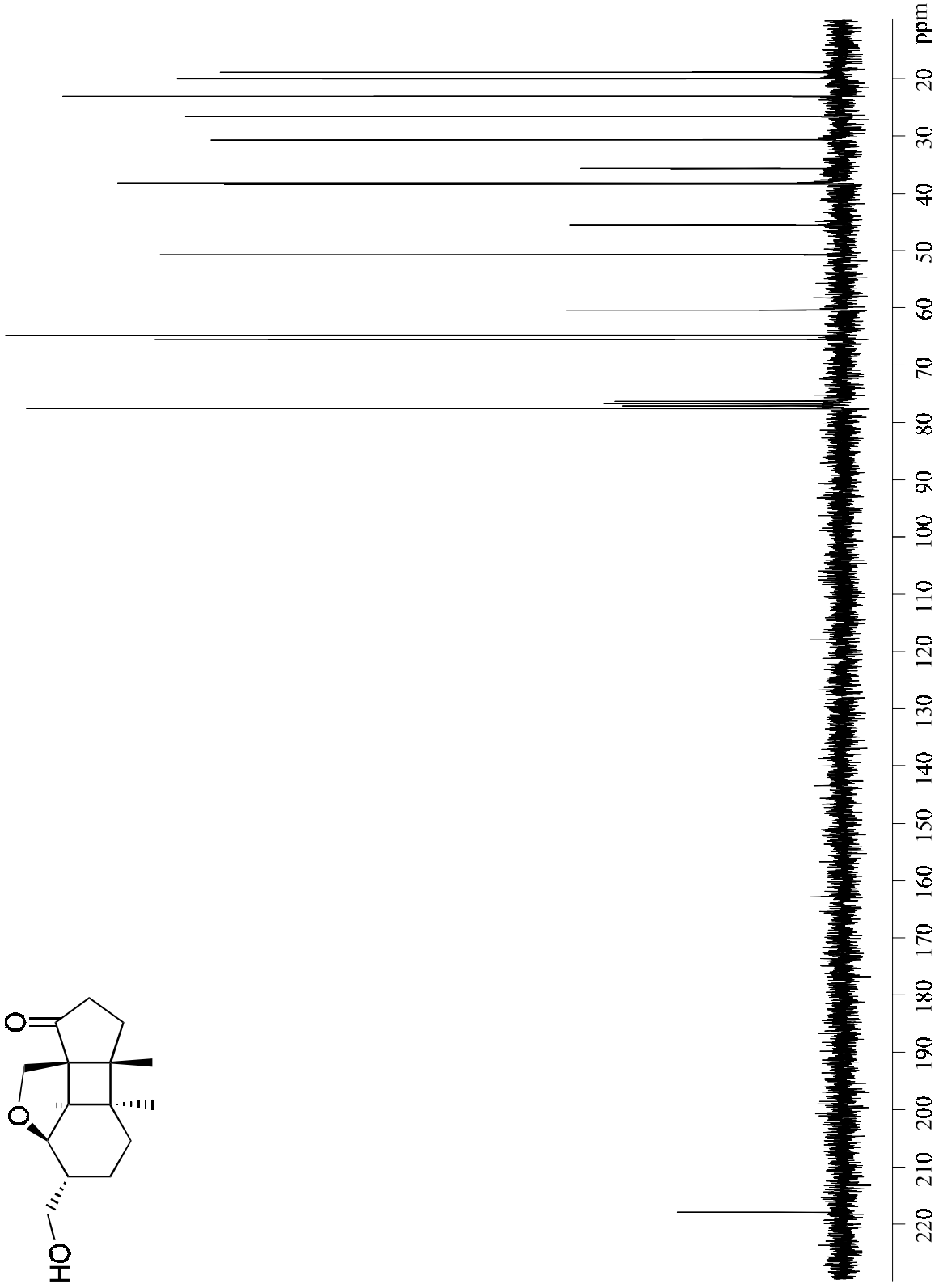
ppm
20
30
40
50
60
70
80
90
100
110
120
130
140
150
160
170
180
190
200
210
220
O
O
HO

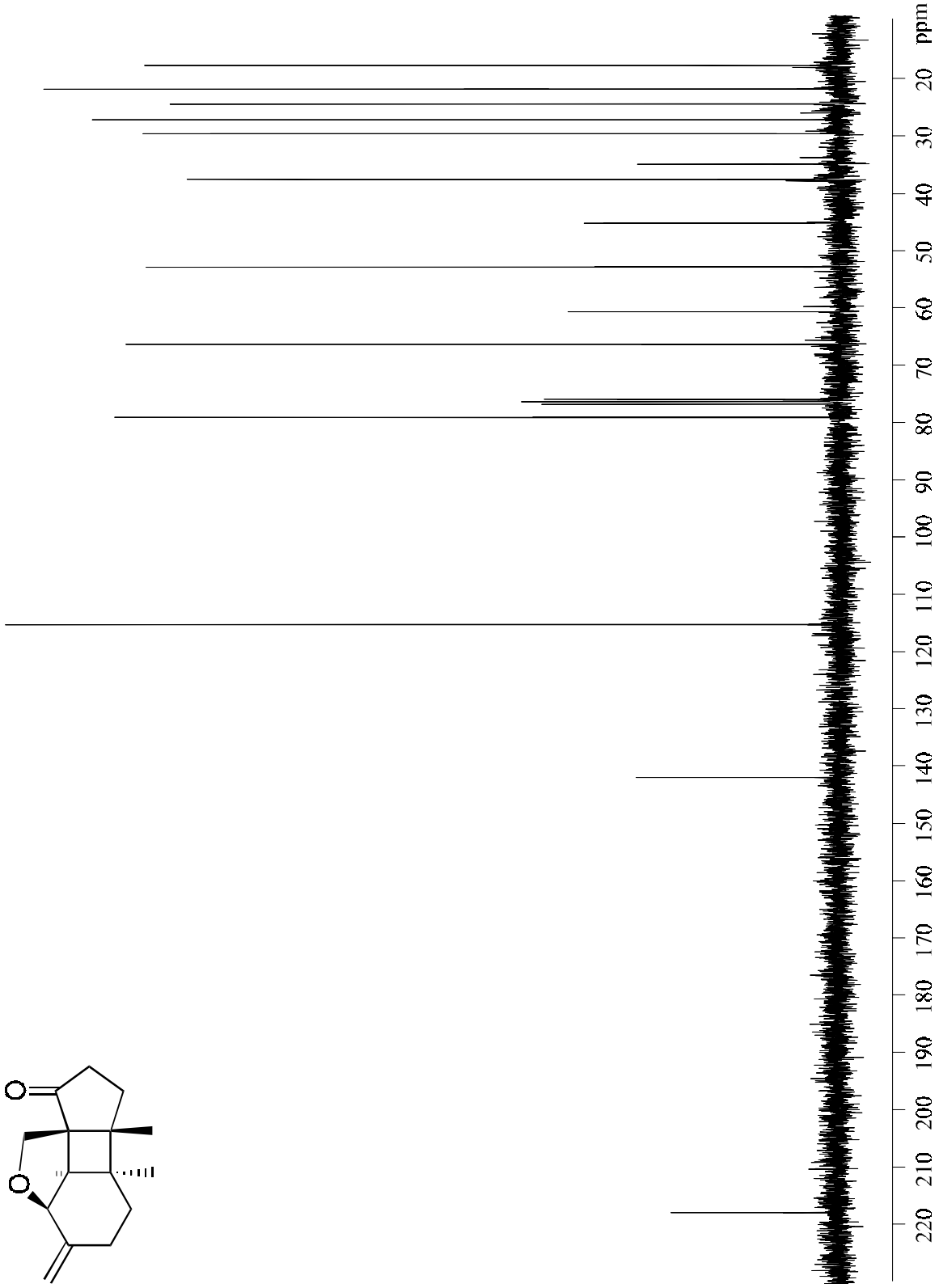
ppm
20
30
40
50
60
70
80
90
100
110
120
130
140
150
160
170
180
190
200
210
220

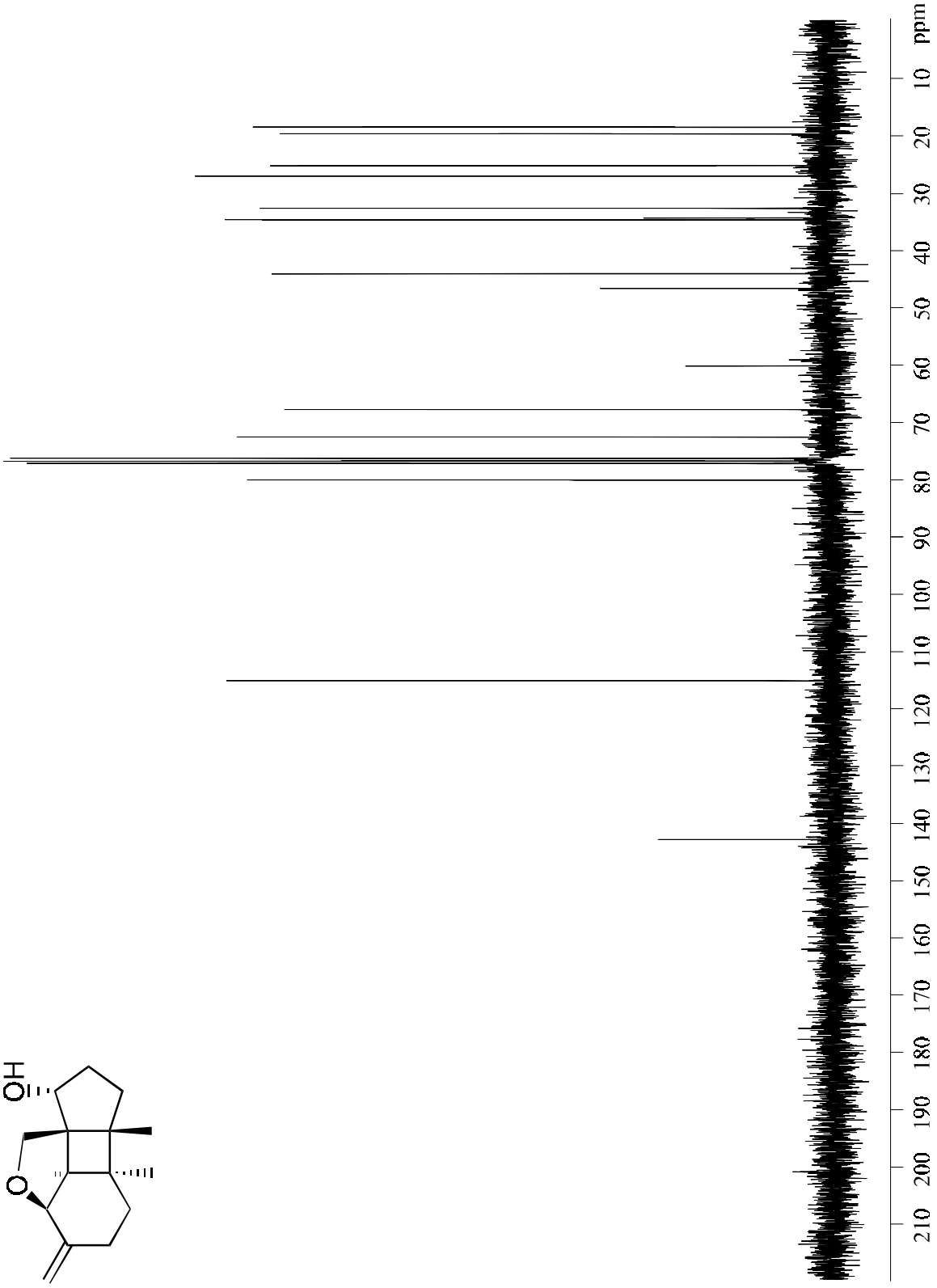
ppm
10
20
30
40
50
60
70
80
90
100
110
120
130
140
150
160
170
180
190
200
210
OH
O

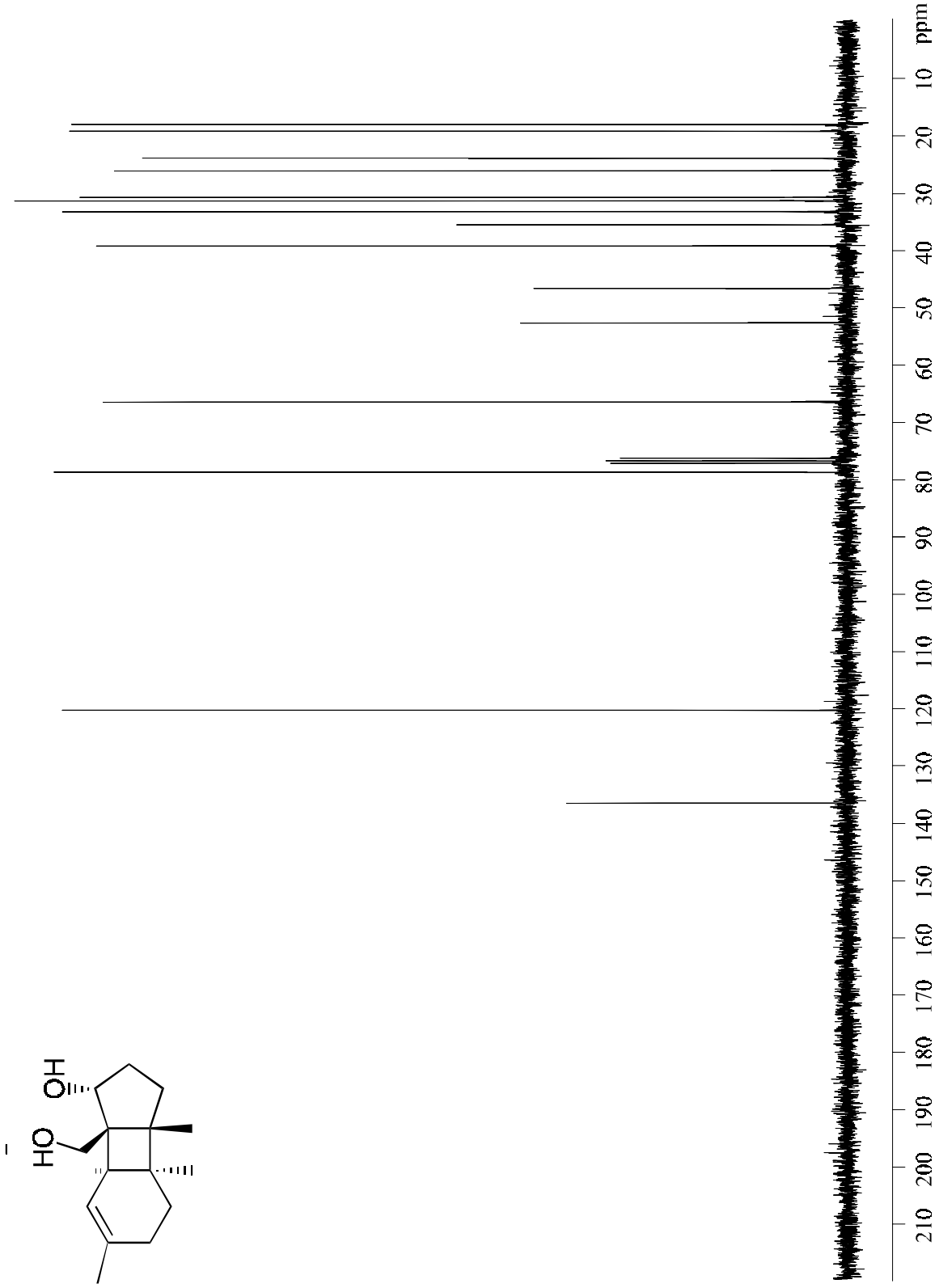
ppm
10
20
30
40
50
60
70
80
90
100
110
120
130
140
150
160
170
180
190
200
210
HO
HO

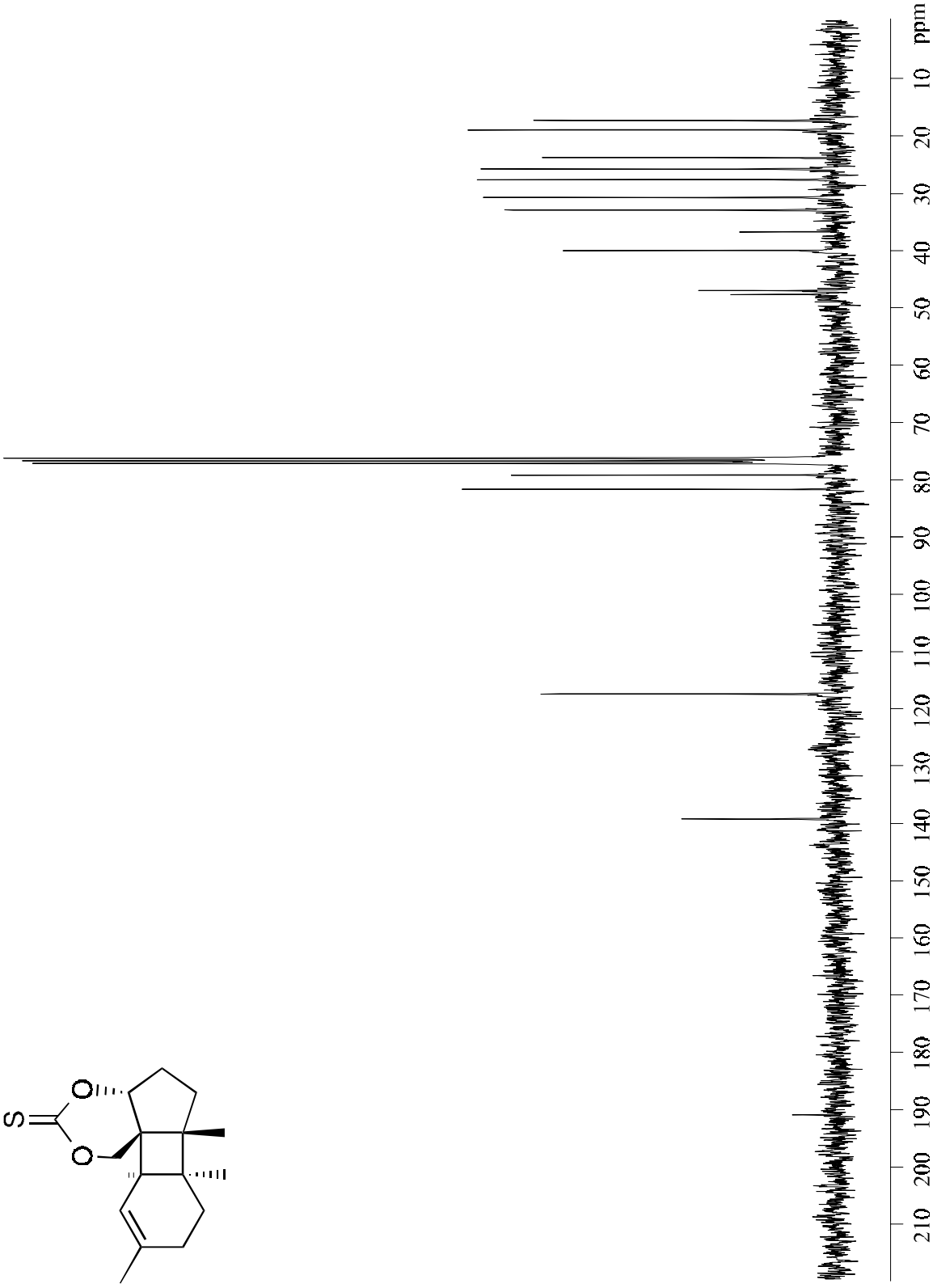
ppm
10
20
30
40
50
60
70
80
90
100
110
120
130
140
150
160
170
180
190
200
210
S
O
O

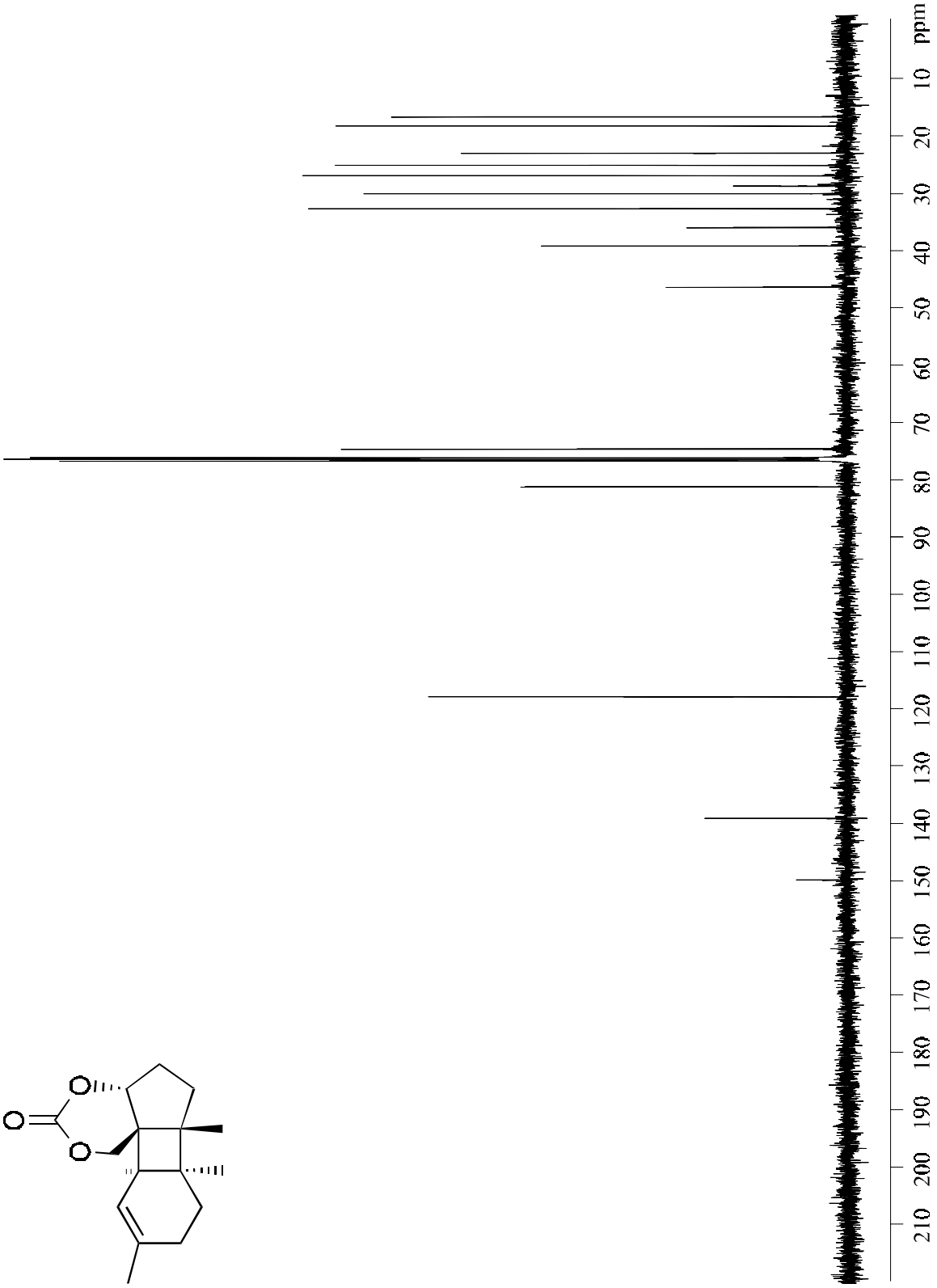
ppm
10
20
30
40
50
60
70
80
90
100
110
120
130
140
150
160
170
180
190
200
210

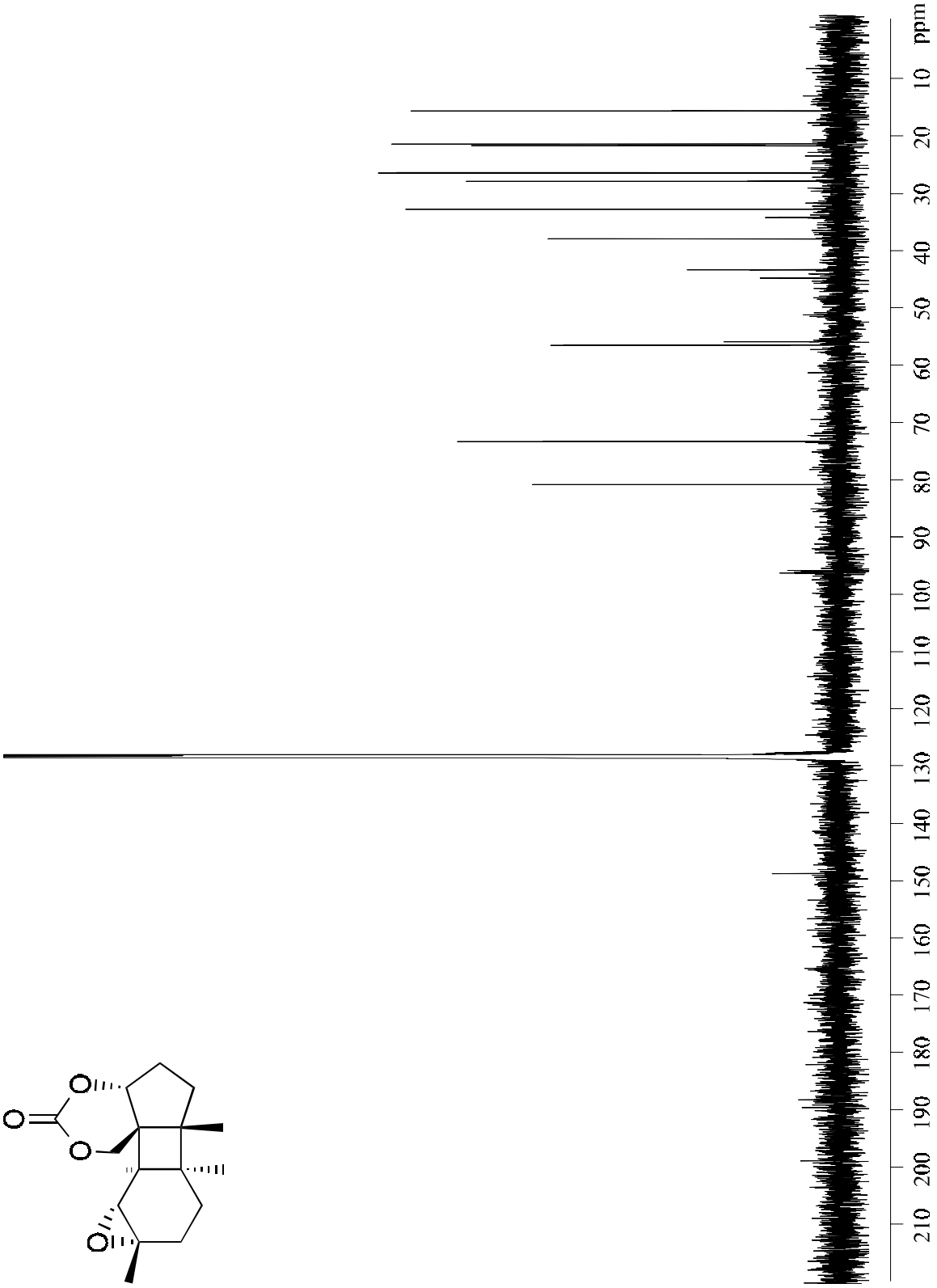
ppm
10
20
30
40
50
60
70
80
90
100
110
120
130
140
150
160
170
180
190
200
210
O
O
O
O

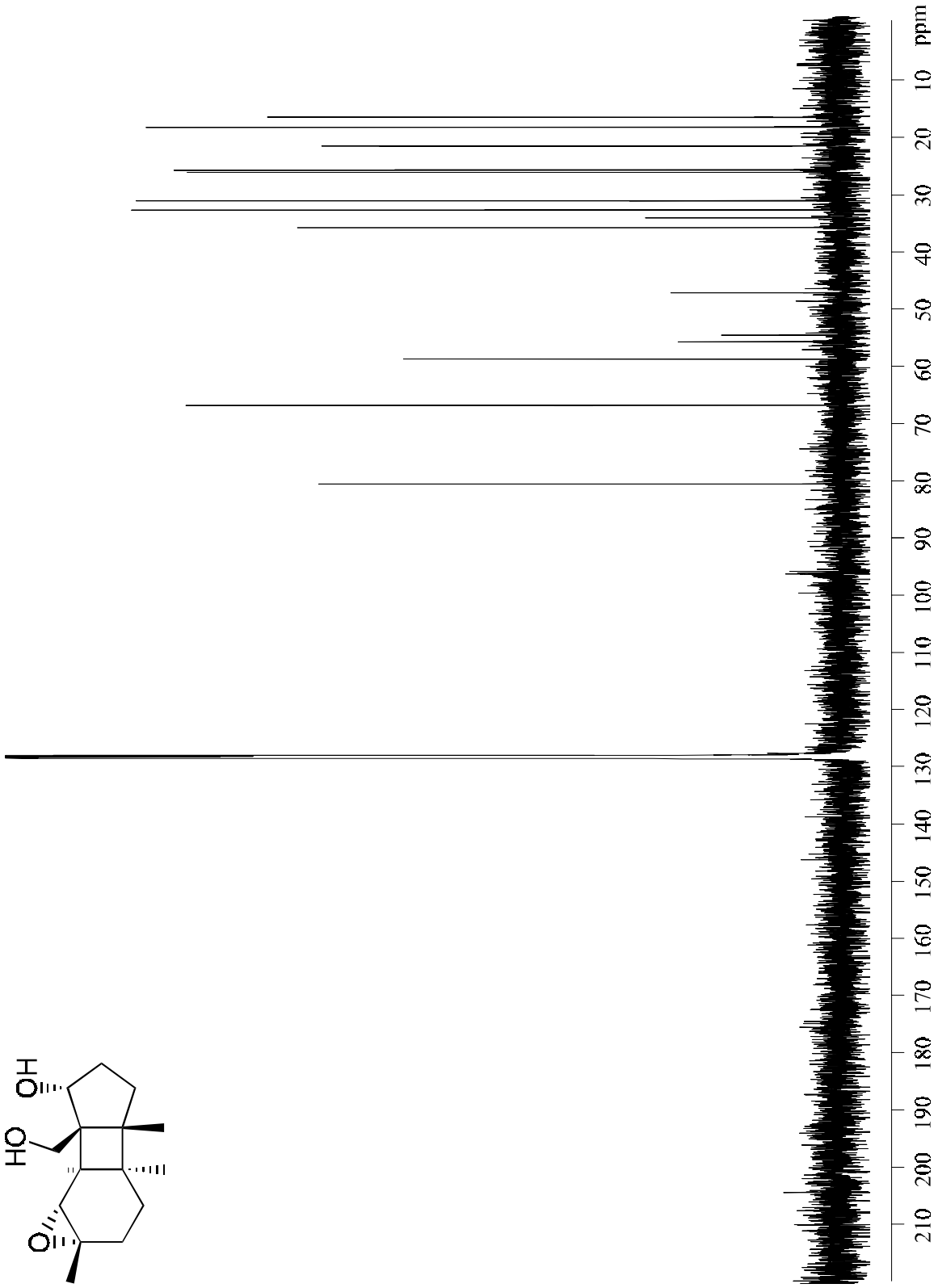
ppm
10
20
30
40
50
60
70
80
90
100
110
120
130
140
150
160
170
180
190
200
210
OH
HO
O

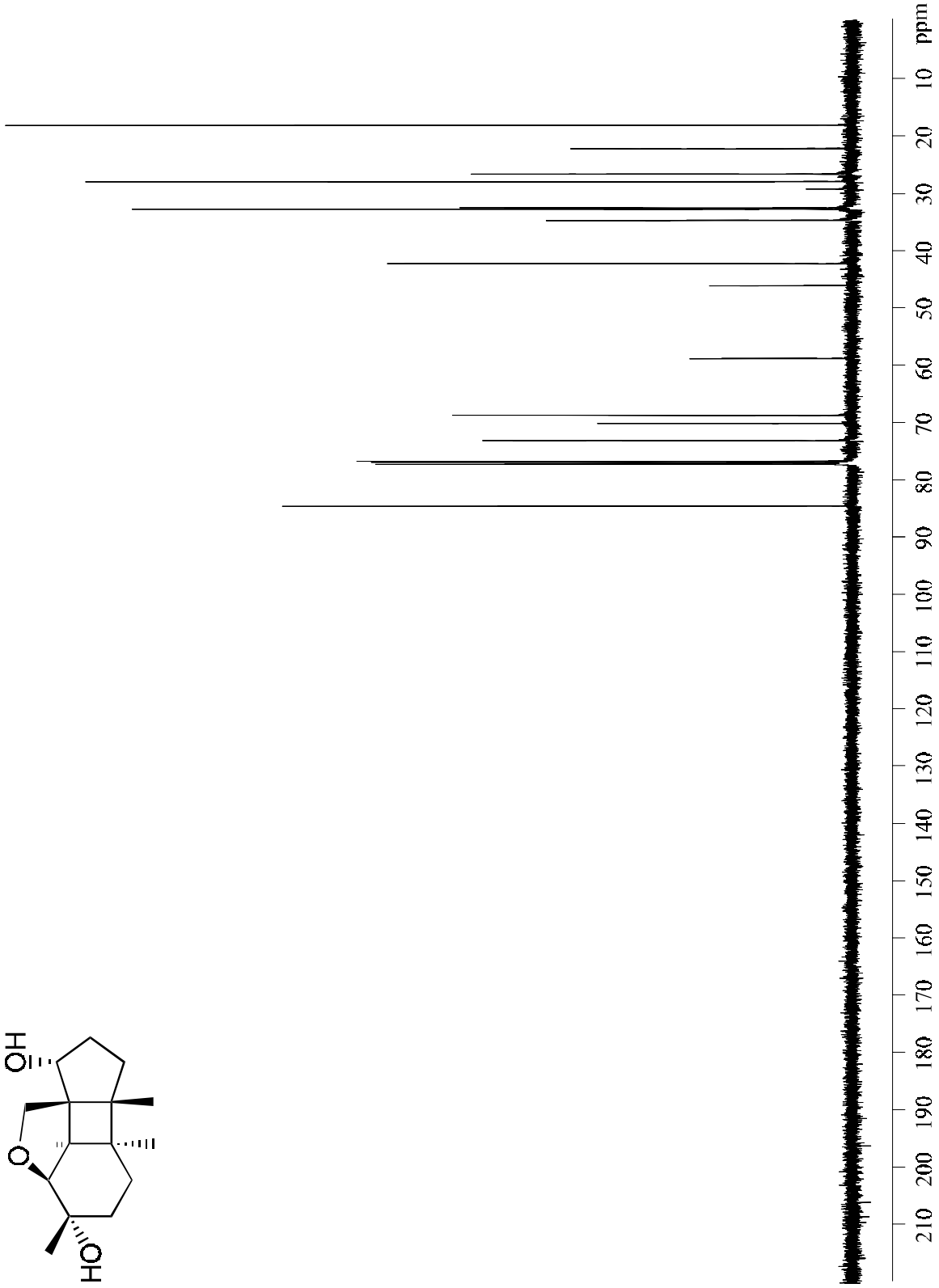
ppm
10
20
30
40
50
60
70
80
90
100
110
120
130
140
150
160
170
180
190
200
210
OH
O
HO

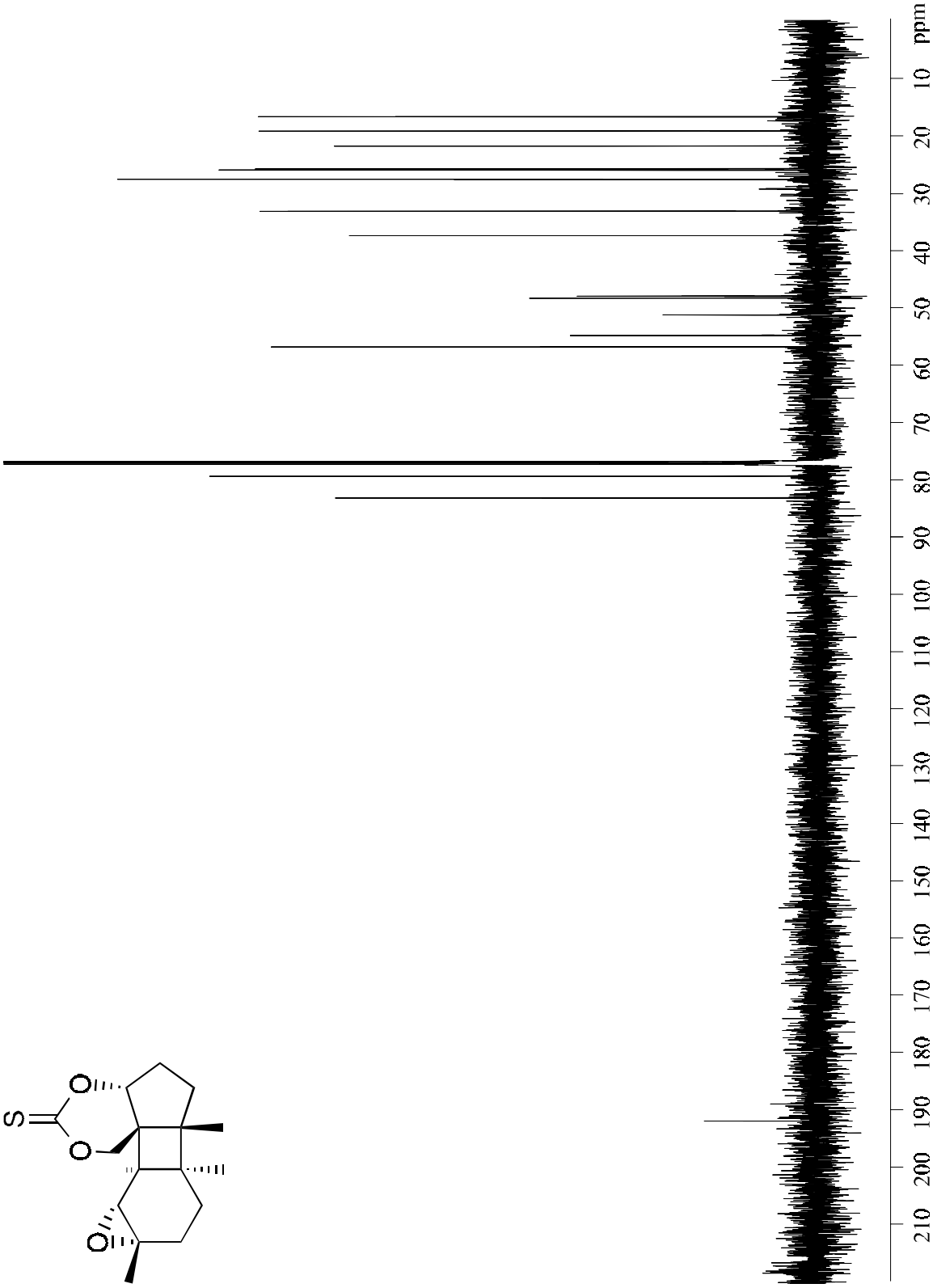
ppm
10
20
30
40
50
60
70
80
90
100
110
120
130
140
150
160
170
180
190
200
210
S
O
O
O

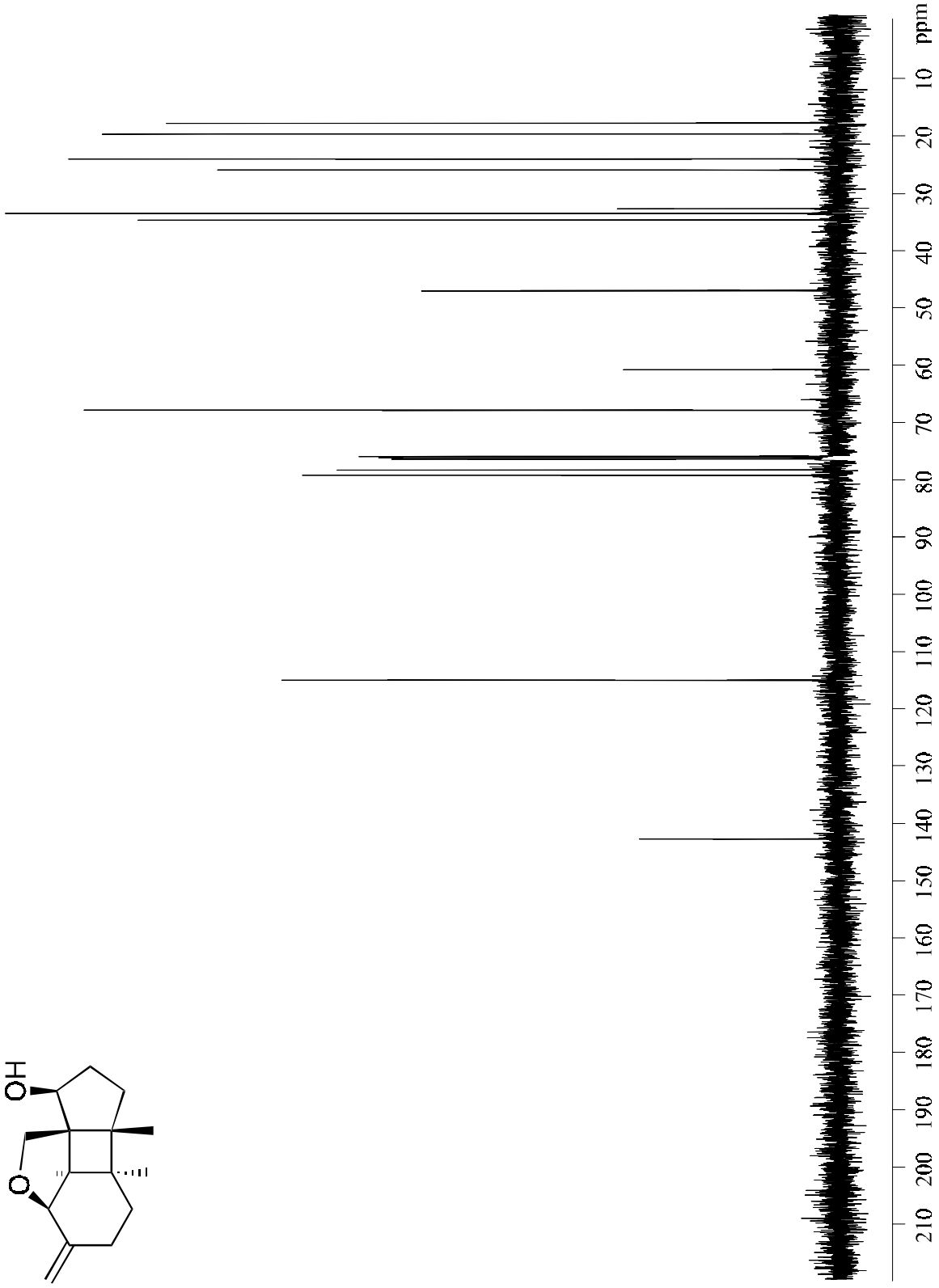
ppm
10
20
30
40
50
60
70
80
90
100
110
120
130
140
150
160
170
180
190
200
210
OH
O

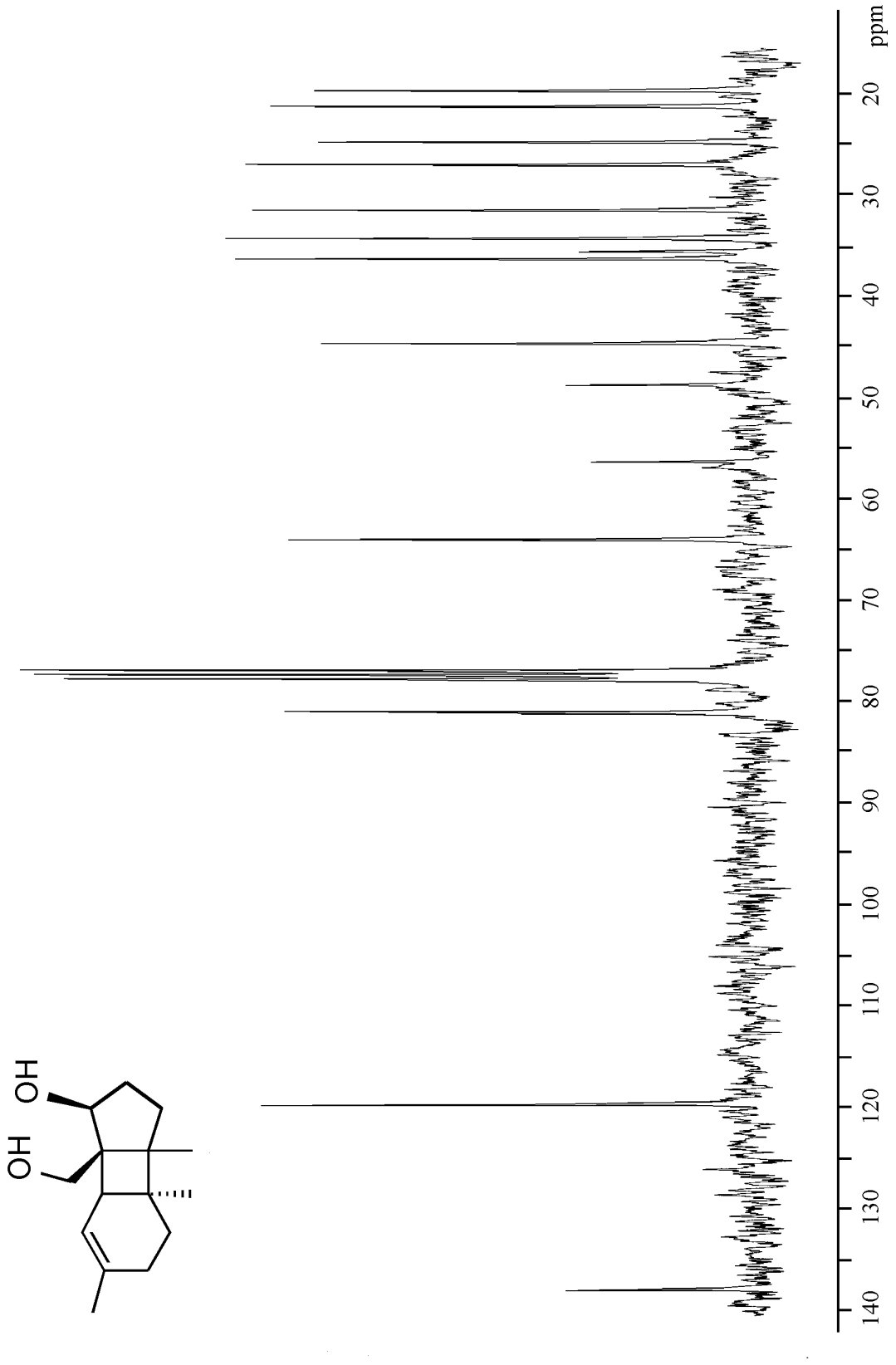
ppm
20
30
40
50
60
70
80
90
100
110
120
130
140
OH
OH

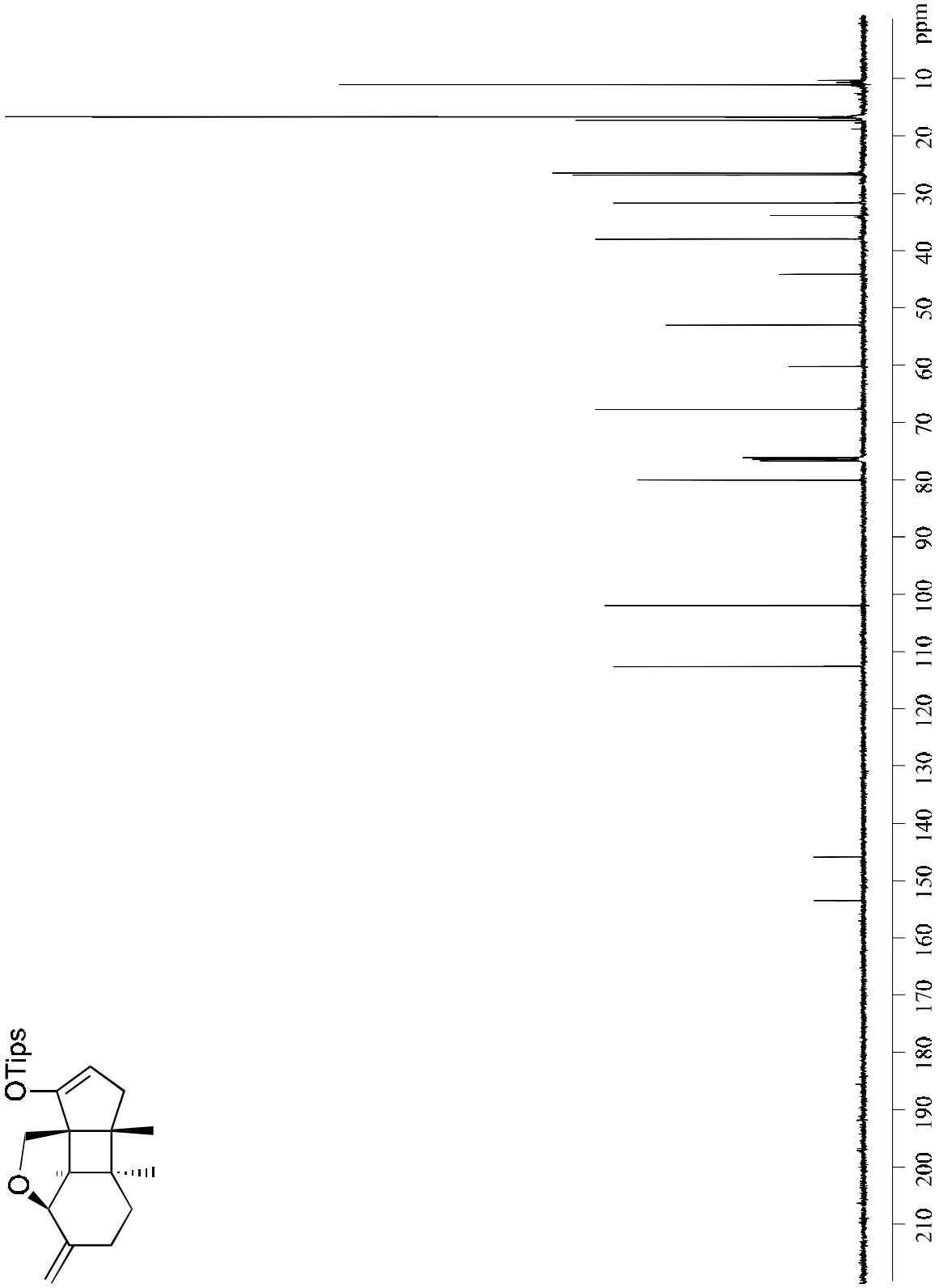
OTips
O
ppm
10
20
30
40
50
60
70
80
90
100
110
120
130
140
150
160
170
180
190
200
210

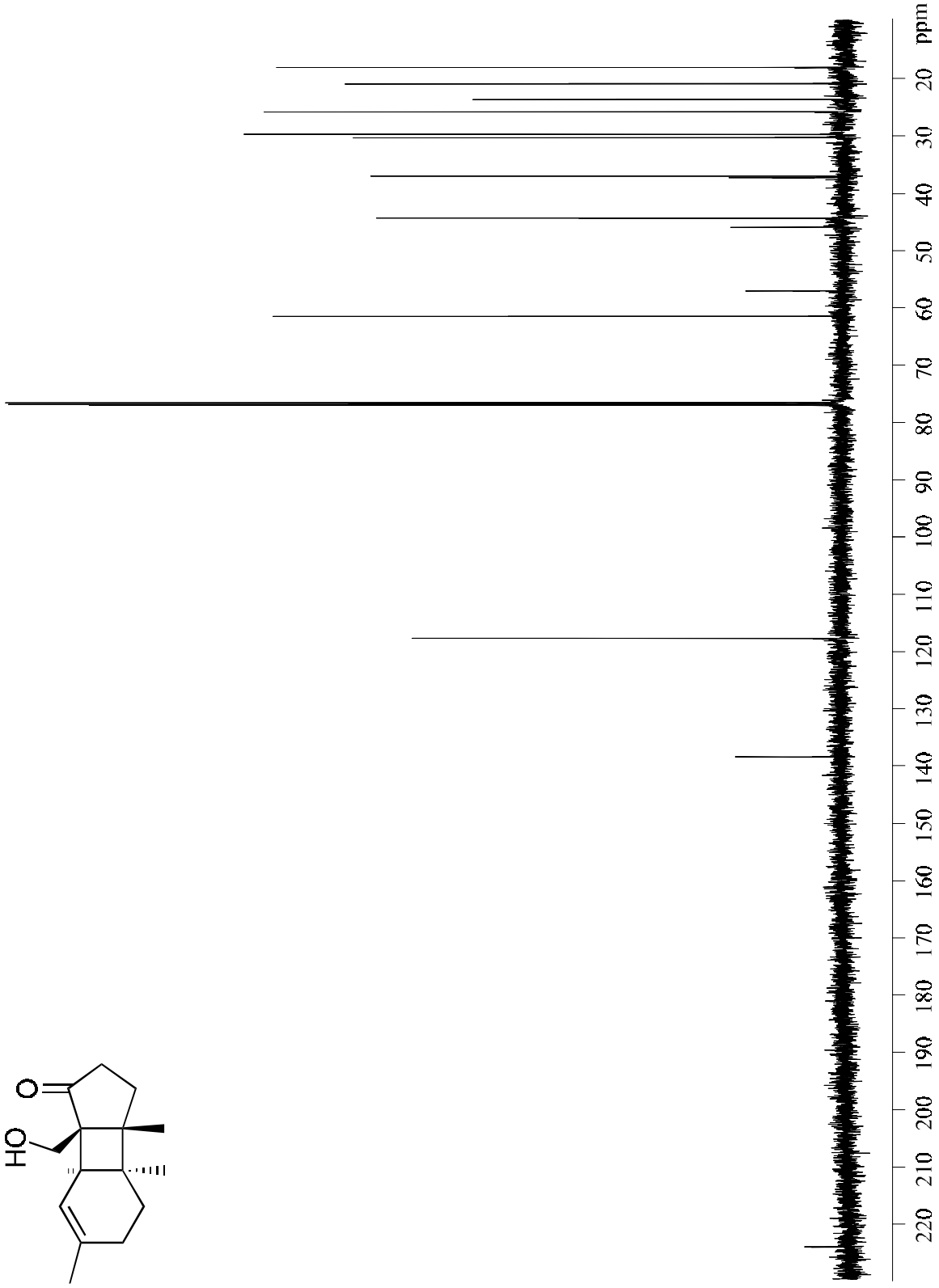
ppm
20
30
40
50
60
70
80
90
100
110
120
130
140
150
160
170
180
190
200
210
220
O
HO

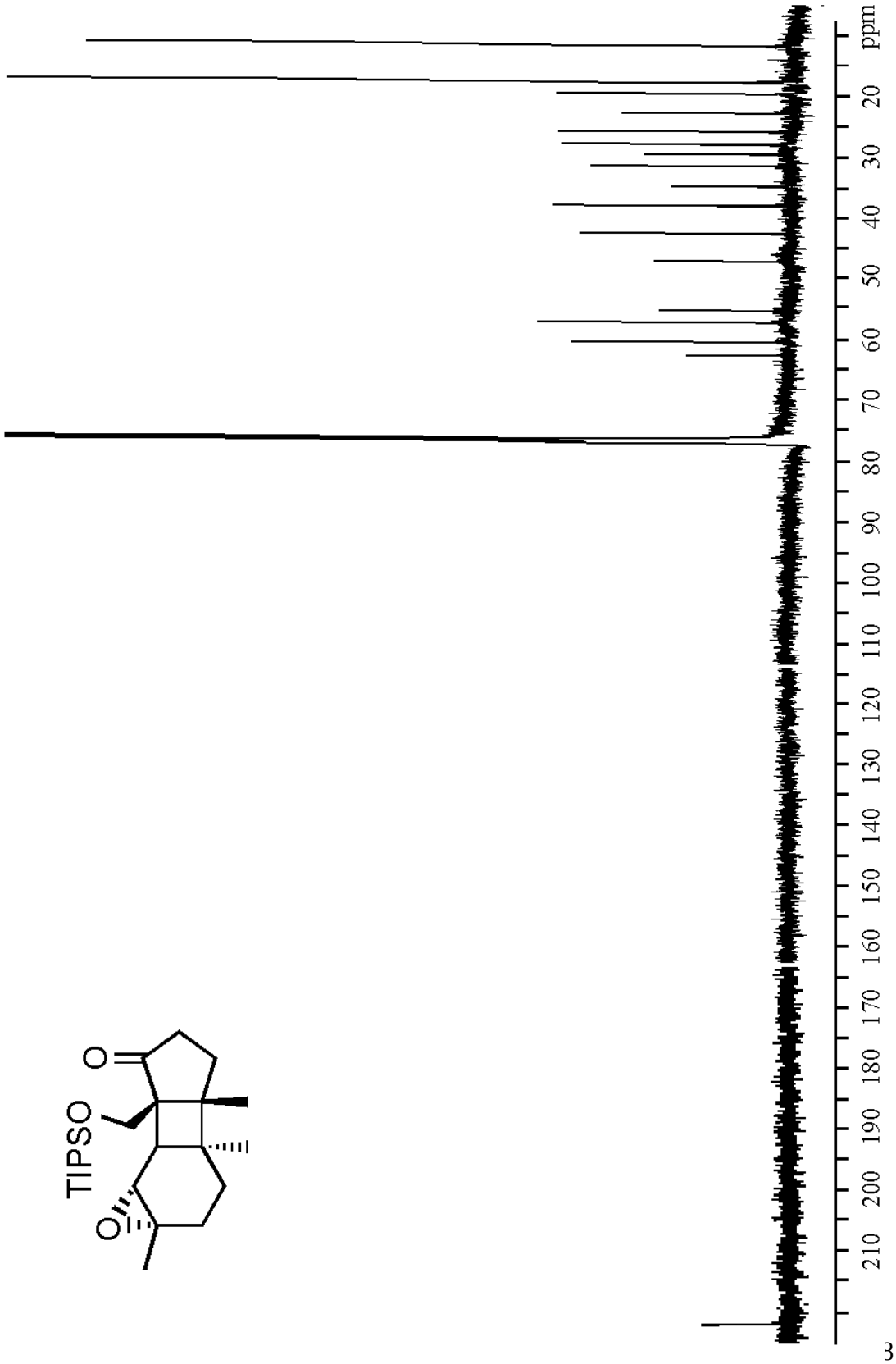
ppm
20
30
40
50
60
70
80
90
100
110
120
130
140
150
160
170
180
190
200
210
TIPSO
O
O

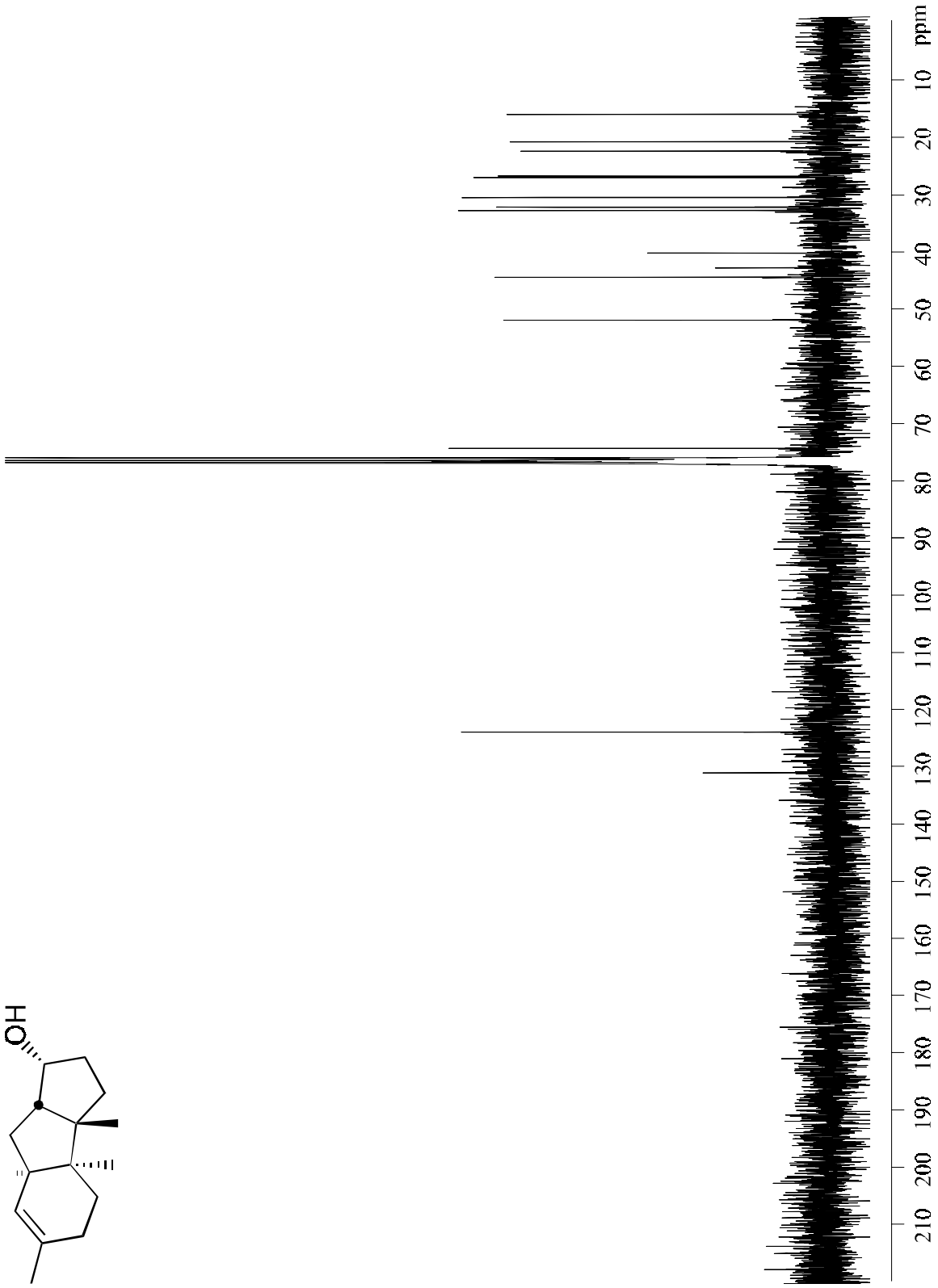
OH
ppm
10
20
30
40
50
60
70
80
90
100
110
120
130
140
150
160
170
180
190
200
210

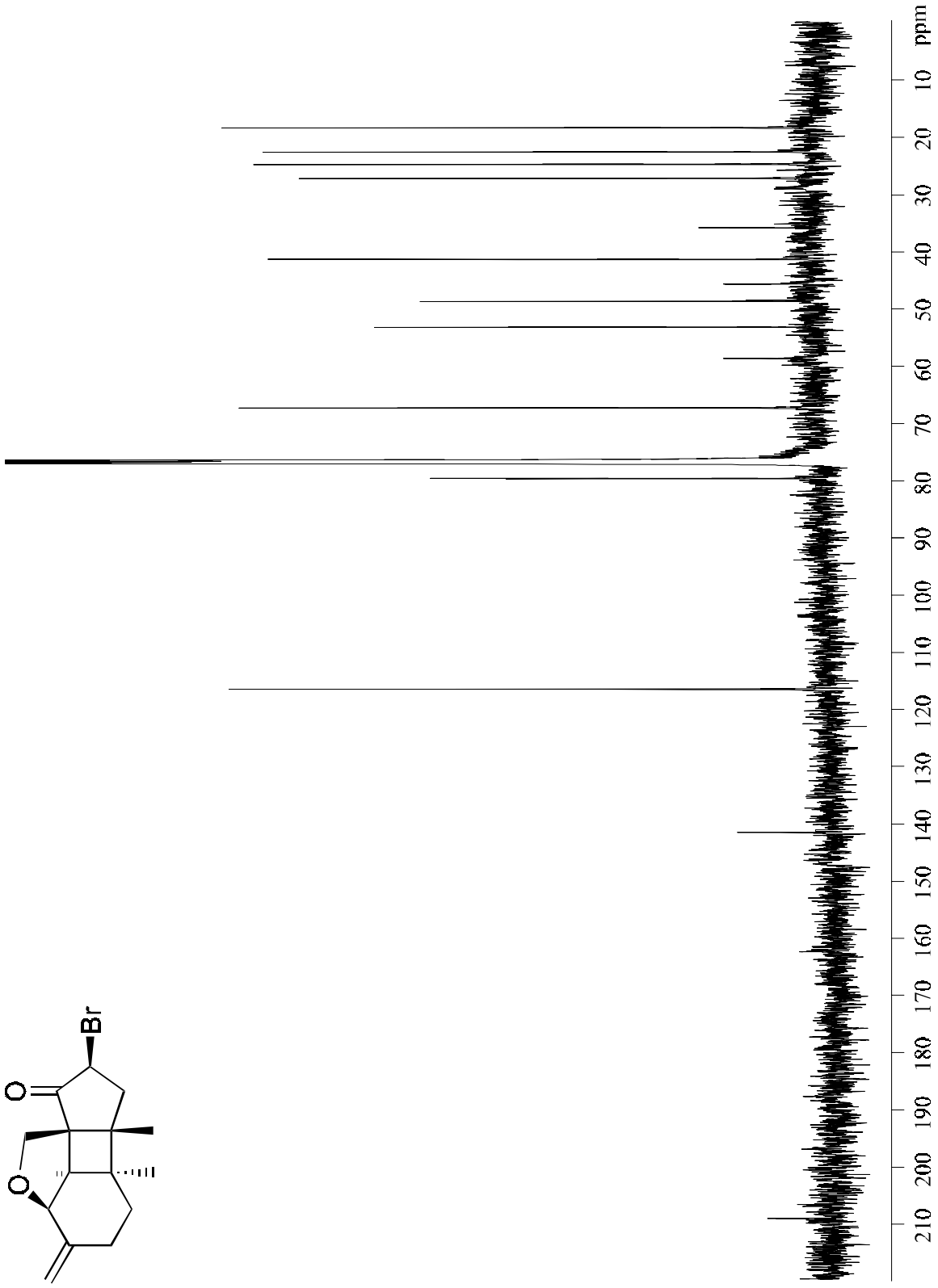
ppm
10
20
30
40
50
60
70
80
90
100
110
120
130
140
150
160
170
180
190
200
210
Br
O
O

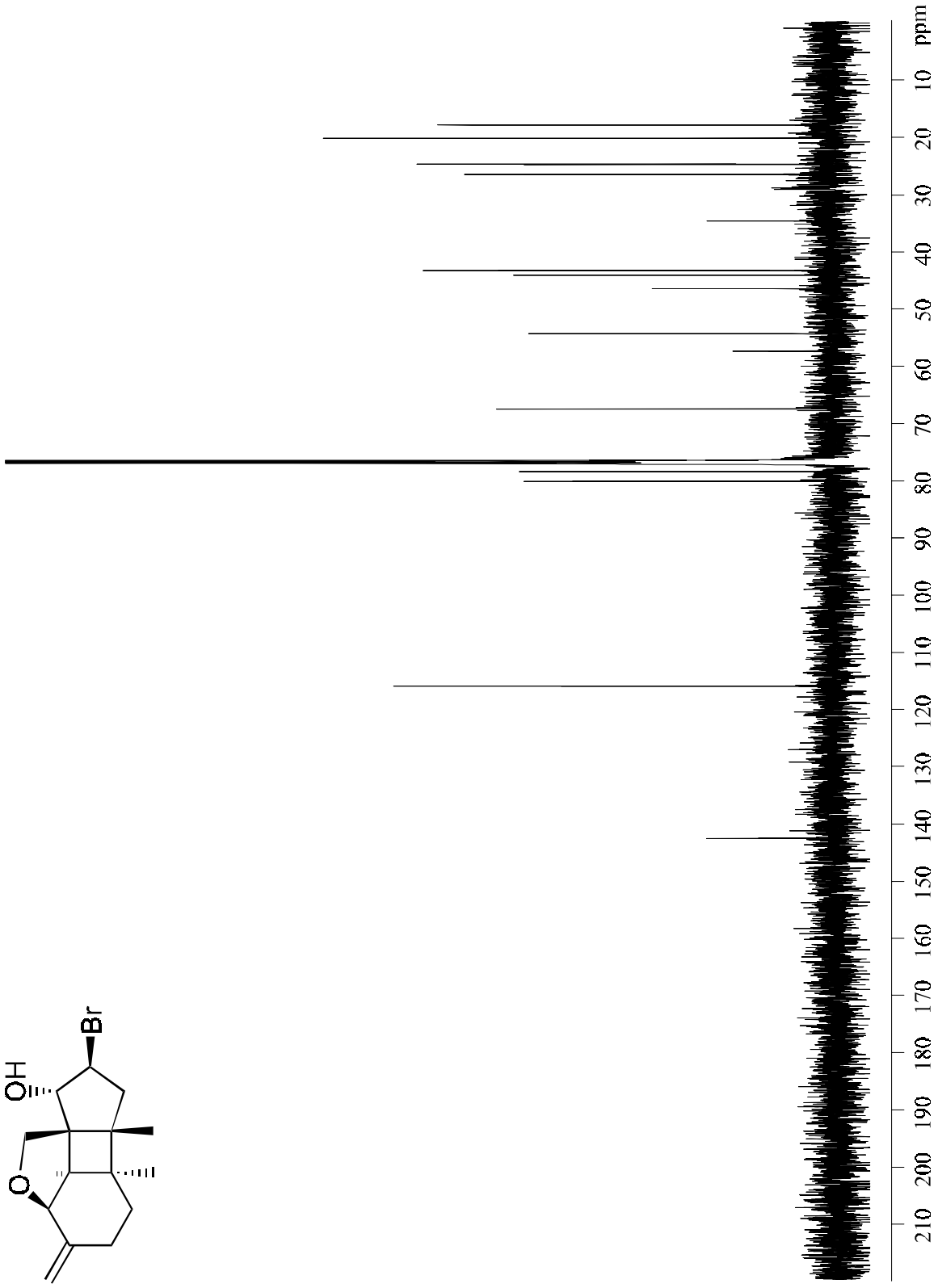
ppm
10
20
30
40
50
60
70
80
90
100
110
120
130
140
150
160
170
180
190
200
210
Br
OH
O

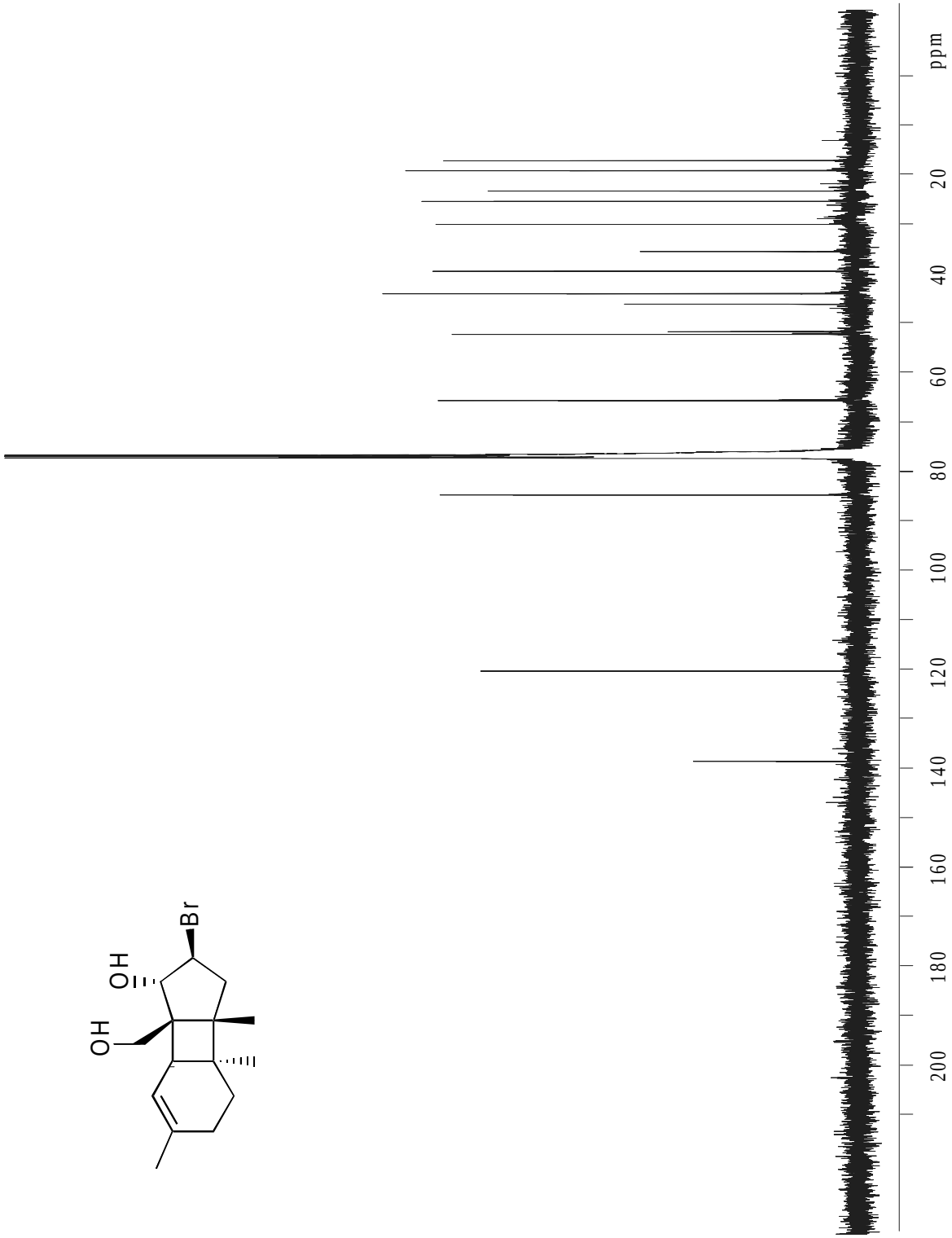
ppm
200
180
160
140
120
100
80
60
40
20
Br
OH
OH

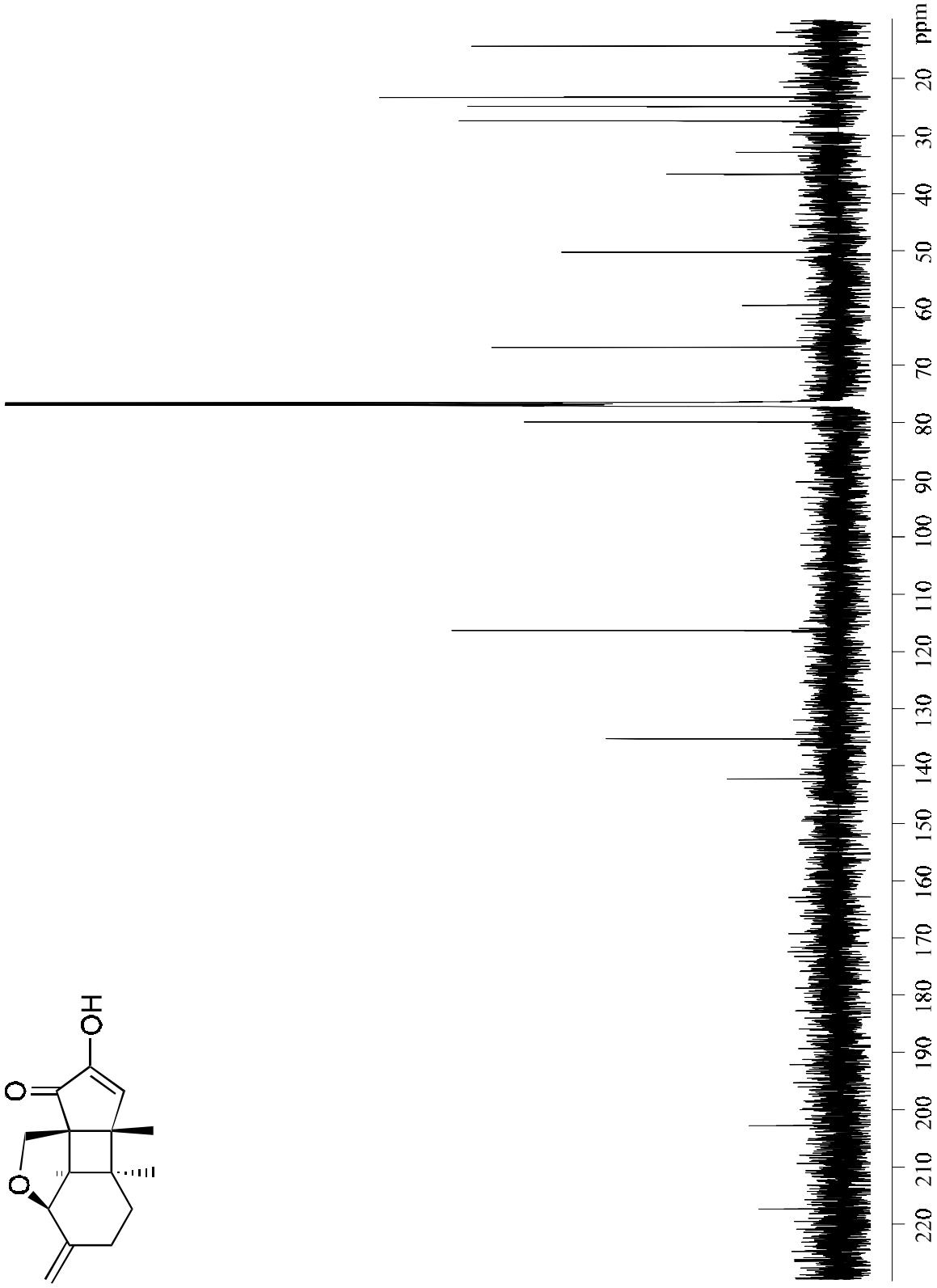
ppm
20
30
40
50
60
70
80
90
100
110
120
130
140
150
160
170
180
190
200
210
220
OH
O
O

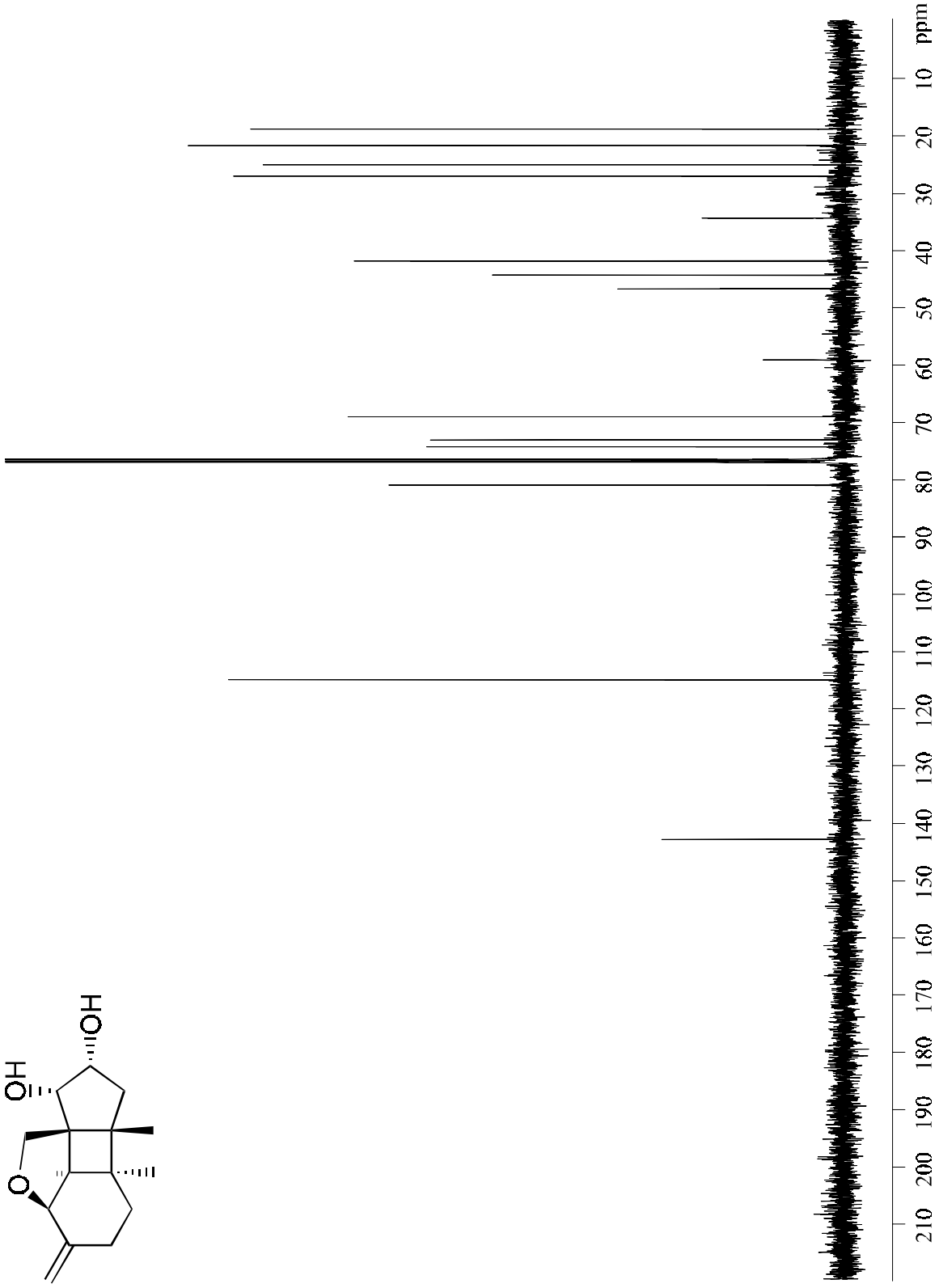
ppm
10
20
30
40
50
60
70
80
90
100
110
120
130
140
150
160
170
180
190
200
210
OH
OH
O

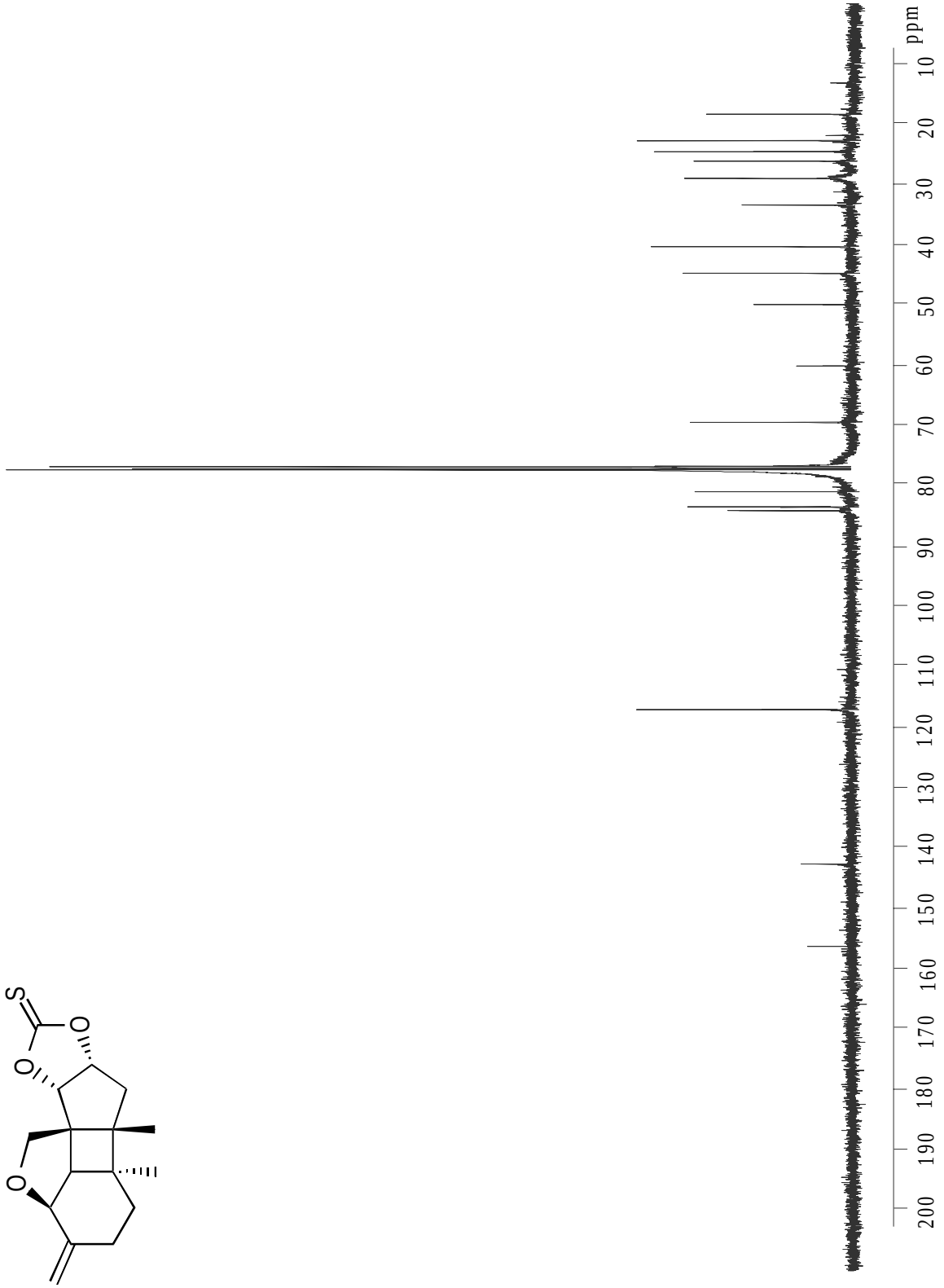
ppm
10
20
30
40
50
60
70
80
90
100
110
120
130
140
150
160
170
180
190
200
S
O
O
O

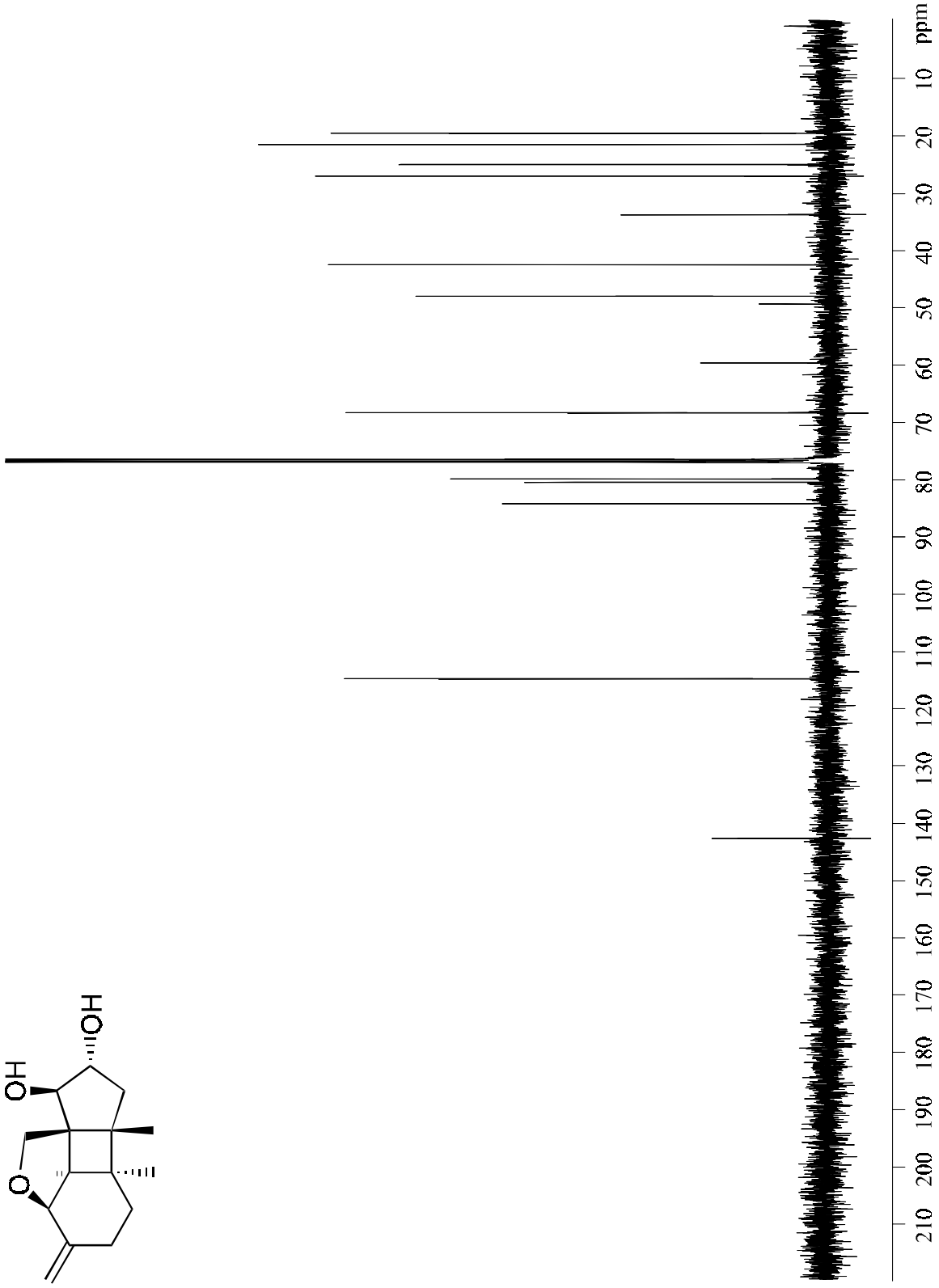
ppm
10
20
30
40
50
60
70
80
90
100
110
120
130
140
150
160
170
180
190
200
210
OH
OH
O

ADDENDUM III: *CONFORMATION ANALYSIS OF FS-2 - MONTE CARLO SIMULATION*

Conformation analysis of the two possible configurations proposed for FS-2[197] was conducted using the Monte Carlo simulation package available in MacroModel[198]. The simulations were carried out in the gas phase using the MM2 method and the PROCG force field. One thousand interactions were performed for each configuration and those that were not within 50 KJ/mol (~ 12 Kcal/mol) of the lowest energy structure were discarded. The structures with 9-S configuration (α-OH) will be reffered as the Tempesta series, and the structures with 9-R configuration (β-OH) will be reffered as the Gilbert series.

For the Tempesta series, 303 different structures were found within the limit of 50 KJ/mol and these could be distributed within six main conformations[199]. The lowest energy structure for each of the six conformations was examined and they were found to be within 4 Kcal/mol of each other, making it difficult to rule out conformations based on thermodynamic arguments alone.

For the Gilbert series, 346 different structures were found distributed within sixteen main conformations. Again, the lowest energy structure for each conformation

---

[197] See Chapter 1 "Revised Structure"

[198] MacroModel (version 4.5) was developed by Prof. Clark Still at Columbia University - www.cc.columbia.edu/cu/chemistry/mmod/mmod.html.

[199] Many structures were found within the same conformation classification due to small variations on angles and/or orientation of OH bonds, etc., which were considered different structures by the computer.

was examined. Of these, nine of the structures lie within 4 Kcal/mol of the overall lowest Gilbert structure energy, only these nine conformations were analyzed further. Four of those conformations contained hydrogen bonds that helped stabilize their structures.

The Nuclear Overhauser Effect data reported for FS-2 by Tempesta[200] was used to help decide which of the two configurations best fit the experimental data. The proton-proton distances from the calculated structures (Monte Carlo simulations) were compared to the experimental data. The NOEs reported were assumed to involve atoms within 3Å of each other. It was considered a violation if the distance between two protons was larger than 4Å and there was an observed NOE, or if the distance was less than 3Å and there was no reported NOE. In some instances the chemical shift dispersion of the two nuclei in question was not enough for NOEs to be observed even though it satisfied the distance criteria and these were dismissed.

The results for the analysis of each conformation are presented below. Only one conformation (Tempesta #3) meets the criteria described above for satisfying the experimental NMR data. Shown are a representative model and description for each conformer next to a graph of the distribution of that conformer's energy with respect to all its structures.

[200] Corley, D. G.; Rottinghaus, G. E.; Tempesta, M. S. *J. Org. Chem.* **1987**, *52*, 4405.

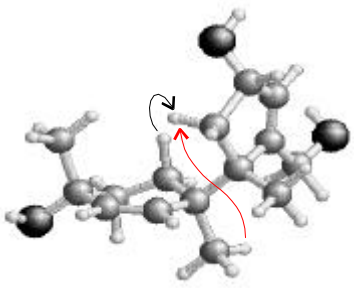

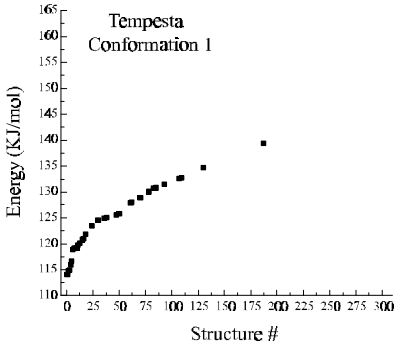

Tempesta #1

Lowest energy structure: structure #1, E = 114.06 KJ/mol (27.26 Kcal/mol).

Description: Quaternary methyls gauche, pseudo chair, methyl front and primary OH back.

NOE violations: one (4.579 Å) - seen in red.

Expected NOEs not seen: one (2.180 Å) - seen in black.

PDB-format file:

```
ATOM      1    C                0.000   0.000   0.000
ATOM      2    C                0.000   0.000   1.341
ATOM      3    C                1.238   0.000  -0.884
ATOM      4    H               -0.978   0.017  -0.508
ATOM      5    C                1.245  -0.014   2.194
ATOM      6    C                2.500  -0.234  -0.013
ATOM      7    C                1.304   1.422  -1.489
ATOM      8    C                1.083  -1.111  -1.979
ATOM      9    H               -0.966   0.004   1.875
ATOM     10    C                2.447   0.456   1.357
ATOM     11    O                1.103   0.894   3.271
ATOM     12    C                1.458  -1.421   2.782
ATOM     13    C                2.373  -1.574  -2.648
ATOM     14    C                0.582  -2.442  -1.336
ATOM     15    H                0.376   1.693  -2.041
ATOM     16    H                1.421   2.203  -0.705
ATOM     17    H                2.157   1.542  -2.191
ATOM     18    C                0.102  -0.743  -3.115
ATOM     19    H                3.411   0.122  -0.544
ATOM     20    H                2.671  -1.320   0.159
ATOM     21    C                2.461  -2.911  -2.680
ATOM     22    C                1.276  -3.601  -2.072
ATOM     23    H                0.390   0.606   3.815
ATOM     24    H                2.374  -1.459   3.414
ATOM     25    H                0.597  -1.722   3.423
ATOM     26    H                1.562  -2.195   1.990
ATOM     27    H               -0.529  -2.546  -1.343
ATOM     28    H                0.886  -2.497  -0.267
ATOM     29    H                2.387   1.559   1.209
ATOM     30    H                3.393   0.273   1.921
ATOM     31    H               -0.048  -1.598  -3.814
ATOM     32    H               -0.904  -0.465  -2.731
ATOM     33    H                0.468   0.105  -3.736
ATOM     34    C                3.341  -0.648  -3.344
ATOM     35    H                0.635  -4.040  -2.875
```

```
ATOM     36    O                    1.648  -4.619  -1.170
ATOM     37    H                    3.268  -3.484  -3.164
ATOM     38    O                    4.325  -1.325  -4.099
ATOM     39    H                    2.787  -0.001  -4.062
ATOM     40    H                    3.878   0.002  -2.617
ATOM     41    H                    2.005  -5.335  -1.669
ATOM     42    H                    4.873  -1.805  -3.500
CONECT    1    2    3    4
CONECT    2    1    5    9
CONECT    3    6    1    7    8
CONECT    4    1
CONECT    5    2   10   11   12
CONECT    6   10    3   19   20
CONECT    7    3   15   16   17
CONECT    8    3   13   14   18
CONECT    9    2
CONECT   10    5    6   29   30
CONECT   11    5   23
CONECT   12    5   24   25   26
CONECT   13    8   21   34
CONECT   14   22    8   27   28
CONECT   15    7
CONECT   16    7
CONECT   17    7
CONECT   18    8   31   32   33
CONECT   19    6
CONECT   20    6
CONECT   21   13   22   37
CONECT   22   21   14   35   36
CONECT   23   11
CONECT   24   12
CONECT   25   12
CONECT   26   12
CONECT   27   14
CONECT   28   14
CONECT   29   10
CONECT   30   10
CONECT   31   18
CONECT   32   18
CONECT   33   18
CONECT   34   13   38   39   40
CONECT   35   22
CONECT   36   22   41
CONECT   37   21
CONECT   38   34   42
CONECT   39   34
CONECT   40   34
CONECT   41   36
CONECT   42   38
END
```

Tempesta #2

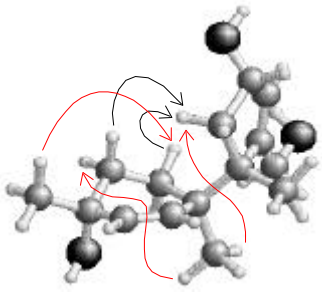

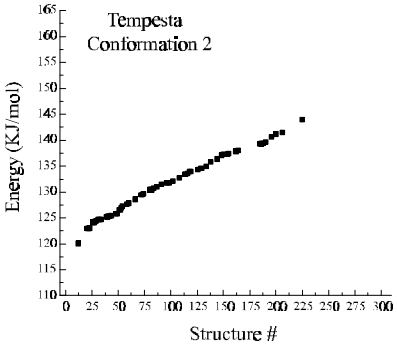

Lowest energy structure: structure #12, E = 120.06 KJ/mol (28.70 Kcal/mol).

Description: Quaternary methyls gauche, twisted chair, methyl front, primary OH back.

NOE violations: three (4.290 Å, 4.612 Å, 4.844 Å) - seen in red.

Expected NOEs not seen: two (2.203 Å, 2.631 Å) - seen in black.

PDB-format file:

```
ATOM      1    C                0.000   0.000   0.000
ATOM      2    C                0.000   0.000   1.340
ATOM      3    C                1.248   0.000  -0.874
ATOM      4    H               -0.978   0.036  -0.506
ATOM      5    C                1.269  -0.044   2.151
ATOM      6    C                2.511  -0.373  -0.044
ATOM      7    C                1.371   1.480  -1.319
ATOM      8    C                1.037  -0.963  -2.092
ATOM      9    H               -0.959   0.026   1.885
ATOM     10    C                2.263  -0.917   1.372
ATOM     11    O                1.811   1.255   2.281
ATOM     12    C                1.020  -0.615   3.558
ATOM     13    C                2.292  -1.379  -2.853
ATOM     14    C                0.531  -2.352  -1.602
ATOM     15    H                0.457   1.852  -1.832
ATOM     16    H                1.519   2.157  -0.446
ATOM     17    H                2.229   1.651  -2.004
ATOM     18    C                0.046  -0.436  -3.155
ATOM     19    H                3.165   0.524   0.063
ATOM     20    H                3.149  -1.114  -0.575
ATOM     21    C                2.308  -2.695  -3.102
ATOM     22    C                1.100  -3.408  -2.566
ATOM     23    H                1.196   1.785   2.760
ATOM     24    H                1.967  -0.667   4.142
ATOM     25    H                0.307   0.019   4.133
ATOM     26    H                0.596  -1.644   3.507
ATOM     27    H               -0.579  -2.416  -1.507
ATOM     28    H                0.953  -2.563  -0.594
ATOM     29    H                3.229  -0.980   1.929
ATOM     30    H                1.869  -1.959   1.316
ATOM     31    H               -0.149  -1.196  -3.946
ATOM     32    H               -0.945  -0.174  -2.722
ATOM     33    H                0.432   0.465  -3.682
ATOM     34    C                3.319  -0.401  -3.369
ATOM     35    H                0.397  -3.656  -3.398
ATOM     36    O                1.432  -4.591  -1.875
ATOM     37    H                3.081  -3.228  -3.678
```

```
ATOM     38    O                   4.307  -0.999  -4.181
ATOM     39    H                   2.816   0.371  -3.998
ATOM     40    H                   3.846   0.100  -2.524
ATOM     41    H                   1.714  -5.231  -2.508
ATOM     42    H                   4.804  -1.593  -3.644
CONECT    1    2    3    4
CONECT    2    1    5    9
CONECT    3    6    1    7    8
CONECT    4    1
CONECT    5    2   10   11   12
CONECT    6   10    3   19   20
CONECT    7    3   15   16   17
CONECT    8    3   13   14   18
CONECT    9    2
CONECT   10    5    6   29   30
CONECT   11    5   23
CONECT   12    5   24   25   26
CONECT   13    8   21   34
CONECT   14   22    8   27   28
CONECT   15    7
CONECT   16    7
CONECT   17    7
CONECT   18    8   31   32   33
CONECT   19    6
CONECT   20    6
CONECT   21   13   22   37
CONECT   22   21   14   35   36
CONECT   23   11
CONECT   24   12
CONECT   25   12
CONECT   26   12
CONECT   27   14
CONECT   28   14
CONECT   29   10
CONECT   30   10
CONECT   31   18
CONECT   32   18
CONECT   33   18
CONECT   34   13   38   39   40
CONECT   35   22
CONECT   36   22   41
CONECT   37   21
CONECT   38   34   42
CONECT   39   34
CONECT   40   34
CONECT   41   36
CONECT   42   38
END
```

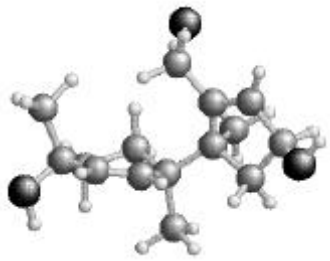

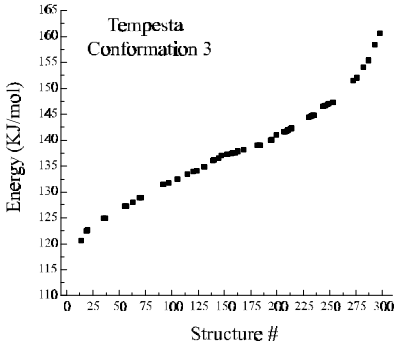

Tempesta #3

Lowest energy structure: structure #14, E = 120.55 KJ/mol (28.81 Kcal/mol).

Description: Quaternary methyls gauche, pseudo chair, methyl back and secondary OH front.

NOE violations: **none**.

Expected NOEs not seen: **none**.

This is the structure that best fits the experimental data available on the molecule. It is 1.55 Kcal/mol more energetic than the lowest energy overall structure for the Tempesta configuration and 3.9 Kcal/mol more energetic than the lowest energy structure for the Gilbert configuration.

PDB-format file:

```
ATOM      1    C                0.000   0.000   0.000
ATOM      2    C                0.000   0.000   1.341
ATOM      3    C                1.244   0.000  -0.869
ATOM      4    H               -0.977   0.016  -0.510
ATOM      5    C                1.238  -0.023   2.208
ATOM      6    C                2.458  -0.416   0.001
ATOM      7    C                1.469   1.466  -1.320
ATOM      8    C                1.048  -0.938  -2.111
ATOM      9    H               -0.968   0.007   1.871
ATOM     10    C                2.502   0.265   1.378
ATOM     11    O                1.132   0.967   3.214
ATOM     12    C                1.336  -1.382   2.926
ATOM     13    C                0.286  -2.237  -1.857
ATOM     14    C                0.126  -0.309  -3.202
ATOM     15    H                0.611   1.888  -1.887
ATOM     16    H                1.600   2.162  -0.462
ATOM     17    H                2.372   1.565  -1.962
ATOM     18    C                2.385  -1.314  -2.789
ATOM     19    H                3.410  -0.193  -0.535
ATOM     20    H                2.451  -1.513   0.178
ATOM     21    C               -0.572  -2.513  -2.850
ATOM     22    C               -0.573  -1.471  -3.930
ATOM     23    H                1.017   1.805   2.796
ATOM     24    H                2.210  -1.410   3.617
ATOM     25    H                0.426  -1.582   3.537
ATOM     26    H                1.452  -2.226   2.211
```

```
ATOM     27    H                    0.665   0.367  -3.906
ATOM     28    H                   -0.682   0.287  -2.720
ATOM     29    H                    2.624   1.363   1.241
ATOM     30    H                    3.409  -0.059   1.942
ATOM     31    H                    2.227  -1.892  -3.728
ATOM     32    H                    2.973  -0.411  -3.065
ATOM     33    H                    3.024  -1.955  -2.142
ATOM     34    C                    0.562  -3.164  -0.701
ATOM     35    H                   -0.004  -1.833  -4.821
ATOM     36    O                   -1.873  -1.105  -4.332
ATOM     37    H                   -1.196  -3.418  -2.924
ATOM     38    O                   -0.186  -4.362  -0.744
ATOM     39    H                    1.636  -3.461  -0.706
ATOM     40    H                    0.312  -2.659   0.259
ATOM     41    H                   -2.240  -1.821  -4.823
ATOM     42    H                   -1.098  -4.139  -0.659
CONECT    1    2    3    4
CONECT    2    1    5    9
CONECT    3    6    1    7    8
CONECT    4    1
CONECT    5    2   10   11   12
CONECT    6   10    3   19   20
CONECT    7    3   15   16   17
CONECT    8    3   13   14   18
CONECT    9    2
CONECT   10    5    6   29   30
CONECT   11    5   23
CONECT   12    5   24   25   26
CONECT   13    8   21   34
CONECT   14   22    8   27   28
CONECT   15    7
CONECT   16    7
CONECT   17    7
CONECT   18    8   31   32   33
CONECT   19    6
CONECT   20    6
CONECT   21   13   22   37
CONECT   22   21   14   35   36
CONECT   23   11
CONECT   24   12
CONECT   25   12
CONECT   26   12
CONECT   27   14
CONECT   28   14
CONECT   29   10
CONECT   30   10
CONECT   31   18
CONECT   32   18
CONECT   33   18
CONECT   34   13   38   39   40
CONECT   35   22
CONECT   36   22   41
CONECT   37   21
CONECT   38   34   42
CONECT   39   34
CONECT   40   34
CONECT   41   36
CONECT   42   38
END
```

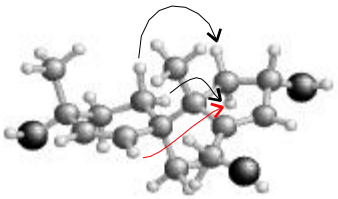

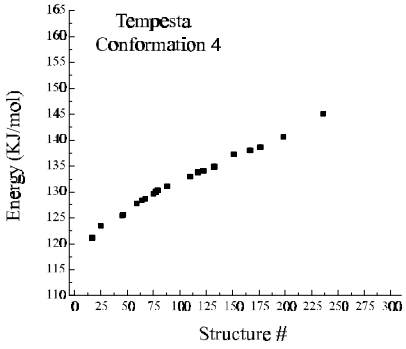

Tempesta #4

Lowest energy structure: structure #17, E = 121.18 KJ/mol (28.96 Kcal/mol).

Description: Quaternary methyls anti, pseudo chair, primary OH front, "flat structure".

NOE violations: one (4.639 Å) - seen in red.

Expected NOEs not seen: two (2.301 Å, 2.541 Å) - seen in black.

PDB-format file:

```
ATOM      1    C                0.000   0.000   0.000
ATOM      2    C                0.000   0.000   1.341
ATOM      3    C                1.231   0.000  -0.890
ATOM      4    H               -0.982   0.027  -0.495
ATOM      5    C                1.244  -0.024   2.194
ATOM      6    C                2.487  -0.256  -0.011
ATOM      7    C                1.353   1.423  -1.486
ATOM      8    C                1.103  -1.099  -2.002
ATOM      9    H               -0.965   0.010   1.876
ATOM     10    C                2.447   0.440   1.356
ATOM     11    O                1.110   0.880   3.275
ATOM     12    C                1.440  -1.437   2.773
ATOM     13    C                0.221  -0.776  -3.208
ATOM     14    C                2.468  -1.337  -2.717
ATOM     15    H                0.495   1.698  -2.135
ATOM     16    H                1.390   2.202  -0.692
ATOM     17    H                2.269   1.553  -2.103
ATOM     18    C                0.606  -2.452  -1.438
ATOM     19    H                3.412   0.064  -0.543
ATOM     20    H                2.617  -1.344   0.178
ATOM     21    C                0.812  -1.125  -4.361
ATOM     22    C                2.166  -1.741  -4.170
ATOM     23    H                0.393   0.598   3.817
ATOM     24    H                2.367  -1.496   3.389
ATOM     25    H                0.585  -1.725   3.427
ATOM     26    H                1.512  -2.210   1.975
ATOM     27    H                3.121  -2.080  -2.201
ATOM     28    H                3.040  -0.384  -2.769
ATOM     29    H                2.396   1.543   1.206
ATOM     30    H                3.392   0.249   1.918
ATOM     31    H                0.582  -3.239  -2.226
ATOM     32    H                1.258  -2.840  -0.625
ATOM     33    H               -0.425  -2.386  -1.024
ATOM     34    C               -1.219  -0.327  -3.116
ATOM     35    H                2.108  -2.849  -4.305
```

```
ATOM     36    O                   3.131  -1.217  -5.053
ATOM     37    H                   0.351  -1.063  -5.359
ATOM     38    O                  -1.876  -0.275  -4.366
ATOM     39    H                  -1.792  -1.052  -2.493
ATOM     40    H                  -1.306   0.687  -2.665
ATOM     41    H                   2.942  -1.542  -5.918
ATOM     42    H                  -1.457   0.391  -4.887
CONECT    1    2    3    4
CONECT    2    1    5    9
CONECT    3    6    1    7    8
CONECT    4    1
CONECT    5    2   10   11   12
CONECT    6   10    3   19   20
CONECT    7    3   15   16   17
CONECT    8    3   13   14   18
CONECT    9    2
CONECT   10    5    6   29   30
CONECT   11    5   23
CONECT   12    5   24   25   26
CONECT   13    8   21   34
CONECT   14   22    8   27   28
CONECT   15    7
CONECT   16    7
CONECT   17    7
CONECT   18    8   31   32   33
CONECT   19    6
CONECT   20    6
CONECT   21   13   22   37
CONECT   22   21   14   35   36
CONECT   23   11
CONECT   24   12
CONECT   25   12
CONECT   26   12
CONECT   27   14
CONECT   28   14
CONECT   29   10
CONECT   30   10
CONECT   31   18
CONECT   32   18
CONECT   33   18
CONECT   34   13   38   39   40
CONECT   35   22
CONECT   36   22   41
CONECT   37   21
CONECT   38   34   42
CONECT   39   34
CONECT   40   34
CONECT   41   36
CONECT   42   38
END
```

Tempesta #5

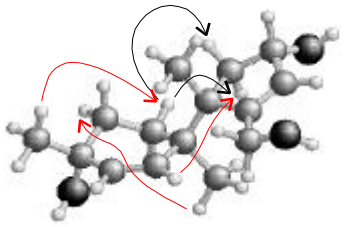

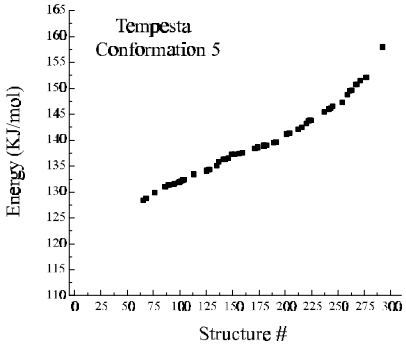

Lowest energy structure: structure #65, E = 128.41 KJ/mol (30.69 Kcal/mol).

Description: Quaternary methyls anti, twisted chair, primary OH front, "flat structure".

NOE violations: three (4.631 Å, 4.643 Å, 4.688 Å) - seen in red.

Expected NOEs not seen: two (2.308 Å, 2.346 Å) - seen in black.

PDB-format file:

```
ATOM      1    C                0.000   0.000   0.000
ATOM      2    C                0.000   0.000   1.341
ATOM      3    C                1.228   0.000  -0.896
ATOM      4    H               -0.984   0.014  -0.491
ATOM      5    C                1.244   0.037   2.193
ATOM      6    C                2.491   0.182  -0.006
ATOM      7    C                1.126   1.277  -1.773
ATOM      8    C                1.265  -1.292  -1.791
ATOM      9    H               -0.966   0.010   1.874
ATOM     10    C                2.435  -0.485   1.375
ATOM     11    O                1.516   1.375   2.564
ATOM     12    C                1.061  -0.795   3.474
ATOM     13    C                0.288  -1.334  -2.970
ATOM     14    C                2.618  -1.429  -2.556
ATOM     15    H                0.273   1.258  -2.484
ATOM     16    H                0.979   2.188  -1.148
ATOM     17    H                2.043   1.454  -2.378
ATOM     18    C                1.025  -2.598  -1.002
ATOM     19    H                2.645   1.268   0.194
ATOM     20    H                3.419  -0.131  -0.532
ATOM     21    C                0.880  -1.764  -4.094
ATOM     22    C                2.328  -2.105  -3.906
ATOM     23    H                0.796   1.691   3.084
ATOM     24    H                1.986  -0.784   4.095
ATOM     25    H                0.231  -0.398   4.104
ATOM     26    H                0.825  -1.857   3.234
ATOM     27    H                3.403  -1.975  -1.983
ATOM     28    H                3.028  -0.421  -2.788
ATOM     29    H                3.383  -0.296   1.933
ATOM     30    H                2.361  -1.589   1.270
ATOM     31    H                0.975  -3.483  -1.678
ATOM     32    H                1.850  -2.817  -0.292
ATOM     33    H                0.073  -2.580  -0.426
ATOM     34    C               -1.204  -1.124  -2.852
ATOM     35    H                2.460  -3.214  -3.869
```

```
ATOM     36    O                  3.147  -1.576  -4.925
ATOM     37    H                  0.373  -1.946  -5.054
ATOM     38    O                 -1.926  -1.548  -3.990
ATOM     39    H                 -1.593  -1.729  -2.000
ATOM     40    H                 -1.454  -0.051  -2.691
ATOM     41    H                  2.982  -2.063  -5.715
ATOM     42    H                 -1.696  -0.983  -4.709
CONECT    1    2    3    4
CONECT    2    1    5    9
CONECT    3    6    1    7    8
CONECT    4    1
CONECT    5    2   10   11   12
CONECT    6   10    3   19   20
CONECT    7    3   15   16   17
CONECT    8    3   13   14   18
CONECT    9    2
CONECT   10    5    6   29   30
CONECT   11    5   23
CONECT   12    5   24   25   26
CONECT   13    8   21   34
CONECT   14   22    8   27   28
CONECT   15    7
CONECT   16    7
CONECT   17    7
CONECT   18    8   31   32   33
CONECT   19    6
CONECT   20    6
CONECT   21   13   22   37
CONECT   22   21   14   35   36
CONECT   23   11
CONECT   24   12
CONECT   25   12
CONECT   26   12
CONECT   27   14
CONECT   28   14
CONECT   29   10
CONECT   30   10
CONECT   31   18
CONECT   32   18
CONECT   33   18
CONECT   34   13   38   39   40
CONECT   35   22
CONECT   36   22   41
CONECT   37   21
CONECT   38   34   42
CONECT   39   34
CONECT   40   34
CONECT   41   36
CONECT   42   38
END
```

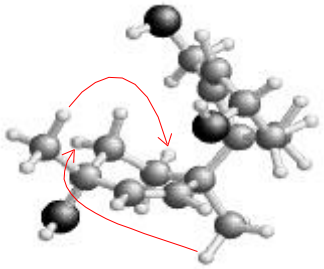

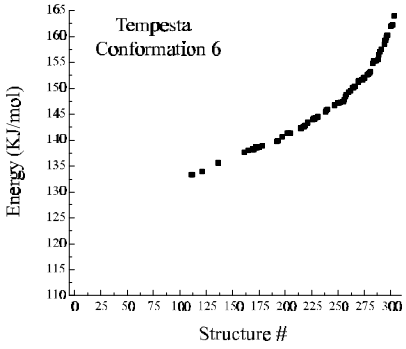

Tempesta #6

Lowest energy structure: structure #111, E = 133.38 KJ/mol (31.88 Kcal/mol).

Description: Quaternary methyls gauche, twisted chair, secondary OH front, methyl back.

NOE violations: two (4.717 Å, 4.924 Å) - seen in red.

Expected NOEs not seen: **none**.

PDB-format file:

```
ATOM      1    C                0.000   0.000   0.000
ATOM      2    C                0.000   0.000   1.341
ATOM      3    C                1.232   0.000  -0.893
ATOM      4    H               -0.984   0.045  -0.494
ATOM      5    C                1.244   0.026   2.193
ATOM      6    C                2.466   0.306  -0.010
ATOM      7    C                1.029   1.238  -1.810
ATOM      8    C                1.362  -1.305  -1.770
ATOM      9    H               -0.966   0.024   1.874
ATOM     10    C                2.448  -0.416   1.346
ATOM     11    O                1.481   1.347   2.640
ATOM     12    C                1.084  -0.883   3.425
ATOM     13    C                1.882  -2.548  -1.051
ATOM     14    C               -0.025  -1.849  -2.238
ATOM     15    H                0.197   1.092  -2.535
ATOM     16    H                0.780   2.151  -1.221
ATOM     17    H                1.948   1.490  -2.386
ATOM     18    C                2.249  -1.084  -3.019
ATOM     19    H                2.505   1.396   0.220
ATOM     20    H                3.408   0.113  -0.570
ATOM     21    C                0.905  -3.421  -0.774
ATOM     22    C               -0.438  -2.993  -1.288
ATOM     23    H                0.747   1.617   3.166
ATOM     24    H                2.010  -0.886   4.044
ATOM     25    H                0.246  -0.543   4.076
ATOM     26    H                0.872  -1.935   3.124
ATOM     27    H                0.101  -2.318  -3.243
ATOM     28    H               -0.814  -1.079  -2.393
ATOM     29    H                3.397  -0.226   1.901
ATOM     30    H                2.379  -1.515   1.201
ATOM     31    H                2.422  -2.032  -3.578
ATOM     32    H                1.781  -0.388  -3.750
ATOM     33    H                3.252  -0.681  -2.752
ATOM     34    C                3.349  -2.854  -0.841
ATOM     35    H               -0.958  -3.818  -1.835
```

```
ATOM     36    O                -1.280  -2.549  -0.250
ATOM     37    H                 1.048  -4.407  -0.303
ATOM     38    O                 3.576  -3.884   0.098
ATOM     39    H                 3.791  -3.189  -1.807
ATOM     40    H                 3.926  -1.967  -0.498
ATOM     41    H                -1.611  -3.306   0.203
ATOM     42    H                 3.222  -3.607   0.926
CONECT    1    2    3    4
CONECT    2    1    5    9
CONECT    3    6    1    7    8
CONECT    4    1
CONECT    5    2   10   11   12
CONECT    6   10    3   19   20
CONECT    7    3   15   16   17
CONECT    8    3   13   14   18
CONECT    9    2
CONECT   10    5    6   29   30
CONECT   11    5   23
CONECT   12    5   24   25   26
CONECT   13    8   21   34
CONECT   14   22    8   27   28
CONECT   15    7
CONECT   16    7
CONECT   17    7
CONECT   18    8   31   32   33
CONECT   19    6
CONECT   20    6
CONECT   21   13   22   37
CONECT   22   21   14   35   36
CONECT   23   11
CONECT   24   12
CONECT   25   12
CONECT   26   12
CONECT   27   14
CONECT   28   14
CONECT   29   10
CONECT   30   10
CONECT   31   18
CONECT   32   18
CONECT   33   18
CONECT   34   13   38   39   40
CONECT   35   22
CONECT   36   22   41
CONECT   37   21
CONECT   38   34   42
CONECT   39   34
CONECT   40   34
CONECT   41   36
CONECT   42   38
END
```

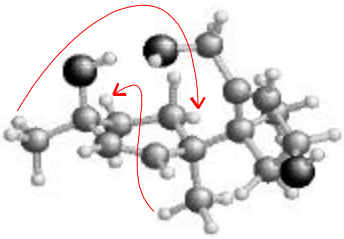

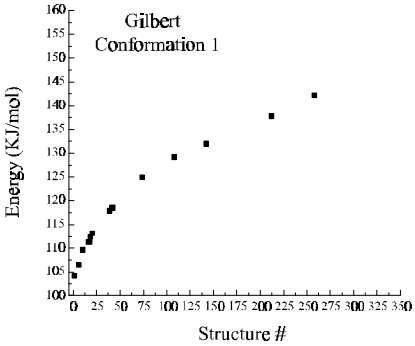

Gilbert #1

Lowest energy structure: structure #1, E = 104.20 KJ/mol (24.91 Kcal/mol).

Description: Quaternary methyls gauche, pseudo chair, H-bond with primary OH (1.911 Å), six-membered ring donor, secondary OH front, methyl back.

NOE violations: two (3.755 Å, 4.842 Å) - seen in red.

Expected NOEs not seen: **none**.

PDB-format file:

```
ATOM      1    C                0.000   0.000   0.000
ATOM      2    C                0.000   0.000   1.341
ATOM      3    C                1.244   0.000  -0.873
ATOM      4    H               -0.980   0.036  -0.503
ATOM      5    C                1.245  -0.086   2.192
ATOM      6    C                2.483  -0.353  -0.012
ATOM      7    C                1.421   1.465  -1.353
ATOM      8    C                1.074  -0.965  -2.098
ATOM      9    H               -0.966   0.014   1.874
ATOM     10    C                2.488   0.307   1.374
ATOM     11    C                1.113   0.824   3.427
ATOM     12    O                1.400  -1.412   2.664
ATOM     13    C                0.432  -2.323  -1.819
ATOM     14    C                0.071  -0.408  -3.158
ATOM     15    H                0.549   1.849  -1.927
ATOM     16    H                1.534   2.177  -0.506
ATOM     17    H                2.319   1.587  -1.999
ATOM     18    C                2.410  -1.245  -2.825
ATOM     19    H                3.419  -0.071  -0.548
ATOM     20    H                2.544  -1.450   0.152
ATOM     21    C               -0.470  -2.651  -2.755
ATOM     22    C               -0.612  -1.613  -3.828
ATOM     23    H                0.545   0.274  -3.902
ATOM     24    H               -0.739   0.170  -2.659
ATOM     25    H                2.530   1.414   1.263
ATOM     26    H                3.413   0.026   1.932
ATOM     27    H                2.258  -1.849  -3.749
ATOM     28    H                2.915  -0.305  -3.140
ATOM     29    H                3.125  -1.819  -2.196
ATOM     30    C                0.857  -3.295  -0.748
ATOM     31    H                2.032   0.780   4.056
ATOM     32    H                0.953   1.886   3.131
ATOM     33    H                0.255   0.519   4.069
ATOM     34    H                1.306  -2.011   1.938
ATOM     35    H               -0.089  -1.944  -4.758
```

```
ATOM     36    O                -1.959  -1.328  -4.133
ATOM     37    H                -1.010  -3.611  -2.798
ATOM     38    O                 0.395  -2.925   0.530
ATOM     39    H                 0.446  -4.312  -0.956
ATOM     40    H                 1.966  -3.398  -0.717
ATOM     41    H                -2.317  -2.064  -4.599
ATOM     42    H                -0.549  -2.965   0.523
CONECT    1    2    3    4
CONECT    2    1    5    9
CONECT    3    6    1    7    8
CONECT    4    1
CONECT    5    2   10   11   12
CONECT    6   10    3   19   20
CONECT    7    3   15   16   17
CONECT    8    3   13   14   18
CONECT    9    2
CONECT   10    5    6   25   26
CONECT   11    5   31   32   33
CONECT   12    5   34
CONECT   13    8   21   30
CONECT   14   22    8   23   24
CONECT   15    7
CONECT   16    7
CONECT   17    7
CONECT   18    8   27   28   29
CONECT   19    6
CONECT   20    6
CONECT   21   13   22   37
CONECT   22   21   14   35   36
CONECT   23   14
CONECT   24   14
CONECT   25   10
CONECT   26   10
CONECT   27   18
CONECT   28   18
CONECT   29   18
CONECT   30   13   38   39   40
CONECT   31   11
CONECT   32   11
CONECT   33   11
CONECT   34   12
CONECT   35   22
CONECT   36   22   41
CONECT   37   21
CONECT   38   30   42
CONECT   39   30
CONECT   40   30
CONECT   41   36
CONECT   42   38
END
```

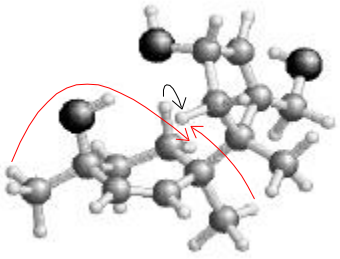

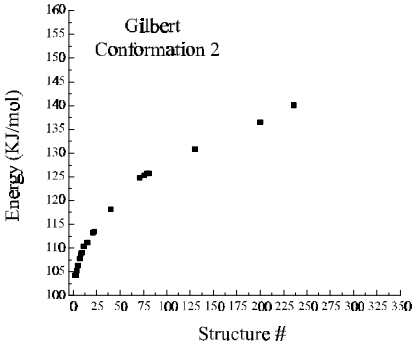

Gilbert #2

Lowest energy structure: structure #2, E = 104.30 KJ/mol (24.93 Kcal/mol).

Description: Quaternary methyls gauche, pseudo chair, H-bond with secondary OH (1.963 Å), six-membered ring donor, primary OH back, methyl front.

NOE violations: two (4.329 Å, 4.879 Å) - seen in red.

Expected NOEs not seen: one (3.245 Å)* - seen in black.

PDB-format file:

```
ATOM      1    C                0.000   0.000   0.000
ATOM      2    C                0.000   0.000   1.340
ATOM      3    C                1.240   0.000  -0.880
ATOM      4    H               -0.975   0.004  -0.516
ATOM      5    C                1.261  -0.002   2.167
ATOM      6    C                2.533  -0.002  -0.024
ATOM      7    C                1.189   1.369  -1.606
ATOM      8    C                1.174  -1.226  -1.863
ATOM      9    H               -0.963  -0.006   1.879
ATOM     10    C                2.384   0.661   1.352
ATOM     11    C                1.043   0.759   3.488
ATOM     12    O                1.620  -1.330   2.501
ATOM     13    C                2.545  -1.722  -2.308
ATOM     14    C                0.624  -2.525  -1.184
ATOM     15    H                0.229   1.540  -2.144
ATOM     16    H                1.282   2.216  -0.888
ATOM     17    H                2.011   1.486  -2.346
ATOM     18    C                0.308  -0.945  -3.113
ATOM     19    H                3.373   0.477  -0.577
ATOM     20    H                2.879  -1.036   0.167
ATOM     21    C                2.871  -2.897  -1.750
ATOM     22    C                1.807  -3.451  -0.847
ATOM     23    H               -0.008  -3.082  -1.914
ATOM     24    H               -0.041  -2.370  -0.306
ATOM     25    H                2.162   1.746   1.219
ATOM     26    H                3.347   0.600   1.914
ATOM     27    H                0.274  -1.822  -3.799
ATOM     28    H               -0.742  -0.704  -2.832
ATOM     29    H                0.698  -0.105  -3.729
ATOM     30    C                3.422  -0.956  -3.268
ATOM     31    H                1.976   0.782   4.096
ATOM     32    H                0.733   1.813   3.302
ATOM     33    H                0.253   0.278   4.110
ATOM     34    H                1.668  -1.865   1.721
ATOM     35    H                1.585  -4.522  -1.074
```

```
ATOM     36    O                   2.140  -3.345   0.520
ATOM     37    H                   3.816  -3.438  -1.916
ATOM     38    O                   4.658  -1.589  -3.529
ATOM     39    H                   2.903  -0.850  -4.249
ATOM     40    H                   3.650   0.058  -2.869
ATOM     41    H                   2.772  -4.016   0.725
ATOM     42    H                   5.149  -1.609  -2.724
CONECT    1    2    3    4
CONECT    2    1    5    9
CONECT    3    6    1    7    8
CONECT    4    1
CONECT    5    2   10   11   12
CONECT    6   10    3   19   20
CONECT    7    3   15   16   17
CONECT    8    3   13   14   18
CONECT    9    2
CONECT   10    5    6   25   26
CONECT   11    5   31   32   33
CONECT   12    5   34
CONECT   13    8   21   30
CONECT   14   22    8   23   24
CONECT   15    7
CONECT   16    7
CONECT   17    7
CONECT   18    8   27   28   29
CONECT   19    6
CONECT   20    6
CONECT   21   13   22   37
CONECT   22   21   14   35   36
CONECT   23   14
CONECT   24   14
CONECT   25   10
CONECT   26   10
CONECT   27   18
CONECT   28   18
CONECT   29   18
CONECT   30   13   38   39   40
CONECT   31   11
CONECT   32   11
CONECT   33   11
CONECT   34   12
CONECT   35   22
CONECT   36   22   41
CONECT   37   21
CONECT   38   30   42
CONECT   39   30
CONECT   40   30
CONECT   41   36
CONECT   42   38
END
```

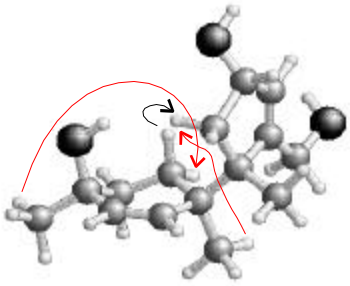

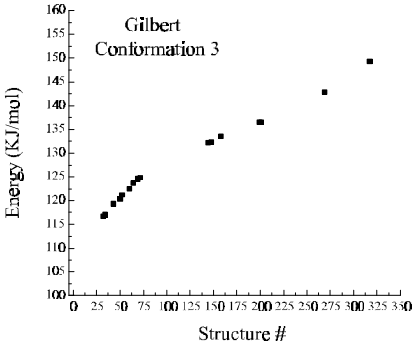

Gilbert #3

Lowest energy structure: structure #12, E = 110.52 KJ/mol (26.42 Kcal/mol).

Description: Quaternary methyls gauche, pseudo chair, primary OH back, methyl front.

NOE violations: two (4.569 Å, 4.850 Å) - seen in red.

Expected NOEs not seen: one (2.193 Å) - seen in black.

PDB-format file:

```
ATOM      1    C                0.000   0.000   0.000
ATOM      2    C                0.000   0.000   1.341
ATOM      3    C                1.239   0.000  -0.884
ATOM      4    H               -0.978   0.022  -0.508
ATOM      5    C                1.251  -0.031   2.183
ATOM      6    C                2.510  -0.197  -0.017
ATOM      7    C                1.283   1.411  -1.516
ATOM      8    C                1.098  -1.136  -1.954
ATOM      9    H               -0.965   0.004   1.876
ATOM     10    C                2.440   0.487   1.356
ATOM     11    C                1.070   0.825   3.450
ATOM     12    O                1.510  -1.356   2.605
ATOM     13    C                2.395  -1.593  -2.614
ATOM     14    C                0.619  -2.459  -1.277
ATOM     15    H                0.349   1.660  -2.069
ATOM     16    H                1.396   2.206  -0.745
ATOM     17    H                2.131   1.529  -2.226
ATOM     18    C                0.108  -0.810  -3.096
ATOM     19    H                3.409   0.186  -0.550
ATOM     20    H                2.712  -1.278   0.154
ATOM     21    C                2.515  -2.927  -2.601
ATOM     22    C                1.351  -3.625  -1.962
ATOM     23    H               -0.488  -2.589  -1.296
ATOM     24    H                0.907  -2.472  -0.201
ATOM     25    H                2.346   1.589   1.216
ATOM     26    H                3.391   0.324   1.917
ATOM     27    H               -0.026  -1.682  -3.776
ATOM     28    H               -0.902  -0.544  -2.714
ATOM     29    H                0.456   0.033  -3.734
ATOM     30    C                3.342  -0.666  -3.339
ATOM     31    H                1.997   0.825   4.068
ATOM     32    H                0.833   1.883   3.193
ATOM     33    H                0.243   0.438   4.089
ATOM     34    H                1.534  -1.924   1.855
ATOM     35    H                0.726  -4.121  -2.744
ATOM     36    O                1.756  -4.586  -1.014
ATOM     37    H                3.336  -3.496  -3.067
```

```
ATOM     38    O                    4.330  -1.344  -4.087
ATOM     39    H                    2.771  -0.045  -4.068
ATOM     40    H                    3.873   0.008  -2.631
ATOM     41    H                    2.140  -5.313  -1.477
ATOM     42    H                    4.895  -1.796  -3.483
CONECT    1    2    3    4
CONECT    2    1    5    9
CONECT    3    6    1    7    8
CONECT    4    1
CONECT    5    2   10   11   12
CONECT    6   10    3   19   20
CONECT    7    3   15   16   17
CONECT    8    3   13   14   18
CONECT    9    2
CONECT   10    5    6   25   26
CONECT   11    5   31   32   33
CONECT   12    5   34
CONECT   13    8   21   30
CONECT   14   22    8   23   24
CONECT   15    7
CONECT   16    7
CONECT   17    7
CONECT   18    8   27   28   29
CONECT   19    6
CONECT   20    6
CONECT   21   13   22   37
CONECT   22   21   14   35   36
CONECT   23   14
CONECT   24   14
CONECT   25   10
CONECT   26   10
CONECT   27   18
CONECT   28   18
CONECT   29   18
CONECT   30   13   38   39   40
CONECT   31   11
CONECT   32   11
CONECT   33   11
CONECT   34   12
CONECT   35   22
CONECT   36   22   41
CONECT   37   21
CONECT   38   30   42
CONECT   39   30
CONECT   40   30
CONECT   41   36
CONECT   42   38
END
```

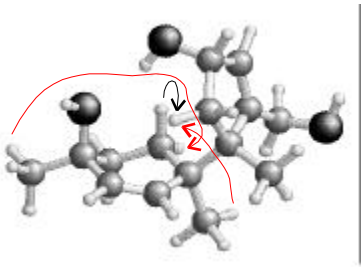

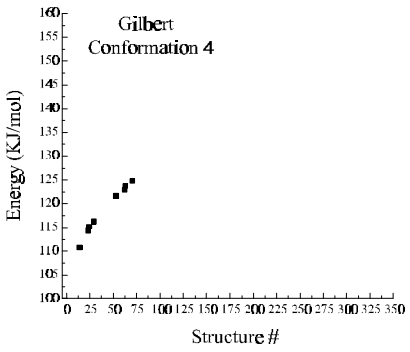

Gilbert #4

Lowest energy structure: structure #14, E = 110.91 KJ/mol (26.51 Kcal/mol).

Description: Quaternary methyls gauche, pseudo chair, H-bond with secondary OH (2.116 Å)*, five-membered ring donor, primary OH back, methyl front.

NOE violations: two (4.372 Å, 4.891 Å) - seen in red.

Expected NOEs not seen: one (3.029 Å)* - seen in black.

PDB-format file:

```
ATOM      1    C                0.000   0.000   0.000
ATOM      2    C                0.000   0.000   1.340
ATOM      3    C                1.246   0.000  -0.874
ATOM      4    H               -0.974   0.009  -0.518
ATOM      5    C                1.266  -0.030   2.159
ATOM      6    C                2.537   0.023  -0.017
ATOM      7    C                1.163   1.358  -1.617
ATOM      8    C                1.219  -1.252  -1.824
ATOM      9    H               -0.961  -0.001   1.882
ATOM     10    C                2.368   0.684   1.358
ATOM     11    C                1.067   0.640   3.529
ATOM     12    O                1.656  -1.376   2.364
ATOM     13    C                2.602  -1.703  -2.280
ATOM     14    C                0.725  -2.544  -1.086
ATOM     15    H                0.208   1.491  -2.173
ATOM     16    H                1.218   2.213  -0.905
ATOM     17    H                1.990   1.503  -2.345
ATOM     18    C                0.331  -1.035  -3.068
ATOM     19    H                3.370   0.515  -0.573
ATOM     20    H                2.895  -1.010   0.176
ATOM     21    C                2.956  -2.892  -1.776
ATOM     22    C                1.911  -3.511  -0.899
ATOM     23    H               -0.033  -3.068  -1.715
ATOM     24    H                0.204  -2.369  -0.120
ATOM     25    H                2.113   1.762   1.234
ATOM     26    H                3.331   0.644   1.921
ATOM     27    H                0.314  -1.937  -3.723
ATOM     28    H               -0.722  -0.813  -2.784
ATOM     29    H                0.693  -0.201  -3.710
ATOM     30    C                3.483  -0.937  -3.233
ATOM     31    H                2.009   0.624   4.124
ATOM     32    H                0.757   1.704   3.414
ATOM     33    H                0.284   0.121   4.128
ATOM     34    H                1.028  -1.783   2.939
ATOM     35    H                1.673  -4.544  -1.257
```

```
ATOM     36    O                   2.308  -3.606   0.452
ATOM     37    H                   3.910  -3.400  -1.989
ATOM     38    O                   3.111  -1.155  -4.577
ATOM     39    H                   3.460   0.157  -3.036
ATOM     40    H                   4.544  -1.266  -3.129
ATOM     41    H                   2.229  -2.768   0.879
ATOM     42    H                   3.251  -2.067  -4.770
CONECT    1    2    3    4
CONECT    2    1    5    9
CONECT    3    6    1    7    8
CONECT    4    1
CONECT    5    2   10   11   12
CONECT    6   10    3   19   20
CONECT    7    3   15   16   17
CONECT    8    3   13   14   18
CONECT    9    2
CONECT   10    5    6   25   26
CONECT   11    5   31   32   33
CONECT   12    5   34
CONECT   13    8   21   30
CONECT   14   22    8   23   24
CONECT   15    7
CONECT   16    7
CONECT   17    7
CONECT   18    8   27   28   29
CONECT   19    6
CONECT   20    6
CONECT   21   13   22   37
CONECT   22   21   14   35   36
CONECT   23   14
CONECT   24   14
CONECT   25   10
CONECT   26   10
CONECT   27   18
CONECT   28   18
CONECT   29   18
CONECT   30   13   38   39   40
CONECT   31   11
CONECT   32   11
CONECT   33   11
CONECT   34   12
CONECT   35   22
CONECT   36   22   41
CONECT   37   21
CONECT   38   30   42
CONECT   39   30
CONECT   40   30
CONECT   41   36
CONECT   42   38
END
```

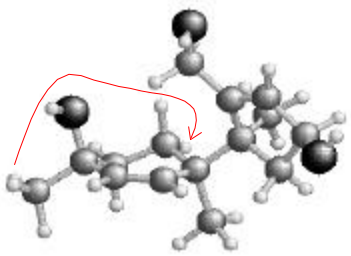

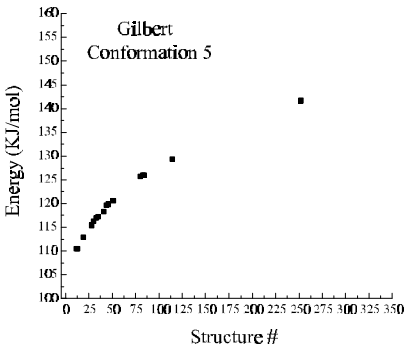

Gilbert #5

Lowest energy structure: structure #25, E = 115.33 KJ/mol (27.57 Kcal/mol).

Description: Quaternary methyls gauche, pseudo chair, secondary OH front, methyl back.

NOE violations: one (4.867 Å) - seen in red.

Expected NOEs not seen: **none**.

PDB-format file:

```
ATOM      1    C                0.000   0.000   0.000
ATOM      2    C                0.000   0.000   1.341
ATOM      3    C                1.243   0.000  -0.872
ATOM      4    H               -0.978   0.029  -0.508
ATOM      5    C                1.244  -0.060   2.196
ATOM      6    C                2.484  -0.321   0.001
ATOM      7    C                1.411   1.451  -1.395
ATOM      8    C                1.078  -1.004  -2.065
ATOM      9    H               -0.967   0.010   1.873
ATOM     10    C                2.471   0.368   1.374
ATOM     11    C                1.094   0.831   3.442
ATOM     12    O                1.453  -1.391   2.628
ATOM     13    C                0.378  -2.320  -1.735
ATOM     14    C                0.120  -0.471  -3.174
ATOM     15    H                0.527   1.818  -1.962
ATOM     16    H                1.540   2.186  -0.571
ATOM     17    H                2.296   1.550  -2.061
ATOM     18    C                2.424  -1.354  -2.741
ATOM     19    H                3.419  -0.038  -0.537
ATOM     20    H                2.555  -1.414   0.189
ATOM     21    C               -0.480  -2.681  -2.699
ATOM     22    C               -0.540  -1.697  -3.830
ATOM     23    H                0.623   0.188  -3.920
ATOM     24    H               -0.706   0.119  -2.716
ATOM     25    H                2.475   1.475   1.248
ATOM     26    H                3.404   0.123   1.936
ATOM     27    H                2.282  -1.986  -3.647
ATOM     28    H                2.968  -0.440  -3.070
ATOM     29    H                3.101  -1.930  -2.071
ATOM     30    C                0.715  -3.179  -0.542
ATOM     31    H                2.016   0.803   4.069
ATOM     32    H                0.908   1.892   3.158
ATOM     33    H                0.245   0.500   4.083
ATOM     34    H                0.718  -1.652   3.157
ATOM     35    H                0.031  -2.080  -4.711
```

```
ATOM     36    O                  -1.860  -1.407  -4.229
ATOM     37    H                  -1.063  -3.616  -2.720
ATOM     38    O                  -0.002  -4.396  -0.503
ATOM     39    H                   1.796  -3.448  -0.567
ATOM     40    H                   0.484  -2.635   0.401
ATOM     41    H                  -2.203  -2.162  -4.677
ATOM     42    H                  -0.916  -4.189  -0.404
CONECT    1    2    3    4
CONECT    2    1    5    9
CONECT    3    6    1    7    8
CONECT    4    1
CONECT    5    2   10   11   12
CONECT    6   10    3   19   20
CONECT    7    3   15   16   17
CONECT    8    3   13   14   18
CONECT    9    2
CONECT   10    5    6   25   26
CONECT   11    5   31   32   33
CONECT   12    5   34
CONECT   13    8   21   30
CONECT   14   22    8   23   24
CONECT   15    7
CONECT   16    7
CONECT   17    7
CONECT   18    8   27   28   29
CONECT   19    6
CONECT   20    6
CONECT   21   13   22   37
CONECT   22   21   14   35   36
CONECT   23   14
CONECT   24   14
CONECT   25   10
CONECT   26   10
CONECT   27   18
CONECT   28   18
CONECT   29   18
CONECT   30   13   38   39   40
CONECT   31   11
CONECT   32   11
CONECT   33   11
CONECT   34   12
CONECT   35   22
CONECT   36   22   41
CONECT   37   21
CONECT   38   30   42
CONECT   39   30
CONECT   40   30
CONECT   41   36
CONECT   42   38
END
```

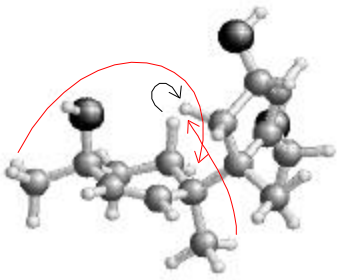

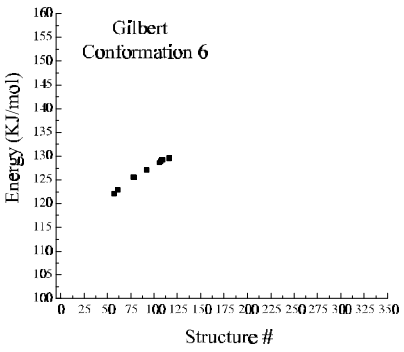

Gilbert #6

Lowest energy structure: structure #31, E = 116.37 KJ/mol (27.82 Kcal/mol).

Description: Quaternary methyls gauche, pseudo chair, primary OH back, methyl front.

NOE violations: two (4.564 Å, 4.882 Å) - seen in red.

Expected NOEs not seen: one (2.272 Å) - seen in black.

PDB-format file:

```
ATOM      1    C                0.000   0.000   0.000
ATOM      2    C                0.000   0.000   1.341
ATOM      3    C                1.244   0.000  -0.877
ATOM      4    H               -0.975   0.025  -0.516
ATOM      5    C                1.253  -0.040   2.181
ATOM      6    C                2.514  -0.180  -0.010
ATOM      7    C                1.262   1.419  -1.497
ATOM      8    C                1.121  -1.153  -1.932
ATOM      9    H               -0.965   0.007   1.876
ATOM     10    C                2.432   0.510   1.360
ATOM     11    C                1.074   0.770   3.477
ATOM     12    O                1.543  -1.380   2.530
ATOM     13    C                2.423  -1.724  -2.479
ATOM     14    C                0.524  -2.434  -1.268
ATOM     15    H                0.337   1.646  -2.075
ATOM     16    H                1.325   2.209  -0.716
ATOM     17    H                2.124   1.584  -2.176
ATOM     18    C                0.252  -0.785  -3.153
ATOM     19    H                3.407   0.204  -0.555
ATOM     20    H                2.711  -1.261   0.175
ATOM     21    C                2.419  -3.064  -2.499
ATOM     22    C                1.143  -3.653  -1.975
ATOM     23    H               -0.591  -2.464  -1.282
ATOM     24    H                0.834  -2.485  -0.199
ATOM     25    H                2.318   1.610   1.223
ATOM     26    H                3.385   0.360   1.922
ATOM     27    H                0.092  -1.661  -3.823
ATOM     28    H               -0.757  -0.426  -2.851
ATOM     29    H                0.729   0.004  -3.778
ATOM     30    C                3.528  -0.926  -3.118
ATOM     31    H                2.004   0.757   4.090
ATOM     32    H                0.828   1.834   3.256
ATOM     33    H                0.253   0.357   4.107
ATOM     34    H                0.821  -1.719   3.031
ATOM     35    H                0.514  -4.023  -2.822
ATOM     36    O                1.361  -4.709  -1.068
ATOM     37    H                3.224  -3.687  -2.921
```

```
ATOM     38    O                   4.770  -1.145  -2.484
ATOM     39    H                   3.628  -1.223  -4.189
ATOM     40    H                   3.326   0.166  -3.094
ATOM     41    H                   1.674  -5.454  -1.554
ATOM     42    H                   5.001  -2.052  -2.594
CONECT    1    2    3    4
CONECT    2    1    5    9
CONECT    3    6    1    7    8
CONECT    4    1
CONECT    5    2   10   11   12
CONECT    6   10    3   19   20
CONECT    7    3   15   16   17
CONECT    8    3   13   14   18
CONECT    9    2
CONECT   10    5    6   25   26
CONECT   11    5   31   32   33
CONECT   12    5   34
CONECT   13    8   21   30
CONECT   14   22    8   23   24
CONECT   15    7
CONECT   16    7
CONECT   17    7
CONECT   18    8   27   28   29
CONECT   19    6
CONECT   20    6
CONECT   21   13   22   37
CONECT   22   21   14   35   36
CONECT   23   14
CONECT   24   14
CONECT   25   10
CONECT   26   10
CONECT   27   18
CONECT   28   18
CONECT   29   18
CONECT   30   13   38   39   40
CONECT   31   11
CONECT   32   11
CONECT   33   11
CONECT   34   12
CONECT   35   22
CONECT   36   22   41
CONECT   37   21
CONECT   38   30   42
CONECT   39   30
CONECT   40   30
CONECT   41   36
CONECT   42   38
END
```

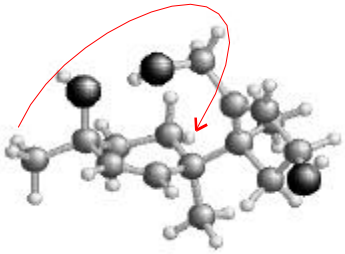

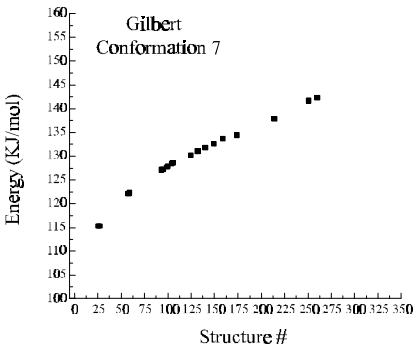

Gilbert #7

Lowest energy structure: structure #32, E = 116.81 KJ/mol (27.92 Kcal/mol).

Description: Quaternary methyls gauche, pseudo chair, H-bond with primary OH (1.908 Å), five-membered ring donor, secondary OH front, methyl back.

NOE violations: one (4.894 Å) - seen in red.

Expected NOEs not seen: **none**.

PDB-format file:

```
ATOM      1    C                0.000   0.000   0.000
ATOM      2    C                0.000   0.000   1.341
ATOM      3    C                1.242   0.000  -0.873
ATOM      4    H               -0.979   0.042  -0.504
ATOM      5    C                1.249  -0.096   2.184
ATOM      6    C                2.499  -0.269  -0.008
ATOM      7    C                1.379   1.447  -1.417
ATOM      8    C                1.093  -1.028  -2.048
ATOM      9    H               -0.965   0.018   1.875
ATOM     10    C                2.459   0.398   1.375
ATOM     11    C                1.088   0.708   3.486
ATOM     12    O                1.453  -1.457   2.519
ATOM     13    C                0.446  -2.370  -1.710
ATOM     14    C                0.103  -0.525  -3.146
ATOM     15    H                0.483   1.795  -1.977
ATOM     16    H                1.510   2.193  -0.602
ATOM     17    H                2.253   1.555  -2.097
ATOM     18    C                2.438  -1.338  -2.743
ATOM     19    H                3.420   0.058  -0.546
ATOM     20    H                2.621  -1.358   0.165
ATOM     21    C               -0.436  -2.745  -2.648
ATOM     22    C               -0.556  -1.764  -3.776
ATOM     23    H                0.582   0.133  -3.909
ATOM     24    H               -0.723   0.061  -2.683
ATOM     25    H                2.417   1.506   1.270
ATOM     26    H                3.400   0.176   1.935
ATOM     27    H                2.300  -1.980  -3.643
ATOM     28    H                2.949  -0.411  -3.087
ATOM     29    H                3.144  -1.887  -2.080
ATOM     30    C                0.838  -3.297  -0.585
ATOM     31    H                2.014   0.663   4.103
ATOM     32    H                0.877   1.781   3.271
ATOM     33    H                0.251   0.314   4.108
ATOM     34    H                2.106  -1.515   3.198
ATOM     35    H               -0.006  -2.138  -4.674
```

```
ATOM     36    O                -1.894  -1.502  -4.132
ATOM     37    H                -0.977  -3.705  -2.653
ATOM     38    O                 0.110  -3.074   0.603
ATOM     39    H                 0.612  -4.347  -0.890
ATOM     40    H                 1.929  -3.273  -0.371
ATOM     41    H                -2.248  -2.280  -4.528
ATOM     42    H                 0.584  -2.467   1.150
CONECT    1    2    3    4
CONECT    2    1    5    9
CONECT    3    6    1    7    8
CONECT    4    1
CONECT    5    2   10   11   12
CONECT    6   10    3   19   20
CONECT    7    3   15   16   17
CONECT    8    3   13   14   18
CONECT    9    2
CONECT   10    5    6   25   26
CONECT   11    5   31   32   33
CONECT   12    5   34
CONECT   13    8   21   30
CONECT   14   22    8   23   24
CONECT   15    7
CONECT   16    7
CONECT   17    7
CONECT   18    8   27   28   29
CONECT   19    6
CONECT   20    6
CONECT   21   13   22   37
CONECT   22   21   14   35   36
CONECT   23   14
CONECT   24   14
CONECT   25   10
CONECT   26   10
CONECT   27   18
CONECT   28   18
CONECT   29   18
CONECT   30   13   38   39   40
CONECT   31   11
CONECT   32   11
CONECT   33   11
CONECT   34   12
CONECT   35   22
CONECT   36   22   41
CONECT   37   21
CONECT   38   30   42
CONECT   39   30
CONECT   40   30
CONECT   41   36
CONECT   42   38
END
```

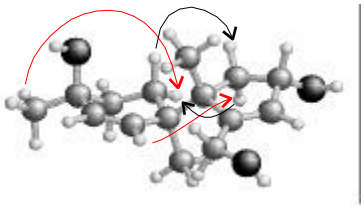

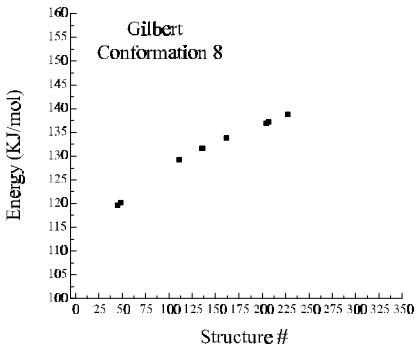

Gilbert #8

Lowest energy structure: structure #36, E = 117.43 KJ/mol (28.07 Kcal/mol).

Description: Quaternary methyls anti, pseudo chair, primary OH front, "flat structure".

NOE violations: two (4.642 Å, 4.878 Å) - seen in red.

Expected NOEs not seen: two (2.309 Å, 2.512 Å) - seen in black.

PDB-format file:

```
ATOM      1    C                0.000   0.000   0.000
ATOM      2    C                0.000   0.000   1.341
ATOM      3    C                1.233   0.000  -0.888
ATOM      4    H               -0.981   0.031  -0.497
ATOM      5    C                1.250  -0.037   2.184
ATOM      6    C                2.497  -0.194  -0.005
ATOM      7    C                1.322   1.406  -1.530
ATOM      8    C                1.131  -1.139  -1.962
ATOM      9    H               -0.965   0.010   1.876
ATOM     10    C                2.424   0.510   1.357
ATOM     11    C                1.071   0.780   3.477
ATOM     12    O                1.538  -1.376   2.538
ATOM     13    C                0.244  -0.877  -3.180
ATOM     14    C                2.502  -1.372  -2.667
ATOM     15    H                0.450   1.647  -2.173
ATOM     16    H                1.359   2.208  -0.759
ATOM     17    H                2.226   1.532  -2.165
ATOM     18    C                0.661  -2.480  -1.350
ATOM     19    H                3.411   0.158  -0.540
ATOM     20    H                2.669  -1.274   0.198
ATOM     21    C                0.844  -1.251  -4.319
ATOM     22    C                2.211  -1.830  -4.105
ATOM     23    H                3.168  -2.085  -2.126
ATOM     24    H                3.054  -0.410  -2.749
ATOM     25    H                2.309   1.609   1.211
ATOM     26    H                3.378   0.365   1.918
ATOM     27    H                0.661  -3.297  -2.107
ATOM     28    H                1.314  -2.820  -0.517
ATOM     29    H               -0.375  -2.422  -0.946
ATOM     30    C               -1.206  -0.455  -3.105
ATOM     31    H                2.001   0.767   4.090
ATOM     32    H                0.828   1.843   3.250
ATOM     33    H                0.249   0.371   4.108
ATOM     34    H                0.831  -1.701   3.070
ATOM     35    H                2.177  -2.943  -4.204
```

```
ATOM     36    O                3.166  -1.316  -5.005
ATOM     37    H                0.384  -1.233  -5.319
ATOM     38    O               -1.865  -0.472  -4.354
ATOM     39    H               -1.762  -1.165  -2.450
ATOM     40    H               -1.315   0.575  -2.698
ATOM     41    H                2.987  -1.674  -5.858
ATOM     42    H               -1.462   0.179  -4.904
CONECT    1    2    3    4
CONECT    2    1    5    9
CONECT    3    6    1    7    8
CONECT    4    1
CONECT    5    2   10   11   12
CONECT    6   10    3   19   20
CONECT    7    3   15   16   17
CONECT    8    3   13   14   18
CONECT    9    2
CONECT   10    5    6   25   26
CONECT   11    5   31   32   33
CONECT   12    5   34
CONECT   13    8   21   30
CONECT   14   22    8   23   24
CONECT   15    7
CONECT   16    7
CONECT   17    7
CONECT   18    8   27   28   29
CONECT   19    6
CONECT   20    6
CONECT   21   13   22   37
CONECT   22   21   14   35   36
CONECT   23   14
CONECT   24   14
CONECT   25   10
CONECT   26   10
CONECT   27   18
CONECT   28   18
CONECT   29   18
CONECT   30   13   38   39   40
CONECT   31   11
CONECT   32   11
CONECT   33   11
CONECT   34   12
CONECT   35   22
CONECT   36   22   41
CONECT   37   21
CONECT   38   30   42
CONECT   39   30
CONECT   40   30
CONECT   41   36
CONECT   42   38
END
```

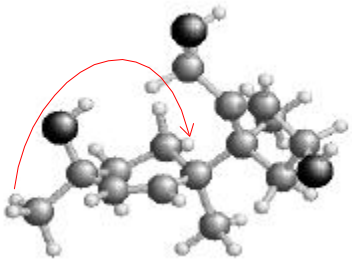

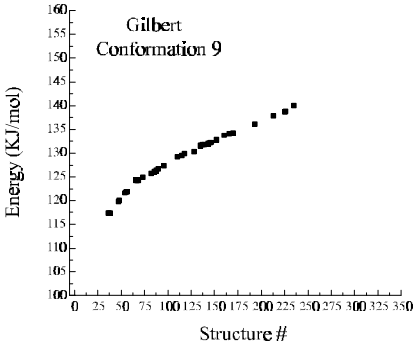

Gilbert #9

Lowest energy structure: structure #45, E = 119.69 KJ/mol (28.61 Kcal/mol).

Description: Quaternary methyls gauche, pseudo chair, secondary OH front, methyl back.

NOE violations: one (4.816 Å) - seen in red.

Expected NOEs not seen: **none**.

PDB-format file:

```
ATOM      1    C                0.000   0.000   0.000
ATOM      2    C                0.000   0.000   1.341
ATOM      3    C                1.244   0.000  -0.871
ATOM      4    H               -0.978   0.033  -0.509
ATOM      5    C                1.240  -0.064   2.202
ATOM      6    C                2.458  -0.427  -0.009
ATOM      7    C                1.478   1.472  -1.304
ATOM      8    C                1.037  -0.926  -2.122
ATOM      9    H               -0.967   0.013   1.872
ATOM     10    C                2.504   0.238   1.375
ATOM     11    C                1.128   0.924   3.378
ATOM     12    O                1.353  -1.360   2.763
ATOM     13    C                0.303  -2.241  -1.865
ATOM     14    C                0.085  -0.295  -3.186
ATOM     15    H                0.627   1.903  -1.875
ATOM     16    H                1.605   2.158  -0.438
ATOM     17    H                2.388   1.576  -1.937
ATOM     18    C                2.366  -1.276  -2.831
ATOM     19    H                3.408  -0.200  -0.545
ATOM     20    H                2.448  -1.525   0.158
ATOM     21    C               -0.601  -2.504  -2.820
ATOM     22    C               -0.666  -1.446  -3.881
ATOM     23    H                0.612   0.364  -3.916
ATOM     24    H               -0.693   0.325  -2.685
ATOM     25    H                2.618   1.338   1.256
ATOM     26    H                3.412  -0.097   1.933
ATOM     27    H                2.194  -1.875  -3.755
ATOM     28    H                2.923  -0.361  -3.136
ATOM     29    H                3.043  -1.886  -2.193
ATOM     30    C                0.645  -3.197  -0.751
ATOM     31    H                2.045   0.897   4.011
ATOM     32    H                0.996   1.969   3.015
ATOM     33    H                0.262   0.681   4.034
ATOM     34    H                1.395  -1.994   2.069
ATOM     35    H               -0.159  -1.797  -4.813
```

```
ATOM     36    O                -1.988  -1.067  -4.191
ATOM     37    H                -1.219  -3.413  -2.879
ATOM     38    O                -0.043  -4.430  -0.829
ATOM     39    H                 1.734  -3.433  -0.776
ATOM     40    H                 0.379  -2.742   0.231
ATOM     41    H                -2.405  -1.782  -4.642
ATOM     42    H                 0.207  -4.854  -1.632
CONECT    1    2    3    4
CONECT    2    1    5    9
CONECT    3    6    1    7    8
CONECT    4    1
CONECT    5    2   10   11   12
CONECT    6   10    3   19   20
CONECT    7    3   15   16   17
CONECT    8    3   13   14   18
CONECT    9    2
CONECT   10    5    6   25   26
CONECT   11    5   31   32   33
CONECT   12    5   34
CONECT   13    8   21   30
CONECT   14   22    8   23   24
CONECT   15    7
CONECT   16    7
CONECT   17    7
CONECT   18    8   27   28   29
CONECT   19    6
CONECT   20    6
CONECT   21   13   22   37
CONECT   22   21   14   35   36
CONECT   23   14
CONECT   24   14
CONECT   25   10
CONECT   26   10
CONECT   27   18
CONECT   28   18
CONECT   29   18
CONECT   30   13   38   39   40
CONECT   31   11
CONECT   32   11
CONECT   33   11
CONECT   34   12
CONECT   35   22
CONECT   36   22   41
CONECT   37   21
CONECT   38   30   42
CONECT   39   30
CONECT   40   30
CONECT   41   36
CONECT   42   38
END
```

ADDENDUM IV: *AB INITIO CALCULATIONS ON THE CYCLIC THIOCARBONATE SYSTEM*

- *Introduction:*

It was observed experimentally[201], that upon homolytic fragmentation of a six-membered ring cyclic thionocarbonate attached to a five-membered ring, the formation of primary or secondary radicals could be controlled through the relative stereochemistry at the ring junction. When the ring junction was *trans*, the major product derived from the primary radical and when the ring junction was *cis* the major product derived from the secondary radical.

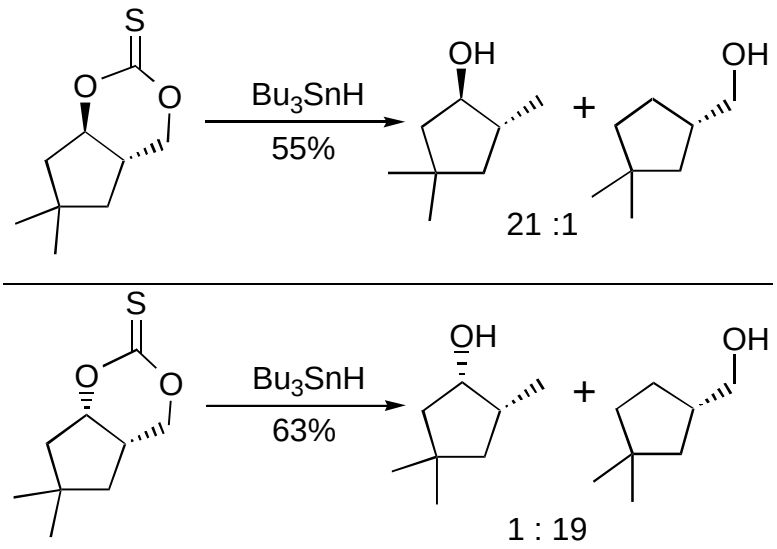

Figure IV.1

[201] (a) Ziegler, F. E.; Zheng, Z. L. *Tetrahedron Lett.* **1987**, *28*, 5973. (b) Ziegler, F. E.; Zheng, Z. L. *J. Org. Chem.* **1990**, *55*, 1416.

Ab initio calculations were used to address the question of whether the bond cleavage selectivity observed was due to thermodynamics and the stability of a specific intermediate, or due to other factors such as charge/spin distribution, ring strain release or orbital overlap.

Geometry calculations were conducted on a simplified version of the fragmentation system shown in Figure IV.1. Initially, a series of molecules was examined to determine if there was something inherently different about the 6-5-ring system (molecules **9** - **12**) *versus* a 6-6-ring system (molecules **7** - **10**) or a dimethyl substituted six-membered ring thionocarbonate (molecules **1** - **4**), in the context of *cis* versus *trans* substitution. Additionally, the effect of replacing sulfur with oxygen was explored in light of previous molecular mechanics studies[201] conducted in carbonates in order to clarify if there were fundamental differences in the thionocarbonate system's reactivity. Finally, the fragmentation reaction itself was examined starting from molecule **11**, representing the *cis* configuration and **12**, representing the *trans* configuration.

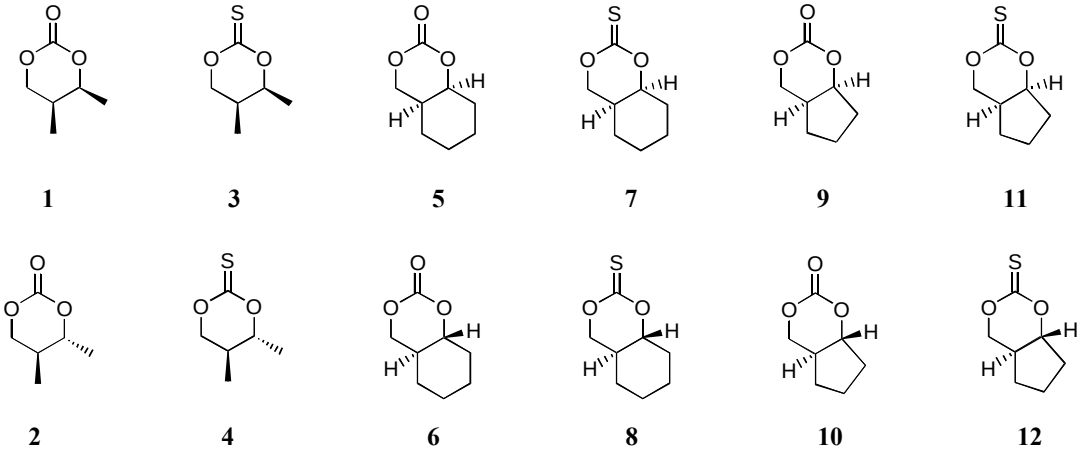

- *The ab initio procedure:*

The *ab initio* calculations were carried out using the software package Gaussian 94, Revision E.1[202]. Geometry calculations were conducted from an internally generated redundant internal coordinate system. Structures were fully optimized[203] at the RHF/6-31G* level[204] (as the highest level) for non-radical molecules and at the UHF/6-31G* level for radical molecules, using the Berny algorithm[205]. The geometries for the transition states were calculated using the Synchronous Transit-Guided Quasi-Newton (STQN) method. This method (keyword: QST3) uses a linear synchronous transit or quadratic synchronous transit approach to get closer to the quadratic region of the energy curve around the transition state, and then uses a quasi-Newton or eigenvector-following algorithm to complete the optimization. This generates a transition state structure that is midway between the reactants and products in terms of redundant internal coordinates, and then goes on to optimize this structure to a first-order saddle point. Assuming

---

[202] Gaussian 94, Revision E.1: M. J. Frisch, G. W. Trucks, H. B. Schlegel, P. M. W. Gill, B. G. Johnson, M. A. Robb, J. R. Cheeseman, T. Keith, G. A. Petersson, J. A. Montgomery, K. Raghavachari, M. A. Al-Laham, V. G. Zakrzewski, J. V. Ortiz, J. B. Foresman, J. Cioslowski, B. B. Stefanov, A. Nanayakkara, M. Challacombe, C. Y. Peng, P. Y. Ayala, W. Chen, M. W. Wong, J. L. Andres, E. S. Replogle, R. Gomperts, R. L. Martin, D. J. Fox, J. S. Binkley, D. J. Defrees, J. Baker, J. P. Stewart, M. Head-Gordon, C. Gonzalez, and J. A. Pople, Gaussian, Inc., Pittsburgh PA, 1995.

[203] Optimizations and vibrational frequency calculations used the analytical first and second derivative methods available with the Gaussian package.

[204] Basis set: 6-31G: Applies to: H-Cl. Polarization functions (3df,3pd). Diffuse functions ++.

[205] At each step of a Berny optimization the following actions are taken: The Hessian is updated; the trust radius (maximum allowed Newton-Raphson step) is updated if a minimum is sought, using the method of Fletcher; if a maximum is sought, the program performs a linear search between the latest point and the best previous point (the previous point having lowest energy). If the latest point is the best so far but if the newest point is not the best, the linear search must return a point in between the most recent and the best step to be acceptable. If all fits fail and the most recent step is the best so far, no linear step is taken. If all fits fail and the most recent step is not the best, the linear step is taken to the midpoint of the line connecting the most recent and the best previous points. Finally, convergence is tested against criteria for

stretching of the bonds involved in the cleavage provided an initial guess for the transition state in these calculations. The calculations were conducted from reagent to product and vice versa with the same results.

Following geometry calculations, frequency analyses were conducted in order to make sure the geometry obtained corresponded to a stable geometry (a minimum for the ground state or a maximum for the transition state). The frequency keyword computes force constants and the resulting vibrational frequencies and their intensities. The force constants were determined analytically whenever possible. The default is to use 298.15 K, 1 atmosphere, and the most abundant isotopes. Unscaled vibrational frequencies for all species were used to characterize stationary points. Each of the ground state structures had no negative eigenvalues and the transition structures had just one negative eigenvalue of the Hessian matrix.

The radicals were also submitted to a stability calculation (keyword: stable) to test the stability of the Hartree-Fock wavefunction. This was accomplished by computing the wavefunction as usual and then verifying if the resulting determinant of the Hessian matrix was a local minimum with the specified number of degrees of freedom. In examining the results prior to a frequency calculation, it sufficed to determine if any singlet instabilities existed for a restricted wavefunction (singlet state molecule) or if any singlet or triplet instability existed for an unrestricted wavefunction (radical).

---

the maximum force component, root-mean-square force, maximum step component, and root-mean-square step. The step is the change between the most recent point and the next to be computed.

Analysis of the calculations utilized the following information: energy[206], charge distribution and geometry. Additionally, the deviation from the ideal angle associated with each molecule or parts of the molecule was evaluated by examining the displacement from the minimized calculated structure to the ideal geometry for each atom as a means of evaluating the bend-angle-strain associated with different portions of the molecule. The strain associated with a molecule has six components, angle strain, torsion strain, strain associated with bond stretching, a cross term that associates stretching with bending, electrostatic interactions and Van der Waals forces. The angle strain portion of the strain was considered important in determining the outcome of the reaction and the one that varied the most throughout the reaction process. A formula was developed (Eq. 1) for qualitatively examining the angle displacement at each atom position in a molecule. This representation of angle displacement was denoted the "offset" and represents a number from 0-1, in which an offset of 0 means the minimized geometry of the molecule is close to the ideal angle distribution and 1 means the maximum possible offset associated with that atom. This offset value could be used to evaluate the ideal angle displacement for the entire molecule or for specific parts of the molecule. This was accomplished by summing the offset on all atoms involved in the region of the molecule being studied.

The offset for an atom was calculated by summing the square of the normalized difference between the energy minimized angle and the ideal hybridization angle (109.6 degrees for an sp^3 center or 120 degrees for an sp^2 center) over all angles involving the atom, then diving by the number of angles.

---

[206] 1 Hartree equals 627.5095 Kcal/mol

$$(1) \qquad offset = \frac{\sum_{i=1}^{N} \left[\left(\theta^{hyb} - \theta_i^{calc} \right) / \theta^{hyb} \right]^2}{N} \qquad \begin{array}{l} \text{for } sp^3 \text{ atom, } ideal\_angle = 109.6^o \\ \text{for } sp^2 \text{ atom, } ideal\_angle = 120^o \end{array} \qquad \text{Eq. 1}$$

Where N is defined as the number of angles involving the atom, θ^{hyb} is the ideal hybridization angle, and θ^{calc} is the calculated angle from the energy-minimized geometry.

- *Sample calculation:*

The steps involved in the calculation of the geometry, frequency and offset-from-the-ideal-angle for the *cis*-dimethyl-carbonate molecule (**1**) are shown below as an example of how these calculations were conducted. First, the actual Gaussian 94 input file for the geometry calculation is displayed; the other Gaussian input files are very similar and will not be shown. Second, summarized results extracted from the Gaussian output "log" files for each calculation are presented. The geometry information obtained by the calculation was transformed into a Protein Data Bank (pdb) file, using the perl script gaussian2pdb.pl, for ease of display. The offset-from-the-ideal-angle was calculated as discussed above by the script angle_strain.pl and the script sum_angle_strain.pl. The angle_strain.pl script creates a text file that can be used along with the pdb file to show the offset-from-the-ideal-angle graphically, as in the drawing in Figure IV.2 (generated using

the Raswin Molecular Graphics[207] package). A similar graphical representation was generated for the display of the charge or spin distribution in the molecule by using the script get_charge.pl.

1. Cis dimethyl carbonate Geometry calculation input file:

```
%chk=ciscarb.chk
%mem=32MB
#P RHF/6-31G* OPT MINPOP

Cis-dimethyl-carbonate geometry calculation

0    1
C
C    1     R2
H    1     R3          2     A3
H    1     R4          2     A4          3     D4          0
H    1     R5          2     A5          3     D5          0
C    2     R6          1     A6          3     D6          0
C    2     R7          1     A7          6     D7          0
H    2     R8          1     A8          6     D8          0
C    6     R9          2     A9          1     D9          0
O    6     R10         2     A10         9     D10         0
O    7     R11         2     A11         1     D11         0
H    6     R12         2     A12         9     D12         0
H    7     R13         2     A13         11    D13         0
H    7     R14         2     A14         11    D14         0
C    10    R15         6     A15         2     D15         0
H    9     R16         6     A16         2     D16         0
H    9     R17         6     A17         16    D17         0
H    9     R18         6     A18         16    D18         0
O    15    R19         10    A19         6     D19         0

R2  =1.5360587
R3  =1.0839627
R4  =1.08196533
R5  =1.08130809
R6  =1.53075197
R7  =1.52752278
R8  =1.08384576
R9  =1.5198039
R10 =1.46029031
R11 =1.45263248
R12 =1.08312181
R13 =1.07692785
R14 =1.0817535
R15 =1.3532833
R16 =1.08166351
R17 =1.0801125
R18 =1.08376274
R19 =1.18917366
A3  = 110.13106118
A4  = 111.30292678
A5  = 110.62137288
A6  = 112.89088224
```

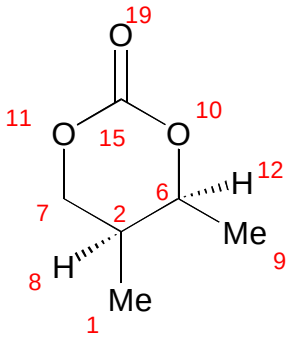

[207] Raswin Molecular Graphics, Windows version 2.6 copyright 1993-1995 R. Sayle, Freeware for molecule visualization downloaded from *http://www.umass.edu/microbio/rasmol*.

```
A7  = 110.90441927
A8  = 110.16877285
A9  = 116.30528266
A10 = 108.71166244
A11 = 110.45216377
A12 = 108.82965216
A13 = 112.42634479
A14 = 110.9286429
A15 = 124.0691475
A16 = 109.27422745
A17 = 110.27567666
A18 = 110.36390674
A19 = 121.96874819
D4  = 119.59575808
D5  =-119.65962609
D6  = 174.55270722
D7  =-118.41023285
D8  = 121.53172655
D9  =  54.46795479
D10 =-118.56875632
D11 =  67.39270586
D12 = 124.56563236
D13 =-117.11771105
D14 = 120.06834693
D15 = -39.00116566
D16 = 179.1315627
D17 = 118.78225922
D18 =-119.9774802
D19 = 190.98539747
```

2. Geometry calculation Results:

Note: HF represents the energy in Hartree units, 1 HF equals 627.5095 Kcal/mol.

G94 - tecate
#P RHF/6-31G* OPT MINPOP
Job CPU time: 9 hours 12 minutes 48.9 seconds.

HF = -457.6374734

Charge distribution

```
  1 C   -0.493262
  2 C   -0.255991
  3 H    0.175311
  4 H   0.179731
  5 H   0.190925
  6 C   0.166100
  7 C   0.007118
  8 H   0.188240
  9 C   -0.490711
 10 O   -0.634657
 11 O   -0.622637
 12 H   0.180208
 13 H   0.202712
 14 H   0.182263
 15 C   1.027624
 16 H   0.195730
 17 H   0.188378
 18 H   0.165337
 19 O   -0.552418
 Sum of Mulliken charges = 0.00000
```

3. Frequency calculation Results:

G94 - tecate

#P RHF/6-31G* FREQ MINPOP
Job CPU time: 0 days 10 hours 56 minutes 35.4 seconds.

NImag=0

4. Geometry pdb file:

```
REMARK Cisdimethylcarbonate geometry calculation.
ATOM      1    C                 0.882  -1.117  -1.582
ATOM      2    C                 0.853  -1.066  -0.051
ATOM      3    H                 1.908  -1.129  -1.935
ATOM      4    H                 0.398  -2.010  -1.956
ATOM      5    H                 0.391  -0.259  -2.026
ATOM      6    C                -0.542  -0.937   0.552
ATOM      7    C                 1.631   0.115   0.501
ATOM      8    H                 1.304  -1.973   0.342
ATOM      9    C                -1.575  -1.945   0.090
ATOM     10    O                -1.078   0.352   0.250
ATOM     11    O                 0.967   1.340   0.236
ATOM     12    H                -0.451  -1.000   1.632
ATOM     13    H                 2.606   0.216   0.047
ATOM     14    H                 1.761   0.025   1.574
ATOM     15    C                -0.353   1.461   0.182
ATOM     16    H                -2.507  -1.784   0.618
ATOM     17    H                -1.769  -1.849  -0.971
ATOM     18    H                -1.232  -2.954   0.296
ATOM     19    O                -0.862   2.514   0.044
CONECT    1    2    3    4    5
CONECT    2    1    6    7    8
CONECT    3    1
CONECT    4    1
CONECT    5    1
CONECT    6    2    9   10   12
CONECT    7    2   11   13   14
CONECT    8    2
CONECT    9    6   16   17   18
CONECT   10    6   15
CONECT   11    7   15
CONECT   12    6
CONECT   13    7
CONECT   14    7
CONECT   15   10   11   19
CONECT   16    9
CONECT   17    9
CONECT   18    9
CONECT   19   15
END
```

5. Calculated Offset-from-the-ideal-angle:

```
Atom number 1 with hybridization sp3 and total strain percentage 0.0268
Atom number 2 with hybridization sp3 and total strain percentage 0.0826
Atom number 6 with hybridization sp3 and total strain percentage 0.0937
Atom number 7 with hybridization sp3 and total strain percentage 0.0482
Atom number 9 with hybridization sp3 and total strain percentage 0.0092
Atom number 10 with hybridization sp3 and total strain percentage 0.2630
Atom number 11 with hybridization sp3 and total strain percentage 0.2180
Atom number 15 with hybridization sp2 and total strain percentage 0.0172

Total conformation strain percent is 0.7587
Total carbonate ring strain percent is 0.7227
Total strain per atom is 0.0948
```

6. Graphical representation:

The graphics in Figure IV.2 were generated using the angle_strain.pl and get_charge.pl scripts respectively to generate scripts that were overlaid on top of the pdb file using the Raswin graphical display package.

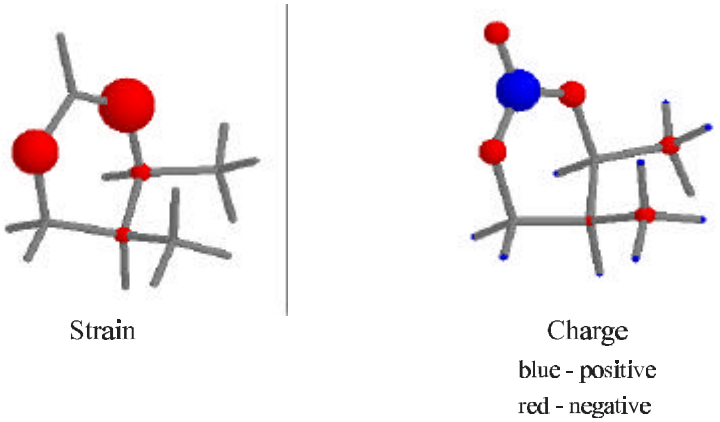

Figure 2: Offset-from-the-ideal-Angle and charge distribution for molecule 1

- *Results: Substituent effects on the carbonate ring:*

Analysis of the effect of substituents on the carbonate ring showed no significant or unexpected difference in energy between the *cis* and the *trans* series (**1** and **2**, **3** and **4**, **5** and **6**, etc).

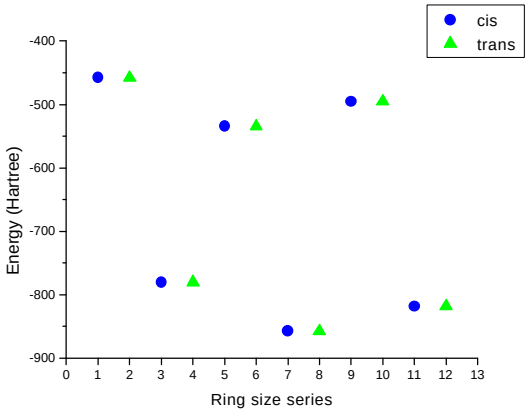

Compound Number	Energy (Hartree) ab initio	Energy (Kcal/mol) MacroModel
1	-457,6375	17,8200
2	-457,6393	17,0400
3	-780,2564	8,5300
4	-780,2582	19,3100
5	-534,5498	21,3400
6	-534,5501	20,3900
7	-857,1689	12,0100
8	-857,1689	23,0100
9	-495,5063	26,0000
10	-495,4997	27,0800
11	-818,1251	23,3100
12	-818,1182	29,7400

Figure IV.3

The energies for these molecules were also calculated using a molecular mechanics methodology with the software package MacroModel. The results from these energy calculations show striking differences between the *cis* and *trans* thiocarbonates pairs (**3** and **4**, **7** and **8**, **11** and **12**), in contrast to the *ab initio* results. This may be attributed to imprecise parameters for calculations involving sulfur atoms or cyclic carbonate and thiocarbonates available with the MM2 package. Figure IV.3 shows a table comparing the results of the *ab initio* and molecular mechanics calculations.

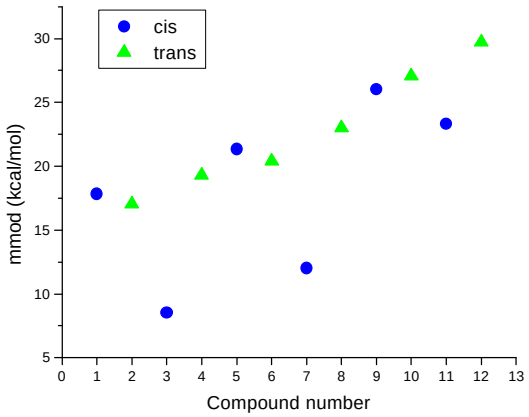

Analysis of charge distribution on the molecules demonstrated that there was very little difference within the series. The trend was that the carbon of the carbonate is positive and the oxygens are negative. There is a larger charge separation for the carbonates when compared to the thionocarbonates.

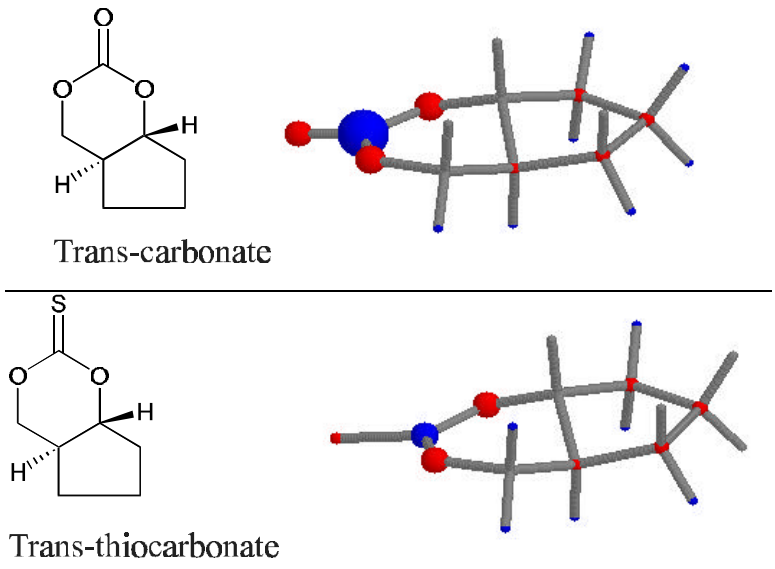

Figure IV.4: carbonate *vs* thiocarbonate charge distribution. Red is negative charge, blue is positive.

The stereochemistry at the ring junction is important in defining the geometrical conformations of the molecules; the *cis* molecules adopted different conformations from the *trans* molecules, as would be expected. The carbonate and thionocarbonate isomer pairs adopted very similar conformations in the 6-6 and dimethyl systems. However, the *cis* compound in the 6-5 ring series carbonate and thiocarbonate (**9** and **11**) adopted different conformations, as shown in Figure IV.5.

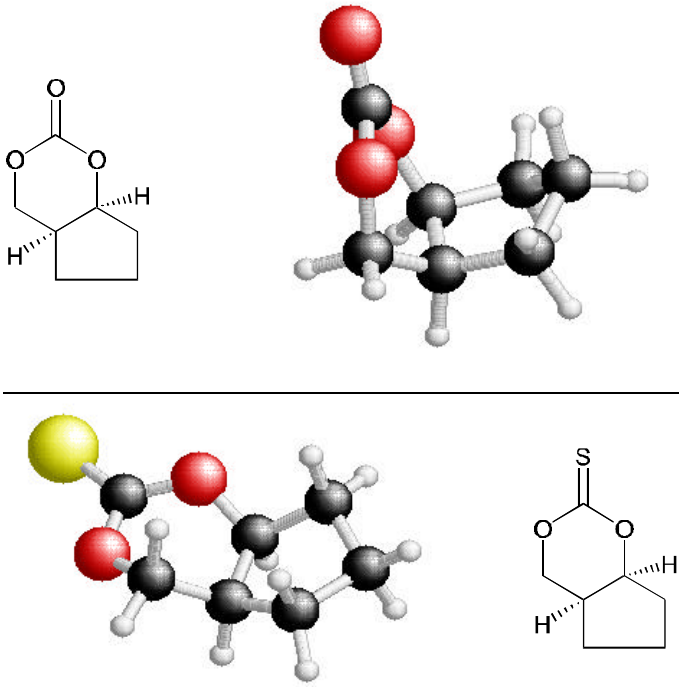

Figure IV.5: Geometry differences in the *cis* 6-5 ring series

Analysis of the distribution of offset-from-the-ideal-angle showed that, unlike the 6-6 system (**5**, **6**, **7**, **8**) and the dimethyl series (**1**, **2**, **3**, **4**), the 6-5 series shows a large difference between the *cis* and the *trans* isomers. The *trans* molecules in the 6-5-ring series (**10, 12**) present a higher offset-from-the-ideal-angle than the *cis* compounds (**9, 11**)

and the *cis* thionocarbonate **11** show less offset-from-the-ideal-angle than its carbonate **9** counterpart. These trends were observed when analyzing the total-offset, the offset-per-atom and the carbonate-offset. Analysis of the ring offset showed a larger offset associated with the five-membered ring (**9**, **10**, **11**, **12**) than the six-membered ring (**5**, **6**, **7**, **8**), but it also showed a larger offset associated with the *trans* compounds **10** and **12** than with the *cis* (**9**, **11**).

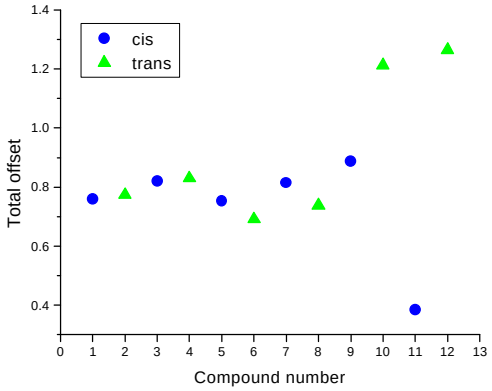

Compound Number	Total Offset	Ring Offset	carbonate Offset	per atom Offset
1	0.7587		0.7227	0.0948
2	0.7741		0.7404	0.0968
3	0.8198		0.7847	0.1025
4	0.8298		0.7979	0.1037
5	0.7533	0.1725	0.6740	0.0753
6	0.6915	0.1341	0.6247	0.0692
7	0.8147	0.1856	0.7341	0.0815
8	0.7375	0.1398	0.6713	0.0738
9	0.8878	0.3824	0.6701	0.0986
10	1.2122	0.5872	0.9816	0.1347
11	0.3847	0.3847	0.2837	0.0427
12	1.2646	0.5961	1.0319	0.1405

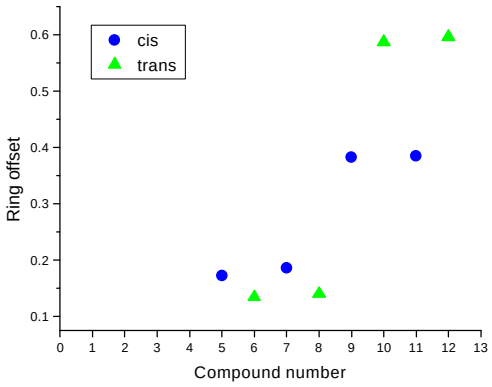

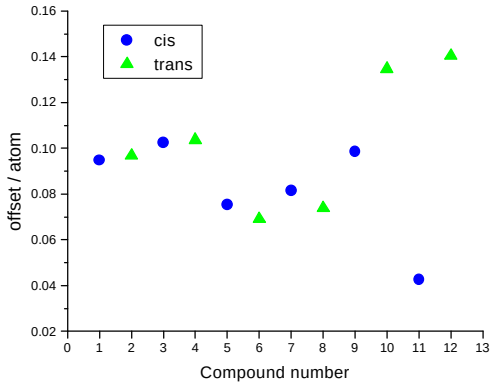

Figure IV.6

The offset-from-the-ideal-angle is slightly larger for the thionocarbonates (**3, 4, 7, and 8**) than the respective carbonates (**1, 2, 5, and 6**) in the dimethyl and 6-6 series. The offset-from-the-ideal-angle is larger for the *trans* thiocarbonate (**12**) than the carbonate counterpart (**10**) in the 6-5 series, while the opposite is true for the *cis* compounds (**11** and **9**).

To conclude, the *ab initio* studies on this series of molecules demonstrated that *cis* and *trans* molecules have similar energies. The molecular mechanics methods do not accurately model these systems and should be avoided, this is probably because they do not model the cyclic thionocarbonates well. The charge distribution results indicated that it does not contribute to the selectivity. The offset-from-the-ideal-angle calculations showed a difference between the thionocarbonates when compared to the carbonates, especially in the 6-5 series.

- *Results: Fragmentation reaction - cis:*

The fragmentation of a cyclic thionocarbonate was examined applying *ab initio* calculations using the methods described in "the *ab initio* procedure" section. The *cis* thionocarbonate fragmentation is examined in this section. The scheme below shows the two possible reaction pathways *via* bond cleavage to give a primary radical (**19**) or a secondary radical (**21**). Experimentally, its been shown that the fragmentation of a *cis* 6-5 system (represented here by compound **11**) gave rise to the product derived from a secondary radical (represented here by compound **29**) as the preferred pathway for the reaction (see Figure IV.1).

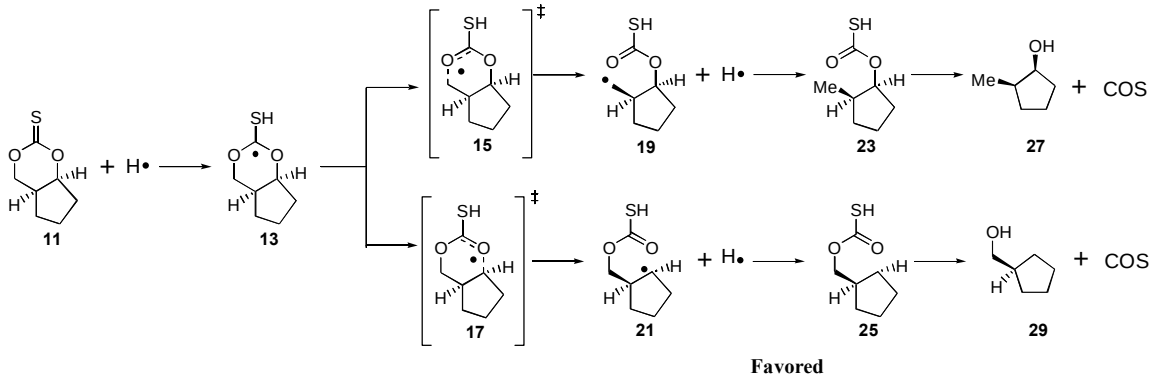

Energy results obtained from the *ab initio* calculations are shown in Figure IV.7. The second column of the table refers to the energy calculated for the compound numbered in the first column. The fourth column represents the energy associated with the complete reaction in each case, *i. e.,* the compound energy plus the value of any extra molecule involved in that reaction step as shown on the third column of the table. The fifth column shows the relative energy for the complete reaction reported in the fourth column converted into Kcal/mol. The graph follows the complete-reaction steps for both the primary and secondary radical paths.

Compd. Number	Energy (Hartree) ab initio		Rxn. Energy (Hartree) ab initio	Rxn. Energy (Kcal/mol) relative
11	-818,1251	H-H	-819,2519	43,6499
13	-818,6578	H•	-819,1560	103,8280
15	-818,6152	H•	-819,1134	130,5599
17	-818,6699	H•	-819,1681	96,2352
19	-818,6884	H•	-819,1867	84,5823
21	-818,6891	H•	-819,1873	84,1807
23	-819,3204		-819,3204	0,6843
25	-819,3145		-819,3145	4,3489
27	-309,0482	COS	-819,3088	7,9195
29	-309,0447	COS	-819,3053	10,1157
H•	-0,4982			
COS	-510,2606			
H-H	-1,1268			

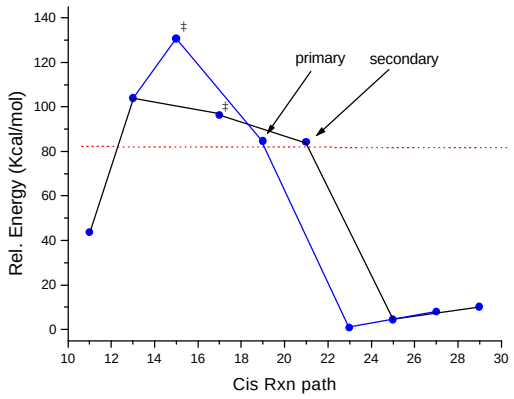

Figure IV.7

Simple thermodynamical analysis would indicate preference for the formation of the secondary radical **21** based on its lower energy as compared to the primary radical **19**. The difference in energy is 6.36 x 10^{-4} Hartree (0.399 Kcal/mol) which gives an approximate 2:1 selectivity at 25^{o} C for formation of the secondary radical. This agrees with what was expected based on stability of secondary *versus* primary radical analysis. This projected 2:1 selectivity[208] value assumes that the formation of the radical is irreversible and thus the rate-determining step. Clearly, this difference in energy is not large enough to justify the selectivity observed experimentally.

Comparison of the difference in energy for the two possible products of the reaction (**27, 29**) gives a difference of 5.8 x 10^{-3} Hartree (3.66 Kcal/mol) favoring formation of the primary product-radical **23**, and 3.5 x 10^{-3} Hartree (2.20 Kcal/mol)

[208] Based on $\Delta G = - RT \ln K$ where R= 1.9872 cal/molK.

favoring the formation of the primary product **27**. This would be the expected result if the fragmentation reaction was reversible.

Both charge and spin distributions are as expected given the atom types and the position of the radicals. The radical was not localized for the transition state **15**; instead it was partially distributed between the thionocarbonate carbon and the emerging carbon radical. For all other species the spin was localized on one carbon.

The cyclic radical **13** adopted the same conformation of the original reagent **11**. The primary radical reaction path (molecules **13** to **27**) evolved through a series of changes in geometry involving different envelope conformations for the five-membered ring. Transition state **15** resembled the geometry of radical **19** (late transition state). The secondary radical reaction path showed similar changes in geometry and a late transition state as well.

Both primary and secondary radicals (**19, 21**) adopted nearly flat conformations, while the cyclic radical **13** is pyramidal. The preferred geometry of tri-coordinated carbon radicals is well known[209], with a planar or nearly planar preferred configuration (around 10^{o} tolerance) with tiny barriers for inversion. Electronegative substituents (oxygen, halogens, etc.) are known to cause a radical to pyramidalize, and raise its barrier to inversion, as was observed for **13**.

Radical reactions usually occur with a transition state that resembles the geometry of the planar radical, a late transition state[209]. The transformation to the planar radical is associated with an increase in bond angles, which reduces the repulsive effects between

---

[209] Ruchardt, C. *Angew. Chem. Int. Ed. Eng.* **1970**, *9*, 830.

substituents. Along the same line, any influence that tends to reduce the angle between the orbitals or bonds encounters strong resistance due to an increase of strain.

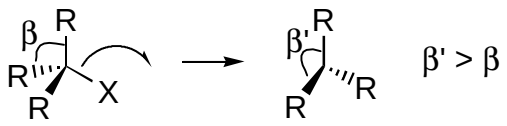

Analysis of the strain associated with angle strain for each molecule was accomplished using the offset-from-the-ideal-angle calculation described in the *ab initio* procedure section of this Addendum. The change in the offset-from-the-ideal-angle associated with the ring portion of the molecule showed an increase for the formation of the radicals (**19**, **21**) leading to both the primary and secondary products (**23**, **25**) as shown in the graphs in Figure IV.8. There was a smaller increase in the offset associated with the formation of the primary radical (**19**). This difference is better demonstrated in the detail graph where the data corresponding to the transition states have been removed for the sake of clarity.

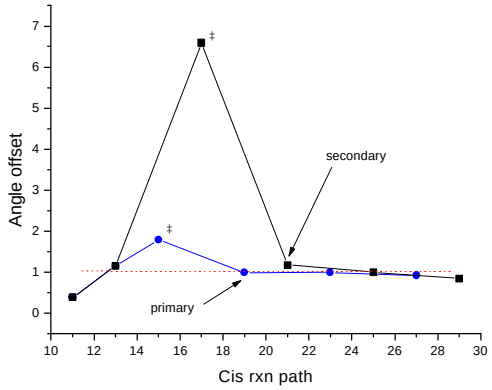

Compound Number	Total Offset	Ring Offset	carbonate Offset
11	0.3847	0.3847	0.2837
13	1.1524	0.3535	0.4543
15	1.7867	0.3979	1.4041
17	6.5950	2.9316	6.0601
19	0.9894	0.4723	
21	1.1768	0.5634	
23	0.9933	0.4667	
25	0.9949	0.3792	
27	0.9197	0.3733	
29	0.8493	0.3352	

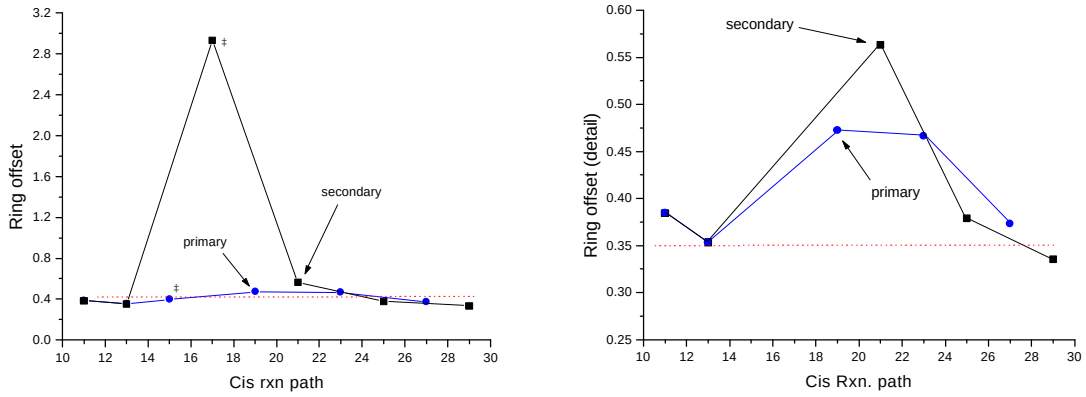

Figure IV.8

Analysis of the offset-from-the-ideal-angle change at each atom position for a specific transition was also considered (see Figure IV.9).

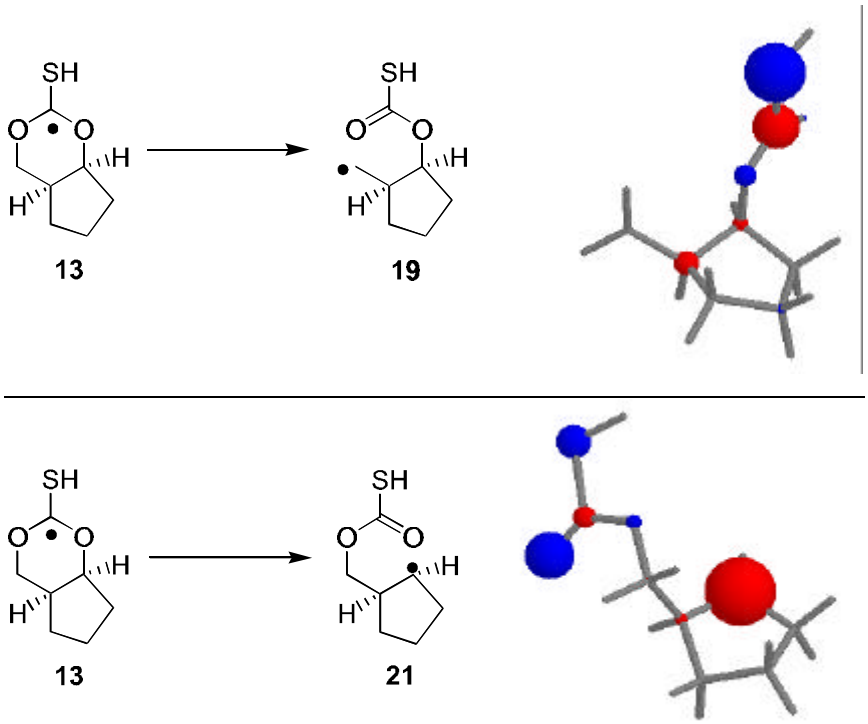

Figure 9: Graphical representation of offset-from-the-ideal-angle change. Red represents an increase in the offset at the indicated position while blue represents a decrease.

Calculation of the change in offset-from-the-ideal-angle for the transformation of cyclic radical **13** into primary radical **19** indicated an increase of ring-offset of 0.12. For the transformation of cyclic radical **13** into secondary radical **21**, the observed change in offset resulted in an increase of ring-offset of 0.21. These values would suggest that formation of the primary radical would be less disfavored due to a smaller increase in the offset and should therefore be the preferred pathway for the reaction. This is not a correct analysis because formation of the secondary radical **21** generates a radical center in the ring, therefore increasing the offset change in the ring for that molecule, while formation of the primary radical **19** does not effect ring-offset. These offset change numbers will be compared instead with the change in offset observed for the trans transformation.

- *Results: Fragmentation reaction - trans:*

The *trans* fragmentation reaction was examined applying similar *ab initio* calculations. The scheme below shows the two possible reaction pathways *via* C-O bond cleavage to give a primary radical (**18**) or a secondary radical (**20**). Experimentally, its been shown that the fragmentation of a *trans* 6-5 system (represented here by compound **12**) gives rise to the product derived from a primary radical (represented here by compound **28**) as the preferred pathway for the reaction (in a ratio of 1:21, see Figure IV.1).

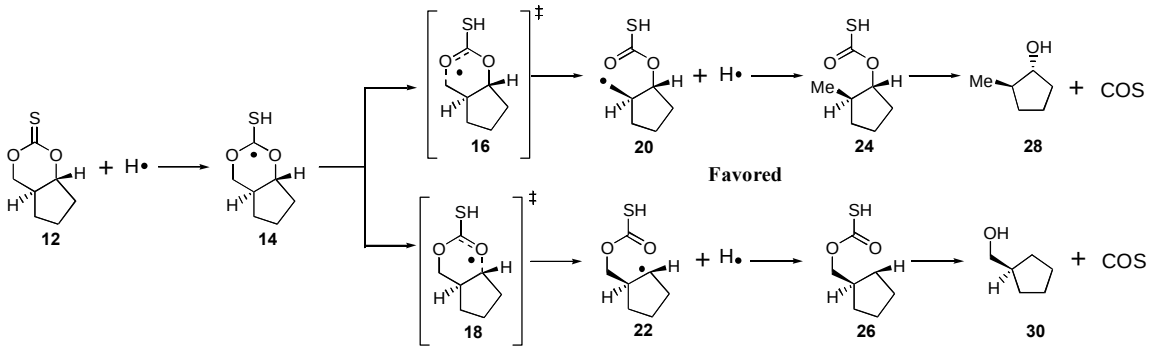

Energy results obtained from the *ab initio* calculations are shown in Figure IV.10. The second column of the table refers to the energy calculated for the compound numbered in the first column. The fourth column represents the energy associated with the complete reaction in each case, *i. e.,* the compound energy plus the value of any extra molecule involved in that reaction step as shown on the third column of the table. The fifth column shows the relative energy for the complete reaction reported in the fourth column converted into Kcal/mol. The graph follows the complete-reaction steps for both the primary and secondary radical paths.

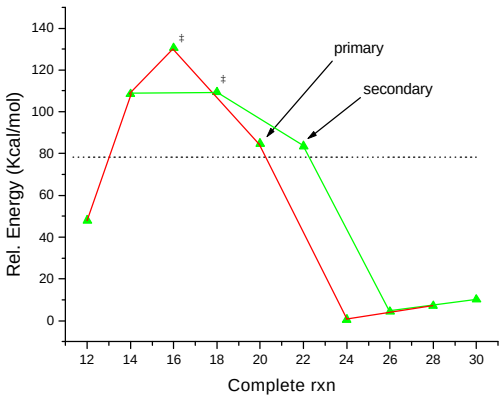

Compd. Number	Energy (Hartree) ab initio		Rxn. Energy (Hartree) ab initio	Rxn. Energy (Kcal/mol) relative
12	-818,1182	H-H	-819,2450	47,9797
14	-818,6504	H•	-819,1486	108,4716
16	-818,6152	H•	-819,1134	130,5599
18	-818,6489	H•	-819,1471	109,4129
20	-818,6881	H•	-819,1863	84,8082
22	-818,6901	H•	-819,1884	83,5281
24	-819,3206		-819,3206	0,5713
26	-819,3145		-819,3145	4,3489
28	-309,0497	COS	-819,3103	7,0033
30	-309,0447	COS	-819,3053	10,1157
H•	-0,4982			
COS	-510,2606			
H-H	-1,1268			

Figure IV.10

Simple thermodynamical analysis would indicate preference for the formation of the secondary radical **22** based on its lower energy as compared to the primary radical **20**, the same behavior observed for the *cis* series. The difference in energy is 2.04 x 10^{-3} Hartree (1.28 Kcal/mol) which gives an approximate 6:1 selectivity[208] at 25° C favoring formation of the secondary radical. This agrees with what was expected based on stability of secondary *versus* primary radical analysis but not with the experimental results obtained for the radical fragmentation of similar compounds. This projected 6:1 selectivity value assumes that the formation of the radical is irreversible and thus the rate-determining step.

Comparison of the difference in energy for the two possible products of the reaction (**28, 30**) gave a difference of 6.0 x 10^{-3} Hartree (3.78 Kcal/mol) favoring formation of the primary product-radical **24** and 5.0 x 10^{-3} Hartree (3.11 Kcal/mol) favoring the formation of the primary product **28**. This would be the expected result if the fragmentation reaction was reversible, but since the reaction is under kinetic control, the stability of the final product should not determine the formation of the final product.

Both charge and spin distributions are as expected given the atom types and the position of the radicals. The radical was not localized for transition state **16**; instead it was partially distributed between the thionocarbonate and the emerging radical carbon. For all other species the spin was localized on one carbon.

The cyclic radical **14** adopted the same conformation as the original reagent **12**. The primary radical reaction pathway evolved through a series of changes in geometry involving the envelope conformation of the five-membered ring. The transition state **16** resembled the geometry of radical **20 (**late transition state). The secondary radical

reaction pathway showed similar changes in geometry, with an early transition state and the spin concentrated in the original thionocarbonate carbon. Both primary and secondary radicals (**20, 22**) were close to flat, while the cyclic radical **14** was pyramidal.

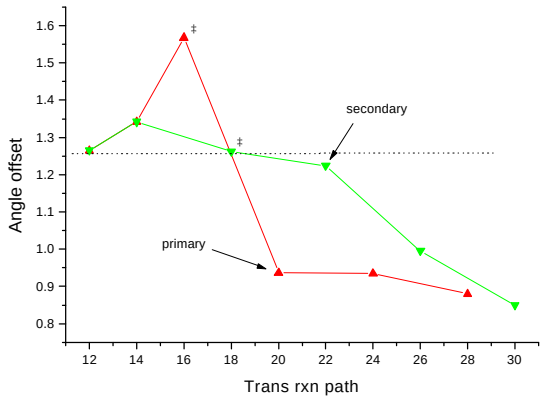

Compound Number	Total Offset	Ring Offset	carbonate Offset
12	1.2646	0.5961	1.0319
14	1.3420	0.5476	0.6243
16	1.5677	0.4528	1.2489
18	1.2623	0.5476	0.8168
20	0.9370	0.4230	
22	1.2241	0.6124	
24	0.9351	0.4144	
26	0.9949	0.3792	
28	0.8803	0.3266	
30	0.8493	0.3352	

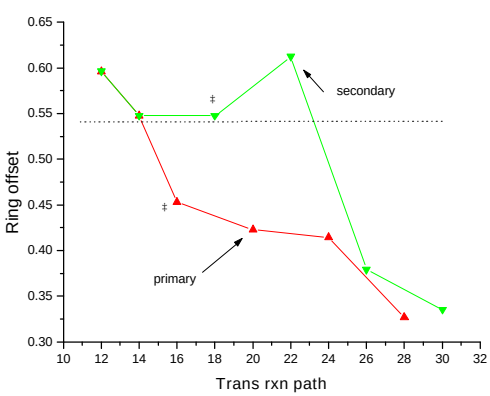

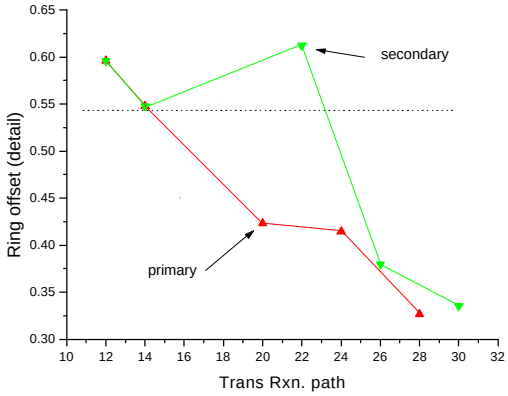

Figure IV.11

Analysis of offset-from-the-ideal-angle associated with each compound showed that formation of the radicals resulted on an increase of ring-offset for the formation of the secondary radical **22** of 0.07 and a release of ring-offset for the formation of primary radical **20** of 0.13. This difference in ring-offset is better demonstrated in the detail graph

where the data corresponding to the transition states have been removed for the sake of clarity (see Figure IV.11).

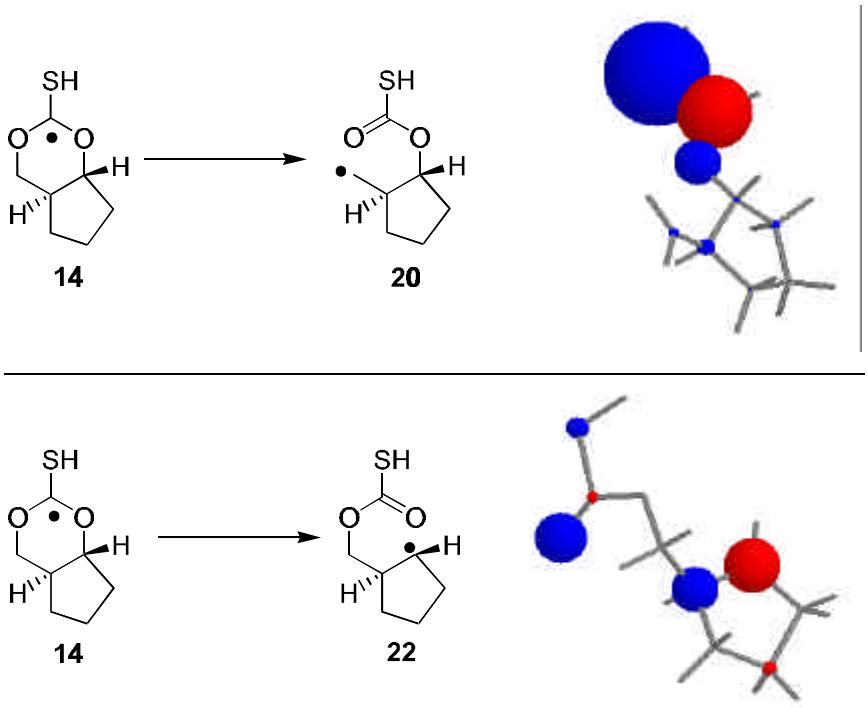

Figure IV.12: Graphical representation of offset-from-the-ideal-angle change. Red represents an increase in angle offset at the indicated position while blue represents a decrease.

Analysis of the change in offset-from-the-ideal-angle at each atom position for a specific transition was considered for the transformation of cyclic radical **14** into primary radical **20** and secondary radical **22** and is illustrated in Figure IV.12. Formation of the primary radical **20** implied in a relief of ring-offset of 0.13 while formation of the secondary radical **22** implied in an increase of the ring-offset of 0.07. These values suggest that formation of the primary radical is favored due to a decrease in ring-offset and should therefore be the preferred pathway for the reaction.

The change in offset observed for the transformation of the *cis* series were compared with the results obtained for the *trans* series. Analysis of the results showed that formation of the primary radical (**19** and **20**) involved increase of the offset for the ring atoms for compound **19** (see Figure 9) and a release of offset for the ring atoms in compound **20** (see Figure 12). For the secondary radical, there was always an increase of the offset associated with the formation of the radical in the ring and therefore it does not play a big role in determining the selectivity of the reaction.

The *trans* series offset is overall laeger than the *cis* series. Under these circumstances release of ring-offset associated with C-O bond cleavage are proportionally more important and thus the offset play a bigger role in defining selectivity towards formation of the primary radical **20** and overcomes the thermodynamical tendencies of the system towards formation of the secondary radical.

ADDENDUM V: *PERL SCRIPTS*

- *Angle_strain.pl*

```
#! /usr/local/bin/perl
# Last update: nov/98, Renata Kover
# angle_strain.pl
# evaluates angle_strain_average in the molecule
# taking into account the hybridization of the atom. The output is a
# script to be used with pdb files for raswin.
# usage: angle_strain.pl inputfile(.log) scaler

# error checking
if ($ARGV[0] eq "") {
        print "\nusage: angle_strain.pl inputfile scaler (default 5)\n";
        print "\n Evaluates angle_strain_average in the molecule from a gaussian \n";
        print " log file taking into account the hybridization of the atom. The output is
a \n";
        print " script to be used with pdb files for raswin.\n \n";
        exit;
}

# Open the log file for reading
$file = shift; $scaler = shift;

open (IN, "< $file") or die "Where is $file?\n";

# First, build the atom number-atom type conversion
$get_names = "";
$line_num = 0;
$input_orientations = 0;
while (<IN>) {
        # Should we begin reading in the atom center/number info?
        if( (/Input orientation/) and ($input_orientations == 0) ) {
                $get_names = "true";
        }

        if( $get_names eq "true" ) {
                ++$line_num;
                next if( $line_num < 6 );
                if( /---------/ ) {
                        $get_names = "false";
                        ++$input_orientations;
                        next;
                }
                ( $center_num, $atom_num ) = split;
                $atom_nums[$center_num] = $atom_num;
                # print "center_num=$center_num atom_num=$atom_num\n";
        }
}

# DEBUG PRINT
# foreach $atom_num ( @atom_nums ) {
#       print "atom_num[$count]=$atom_num\n";
#       ++$count;
# }

# Look in a PERL book and learn how to REWIND a file
```

```
close( IN );
open (IN, "< $file") or die "Where is $file?\n";

while (<IN>) {
        # Begin looking for the angle info after these words
        if (/ Optimized Parameters /) { $opt="t"; }
        next unless ( $opt );

        # Angle info looks like this
        # A1    A(2,1,3)             110.0984         -DE/DX =    0.
        next unless (/\! A/);
        # print;

        # get the desired values out of the file
        if (/ \! A\d+\s+A\((\d+)\,(\d+)\,(\d+)\)\s+(\S+)/) {
                ($a, $b, $c, $deg) = ($1, $2, $3, $4, $5);
                $angle = "A($a,$b,$c)";

                # This is a 2D assoc. array
                $angle{$b}{"$a $c"} = $deg;
                # print "$angle $deg \n";
        }

}
close (IN);

# Grab the atom names
@atoms_mid = sort bynum keys %angle;
#print @atoms_mid, "\n";


foreach $atom_mid ( @atoms_mid ) {
        @atoms_other = keys %{ $angle{$atom_mid} };

        # print "There are ",$#atoms_other+1," angles involving atom $atom_mid\n";

        # If there are 1 or 6 angles then it is sp3 hybridization
        if ( ( $#atoms_other+1 == 6 ) or ( $#atoms_other+1 == 1 ) ) { $hyb{$atom_mid} =
"sp3"; }
        # Otherwise it is sp2 hybridization
        else { $hyb{$atom_mid} = "sp2"; }

        # loop through each angle and print out a report
        $num_angles = $#atoms_other+1;
        # print "Found $num_angles angle on atom number $atom_mid, the hybridization is
$hyb{$atom_mid}\n";

        foreach $atom_other ( @atoms_other ) {

                # Figure out the explicit names of the other atoms
                ($a, $c) = split " ", $atom_other;

                # sp2 carbon atom
                if ( ($hyb{$atom_mid} eq "sp2") && ($atom_nums[$atom_mid]==6) ) {
                        # print "Calculating the offset for an sp2 carbon\n";
                        &calc_offset( 120 );

                # sp3 carbon atom
                } elsif ( ($hyb{$atom_mid} eq "sp3") && ($atom_nums[$atom_mid]==6) ) {
                        # print "Calculating the offset for an sp3 carbon\n";
                        &calc_offset( 109.6 );

                # sp3 oxygen atom
                } elsif ( ($hyb{$atom_mid} eq "sp3") and ($atom_nums[$atom_mid]==8) ) {
                        # print "Calculating the offset for an sp3 oxygen\n";
                        &calc_offset( 109.6 );

                # sp3 sulfur atom
                } elsif ( ($hyb{$atom_mid} eq "sp3") and ($atom_nums[$atom_mid]==16) ) {
                        # print "Calculating the offset for an sp3 sulfur\n";
                        &calc_offset( 92 );

                } else {
```

```
                        print "Whoa there pardner, I don't understand the hybridization of
                        atom $atom_mid\n";
                        print "atom_num=$atom_nums[$atom_mid]\n";
                        exit;
                }

                # print "    found an offset of $offset\n";

                $angle = "A($a,$atom_mid,$c)";
                # printf ("%15s %4s %8.4f %6.2f\n",
                #       $angle, $hyb{$atom_mid}, $angle{$atom_mid}{$atom_other}, $offset );

                # Store the total percentage strain for each mid atom
                $strain{$atom_mid} += $offset;
        }
        # Normalize for the number of angles involved in the strain
        # calculation of each atom
        $strain{$atom_mid} *= 100/$num_angles;

}

# Print a rasmol input script

print "background white\n";
print "select all\n";
print "color label blue\n";
print "label on\n";
print "wireframe 20\n";
print "color bond [155,155,155]\n";

foreach $num ( @atoms_mid ) {
        $size = $strain{$num} * $scaler;
        $hybridization = $hyb{$num};

        print "#####################\n";
        print "# Below is for atom number $num with hybridization $hybridization\n";
        print "# and total strain percentage $strain{$num}\n";
        print "select atomno=$num\n";
        printf ("spacefill %1d\n", $size);
        print "colour red\n";
        # print "colour blue\n" if ($charge >= 0);
        print "\n";
}

sub calc_offset {
        $ideal = shift;

        # Calculate the normalized deflection from the ideal sp3 angle
        $offset = ( $ideal - $angle{$atom_mid}{$atom_other} ) / $ideal;

        # Square this offset value
        $offset *= $offset;
}

sub bynum { $a <=> $b };
```

- *Get_charge.pl*

```
#! /usr/local/bin/perl
# Last update: april/98, Renata Kover
# get_charge.pl
# requires programs:
# evaluates charges in the molecule and writes a script
# to be used with pdb files.
# usage: get_charge.pl scaler <inputfile(.log)

# error checking
if ($ARGV[0] eq "") {
```

```
        print "usage:\n get_charge.pl scaler (default 100) < input file\n";
        exit;
}

$scaler=shift;

while (<>) {

        if (/Optimization completed/) {
                $continue = "t";
        }

        next unless ( $continue );

        # Okay, we are past the "Opt. completed" line

        if (/Total atomic charges/) {
                # Save charge info after the
                # "Total atomic charges" line
                $get_charge = "t";
        }

        if (/Sum of Mulliken charges/) {
                # When we hit the "Sum of..." line,
                # stop getting the charge info
                $get_charge ="";
        }

        next unless ( $get_charge );

        ++$count;
        next unless ( $count > 2 );
        # Count how many lines after "Total atomic..."
        # we are.  Keep only AFTER line 2

        #################
        # The good stuff
        #################

        # Grab the atom number and type
        ( $a, $num, $type, $charge ) = split (/\s+/, $_);

        # print "The charge on atom num $num with type $type is $charge\n";

        $charges[$num] = $charge;

}

# Print a rasmol input script

print "background [200,200,170]\n";
print "select all\n";
print "color label blue\n";
print "label on\n";
print "wireframe 20\n";
print "color bond [155,155,155]\n\n";

foreach $num ( 1 .. $#charges ) {
        $charge = $charges[$num];
        $size = abs( $charge * $scaler );

        print "######################\n";
        print "# Below is for atom number $num with charge $charge\n";
        print "select atomno=$num\n";
        printf ("spacefill %1d\n", $size);
        print "colour red\n" if ($charge < 0);
        print "colour blue\n" if ($charge >= 0);
        print "\n";
}
```

- *Get_spin.pl*

```
#! /usr/local/bin/perl
# Last update: april/98, Renata Kover
# get_spin.pl
# requires programs:
# evaluates spin in the molecule and writes a script
# to be used with pdb files.
# usage: get_spin.pl scaler <inputfile(.log)

# error checking
if ($ARGV[0] eq "") {
        print "usage:\n get_spin.pl scaler (default 100) < input file\n";
        exit;
}

$scaler=shift;

while (<>) {

        if (/The wavefunction is already stable/) {
                $continue = "t";
        }

        next unless ( $continue );

        # Okay, we are past the "Opt. completed" line

        if (/Total atomic spin densities/) {
                # Save charge info after the
                # "Total atomic charges" line
                $get_charge = "t";
        }

        if (/Sum of Mulliken spin densities/) {
                # When we hit the "Sum of..." line,
                # stop getting the charge info
                $get_charge ="";
        }

        next unless ( $get_charge );

        ++$count;

        next unless ( $count > 2 );
        # Count how many lines after "Total atomic..."
        # we are.  Keep only AFTER line 2


        #################
        # The good stuff
        #################

        # Grab the atom number and type
        ( $a, $num, $type, $charge ) = split (/\s+/, $_);

        # print "The charge on atom num $num with type $type is $charge\n";

        $charges[$num] = $charge;

}

# Print a rasmol input script

print "background [170,200,200]\n";
print "select all\n";
print "color label blue\n";
print "label on\n";
print "wireframe 20\n";
print "color bond [155,155,155]\n\n";
```

```
foreach $num (1 .. $#charges) {
        $charge = $charges[$num];
        $size = abs( $charge * $scaler );

        print "######################\n";
        print "# Below is for atom number $num with charge $charge\n";
        print "select atomno=$num\n";
        printf ("spacefill %1d\n", $size);
        print "colour red\n" if ($charge < 0);
        print "colour blue\n" if ($charge >= 0);
        print "\n";
}
```

- *Gaussian2pdb.pl*

```
#! /usr/local/bin/perl
# Last update: Mar/98, Renata Kover
# gaussian2pdb.pl
# requires programs: zmatrix_extract, newzmat and pdbclean.pl
# Converts gaussian ts log files into individual pdb files
# usage: gaussian2pdb.pl inputfile(.log)

# error checking
if ($ARGV[0] eq "") {
        print "usage: gaussian2pdb.pl inputfile(.log)\n";
        exit;
}

$file = shift;

# Keep the word to the left of the period in the filename
$file =~ s/^(\w+).*/$1/;

`zmatrix_extract < $file.log > $file.temp`;

open (IN, "< $file.temp") or die "Where is $file.temp\n";
open (OUT, "> $file.out");

while (<IN>) {

        if ($count > 1) { print OUT; }

        if ( /^#/ ) {
                # This is only true the first time
                next if ( ++$count == 1 );
                print OUT;
                ++$count;
                next;
        }

}

close IN;
close OUT;

`newzmat -izmat -obkv $file.out`;
`pdbclean.pl < $file.bkv > $file.pdb`;

unlink "$file.temp";
unlink "$file.out";
unlink "$file.bkv";


exit;
```

- *Zmatrixextract*

```
#! /usr/bin/awk -f
# @(#) extract Gaussian zmatrix from an archive file

!/#/    {next}  # beginning of the root card

{
        prev = substr($0, index($0, "#"));
        gsub(/\\/, "\n", prev);
        while (getline > 0) {
                sub(/^[ \t]+/, "", $0);
                gsub(/\\/, "\n", $0);
                card = sprintf("%s%s", prev, $0);
                n = index(card, "Version");   # mark the end
                if (n > 0) {   # done
                        printf("%s", substr(card, 1, n-1));
                        break;
                }
                printf("%s", prev);
                prev = $0;
        }
        exit;
}
```

- *Pdbclean.pl*

```
.#! /usr/local/bin/perl
# pdb_clean
# Makes those pesky pdb files better!
# usage: "pdbclean.pl inputfile > outputfile"

foreach (<>) {
    ($first)=(split)[0];

    if (($first eq "COMPND") or ($first eq "CONECT") or
        ($first eq "END") or ($first eq "TER") or
        ($first eq "REMARK")) {
                print;
        } elsif (($first eq "ATOM") || ($first eq "HETATM")) {
                $rec_name="ATOM";
                ($int,$atom_name)=(split)[1,2];

                # Now, substitute nothing for any numbers:
                $atom_name =~ s/[0-9]+//;

                # Now, read in the x,y,z coordinates
                $x=substr($_, 31, 8);
                $y=substr($_, 39, 8);
                $z=substr($_, 47, 8);

                if ($atom_name ne "LP") {
                    write;
                }
        }
}

format STDOUT =
@<<<<< @>>>  @>>              @###.###@###.###@###.###
$rec_name,$int,$atom_name,$x,$y,$z
.
```

- *Sum_angle_strain.pl*

```
#! /usr/local/bin/perl
# Last update: nov/98, Renata Kover
# sum_angle_strain.pl
# evaluates angle_strain of portions of the molecule by adding
# the total angle strain of the individual atoms while
# taking into account the hybridization of the atom. The output is a
# script to be used with pdb files for raswin.
# usage: sum_angle_strain.pl inputfile(.log) (list of atom numbers)

# error checking
if ($ARGV[0] eq "") {
        print "\n Usage: sum_angle_strain.pl inputfile (list of atom numbers)\n";
        print "\n Evaluates angle_strain of portions of the molecule by adding the \n";
    print " total angle strain of the individual atoms while \n";
        print " taking into account the hybridization of the atom. The output is a \n";
        print " script to be used with pdb files for raswin.\n \n";
        exit;
}

# Open the log file for reading
$file = shift;

# Grab all the atoms for which to add up the strain
@sum_atoms = @ARGV;

print "Working on atoms ";
foreach $atom ( @sum_atoms ) {
        print "$atom ";
}
print "\n";

open (IN, "< $file") or die "ERROR: Cannot find $file?\n";

# First, build the atom number-atom type conversion
$get_names = "";
$line_num = 0;
$input_orientations = 0;
while (<IN>) {
        # Should we begin reading in the atom center/number info?
        if( (/Input orientation/) and ($input_orientations == 0) ) {
                $get_names = "true";
        }

        if( $get_names eq "true" ) {
                ++$line_num;
                next if( $line_num < 6 );
                if( /---------/ ) {
                        $get_names = "false";
                        ++$input_orientations;
                        next;
                }
                ( $center_num, $atom_num ) = split;
                $atom_nums[$center_num] = $atom_num;
                # print "center_num=$center_num atom_num=$atom_num\n";
        }
}

# DEBUG PRINT
# foreach $atom_num ( @atom_nums ) {
#       print "atom_num[$count]=$atom_num\n";
#       ++$count;
# }

# Look in a PERL book and learn how to REWIND a file
close( IN );
open (IN, "< $file") or die "Where is $file?\n";

while (<IN>) {
        # Begin looking for the angle info after these words
```

```
        if (/ Optimized Parameters /) { $opt="t"; }
        next unless ( $opt );

        # Angle info looks like this
        # A1    A(2,1,3)              110.0984         -DE/DX =    0.
        next unless (/\! A/);
        # print;

        # get the desired values out of the file
        if (/ \! A\d+\s+A\((\d+)\,(\d+)\,(\d+)\)\s+(\S+)/) {
                ($a, $b, $c, $deg) = ($1, $2, $3, $4, $5);
                $angle = "A($a,$b,$c)";

                # This is a 2D assoc. array
                $angle{$b}{"$a $c"} = $deg;
        }


}
close (IN);

# Grab the atom names
@atoms_mid = sort bynum keys %angle;
# print @atoms, "\n";


foreach $atom_mid ( @atoms_mid ) {
        @atoms_other = keys %{ $angle{$atom_mid} };

        # print "There are ",$#atoms_other+1," angles involving atom $atom_mid\n";

        # If there are 1 or 6 angles then it is sp3 hybridization
        if ( ( $#atoms_other+1 == 6 ) or ( $#atoms_other+1 == 1 ) ) { $hyb{$atom_mid} =
"sp3"; }
        # Otherwise it is sp2 hybridization
        else { $hyb{$atom_mid} = "sp2"; }

        # loop through each angle and print out a report
        $num_angles = $#atoms_other+1;

        foreach $atom_other ( @atoms_other ) {

                # Figure out the explicit names of the other atoms
                ($a, $c) = split " ", $atom_other;

                # sp2 carbon atom
                if ( ($hyb{$atom_mid} eq "sp2") && ($atom_nums[$atom_mid]==6) ) {
                        # print "Calculating the offset for an sp2 carbon\n";
                        &calc_offset( 120 );

                # sp3 carbon atom
                } elsif ( ($hyb{$atom_mid} eq "sp3") && ($atom_nums[$atom_mid]==6) ) {
                        # print "Calculating the offset for an sp3 carbon\n";
                        &calc_offset( 109.6 );

                # sp3 oxygen atom
                } elsif ( ($hyb{$atom_mid} eq "sp3") and ($atom_nums[$atom_mid]==8) ) {
                        # print "Calculating the offset for an sp3 oxygen\n";
                        &calc_offset( 109.6 );

                # sp3 sulfur atom
                } elsif ( ($hyb{$atom_mid} eq "sp3") and ($atom_nums[$atom_mid]==16) ) {
                        # print "Calculating the offset for an sp3 sulfur\n";
                        &calc_offset( 92 );

                } else {
                        print "Whoa there pardner, I dont understand the hybridization of
atom $atom_mid\n";
                        print "atom_num=$atom_nums[$atom_mid]\n";
                        exit;
                }

                $angle = "A($a,$atom_mid,$c)";
                # printf ("%15s %4s %8.4f %6.2f\n",
```

```
                #       $angle, $hyb{$atom_mid}, $angle{$atom_mid}{$atom_other}, $per );


                # Store the total strain for each mid atom
                $strain{$atom_mid} += $offset ;
        }
        # Normalize for the number of angles involved in the strain
        # calculation of each atom
        $strain{$atom_mid} *= 100/$num_angles;

        printf( "The strain at atom_mid, %2d, with hybridization $hyb{$atom_mid}, is %7.3f
percent\n", $atom_mid, $strain{$atom_mid} );

}

# Sum up the total strain
$total_strain = 0;
foreach $atom ( @sum_atoms ) {
        $total_strain += $strain{$atom};
}

# Print a mini strain report
print "The sum of the strain at atoms ";
foreach $atom ( @sum_atoms ) {
        print " $atom";
}
printf( " is %8.4f\n", $total_strain );
exit;

sub calc_offset {
        $ideal = shift;

        # Calculate the normalized deflection from the ideal sp3 angle
        $offset = ( $ideal - $angle{$atom_mid}{$atom_other} ) / $ideal;

        # Square this offset value
        $offset *= $offset;
}

sub bynum { $a <=> $b };
```